

ISSN 1854-6250

APEM
journal

Advances in Production Engineering & Management

Volume 11 | Number 4 | December 2016



University of Maribor

Published by PEI
apem-journal.org

Advances in Production Engineering & Management

Identification Statement

	ISSN 1854-6250 Abbreviated key title: Adv produc engineer manag Start year: 2006 ISSN 1855-6531 (on-line)
	Published quarterly by Production Engineering Institute (PEI), University of Maribor Smetanova ulica 17, SI – 2000 Maribor, Slovenia, European Union (EU) Phone: 00386 2 2207522, Fax: 00386 2 2207990 Language of text: English APEM homepage: apem-journal.org University homepage: www.um.si

APEM Editorial

Editor-in-Chief

Miran Brezocnik

editor@apem-journal.org, info@apem-journal.org
University of Maribor, Faculty of Mechanical Engineering
Smetanova ulica 17, SI – 2000 Maribor, Slovenia, EU

Desk Editor

Tomaz Irgolic

desk1@apem-journal.org

Website Technical Editor

Lucija Brezocnik

lucija.brezocnik@um.si

Editorial Board Members

Eberhard Abele, Technical University of Darmstadt, Germany
Bojan Acko, University of Maribor, Slovenia
Joze Balic, University of Maribor, Slovenia
Agostino Bruzzone, University of Genoa, Italy
Borut Buchmeister, University of Maribor, Slovenia
Ludwig Cardon, Ghent University, Belgium
Nirupam Chakraborti, Indian Institute of Technology, Kharagpur, India
Edward Chlebus, Wroclaw University of Technology, Poland
Franci Cus, University of Maribor, Slovenia
Igor Drstvensek, University of Maribor, Slovenia
Illes Dudas, University of Miskolc, Hungary
Mirko Ficko, University of Maribor, Slovenia
Vlatka Hlupic, University of Westminster, UK
David Hui, University of New Orleans, USA

Pramod K. Jain, Indian Institute of Technology Roorkee, India
Isak Karabegović, University of Bihać, Bosnia and Herzegovina
Janez Kopac, University of Ljubljana, Slovenia
Iztok Palcic, University of Maribor, Slovenia
Krsto Pandza, University of Leeds, UK
Andrej Polajnar, University of Maribor, Slovenia
Antonio Pouzada, University of Minho, Portugal
Rajiv Kumar Sharma, National Institute of Technology, India
Katica Simunovic, J. J. Strossmayer University of Osijek, Croatia
Daizhong Su, Nottingham Trent University, UK
Soemon Takakuwa, Nagoya University, Japan
Nikos Tsourveloudis, Technical University of Crete, Greece
Tomo Udiljak, University of Zagreb, Croatia
Ivica Veza, University of Split, Croatia

Limited Permission to Photocopy: Permission is granted to photocopy portions of this publication for personal use and for the use of clients and students as allowed by national copyright laws. This permission does not extend to other types of reproduction nor to copying for incorporation into commercial advertising or any other profit-making purpose.

Subscription Rate: 120 EUR for 4 issues (worldwide postage included); 30 EUR for single copies (plus 10 EUR for postage); for details about payment please contact: info@apem-journal.org

Cover and interior design: Miran Brezocnik

Printed: Tiskarna Koštomaj, Celje, Slovenia

Subsidizer: The journal is subsidized by Slovenian Research Agency

Statements and opinions expressed in the articles and communications are those of the individual contributors and not necessarily those of the editors or the publisher. No responsibility is accepted for the accuracy of information contained in the text, illustrations or advertisements. Production Engineering Institute assumes no responsibility or liability for any damage or injury to persons or property arising from the use of any materials, instructions, methods or ideas contained herein.

Copyright © 2016 PEI, University of Maribor. All rights reserved.

Advances in Production Engineering & Management is indexed and abstracted in the **WEB OF SCIENCE** (maintained by **THOMSON REUTERS**): **Science Citation Index Expanded**, **Journal Citation Reports** – Science Edition, **Current Contents** – Engineering, Computing and Technology • **Scopus** (maintained by **Elsevier**) • **Inspec** • **EBSCO**: Academic Search Alumni Edition, Academic Search Complete, Academic Search Elite, Academic Search Premier, Engineering Source, Sales & Marketing Source, TOC Premier • **ProQuest**: CSA Engineering Research Database – Cambridge Scientific Abstracts, Materials Business File, Materials Research Database, Mechanical & Transportation Engineering Abstracts, ProQuest SciTech Collection • **TEMA (DOMA)** • The journal is listed in **Ulrich's** Periodicals Directory and **Cabell's** Directory



University of Maribor
Production Engineering Institute (PEI)

Advances in Production Engineering & Management

Volume 11 | Number 4 | December 2016 | pp 255–380

Contents

Scope and topics	258
A combined zone-LP and simulated annealing algorithm for unequal-area facility layout problem	259
Xiao, Y.J.; Zheng, Y.; Zhang, L.M.; Kuo, Y.H.	
A new multi-objective Jaya algorithm for optimization of modern machining processes	271
Rao, R.V.; Rai, D.P.; Ramkumar, J.; Balic, J.	
Finite element method for optimum design selection of carport structures under multiple load cases	287
Özkal, F.M.; Cakir, F.; Arkun, A.K.	
Applying multi-phase particle swarm optimization to solve bulk cargo port scheduling problem	299
Tang, M.; Gong, D.; Liu, S.; Zhang, H.	
A case-based reasoning approach for non-traditional machining processes selection	311
Boral, S.; Chakraborty, S.	
Dimensional accuracy of camera casing models 3D printed on Mcor IRIS: A case study	324
Mandić, M.; Galeta, T.; Raos, P.; Jugović, V.	
Effect of delayed differentiation on a multiproduct vendor-buyer integrated inventory system with rework	333
Chiu, Y.-S.P.; Kuo, J.-S.; Chiu, S.W.; Hsieh, Y.-T.	
Experimental modeling of fluid pressure during hydroforming of welded plates	345
Karabegović, E.; Poljak, J.	
An integrated lean approach to Process Failure Mode and Effect Analysis (PFMEA): A case study from automotive industry	355
Banduka, N.; Veža, I.; Bilić, B.	
Multi-objective optimization of the turning process using a Gravitational Search Algorithm (GSA) and NSGA-II approach	366
Klančnik, S.; Hrelja, M.; Balic, J.; Brezocnik, M.	
Calendar of events	377
Notes for contributors	379

Journal homepage: apem-journal.org

ISSN 1854-6250 (print)

ISSN 1855-6531 (on-line)

©2016 PEI, University of Maribor. All rights reserved.

Scope and topics

Advances in Production Engineering & Management (APEM journal) is an interdisciplinary refereed international academic journal published quarterly by the *Production Engineering Institute* at the *University of Maribor*. The main goal of the *APEM journal* is to present original, high quality, theoretical and application-oriented research developments in all areas of production engineering and production management to a broad audience of academics and practitioners. In order to bridge the gap between theory and practice, applications based on advanced theory and case studies are particularly welcome. For theoretical papers, their originality and research contributions are the main factors in the evaluation process. General approaches, formalisms, algorithms or techniques should be illustrated with significant applications that demonstrate their applicability to real-world problems. Although the *APEM journal* main goal is to publish original research papers, review articles and professional papers are occasionally published.

Fields of interest include, but are not limited to:

Additive Manufacturing Processes	Machine Learning in Production
Advanced Production Technologies	Machine Tools
Artificial Intelligence in Production	Machining Systems
Assembly Systems	Manufacturing Systems
Automation	Materials Science, Multidisciplinary
Computer-Integrated Manufacturing	Mechanical Engineering
Cutting and Forming Processes	Mechatronics
Decision Support Systems	Metrology
Discrete Systems and Methodology	Modelling and Simulation
e-Manufacturing	Numerical Techniques
Evolutionary Computation in Production	Operations Research
Fuzzy Systems	Operations Planning, Scheduling and Control
Human Factor Engineering, Ergonomics	Optimisation Techniques
Industrial Engineering	Project Management
Industrial Processes	Quality Management
Industrial Robotics	Risk and Uncertainty
Intelligent Manufacturing Systems	Self-Organizing Systems
Joining Processes	Statistical Methods
Knowledge Management	Supply Chain Management
Logistics	Virtual Reality in Production

A combined zone-LP and simulated annealing algorithm for unequal-area facility layout problem

Xiao, Y.J.^{a,b}, Zheng, Y.^c, Zhang, L.M.^{d,*}, Kuo, Y.H.^e

^aJiangsu Key Laboratory of Modern Logistics, School of Marketing and Logistic Management, Nanjing University of Finance and Economics, Nanjing, China

^bBusiness school, Nanjing University, Nanjing, China

^cCollege of Automobile and Traffic Engineering, Nanjing Forestry University, Nanjing, China

^dSchool of Management and Engineering, Nanjing University, Nanjing, China

^eStanley Ho Big Data Decision Analytics Research Centre, The Chinese University of Hong Kong, Shatin, New Territories, Hong Kong

ABSTRACT

Facility layout problem (FLP) is one of well-known NP-hard problems and has been demonstrated to be useful in enhancing the productivity of manufacturing systems in practice. This paper focuses on the unequal-area FLP (UA-FLP) whose goal is to locate departments with different areas within a given facility so as to minimize the total material handling cost. A novel approach, which we call a combined zone-linear programming (zone-LP) and simulated annealing algorithm, is developed for solving the UA-FLP. The zone-LP approach is a layout construction technique for the unequal-area departments and consists of two phases. In the first phase, a zoning algorithm is implemented to determine the relative positions between the departments. In this algorithm, for the sake of problem simplification and computational efficiency, each department is treated as a rectangle with an allowable aspect ratio and the area of the facility is assumed to be unbounded. In the second phase, by using the relative positions obtained in the first phase as input, a linear programming (LP) model is developed to identify the exact locations and dimensions of departments within the facility with specified sizes while satisfying their maximum aspect ratio requirement and the shape constraints. We also design a simulated annealing algorithm to improve the placing sequence. Finally, our computational results suggest that our proposed algorithm is efficient compared with the best existing approach in the literature.

© 2016 PEI, University of Maribor. All rights reserved.

ARTICLE INFO

Keywords:

Facility layout problem
Unequal area
Zone-LP approach
Simulated annealing

*Corresponding author:

zhanglm@nju.edu.cn
(Zhang, L.M.)

Article history:

Received 10 August 2016
Revised 9 October 2016
Accepted 15 October 2016

1. Introduction

As the competition among the global marketplaces increases rapidly, the provision of high-quality products or services at low cost to customers becomes more and more crucial for companies to capture the mass market. Facilities planning “determines how an activity’s tangible fixed assets best support achieving the activity objectives” [1] and thus plays an important role in the cost reduction and productivity gain in industrial firms.

Facility planning consists of facilities location, facility system design, facility layout design and handling system design. As a crucial part of facilities planning, facility layout design is to arrange departments interacting with each other within a facility so as to minimize the total material handling cost. The layout design of a facility significantly impacts manufacturing cost and the productivity and efficiency of the system. According to [1], material handling cost ac-

counts for 20 % to 50 % of the total manufacturing cost; an effective planning of facilities can reduce such cost by at least 10 % to 30 %. It is essential to design an efficient layout before manufacturing system design since future rearrangement of departments can result in a considerable expense. For these reasons, facility layout problem (FLP) has been studied extensively for over three decades [2-10].

There have been numerous studies adopting mathematical programming approaches to obtain optimal solutions for FLP. Montreuil [11] proposed the first mixed integer programming (MIP) model for solving the UA-FLP. However, their proposed MIP model can be solved for the problems with no more than six departments. Meller et al. [12] improved the formulation of the MIP model of Montreuil [11] by introducing a tightened department area constraint and several classes of valid inequalities. By their enhancement, the number of departments of the solvable problems increased to eight. Motivated by Meller et al. [12], Sherali et al. [13] further improved the accuracy for approximating the department areas by using a polyhedral outer approximation scheme. Moreover, Sherali et al. [13] investigated the effectiveness of the classes of valid inequalities proposed by Meller et al. [12] and reported that the MIP model was solved most efficiently by incorporating only two inequalities among them into the formulation. With this finding, the problems with up to nine departments could be optimally solved. Recently, Meller et al. [14] developed a new mathematical formulation for UA-FLP based on a sequence-pair representation. In this formulation, the feasible region of the problem was tightened such that the number of departments of the solvable problems has become eleven.

Exact solution methods such as mathematical programming approaches are not applicable to obtain optimal solutions for large-scale problems since FLP is NP-hard [2]. Hence, heuristic approaches based on MIP models have been designed to construct layout solutions of high quality efficiently [15-17]. One of the well-known algorithms for solving FLP is based on the use of a slicing tree [18, 19], which is a binary tree used to form a subdivision of a rectangle by recursive computations. In the slicing tree, each inner node contains a guillotine cut operator (which cuts the area horizontally or vertically), and each leaf node represents a department. A layout can be generated according to a slicing tree by applying a set of guillotine cuts. Liu and Meller [20] developed a sequence-pair approach, where a pair of sequences is used to determine the relative locations between departments. By employing those relative locations, a reduced MIP model is utilized to construct the layout solutions. Both of above method are primarily proposed in the VLSI (very large Scale Integration) design. Similarly, Bozer and Wang [21] presented a graph-pair technique to fix the relative locations between departments and then a linear program (LP) is solved to obtain the layout solutions.

This paper proposes a novel approach, which we call a combined zone-LP and simulated annealing (SA) algorithm, to solve the problem efficiently. The zone-LP approach is a layout construction technique for the UA-FLP and consists of two phases. In the first phase, the zone algorithm is implemented to determine the relative positions between departments. In this algorithm, for the sake of problem simplification and computational efficiency, each department is considered to be a rectangle with an allowable aspect ratio and the area of the facility is assumed to be unbounded. In the second phase, by using the relative positions obtained in the first phase as input, an LP is solved to determine the exact locations and dimensions of departments within the facility with specified sizes while satisfying their maximum aspect ratio requirement and the shape constraints. Furthermore, we also develop an SA algorithm to improve the solution quality. Finally, we conduct a computational study to examine the performance of our proposed algorithm and compare it with other existing solution approaches in the literature.

Our paper is organized as follows. In the next section, we will describe the problem of UA-FLP. Section 3 will present our proposed solution methodology. In Section 4, we conduct computational experiments to study the performance of our proposed algorithm. Section 5 concludes our paper.

2. Problem description

In UA-FLP, the areas of the departments are given and their dimensions are limited by a maximum aspect ratio (MAR), which is defined as the largest allowable ratio of the longest side to the

shortest side of the department. The aspect ratio of a department ranges from $1/MAR$ to MAR . Furthermore, material flow quantities and the location of input/output (I/O) points are given. In the problem, the I/O points are assumed to be located at the centroids of departments. During the manufacturing process, materials are transferred between I/O points for each pair of departments. The objective is to minimize the total travel distance (TTD), which is the sum product of the distances between departments and their material flow quantities. For simplicity, the distance between departments is defined as the rectilinear distance between the input point and the output point.

Table 1 provides an example of a setting of six departments with their required areas (a_m) and maximum aspect ratio (MAR_m) and the material flow quantities between each pair of the departments.

Table 1 An example of a setting of six departments with their required areas (a_m) and maximum aspect ratio (MAR_m) and the material flow quantities between each pair of the departments

m	Material flow quantities						a_m	MAR_m
	1	2	3	4	5	6		
1	—	4	2	5	7	1	16	4
2	—	—	4	3	3	4	16	4
3	—	—	—	2	2	6	25	4
4	—	—	—	—	7	4	36	4
5	—	—	—	—	—	3	36	4
6	—	—	—	—	—	—	9	4

3. Solution methodology

It is well-known that UA-FLP is NP-hard. For this reason, we develop a heuristic algorithm to solve UA-FLP of large size. One complicating factor of UA-FLP is to determine the relative positions between the departments subject to the condition that their areas do not overlap. To circumvent this difficulty, we propose a solution methodology that integrates the zone-LP approach and an SA algorithm to obtain good-quality solutions. The zone-LP approach is a newly proposed layout construction technique based on an improved zone algorithm and the solution for an LP. When an initial solution is obtained from the previous stage, SA is employed to search within the solution space and acts to avoid the search procedure being trapped at a local optimum.

3.1 Zone-LP approach

The zone-LP approach consists of two phases. In the first phase, for the simplification of the problem and more efficient computations, we consider the shape of each department as a rectangle with an allowable aspect ratio. As an example, as shown in Fig. 1, the six departments in Table 1 are treated as squares. Given the allowable aspect ratios of the departments, we develop an improved zone algorithm to determine their relative positions. The zone concept for UA-FLP is first introduced by Xiao et al. [22] to reduce its computational complexity and has been shown to be computationally efficient. In the second phase, by using the relative positions obtained in the first phase as input, we solve an LP to obtain the exact locations of the departments within the facility, and their dimensions subject to their shape constraints are satisfied.

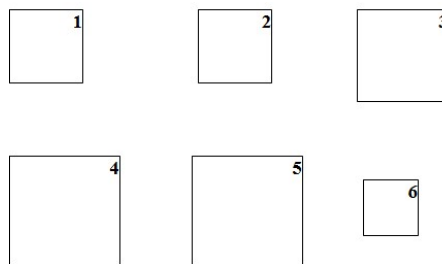


Fig. 1 Six departments to be located within the facility where each of them is of a fixed aspect ratio

3.2 Improved zone algorithm

The improved zone algorithm locates departments one by one according to a sequence such that a unique layout is generated. Given an initial sequence for locating the departments within the facility, say [1-4-2-5-3-6], we begin the algorithm by placing the first department in the sequence (i.e. Department 1) at the center of the facility. Then, four zones that are respectively on the left, above, on the right, and below this department can be identified. As an example, the four zones are shaded in the graphs of Fig. 2. The next step is to determine the zone that the following department in the sequence (i.e. Department 4) to be located. We first determine the optimal locations of this department within the four zones by using a median point (MP) method. The department will then be located at the best zone that results in the minimum total distance. Once the department is located within the facility, the set of zones will be updated for the determination of the location of the next department in the sequence. That procedure is repeated until all departments are located. For more detail about zone updating procedure, we refer the reader to Xiao et al. [22].

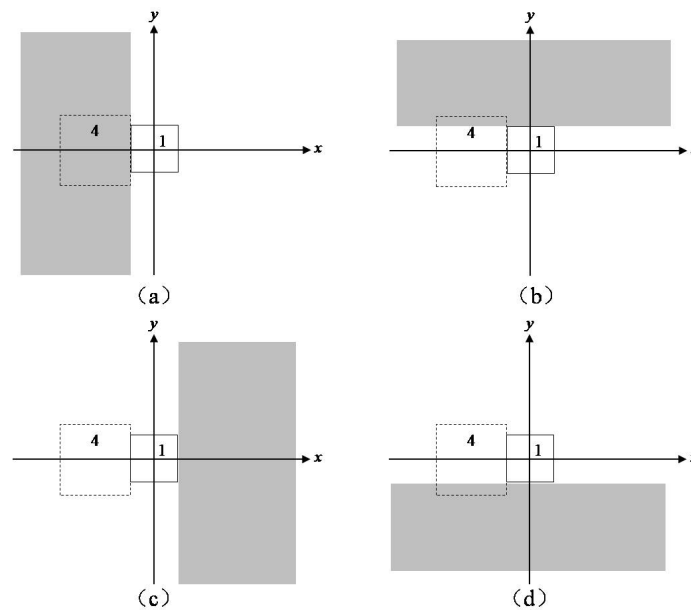


Fig 2 The four zones (shaded in grey) for the possible location of the department in our example

To generalize the expressions of the zones, for $i = 1, \dots, N$, let F_i be the i -th department in the sequence and let $Z(i) = \{z_1^i, \dots, z_j^i, \dots, z_j^i\}$ be the set of zones that F_i can be located, where j is the index of zone. Note that $Z^{(1)}$ consists of only one zone that is the entire rectangle facility. For each zone of F_j , z_j^i is represented by $\{(x_{j1}^i, y_{j1}^i), (x_{j2}^i, y_{j2}^i)\}$, where (x_{j1}^i, y_{j1}^i) and (x_{j2}^i, y_{j2}^i) are the coordinates of the bottom left corner and the top right corner of the zone, respectively. For step of determining the location of the department, the MP method is applied to obtain the optimal position of F_i within each zone in $Z^{(i)}$. In this MP method, an ideal location of the centroid of F_i is first identified in such a way that the sum of rectilinear distances weighted by the flow quantities between F_i and the departments that have previously been located, denoted by the set B , is minimized. The objective function is formulated as follows:

$$\text{Minimize } TTD_i = \sum_{n \in B} f_{mn} (|x_i - x_n| + |y_i - y_n|) \tag{1}$$

To determine the optimal location, (x_i^*, y_i^*) , the objective function Eq. 1 is reformulated as Equations Eq. 2 and Eq. 3. Therefore, the values of x_i^* and y_i^* can be calculated separately. In Equations Eq. 2 and Eq. 3, $TTD_i(x)$ and $TTD_i(y)$ are piecewise linear and convex functions, where all x_n (y_n), for $n \in B$, are arranged in increasing order, i.e. $x_1' \leq x_t' \leq \dots \leq x_{|B|}'$ ($y_1' \leq y_t' \leq \dots \leq y_{|B|}'$). The flow quantities f_{mn} associated with x_n (y_n), for $n \in B$, are also sorted by

$[w_1^x, w_t^x, \dots, w_{|B|}^x]$ ($[w_1^y, w_t^y, \dots, w_{|B|}^y]$). To determine the values of x_i^* and y_i^* , we make use of Property 1.

$$\text{Minimize } TTD_i(x) = \sum_{n \in B} f_{mn} |x_i - x_n| = w_1^x |x_i - x_1'| - w_2^x |x_i - x_2'| + \dots + w_{|B|}^x |x_i - x_{|B|}'| \quad (2)$$

$$\text{Minimize } TTD_i(y) = \sum_{n \in B} f_{mn} |y_i - y_n| = w_1^y |y_i - y_1'| - w_2^y |y_i - y_2'| + \dots + w_{|B|}^y |y_i - y_{|B|}'| \quad (3)$$

Property 1. Suppose that x_i^* is the MP and x_c' satisfies the median condition, i.e. $\sum_{t=1}^{c-1} w_t^x \leq \sum_{t=c}^{|B|} w_t^x / 2$ and $\sum_{t=c+1}^{|B|} w_t^x \leq \sum_{t=1}^{|B|} w_t^x / 2$. Then $x_i^* = x_c'$. Similarly, if y_i^* MP and y_c' , satisfies the MP condition $\sum_{t=1}^{c-1} w_t^y \leq \sum_{t=1}^{|B|} w_t^y / 2$ and $\sum_{t=c+1}^{|B|} w_t^y \leq \sum_{t=1}^{|B|} w_t^y / 2$ then, $y_i^* = y_c'$.

By Property 1, the optimal location of F_i (i.e. the optimal solution for formulation Eq. 1) can be determined by searching the MP such that both of the total weights summing over those before the MP in the sequence and summing over those after the MP in the sequence is no more than the total weight summing over all the departments. In other words, the MP is the first point where the partial sum of weights from the first department in the sequence to itself is no less than half of the total weights of all departments. Let $W_x(t), W_y(t)$ be the partial sums of the weights at point summing from the first department in the sequence in x -direction and y -direction respectively, and W be the total weights summing over all departments. With the sequence [1-4-2-5-3-6] for locating the departments within the facility in the previous example, we illustrate in Fig. 3 for how the aforementioned procedure can determine the MP. In Fig. 3, the locations of four departments have previously been determined. The TTD between F_5 , i.e. Department 3 and the four departments that have been located in x -direction is: $TTD_5(x) = 2|x_5 - (-5)| + 2|x_5 - 0| + 4|x_5 - 0| + 2|x_5 - 7|$. In this example, $W = 11, W_x(1) = 2, W_x(2) = 2 + 2 = 4, W_x(3) = 2 + 2 + 4 = 8 > W/2$. Hence, the MP is $x_3' = 0$ and $x_5^* = x_3' = 0$. Similarly, $TTD_5(y) = 2|y_5 - 0| + 2|y_5 - 0| + 2|y_5 - 0| + 4|y_5 - 4|$. And $W_y(1) = 2, W_y(2) = 2 + 2 = 4, W_y(3) = 2 + 2 + 2 = 6 > W/2$. Hence, the MP in y -direction is $y_3' = 0$ and $y_5^* = y_3' = 0$. Therefore, the optimal location of Department 3 is $(0, 0)$, which is marked by the dashed rectangle in Fig. 3.

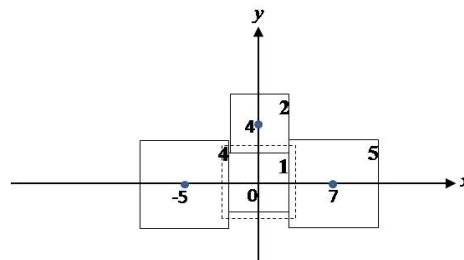


Fig. 3 Optimal location of Department 3 (represented by a dotted square)

Nevertheless, this optimal location determined for Department 3, in fact, is infeasible because it overlaps with the other departments as shown in in Fig. 3. In this case, we have to determine a new location for Department 3 to continue our UA-FLP procedure. To this end, we determine the location in each zone for Department 3 such that the location is closest to the previously determined optimal location in both x -direction and y -direction. The rationale is that such position can minimize TTD for each zone. For example, the best positions for Department 3 in those considered zones are shown in Fig. 4(a)-4(f), which are respectively the closest locations to the optimal location that was previously determined. The department is to be located at the best position that attains the minimum TTD_{ij} among those zones. In this example, Department 3 has the same TTD_{ij} at the positions as shown in Fig. 4(b) and Fig. 4(d). Thus, this tie is broken by randomly picking one of the two positions for locating Department 3. The location of the last department in the sequence of this example is also determined in the same way. Fig. 5 shows the final layout of the facility.

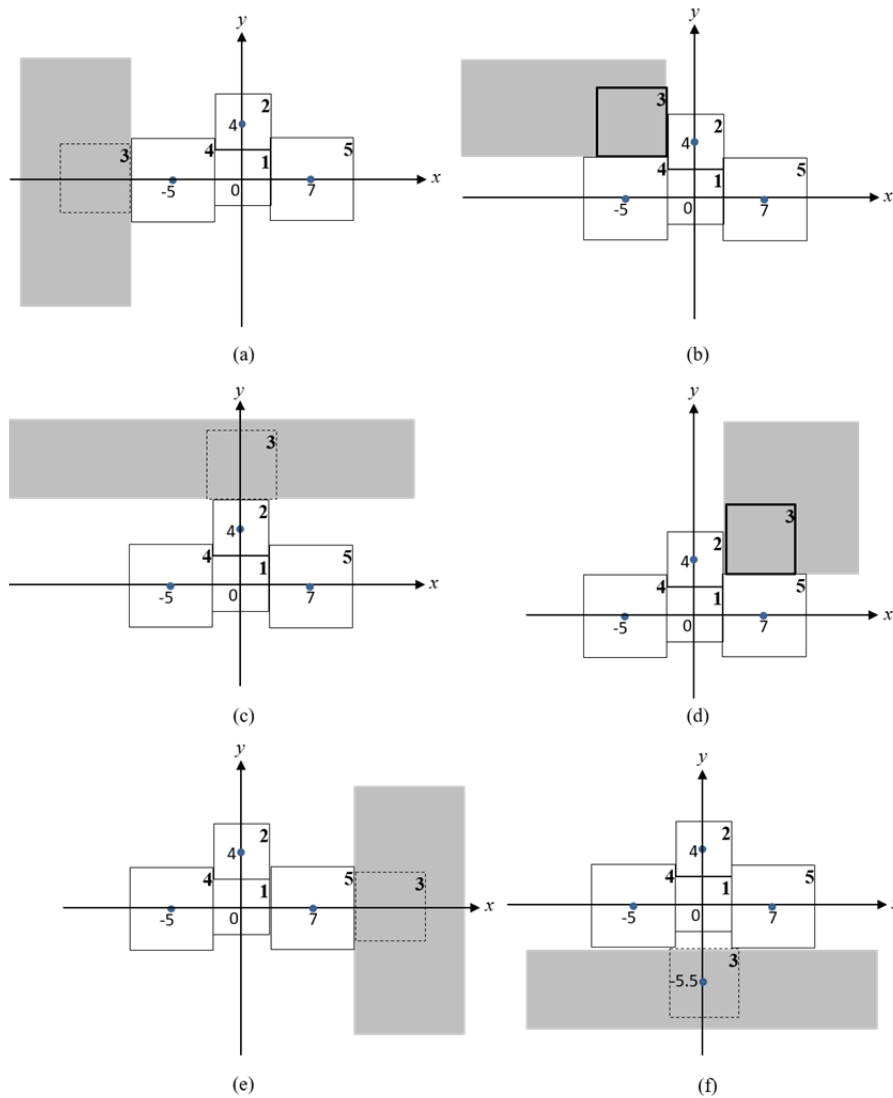


Fig. 4 Closest location in each zone to the optimal location

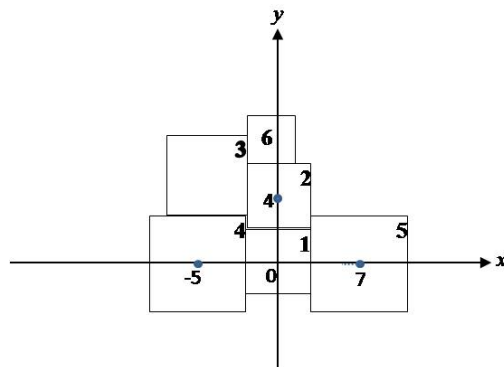


Fig. 5 Layout of the six departments of fixed shapes

To determine if the department can be located at the intended position, we also have to consider the dimension of each zone z_j^i which can be measured by $w_j^i = x_{j2}^i - x_{j1}^i$ and $h_j^i = y_{j2}^i - y_{j1}^i$, where w_j^i and h_j^i are respectively the width and the height of the zone. Let d_{wm} and d_{hm} be the width and the height of the department to be located, respectively. If a zone satisfies the conditions that $w_j^i \geq d_{wm}$ and $h_j^i \geq d_{hm}$, it is feasible to locate Department m in this zone; otherwise, check if the subsequent zone can accommodate Department m . The procedure of the modified zone algorithm is summarized as follows:

- Step 1.* Set $i = 1$. The centroid of F_i is placed at $(0, 0)$ in the coordinate system.
- Step 2.* Set $i = i + 1$. Create the zone set, $Z^{(i)} = \{z_j^i | j = 1, \dots, J\}$, by using the zone updating procedure. Determine the optimal location, (x_i^*, y_i^*) , for F_i . Let TTD_i^* be the minimum TTD_{ij} among the zones contained in the zone set. Set $j = 1, TTD_i^* = +\infty$.
- Step 3.* If $x_{j_1}^i + d_{wm}/2 \leq x_i^* \leq x_{j_2}^i - d_{wm}/2$ and $y_{j_1}^i + d_{hm}/2 \leq y_i^* \leq y_{j_2}^i - d_{hm}/2$ (i.e. F_i with its centroid located at the optimal location can fit entirely within zone z_j^i), go to Step 3.1; otherwise, go to Step 3.2.
- Step 3.1 F_i is optimally located at (x_i^*, y_i^*) . Go to Step 5.
- Step 3.2 If $w_j^i \geq d_{wm}$ and $w_j^i \geq d_{hm}$, locate D_i at the closest possible position in z_j^i to the optimal location. Calculate TTD_{ij} . If $TTD_{ij} \leq TTD_i^*$, then $TTD_i^* = TTD_{ij}$; else, TTD_i^* keeps unchanged.
- Step 3.3 Set $j = j + 1$. If $j \leq J$, go to Step 3; otherwise, go to Step 4.
- Step 4.* F_i is placed in the zone whose TTD_{ij} attains TTD_i^* , go to Step 5.
- Step 5.* If $i \leq N$, go to Step 2; otherwise, all the departments have already been located within the facility. Terminate the procedure.

3.3 Linear programming (LP)

With facility layout determined by the improved zoning algorithm in the first phase, the relative positions of each pair of departments can be obtained. By using this information, an LP model is formulated to optimize the dimensions of departments within a specified facility while satisfying the physical constraints imposed on their dimensions. The additional notations used in this formulation are listed as follows:

W	Width of the facility on the floor plan
H	Height of the facility on the floor plan
N	Total number of departments to be located
m, n	Indices used to represent the departments, $m = 1, \dots, N$ and $n = 1, \dots, N$.
f_{mn}	Material flow quantity from Department m to Department n ($m \neq n$).
a_m	Area requirement of department m
α_m	Maximum aspect ratio of department m
ub_m^x, lb_m^x	Upper and lower bound of the length of Department m in the x-direction
ub_m^y, lb_m^y	Upper and lower bound of the length of Department m in the y-direction
r_{mn}, s_{mn}	Indicators to denote if Department m is on the right/below Department n respectively. More specifically, $r_{mn} = 1$ if Department m is on the left of Department n , and 0 otherwise; $s_{mn} = 1$ if Department m is to below Department n , and 0 otherwise
\bar{x}	The value of the tangential support point for the polyhedral outer approximation to the area constraints, $lb^x m / 2 \leq \bar{x} \leq ub^x m / 2$
Δ	Number of tangential support points, $\Delta \geq 2$
C	penalty for the violation of the floor boundary condition, $C = \sum_m \sum_{n>m} f_{mn}(W + H)$
w_m, h_m	Half of width and height of Department m
$v^x m, v^y m$	Amount of violation of the floor boundary condition for Department m in the x-direction and the y-direction, respectively

Our LP model to determine the dimensions of the departments is derived from the MIP formulated by Sherali et al. [13] and presented below:

Minimize
$$TTD = \sum_m \sum_{n>m} f_{mn}(d_{mn}^x + d_{mn}^y) + C(\sum_m v_m^x + \sum_m v_m^y) \tag{4}$$

subject to

$$d_{mn}^x \geq x_m - x_n \quad \forall m < n \tag{5}$$

$$d_{mn}^x \geq x_n - x_m \quad \forall m < n \tag{6}$$

$$d_{mn}^y \geq y_m - y_n \quad \forall m < n \tag{7}$$

$$d_{mn}^y \geq y_n - y_m \quad \forall m < n \tag{8}$$

$$w_m \leq x_m \leq W - w_m + v_m^x \quad \forall m \tag{9}$$

$$h_m \leq y_m \leq H - h_m + v_m^y \quad \forall m \tag{10}$$

$$lb_m^x \leq 2w_m \leq ub_m^x \quad \forall m \tag{11}$$

$$lb_m^y \leq 2h_m \leq ub_m^y \quad \forall m \tag{12}$$

$$x_m + w_m \leq x_n - w_n \quad \forall m, n, m \neq n: r_{mn} = 1 \tag{13}$$

$$y_m + h_m \leq y_n - h_n \quad \forall m, n, m \neq n: s_{mn} = 1 \tag{14}$$

$$a_m w_m + 4\bar{x}_{mp}^2 h_m \geq 2a_m \bar{x}_{mp} \quad \forall m, p \tag{15}$$

$$\bar{x}_{mp} = lb_m^x / 2 + \frac{p}{\Delta - 1} (ub_m^x / 2 - lb_m^x / 2) \quad \forall m, p = 0, \dots, \Delta - 1 \tag{16}$$

$$x_m, y_m, w_m, h_m, v_m^x, v_m^y \geq 0 \quad \forall m \tag{17}$$

$$d_{mn}^x, d_{mn}^y \geq 0 \quad \forall m < n \tag{18}$$

Objective function Eq. 4 consists of two terms: *TTD* between departments and the penalty for violation of the floor boundary condition. Constraints Eq. 5 to Eq. 8 determine the *TTD* between departments. Constraints Eq. 9 and Eq. 10 measure the violation of the floor boundary condition (in *x*-direction and *y*-direction, respectively), if it is infeasible to locate all the departments within the facility. Constraints Eq. 11 and Eq. 12 impose the bounds on the width and height for each department, where the upper bounds $ub_m^x = \min\{W, \sqrt{a_m a_m}\}$, $ub_m^y = \min\{H, \sqrt{a_m a_m}\}$, and lower bounds $lb_m^x = a_m / ub_m^y$, $lb_m^y = a_m / ub_m^x$. Constraints Eq. 13 and Eq. 14 ensure that the departments do not overlap with each other. Constraint Eq. 15 is the polyhedral outer approximation for the area function, $a_i = 4w_m h_m$, with the number of tangential support points equal to Δ . The value of the tangential support points \bar{x} is given in Eq. (16).

As an example, with the relative positions of the departments obtained by the improved zone algorithm (as shown in Fig. 5), the final facility layout for locating the six departments with the exact dimensions can now be obtained by the LP. Their positions and dimensions are shown in Fig. 6.

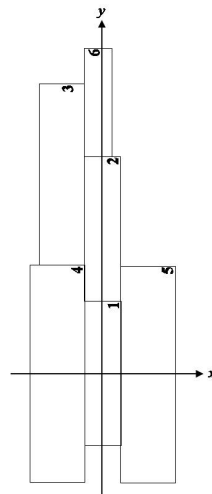


Fig. 6 Layout solution of the six departments with their dimensions determined

3.4 SA algorithm

With the facility layout solution obtained by the zone-LP approach, we implement an SA algorithm to improve the quality of the solution. The SA algorithm that we adopt is the same as the procedure proposed in Xiao et al. [22]. For the detail of the algorithm, we refer the reader to Xiao et al. [22].

4. Computational experiments

In this section, we conduct computational experiments to evaluate the performance of our proposed solution methodology for UA-FLP – an integrated method of zone-LP approach and SA algorithm. We use a set of widely tested instances in the literature to examine the efficiency of the solution methodology. There are five instances of different problem sizes included in the computational experiments: Problems O7 (with 7 departments), O8 (with 8 departments) and O9 (with 9 departments) from Meller et al. [12] and Two largest instances SC30 (with 30 departments) and SC35 (with 35 departments) from Liu and Meller [20].

The combined zone-LP and SA algorithm is run ten times for each computational instance. In the first phase of zone-LP algorithm, the dimensions of departments are fixed with the MAR because all departments tend to have a narrower rectangular shape to get a lower *TTD*. The parameter combination used in SA was $T = 200^\circ$, $R = 0.8$, and $L = 1000$ from Xiao et al. [21]. The results on the computational performance of our proposed approach are shown in Table 2. We present the averages and the standard deviations of the costs to examine the robustness of our proposed method. The computational results suggest that the proposed algorithm appears to be quite robust. For the three small-sized problems (O7, O8, O9), the standard deviation is quite small, ranging from 0 to 0.57 (less than 0.5 % of the average). Although the magnitude of the standard deviation becomes large for the large-sized problems (SC30, SC35), its relative value is still small (less than 3 % of the average). For the computational efficiency, our proposed solution methodology can obtain the final solution within a reasonable time frame (less than 1 minute for the small-sized problems and less than 4 minutes for the large-sized problems). Given that facility layout planning is not a daily practice (is usually determined for several years), this computational time is negligible, and our method is suitable for the application in practice.

Table 2 Objective values and the computing time obtained by the proposed algorithm

Problem	Best	Mean	Worst	Standard deviation	Average time (s)
O7	89.25	89.25	89.25	0	33.13
O8	185.00	185.30	186.00	0.46	36.93
O9	185.00	185.45	186.5	0.57	41.80
SC30	3441.57	3663.21	3792.71	103.50	180.27
SC35	3347.94	3423.70	3555.89	69.06	225.94

Table 3 Objective values, dimensions of the facilities, space utilizations resulting from the best solutions found by GRAPH [21] and our proposed algorithm

Problem	GRAPH[21]			The proposed algorithm			Diff. in TTD (%)
	TTD	Layout dimension ($W \times H$)	Space utilization (%)	TTD	Layout dimension ($W \times H$)	Space utilization (%)	
O7	115.93		96.00	89.25	12×13.5	68.52	23.01
O8	239.00		96.00	185.00	12×16.5	74.24	22.59
O9	227.10		96.00	185.00	15×16.5	63.03	18.54
SC30	3601.20	15×12	90.56	3441.57	12.75×21.59	59.21	4.43
SC35	3351.12	16×15	80.00	3347.94	15.14×24.7	51.34	0.09

We also compare our proposed solution methodology with other existing algorithms in the literature and use them as benchmarks. We first compare the solution qualities obtained by our approach and the GRAPH algorithm [21], which attains the best known solutions for the computational instances. As shown in Table 3, our proposed outperforms GRAPH [21] in terms of TTD for all computational instances, but the space utilizations resulting from our algorithm are less than those from GRAPH. In our UA-FLPs, departments are arranged within an open-field floor

(as shown in Fig. 4 and Fig. 5) and the loss of consideration on space utilization in the objective function of the proposed model mainly causes the poor performance on space utilization. Therefore, a multi-objective optimization considering minimization of TTD and maximization of space utilization may be our future research topic. For reference, the best layouts solutions obtained by our proposed approach are shown in Appendix 1. The proposed algorithm also has an advantage of a shorter computing time due to its capability of searching in the restricted solution spaced. We conduct another study to examine the efficiency of our proposed methodology. In addition to GRAPH [21], we also include SEQUENCE [20] for the comparison of computational efficiencies of the different approaches. Computational results in Table 4 suggest that our algorithm takes a significantly shorter time to solve the UA-FLP. More importantly, the computing time appears to grow almost linearly as the number of departments increases. Compared with the approaches that appear to have an exponential computing time in the number of departments, our approach is apparently more suitable for problems of a larger size. The linear increase of computing time may be attributed to the proposed zone-LP algorithm which can construct the layout solution effectively. In each iteration of SA, the number of zones produced for putting departments by MP method is $O(N)$ according to the zone algorithm. The proposed LP model is just used to determine the dimensions of departments. In general, the computing time is approximately proportional to the number of generated zones in each SA iteration and thus grows almost linearly as the number of departments increases. This further demonstrates the value of our proposed approach in advancing the computational performance for solving UA-FLP.

Table 4 Average computing times of the SEQUENCE [20], GRAPH [21], and our proposed algorithm

Instance	Computing time (s)		
	SEQUENCE [20]	GRAPH [21]	Our proposed algorithm
07	1644.0	228.0	33.13
08	3056.0	390.0	36.93
09	3879.0	222.0	41.80
SC30	7282.8	2442.0	180.27
SC35	9590.4	4728.0	225.94

5. Conclusion and future research

This paper deals with UA-FLP and proposes a novel approach, which we call a combined zone-LP and SA algorithm, for solving large-sized UA-FLP. The zone-LP algorithm is a new layout construction method and consists of two phases. In the first phase, the shapes of departments are fixed to a rectangle with an allowable aspect ratio. Those departments of fixed shapes are then placed sequentially by using an improved zone algorithm, where an MP method is proposed to locating departments. By using relative positions of the departments obtained in this first phase, an LP is formulated to determine the exact locations and dimensions of departments. We also implement an SA algorithm to search the sequences of locating the departments within the facility and to prevent the search procedure from getting trapped at a local optimum. Computational experiments indicate that our proposed combined zone-LP and SA has a reasonably good performance, compared with existing algorithms in the literature on widely tested computational instances.

We also note that there can be future directions extended from this research. In reality, departments of irregular shapes are commonplace; a future study may consider the facility layout problem with the consideration of departments with irregular shapes. Moreover, the results of computing experiments suggest that our proposed solution methodology may generate solutions leading to a low space utilization. For this case, we may adopt a multi-objective optimization approach whose goals are to minimize the material handling cost and to maximize space utilization. The trade-off between these two performance measures would also be an interesting research topic for investigation in the future.

Acknowledgement

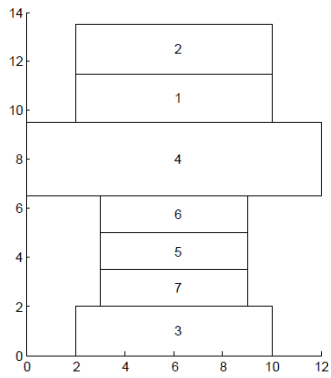
The research has been supported by the National Natural Science Foundation of China (Grant No. 71501090, 71501093), the Natural Science Foundation of Jiangsu Higher Education Institutions of China (Grant No. 14KJD410001), the Natural Science Foundation of Jiangsu Province (Grant No. BK20150566), and the General Research Fund of Research Grants Council of Hong Kong (Grant No. 414313).

References

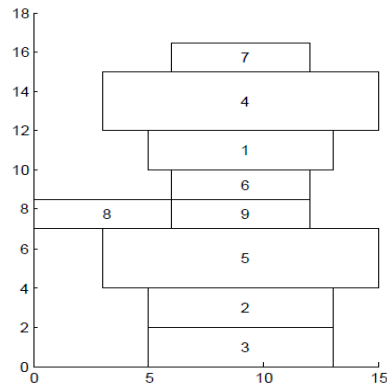
- [1] Tompkins, J.A., White, J.A., Bozer, Y.A., Tanchoco, J.M.A. (2010). *Facilities Planning*, 4th edition, John Wiley & Sons, New York, USA.
- [2] Kusiak, A., Heragu, S.S. (1987). The facility layout problem, *European Journal of Operational Research*, Vol. 29, No. 3, 229-251, doi: [10.1016/0377-2217\(87\)90238-4](https://doi.org/10.1016/0377-2217(87)90238-4).
- [3] Meller, R.D., Gau, K.Y. (1996). The facility layout problem: Recent and emerging trends and perspectives, *Journal of Manufacturing Systems*, Vol. 15, No. 5, 351-366, doi: [10.1016/0278-6125\(96\)84198-7](https://doi.org/10.1016/0278-6125(96)84198-7).
- [4] Singh, S.P., Sharma, R.R.K. (2006). A review of different approaches to the facility layout problems, *The International Journal of Advanced Manufacturing Technology*, Vol.30, No.5-6,425-433,doi:[10.1007/s00170-005-0087-9](https://doi.org/10.1007/s00170-005-0087-9).
- [5] Drira, A., Pierreval, H., Hajri-Gabouj, S. (2007). Facility layout problems: A survey, *Annual Review in Control*, Vol. 31, No. 2, 255-267, doi: [10.1016/j.arcontrol.2007.04.001](https://doi.org/10.1016/j.arcontrol.2007.04.001).
- [6] Kulturel-Konak, S., Konak, A. (2011). Unequal area flexible bay facility layout using ant colony optimisation, *International Journal of Production Research*, Vol. 49, No.7, 1877-1902, doi: [10.1080/00207541003614371](https://doi.org/10.1080/00207541003614371).
- [7] Jolai, F., Tavakkoli-Moghaddam, R., Taghipour, M. (2012). A multi-objective particle swarm optimisation algorithm for unequal sized dynamic facility layout problem with pickup/drop-off locations, *International Journal of Production Research*, Vol. 50, No. 15, 4279-4293, doi: [10.1080/00207543.2011.613863](https://doi.org/10.1080/00207543.2011.613863).
- [8] Navidi, H., Bashiri, M., Bidgoli, M.M. (2012). A heuristic approach on the facility layout problem based on game theory, *International Journal of Production Research*, Vol. 50, No. 6, 1512-1527, doi: [10.1080/00207543.2010.550638](https://doi.org/10.1080/00207543.2010.550638).
- [9] Ficko, M., Palcic, I. (2013). Designing a layout using the modified triangle method, and genetic algorithms, *International Journal of Simulation Modelling*, Vol. 12, No. 4, 237-251, doi: [10.2507/IJSIMM12\(4\)3.244](https://doi.org/10.2507/IJSIMM12(4)3.244).
- [10] Ficko, M., Brezovnik, S., Klančnik, S., Balic, J., Brezocnik, M., Pahole, I. (2010). Intelligent design of an unconstrained layout for a flexible manufacturing system, *Neurocomputing*, Vol. 73, No. 4-6, 639-647, doi: [10.1016/j.neucom.2009.06.019](https://doi.org/10.1016/j.neucom.2009.06.019).
- [11] Montreuil, B. (1991). A modelling framework for integrating layout design and flow network design, *Progress in Materials Handling Research*, Vol. 2, 95-115, doi: [10.1007/978-3-642-84356-3_8](https://doi.org/10.1007/978-3-642-84356-3_8).
- [12] Meller, R.D., Narayanan, V., Vance, P.H. (1998). Optimal facility layout design, *Operations Research Letters*, Vol. 23, No. 3-5, 117-127, doi: [10.1016/S0167-6377\(98\)00024-8](https://doi.org/10.1016/S0167-6377(98)00024-8).
- [13] Sherali, H.D., Fraticelli, B.M.P., Meller, R.D. (2003). Enhanced model formulations for optimal facility layout, *Operations Research*, Vol. 51, No. 4, 629-644, doi: [10.1287/opre.51.4.629.16096](https://doi.org/10.1287/opre.51.4.629.16096).
- [14] Meller, R.D., Chen, W., Sherali, H.D. (2007). Applying the sequence-pair representation to optimal facility layout design, *Operations Research Letters*, Vol. 35, No. 5, 651-659, doi: [10.1016/j.orl.2006.10.007](https://doi.org/10.1016/j.orl.2006.10.007).
- [15] Kim, J.G., Kim, Y.D. (2000). Layout planning for facilities with fixed shapes and input and output points, *International Journal of Production Research*, Vol. 38, No. 18, 4635-4653, doi: [10.1080/00207540050205550](https://doi.org/10.1080/00207540050205550).
- [16] Das, S.K. (1993). A facility layout method for flexible manufacturing systems, *International Journal of Production Research*, Vol. 31, No. 2, 279-297, doi: [10.1080/00207549308956725](https://doi.org/10.1080/00207549308956725).
- [17] Rajasekharan, M., Peters, B.A., Yang, T. (1998). A genetic algorithm for facility layout design in flexible manufacturing systems, *International Journal of Production Research*, Vol. 36, No. 1, 95-110, doi: [10.1080/002075498193958](https://doi.org/10.1080/002075498193958).
- [18] Scholz, D., Petrick, A., Domschke, W. (2009). STaTS: A Slicing Tree and Tabu Search based heuristic for unequal area facility layout problem, *European Journal of Operational Research*, Vol. 197, No. 1, 166-178, doi: [10.1016/j.ejor.2008.06.028](https://doi.org/10.1016/j.ejor.2008.06.028).
- [19] Komarudin, Wong, K.Y. (2010). Applying ant system for solving unequal area facility layout problems, *European Journal of Operational Research*, Vol. 202, No. 3, 730-746, doi: [10.1016/j.ejor.2009.06.016](https://doi.org/10.1016/j.ejor.2009.06.016).
- [20] Liu, Q., Meller, R.D. (2007). A sequence-pair representation and MIP model based heuristic for the facility layout problem with rectangular departments, *IIE Transactions*, Vol. 39, No. 4, 337-394, doi: [10.1080/07408170600844108](https://doi.org/10.1080/07408170600844108).
- [21] Bozer, Y.A., Wang, C.T. (2012). A graph-pair representation and MIP-model-based heuristic for the unequal-area facility layout problem, *European Journal of Operational Research*, Vol. 218, No. 2, 382-391, doi: [10.1016/j.ejor.2011.10.052](https://doi.org/10.1016/j.ejor.2011.10.052).
- [22] Xiao, Y., Seo, Y., Seo, M. (2013). A two-step heuristic algorithm for layout design of unequal-sized facilities with input/output points, *International Journal of Production Research*, Vol. 51, No. 14, 4200-4222, doi: [10.1080/00207543.2012.752589](https://doi.org/10.1080/00207543.2012.752589).

Appendix 1

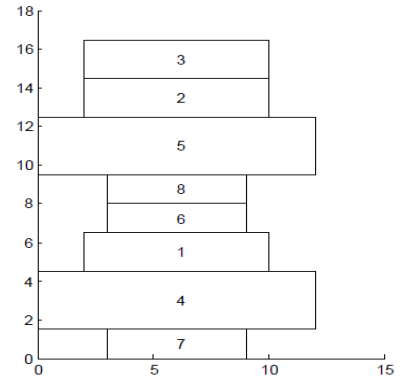
The best layouts obtained by our proposed algorithm for the experimental instances from Meller *et al.* [10] and Liu and Meller [19].



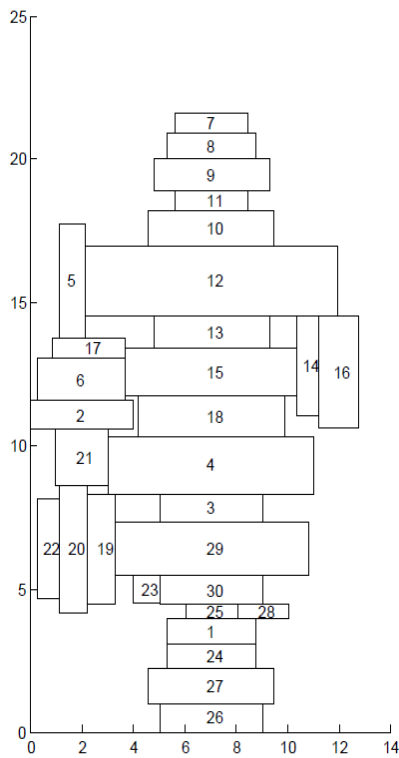
Layout with seven departments



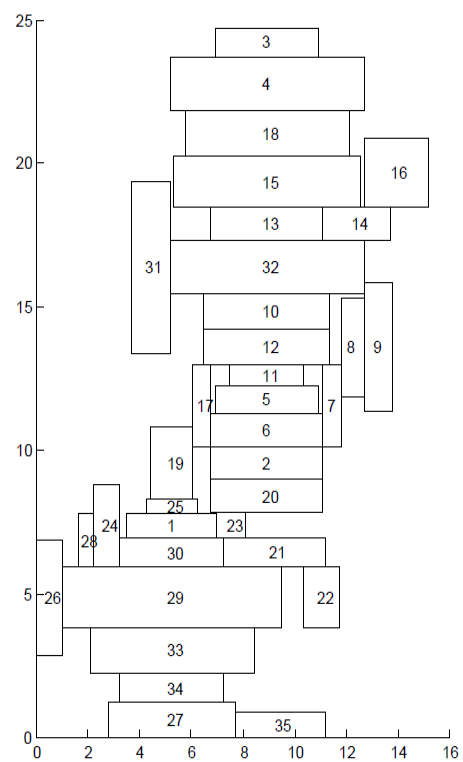
Layout with eight departments



Layout with nine departments



Layout with 30 departments



Layout with 35 departments

A new multi-objective Jaya algorithm for optimization of modern machining processes

Rao, R.V.^{a,*}, Rai, D.P.^a, Ramkumar, J.^b, Balic, J.^c

^aDepartment of Mechanical Engineering, Sardar Vallabhbhai National Institute of Technology, Surat, India

^bDepartment of Mechanical Engineering, Indian Institute of Technology, Kanpur, India

^cProduction Engineering Institute, Faculty of Mechanical Engineering, University of Maribor, Slovenia

ABSTRACT

In this work, the multi-objective optimization aspects of plasma arc machining (PAM), electro-discharge machining (EDM), and micro electro-discharge machining (μ -EDM) processes are considered. Experiments are performed and actual experimental data is used to develop regression models for the considered machining processes. A posteriori version of Jaya algorithm (MO-Jaya algorithm) is proposed to solve the multi-objective optimization models in a single simulation run. The PAM, EDM and μ -EDM processes are optimized using MO-Jaya algorithm and a set of Pareto-efficient solutions is obtained for each of the considered machining processes and the same is reported in this work. This Pareto optimal set of solutions will provide flexibility to the process planner to choose the best setting of parameters depending on the application. The aim of this work is to demonstrate the performance of MO-Jaya algorithm and to show its effectiveness in solving the multi-objective optimization problems of machining processes.

© 2016 PEI, University of Maribor. All rights reserved.

ARTICLE INFO

Keywords:

Plasma arc machining
Electro-discharge machining
Micro-electro-discharge machining
Multi-objective optimization
Jaya algorithm
Posteriori approach
Sustainability

*Corresponding author:

ravipudirao@gmail.com
(Rao, R.V.)

Article history:

Received 10 November 2016

Revised 25 November 2016

Accepted 1 December 2016

1. Introduction

In order to survive in a fierce market scenario manufacturing industries are required to maintain high quality standards, produce at lowest cost, increase production rate, conserve resources and at the same time minimize the environmental impact of the processes they use. Machine tools are major pillars of any manufacturing system and are used on a large scale for processing of materials. However, machining processes are characterized by high energy consumption, high tool wear rate, poor surface quality and generation of large scale waste products in the form of used lubricants, coolants, dielectric or electrolytic fluids, chips and debris of tool or workpiece materials, etc. Thus, for success of any manufacturing system in terms of economy and to reduce its impact on the ecology it is crucial to improve the efficiency of these machine tools. Furthermore, in order to improve the sustainability of the process it is imminent that the machines are operated as efficiently as possible.

The performance of any machining process extensively depends upon the choice of process parameters. Therefore, for best performance from any machining process it is important to set the process parameters optimally. In order to determine the optimal setting of process parameters it is important to map the relationship between input and output parameters. De Wolf et al. [1] investigated the effect of process parameters on material removal rate, electrode wear rate and surface finish in EDM process. Aich and Banerjee [2] applied teaching learning based opti-

mization procedure for the development of support vector machine learned EDM process and its pseudo Pareto optimization. Zhang et al. [3] enumerated and characterized 128 scenarios in sustainable machining operation involving 7 objectives including energy, cost, time, power, cutting force, tool life and surface finish. Gupta et al. [4] presented the results of optimization of machining parameters and cutting fluids during nano-fluid based minimum quantity lubrication turning of titanium alloy by using particle swarm optimization and bacteria foraging optimization techniques.

Researchers have also applied a number of numerical and metaheuristic optimization algorithms for optimal setting of machining process parameters [5-13]. The metaheuristic optimization algorithms are mostly inspired by the theory of evolution or of behavior of a swarm. All evolutionary algorithms or swarm based algorithms require tuning of parameters like population size, number of iterations, elite size, etc. In addition, different algorithms require their own algorithm-specific parameters. The improper tuning of algorithm-specific parameters adversely affects the performance of these algorithms. In addition, the tuning of population size and number of iterations is also required.

Rao [14] proposed the Jaya algorithm which algorithm-specific parameter-less algorithm. The performance of Jaya algorithm has already been tested on a number of unconstrained and constrained benchmark functions and engineering optimization problems. For more details about the algorithm, the readers may refer to <https://sites.google.com/site/jayaalgorithm>. The Jaya algorithm is simple in implementation as a solution is updated only in a single phase using a single equation. However, the multi-objective version of Jaya algorithm is not yet developed.

In the case of machining processes due to co-existence of multiple performance criteria there is a need to formulate and solve multi-objective optimization problems (MOOP). A priori approach such as normalized weighted sum approach, epsilon constraint method, etc. require assigning the weights of importance to the objectives before simulation run of the algorithm. Further, it is required to run the algorithm independently for each set of weights to obtain distinct solutions. A posteriori approach does not require assigning weights of importance to the objectives in advance. This approach provides a set of Pareto-efficient solutions for a MOOP in a single run of simulation. The process planner can then select one out of the set of Pareto-efficient solutions based on the order of importance of objectives.

Thus, in this work a parameter-less posteriori multi-objective version of Jaya algorithm is named as multi-objective Jaya (MO-Jaya) algorithm is proposed and the MOOPs of three modern machining processes namely plasma arc machining (PAM), electro-discharge machining (EDM), and micro electro-discharge machining (μ -EDM) are solved using MO-Jaya algorithm. The Jaya and MO-Jaya algorithms are described in following sections.

2. The Jaya algorithm

In the Jaya algorithm P initial solutions are randomly generated obeying the upper and lower bounds of the process variables. Thereafter, each variable of every solution is stochastically updated using Eq. 1. The best solution is the one with maximum fitness (i.e. best value of objective function) and the worst solution is the one with lowest fitness (i.e. worst value of objective function).

$$O_{p+1,q,r} = O_{p,q,r} + \alpha_{p,q,1} (O_{p,q,best} - \text{abs}(O_{p,q,r})) - \alpha_{p,q,2} (O_{p,q,worst} - \text{abs}(O_{p,q,r})) \quad (1)$$

Here *best* and *worst* represent the index of the best and worst solutions among the population. p , q , r are the index of iteration, variable, and candidate solution. $O_{p,q,r}$ means the q -th variable of r -th candidate solution in p -th iteration. $\alpha_{p,q,1}$ and $\alpha_{p,q,2}$ are numbers generated randomly in the range of [0, 1]. The random numbers $\alpha_{p,q,1}$ and $\alpha_{p,q,2}$ act as scaling factors and ensure exploration. The absolute value of the variable (instead of a signed value) also ensures exploration. Fig. 1 gives the flowchart for Jaya algorithm.

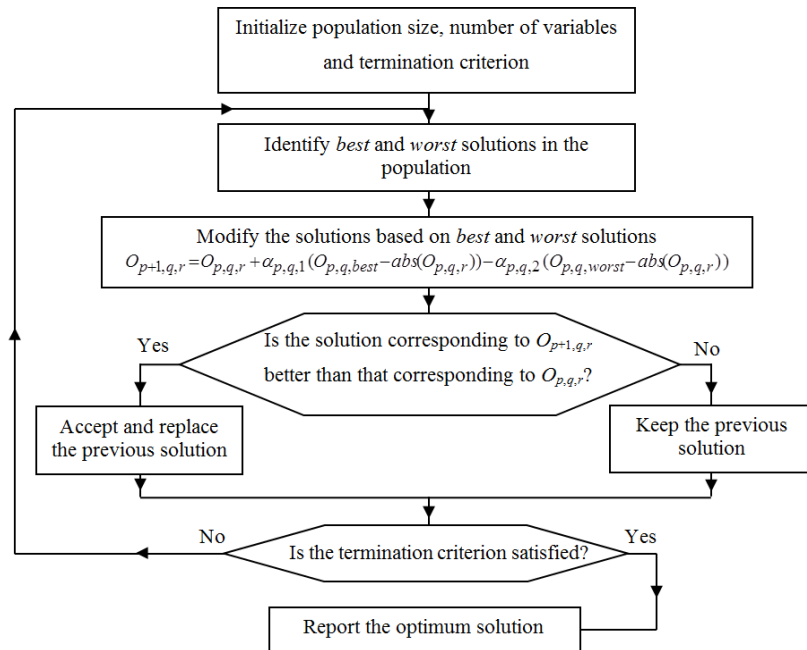


Fig. 1 Flowchart of Jaya algorithm

3. The multi-objective Jaya algorithm

The MO-Jaya algorithm is a posteriori version of Jaya algorithm for solving MOOPs. The solutions in the MO-Jaya algorithm are updated in the similar manner as in the Jaya algorithm based on Eq. 1. In the interest of handling problems in which more than one objective co-exist the MO-Jaya algorithm is embedded with dominance ranking approach and crowding distance evaluation approach.

The MO-Jaya algorithm is a posteriori version of Jaya algorithm for solving MOOPs. The solutions in the MO-Jaya algorithm are updated in the similar manner as in the Jaya algorithm based on Eq. 1. In the interest of handling problems in which more than one objective co-exist the MO-Jaya algorithm is embedded with dominance ranking approach and crowding distance evaluation approach [12].

In the MO-Jaya algorithm, the superiority among the solutions is decided according to the non-dominance rank and value of the density estimation parameter i.e. crowding distance (ξ). The solution with highest rank (rank = 1) and largest value of ξ is chosen as the *best* solution. On the other hand the solution with the lowest rank and lowest value of ξ is selected as the *worst* solution. Such a selection scheme is adopted so that solution in less populous region of the objective space may guide the search process. Once the *best* and *worst* solutions are selected, the solutions are updated based on the Eq. 1.

After all the solutions are updated, the updated solutions are combined with the initial population to so that a set of $2P$ solutions (where P is the size of initial population) is formed. These solutions are again ranked and the ξ value for every solution is computed. Based on the new ranking and ξ value P good solutions are chosen.

The flowchart of MO-Jaya algorithm is given in Fig. 2. For every candidate solution the MO-Jaya algorithm evaluates the objective function only once in each iteration. Therefore, the total no. of function evaluations required by MO-Jaya algorithm = population size \times no. of iterations. However, when the algorithm is run more than once, then the number of function evaluations is to be calculated as: no. of function evaluations = no. of runs \times population size \times number of iterations. The methodology used for ranking of solutions, computing the crowding distance and crowding comparison operator are described in the following sub-sections.

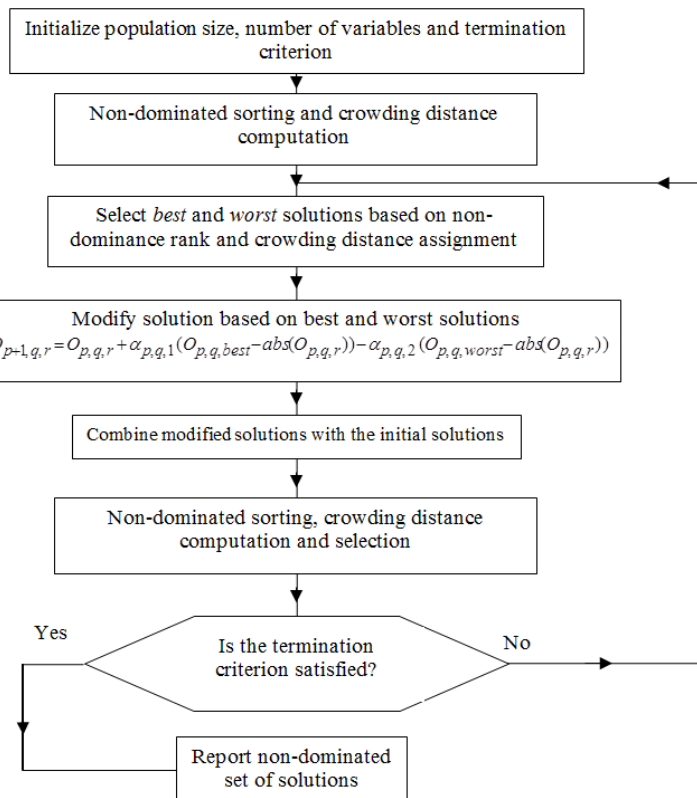


Fig. 2 Flowchart of MO-Jaya algorithm

3.1 Ranking methodology

The approach used for ranking of solutions is based on the non-dominance relation between solutions and is described as follows. In an M objective optimization problem, P is the set of solutions to be sorted and $n = |P|$.

Domination: A solution x_1 is said to dominate another solution x_2 if and only if $f_i(x_1) \leq f_i(x_2)$ for all $1 \leq i \leq M$ and $f_i(x_1) < f_i(x_2)$ for at least one i , where $i \in \{1, \dots, M\}$ (when all objectives are to be minimized).

Non-domination: A solution x^* in P is non-dominated if there does not exist any solution x_j in P which dominates x^* .

Similarly, every solution in P competes with every other solution and the non-dominated solutions are removed from P and assigned rank one. The remaining solutions in P are again sorted in the same way and the non-dominated solutions are removed and assigned rank two. Unless all the solutions in P receive a rank this procedure is continued. A group of solutions with same rank is known as front (F).

3.2 Computing the crowding distance

The crowding distance (ξ_j) is an estimate of the density of the solutions in the vicinity of a particular solution j . For a particular front F , let $l = |F|$ then for each member in F , ξ is calculated as follows.

Step 1: Initialize $\xi_j = 0$

Step 2: Sort all solutions in F the set in the worst order of objective function value f_m .

Step 3: In the sorted list of m^{th} objective assign infinite crowding distance to solutions at the extremes of the sorted list (i.e. $\xi_1 = \xi_l = \infty$), for $j = 2$ to $(l - 1)$, calculate ξ_j as follows:

$$\xi_j = \xi_j \frac{f_m^{j+1} - f_m^{j-1}}{f_m^{\max} - f_m^{\min}} \quad (2)$$

Where j represents a solution in the sorted list, f_m is the objective function value of m -th objective of j -th solution, and are the highest and the lowest values of the m -th objective function in the current population. Likewise, ξ is computed for all the solutions in all F_s .

In the case of MOOPs there exist more than one optimal solution. Therefore, the aim is to find a set of Pareto-efficient solutions. In MO-Jaya algorithm in order to avoid clustering of solutions about a single good (higher rank) solution, the good solutions in the isolated region of the search space are identified based on the ξ value, and a solution with a higher rank and higher ξ value is considered as the best solution in the next generation. Thus, the other solutions in the population will be directed towards the good solution which lies in the less populous (isolated) region of the search space in the next generation. This will prevent the algorithm from converging to single optimum solution and ensure diversity among the solutions. For this purpose a solution from the more isolated region of search space is given more preference than the solution in the crowded region of the search space. In the MO-Jaya algorithm, among the two competing solutions i and j , primarily, the solution with a higher rank is preferred. If the two solutions have equal rank then the solution with a higher ξ value is preferred.

The next section describes the experiments performed on the PAM, EDM and μ -EDM processes. The experiments are performed at the Manufacturing Science Laboratory of IIT Kanpur, India by the team of Professor J. Ramkumar (co-author of this paper) and validation tests are also performed for the considered machining processes.

4. Case studies

The MOOPs of PAM, EDM and μ -EDM processes are described in the following sub-sections and the same are solved using MO-Jaya algorithm. In order to get a set of 50 Pareto-efficient solutions a population size of 50 is chosen for MO-Jaya algorithm. In order to provide enough chance for the search process to evolve and converge at the Pareto-efficient set of solutions, allowable iterations are set to 100. All the simulations are performed on a computer with 2.93 GHz processor and 4 GB RAM. The code for MO-Jaya algorithm is developed in MATLAB R2009a.

4.1 Optimization of plasma arc machining process

This work aims to improve the performance of PAM process by means of process parameter optimization. The regression models for material removal rate ' MRR ' (g/s) and dross formation rate ' DFR ' (g/s) are developed using the data collected by means of actual experimentation, and the same are used as fitness functions for MO-Jaya algorithm in order to obtain multiple trade-off solutions.

The experimental setup consisted of mainly four components i.e. power supply unit, steel trailer, plasma torch, a work-table and a vibration setup. The power supply unit is used to control the current and pressure of gas. The steel trailer is used to move the plasma torch on 2D surface. The plasma torch is used to convert the gas into plasma and the worktable is used to hold the workpiece a vibration setup is also mounted on the worktable. The vibration setup consists of two RM slider assembly, a moving plate and a fixed plate, an induction motor, a variable frequency drive to control the speed of the motor and a cam and spring assembly.

The experiments are performed at Manufacturing Science Laboratory of IIT Kanpur, India and AISI 4340 steel (0.16-0.18 % of C) is used as work material. The experiments are planned according to the central composite design (CCD) and 4 process parameters such as thickness of workpiece ' T ' (mm), current ' I ' (Amp), arc gap voltage ' V_g ' (V) and speed ' S ' (mm/min) are considered each at 5 levels. Table 1 gives the plan of experiments based on CCD.

Table 1 Design of experiments and values of *MRR* and *DFR* measured after experimentation

S. No.	<i>T</i> (mm)	<i>I</i> (A)	<i>V_g</i> (V)	<i>S</i> (mm/min)	<i>MRR</i> (g/s)	<i>DFR</i> (g/s)
1	2	40	135	500	0.1514	0.1164
2	1.5	35	145	600	0.1269	0.1623
3	1.5	45	145	600	0.3088	0.0058
4	2	30	135	700	0.2476	0.02
5	2	40	155	700	0.3529	0.0217
6	1	40	135	700	0.1495	0.0428
7	1.5	25	145	600	0.1367	0.0894
8	1.5	35	145	600	0.2537	0.0204
9	2	40	135	700	0.3206	0.0065
10	2.5	35	145	600	0.2939	0.0643
11	1	40	155	500	0.0696	0.1120
12	1	40	155	700	0.1958	0.0427
13	1	30	155	700	0.1571	0.0495
14	1.5	35	145	400	0.1230	0.0799
15	2	40	155	500	0.2530	0.0484
16	2	30	135	500	0.1791	0.0330
17	1	40	135	500	0.0447	0.0804
18	0.5	35	145	600	0.0023	0.0858
19	1.5	35	145	600	0.15	0.1260
20	2	30	155	500	0.1516	0.1095
21	1.5	35	145	800	0.3106	0.0235
22	1.5	35	125	600	0.1389	0.0899
23	2	30	155	700	0.1351	0.1921
24	1.5	35	145	600	0.1693	0.1144
25	1	30	135	700	0.1330	0.0218
26	1.5	3555	145	600	0.1440	0.1274
27	1.5	35	165	600	0.1308	0.1885
28	1	30	135	500	0.0580	0.0679
29	1.5	35	145	600	0.1711	0.1084
30	1	30	155	500	0.0236	0.1363

Thirty experimental runs are performed and *MRR* and *DFR* are measured and recorded. The weight of each test specimen is measured before and after performing an experimental run, with dross and without dross and the *MRR* and *DFR* are determined according to Eq. 3 to Eq. 5.

$$MRR = (w_1 - w_2)/t \quad (3)$$

$$DFR = (w_2 - w_3)/t \quad (4)$$

$$t = L \cdot 60/S \quad (5)$$

Where w_1 is the weight of the workpiece in grams before cutting; w_2 is the weight of the workpiece in grams after cutting with dross; w_3 is the weight of the workpiece after cutting in grams without dross; t is the cutting time in s and L is the length of cut on each workpiece (125 mm) and S is the cutting speed (mm/min). Thereafter, regression models for *MRR* and *DFR* are developed using a logarithmic scale and are expressed by Eq. 6 and Eq. 7.

$$\begin{aligned}
MRR = \exp \{ & 202.0963939 + 26.97654873 (\log T) - 115.7823 (\log I) \\
& + 36.5388 (\log V_g) - 32.2698 (\log S) - 2.3015 (\log T)^2 + 3.07499 (\log I)^2 \\
& - 10.03049 (\log V_g)^2 + 2.5766 (\log S)^2 + 0.70759 (\log T \cdot \log I) \\
& - 0.25221 (\log T \cdot \log V_g) - 3.92965 (\log T \cdot \log S) + 17.92577 (\log I \cdot \log V_g) \\
& + 0.91766 (\log I \cdot \log S) - 0.07549 (\log V_g \cdot \log S) \} \quad (6)
\end{aligned}$$

($R^2 = 0.95$)

$$\begin{aligned}
DFR = \exp \{ & -310.030243 - 7.0437 (\log T) + 311.642 (\log I) - 169.3030 (\log V_g) \\
& + 56.3056 (\log S)^2 - 0.5839 (\log T)^2 - 16.1736 (\log I)^2 + 17.4766 (\log V_g)^2 \\
& - 8.15487 (\log S)^2 - 4.90491 (\log T \cdot \log I) + 4.68153 (\log T \cdot \log V_g) \\
& + 0.17082 (\log T \cdot \log S) - 28.2996 (\log I \cdot \log V_g) - 8.91918 (\log I \cdot \log S) \\
& + 15.42233 (\log V_g \cdot \log S) \} \quad (7)
\end{aligned}$$

($R^2 = 0.7$)

Now MO-Jaya algorithm is applied to maximize the *MRR* and minimize the *DFR*, simultaneously. The regression models for *MRR* and *DFR* expressed by Eq. 6 and Eq. 7 are used as fitness function for MO-Jaya algorithm. The process parameters limits are expressed by Eqs. 8 to 11.

$$0.5 \leq T \leq 2.5 \tag{8}$$

$$25 \leq I \leq 45 \tag{9}$$

$$125 \leq V_g \leq 165 \tag{10}$$

$$400 \leq S \leq 800 \tag{11}$$

The set of Pareto-efficient solutions provided by MO-Jaya algorithm is reported Table 2 and the Pareto-front is shown in Fig. 3. The MO-Jaya algorithm required 8 iterations to obtain 50 Pareto-efficient solutions. The CPU time required by MO-Jaya algorithm to perform 100 iterations is 7.2 s.

The results of MO-Jaya algorithm have revealed that, the optimal value for current and speed are 45 (A) and 800 (mm/min) to achieve a trade-off between *MRR* and *DFR*. The *MRR* increases continuously from a minimum value of 0.2342 (g/s) to 1.0769 (g/s) as the arc gap voltage increases from 128.2032 (V) to 165 (V). However, the increase in *MRR* is achieved on the expense of increase in *DFR*. Therefore, the best compromised values for *DFR* lie in the range of 0.0004 (g/s) to 0.0026 (g/s). The *DFR* shows an inverse trend with respect to thickness of workpiece. However, as the arc gap voltage increases the *DFR* also increases (refer to Table 2).

Table 2 Pareto optimal solution set provided by MO-Jaya algorithm in a single simulation run for PAM process

S. No.	x_1 (mm)	x_2 (A)	x_3 (V)	x_4 (mm/min)	<i>MRR</i> (g/s)	<i>DFR</i> (g/s)
1	2.5	45	128.2032	800	0.2342	0.0004
2	2.5	45	130.0663	800	0.2573	0.0004
3	2.5	45	134.3141	800	0.3127	0.0004
4	2.5	45	137.139	800	0.3508	0.0005
5	2.5	45	140.1553	800	0.392	0.0005
6	2.5	45	141.3426	800	0.4082	0.0005
7	2.5	45	142.5303	800	0.4243	0.0005
8	2.4048	45	142.5775	800	0.4589	0.0006
9	2.4115	45	144.2314	800	0.4804	0.0006
10	2.3928	45	144.823	800	0.4961	0.0006
11	2.3038	45	143.0715	800	0.5033	0.0006
12	2.4004	45	147.4697	800	0.5308	0.0007
13	2.3995	45	148.7112	800	0.5483	0.0007
14	2.3583	45	148.559	800	0.564	0.0007
15	2.2949	45	148.3905	800	0.5889	0.0008
16	2.3668	45	150.6993	800	0.5898	0.0008
17	2.3144	45	151.253	800	0.6215	0.0008
18	2.268	45	150.9664	800	0.6388	0.0008
19	2.0579	45	146.8665	800	0.6613	0.0009
20	2.1508	45	150.1631	800	0.6794	0.0009
21	2.1876	45	152.6231	800	0.7005	0.001
22	2.1182	45	151.5029	800	0.7152	0.001
23	2.0995	45	152.0345	800	0.7319	0.001
24	2.0861	45	153.623	800	0.7628	0.0011
25	2.0661	45	153.5103	800	0.7701	0.0011
26	2.0207	45	153.3698	800	0.788	0.0011
27	1.985	45	153.4289	800	0.804	0.0012
28	1.9782	45	154.6089	800	0.8259	0.0012
29	1.8797	45	153.3452	800	0.8429	0.0013
30	1.9448	45	155.8998	800	0.8601	0.0013
31	2.0101	45	158.4338	800	0.8681	0.0014
32	1.8571	45	155.9489	800	0.8943	0.0014
33	1.8422	45	156.0147	800	0.9005	0.0015
34	1.7788	45	155.7694	800	0.9156	0.0015
35	1.8493	45	157.9314	800	0.928	0.0016
36	1.8344	45	158.1038	800	0.9358	0.0016
37	1.901	45	160.6495	800	0.9464	0.0017
38	1.8744	45	160.3258	800	0.9528	0.0017
39	1.8186	45	159.9524	800	0.9681	0.0017
40	1.8681	45	161.9012	800	0.9757	0.0018
41	1.8435	45	162.0781	800	0.9874	0.0018
42	1.6871	45	160.0925	800	1.004	0.0019
43	1.6935	45	160.9864	800	1.0155	0.002
44	1.7365	45	162.4991	800	1.0263	0.002
45	1.7111	45	163.0979	800	1.0397	0.0021
46	1.7012	45	163.4105	800	1.0457	0.0022
47	1.7513	45	165	800	1.0518	0.0022
48	1.7091	45	165	800	1.0624	0.0023
49	1.6118	45	165	800	1.076	0.0025
50	1.5829	45	165	800	1.0769	0.0026

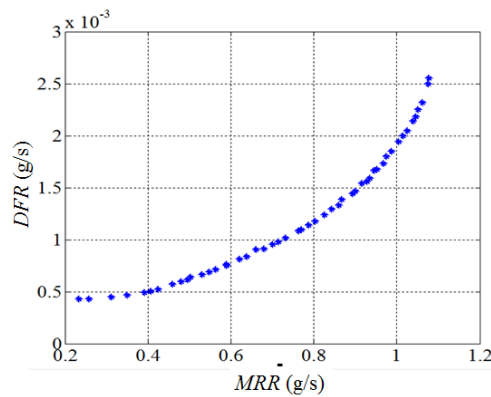


Fig. 3 Pareto-front obtained by MO-Jaya algorithm for PAM process in a single simulation run

4.2 Optimization of electro-discharge machining process

This work aims to maximize the MRR (mg/min), minimize tool wear rate ' TWR ' (mg/min), minimize taper angle θ (degree) and minimize delamination factor ' DF ', simultaneously, by the means of process parameter optimization. For this purpose, experiments are performed and the data collected is used to develop regression models for MRR , TWR , θ and DF and the same are used as fitness functions for MO-Jaya algorithm.

The survey of literature revealed that there are number of process parameters which control the performance of the EDM process such as pulse current, pulse on time, gap voltage, % duty cycle, Z depth, sensitivity, anti-arc sensitivity, work-time, lift time, prepulse sparking current, X displacement, Y displacement, polarity and tool rotation. Therefore, preliminary experiments were conducted to find out the most critical parameters like the gap voltage ' V_g ' (V), pulse current ' I_p ' (A), pulse-on time ' T_{on} ' (μ s) and tool rotation speed ' N ' (rpm).

Design of experiments is used as a tool to generate the experimental procedure. The experiments are planned according to the rotational-central composite design (RCCD) and regression models for MRR , TWR , taper angle and DF are developed. The experiments are conducted with 4 process parameters considering each at 5 levels. The values of other process parameters are maintained as constant such as duty cycle 40 %, Z depth 15 mm, sensitivity 8, anti-arc sensitivity 7, work time 8.0 s, lift time 0.2 s, prepulse sparking current 0 A and straight polarity.

The experiments are performed in the Manufacturing Sciences laboratory of IIT Kanpur, India. ZNC Electronica EDM machine with a copper tool of 3 mm diameter is used for the purpose of experimentation. Carbon-carbon composite materials with 6 % grade with approximate dimensions as 155 mm \times 75 mm \times 3.5 mm is used as the workpiece material. A copper rod of 3 mm diameter and 7 mm length is used as tool. The tool is given negative polarity while the workpiece is given positive polarity. 30 experiments with 6 replicates of centre point are performed. Table 3 gives the experimental plan and results.

For each experiment the initial and final weights of tool and workpiece material is measured using a weighing scale (Citizen CY 204), care is taken to completely remove the moisture from the workpiece material before measurement. The MRR is calculated by taking the ratio of difference between initial and final weights of workpiece to the machining time of through hole. The TWR is calculated by taking the ratio of difference between initial and final weights of the tool to the machining time of through hole.

In the EDM process as the material is removed from tool as well as the workpiece all holes machined have a significant taper angle. To calculate taper angle the nominal diameters of upper and lower part of the machined hole are measured with the help of digital microscope and Dino-lite software. Further, the taper angle is calculated as follows.

$$\theta = \tan^{-1} \left(\frac{D_{top} - D_{bot}}{2 \cdot t} \right) \quad (12)$$

Where D_{top} and D_{bot} are nominal diameters of top and bottom surfaces of the machined hole and t is the thickness of workpiece.

The delamination factor is calculated as the ratio of maximum diameter of the heat affected zone to the nominal diameter of the machined hole. The regression models for MRR , TWR , θ and DF developed using a logarithmic scale with uncoded values of machining parameters and are expressed by Eq. 13 to Eq. 16.

Table 3 Design of experiments and values of MRR , TWR , θ and DF measured after experimentation

S. No.	V_g (V)	I_p (A)	T_{on} (μ s)	N (rpm)	MRR (mg/min)	TWR (mg/min)	θ (degree)	DF
1	40	20	500	250	11.774	15.56	0.49896	1.13765
2	80	20	500	250	18.429	28.071	0.94956	1.17407
3	40	40	500	250	17.984	87.5	2.14977	1.19477
4	80	40	500	250	23.818	169.129	2.93734	1.28756
5	40	20	1000	250	10.485	9.706	1.01307	1.1483
6	80	20	1000	250	21.755	35.145	1.44775	1.18842
7	40	40	1000	250	17.957	89.586	2.34904	1.20387
8	80	40	1000	250	25.836	189.062	3.03773	1.29591
9	40	20	500	350	9.409	12.994	1.21824	1.12567
10	80	20	500	350	14.73	22.858	1.45351	1.16211
11	40	40	500	350	14.251	87.553	2.47527	1.18693
12	80	40	500	350	17.152	141.074	2.73688	1.27143
13	40	20	1000	350	7.567	13.593	1.43657	1.13062
14	80	20	1000	350	12.739	26.774	1.58195	1.16556
15	40	40	1000	350	13.983	88.552	1.86935	1.18385
16	80	40	1000	350	16.643	145.738	2.11996	1.2753
17	25	30	750	300	7.135	13.344	1.56341	1.15768
18	95	30	750	300	17.791	97.223	2.05367	1.20508
19	60	10	750	300	16.462	2.123	0.609447	1.1168
20	60	45	750	300	23.262	189.031	1.93848	1.23504
21	60	30	300	300	19.481	90.738	1.2623	1.23478
22	60	30	2000	300	11.879	63.277	2.5361	1.20539
23	60	30	750	200	23.644	92.36	1.75735	1.24253
24	60	30	750	400	4.167	8.568	1.45485	1.21992
25	60	30	750	300	22.61	76.726	1.54156	1.21704
26	60	30	750	300	22.532	80.963	1.51356	1.21996
27	60	30	750	300	21.873	75.491	1.50756	1.22892
28	60	30	750	300	22.095	79.266	1.53274	1.22455
29	60	30	750	300	20.032	75.118	1.53498	1.2119
30	60	30	750	300	22.263	76.726	1.52827	1.2338

$$\begin{aligned}
 MRR = \exp \{ & -264.7311 + 14.62835 (\log V_g) + 0.633896 (\log I_p) + 8.67444 (\log T_{on}) \\
 & + 74.465 (\log N) - 1.0053 (\log V_g)^2 + 0.2317 (\log I_p)^2 - 0.3459 (\log T_{on})^2 \\
 & - 5.83289 (\log N)^2 - 0.63041 (\log V_g \cdot \log I_p) + 0.16643 (\log V_g \cdot \log T_{on}) \\
 & - 0.87394 (\log V_g \cdot \log N) + 0.12709 (\log I_p \cdot \log T_{on}) - 0.94153 (\log T_{on} \cdot \log N) \} \quad (13) \\
 & (R^2 = 0.855)
 \end{aligned}$$

$$\begin{aligned}
 TWR = \exp \{ & -264.7887 + 16.8 (\log V_g) + 7.1385 (\log I_p) - 1.206 (\log T_{on}) \\
 & + 79.1385 (\log N) - 0.9912 (\log V_g)^2 - 0.5355 (\log I_p)^2 + 0.03906 (\log T_{on})^2 \\
 & - 6.3355 (\log N)^2 - 0.3342 (\log V_g \cdot \log I_p) + 0.4552 (\log V_g \cdot \log T_{on}) \\
 & - 1.6904 (\log V_g \cdot \log N) + 0.06969 (\log I_p \cdot \log T_{on}) - 0.2617 (\log T_{on} \cdot \log N) \} \quad (14) \\
 & (R^2 = 0.926)
 \end{aligned}$$

$$\begin{aligned}
 \theta = \exp \{ & -60.4654 + 3.7949 (\log V_g) + 6.7335 (\log I_p) + 10.0673 (\log T_{on}) \\
 & + 1.58424 (\log N) + 0.6458 (\log V_g)^2 + 0.18217 (\log I_p)^2 + 0.24652 (\log T_{on})^2 \\
 & + 1.2749 (\log N)^2 - 0.2535 (\log V_g \cdot \log I_p) - 0.1392 (\log V_g \cdot \log T_{on}) \\
 & - 1.20511 (\log V_g \cdot \log N) - 0.89575 (\log I_p \cdot \log T_{on}) - 1.6643 (\log T_{on} \cdot \log N) \} \quad (15) \\
 & (R^2 = 0.892)
 \end{aligned}$$

$$\begin{aligned}
 DF = \exp \{ & -0.58509 + 0.15295 (\log V_g) - 0.14645 (\log I_p) + 0.27323 (\log T_{on}) \\
 & - 0.12994 (\log N) - 0.02262 (\log V_g)^2 + 0.00873 (\log I_p)^2 + 7.9329^{-5} (\log T_{on})^2 \\
 & + 0.032075 (\log N)^2 + 0.07168 (\log V_g \cdot \log I_p) - 0.00957 (\log V_g \cdot \log T_{on}) \\
 & - 0.01534 (\log V_g \cdot \log N) - 0.01683 (\log I_p \cdot \log T_{on}) - 0.03149 (\log T_{on} \cdot \log N) \} \quad (16) \\
 & (R^2 = 0.898)
 \end{aligned}$$

Now MO-Jaya algorithm is used to maximize the *MRR*, minimize *TWR*, minimize taper angle and minimize *DF*, simultaneously. The regression models expressed by Eq. 13 to Eq. 16 are used as fitness functions for MO-Jaya algorithm. The process parameter bounds are expressed by Eq. 17 to Eq. 20 as follows.

$$25 \leq V_g \leq 95 \tag{17}$$

$$10 \leq I_p \leq 45 \tag{18}$$

$$300 \leq T_{on} \leq 2000 \tag{19}$$

$$200 \leq N \leq 400 \tag{20}$$

The set of Pareto-efficient solutions provided by MO-Jaya algorithm in a single run of simulation is reported in Table 4 for all 4 objectives. As the optimization problem is having 4 objectives it is not easy to show the 4-dimensional Pareto front and hence the Pareto front for *MRR*, *TWR* and θ is shown as Fig. 4(a) and the Pareto front for *TWR*, θ and *DF* is shown as Fig. 4(b).

Table 4 Pareto optimal solution set provided by MO-Jaya algorithm in a single simulation run for EDM process

S. No.	V_g (V)	I_p (A)	T_{on} (μ s)	N (rpm)	<i>MRR</i> (0.1 mg/s)	<i>TWR</i> (0.1 mg/s)	θ (degree)	<i>DF</i>
1	25	10	1913.724	200	1.2453	0.0965	3.3476	1.1574
2	25.0495	10	1844.116	200	1.2865	0.0986	3.0562	1.1558
3	25	10	1757.623	200	1.3199	0.0996	2.7192	1.1536
4	26.2683	10	2000	200	1.4191	0.1162	3.7259	1.1603
5	25	10	300	200	1.4245	0.2215	0.0811	1.079
6	31.7003	10	2000	200	2.5179	0.2405	3.8046	1.1629
7	28.5	10	932.73	212.1907	3.0999	0.2672	0.6472	1.1259
8	33.8835	10	980.8407	214.6995	5.0426	0.4827	0.7417	1.13
9	39.4565	10	1366.835	200	5.5058	0.5499	1.7016	1.1488
10	39.5125	10	893.006	200	6.1636	0.6041	0.6878	1.1325
11	43.1006	10	785.4233	214.3395	9.0452	1.0027	0.5488	1.1238
12	60.5423	10	300	200	9.4074	1.871	0.159	1.0949
13	50.252	10	951.2899	200	10.0145	1.1314	0.943	1.1347
14	50.4624	10	1094.945	209.8391	11.047	1.3154	1.1924	1.1359
15	95	10	300	370.8176	11.201	1.547	0.5758	1.0749
16	53.9205	10	1193.568	203.7774	11.3644	1.3979	1.5711	1.1404
17	61.7591	10	417.817	200	11.776	1.8677	0.269	1.1054
18	52.3786	10	997.8612	216.286	12.7649	1.5735	0.9942	1.1302
19	59.0602	10	1199.503	212.3769	14.2355	1.9259	1.6368	1.1357
20	62.0647	10	782.3541	212.8126	16.3417	2.1735	0.7642	1.1214
21	57.6466	10	899.7264	241.1095	17.1198	2.3377	0.8244	1.1187
22	78.1695	10	300	303.9107	18.6777	3.184	0.3371	1.0817
23	63.9669	10	721.4555	233.2439	19.5525	2.7339	0.6496	1.1129
24	81.4454	10.4816	300	263.1196	20.3185	4.6091	0.3181	1.0889
25	82.047	10.242	300	276.3105	20.4793	4.1102	0.3279	1.0849
26	81.5354	10	407.3847	289.2469	22.0527	3.4706	0.4306	1.0863
27	93.3095	10	460.6347	290.8624	23.1194	3.5922	0.5781	1.0837
28	77.2987	10	847.0946	243.5197	23.7081	3.6683	1.0182	1.1097
29	84.271	11.0556	628.0503	247.9736	24.8563	5.7193	0.7768	1.1108
30	95	10	680.5518	230.7705	25.9749	4.2886	1.0235	1.101
31	95	10	726.217	247.0427	26.8204	4.4199	1.0638	1.0983
32	63.1759	35.7338	815.4502	250.6803	26.8784	141.1848	1.9473	1.2461
33	46.8665	45	704.2118	262.2001	26.8928	168.1049	2.1411	1.2377
34	66.0972	36.3491	644.0377	251.924	27.032	153.657	1.8928	1.2522
35	63.4694	37.0986	865.4543	259.8581	27.2314	155.9124	2.0329	1.2489
36	65.7791	37.3432	876.1797	259.7034	27.5357	164.2039	2.1005	1.2531
37	48.7786	45	750.8355	259.6498	27.6576	176.157	2.1703	1.2431
38	53.8153	45	571.8286	249.4247	27.9858	200.6127	2.1753	1.2581
39	55.3277	45	591.4365	277.3743	28.3591	208.3648	2.2865	1.2568
40	52.1831	45	875.1416	246.9805	28.454	185.9188	2.3039	1.254
41	55.6714	45	867.8184	251.2169	29.5533	205.7847	2.3407	1.2608
42	56.978	45	895.9178	245.2088	29.6352	208.5368	2.4141	1.265
43	59.1992	45	664.6343	264.8876	29.8885	224.7545	2.3068	1.2662
44	58.1049	45	835.4176	253.878	30.121	218.1782	2.3559	1.2653
45	60.3879	45	738.0855	255.0349	30.42	228.327	2.3521	1.27
46	62.1815	45	846.2731	248.4064	30.6445	233.4057	2.473	1.2745
47	64.936	45	937.1024	251.8109	30.7501	246.4366	2.577	1.278
48	64.7866	45	770.7681	249.6904	30.8257	243.3128	2.4831	1.2792
49	69.817	45	810.0259	259.0902	30.8293	260.9632	2.5826	1.2849
50	68.0958	45	836.1816	252.7234	31.0207	256.4056	2.5864	1.2836

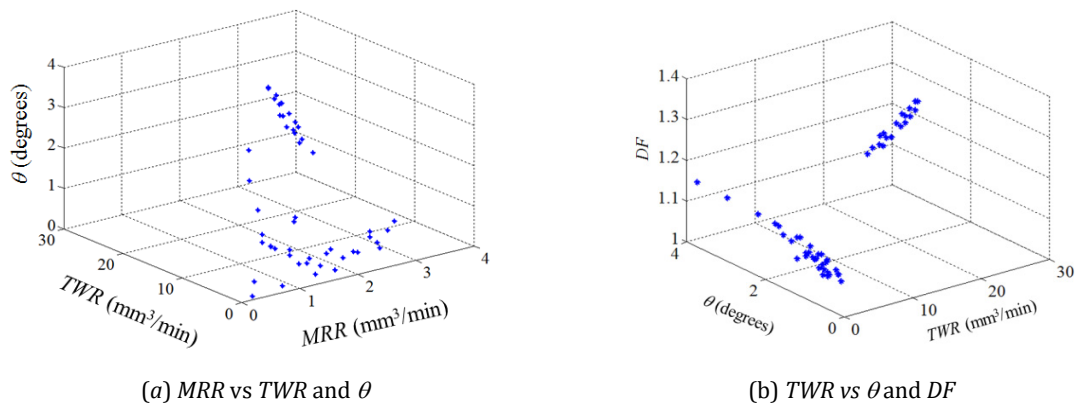


Fig. 4 Pareto-optimal solution obtained by MO-Jaya algorithm for EDM process in a single simulation run

The MO-Jaya algorithm required 20 iterations and it required a CPU time of 7.77 s to perform 100 iterations. The results show that the optimum value of *MRR* lies in the range of 0.12453 (mg/s) to 3.10207 (mg/s). The *MRR* increases with increase in gap voltage and current due to increase in energy input per pulse which causes more melting of the workpiece material. However, a high energy input also results in melting of tool material increasing the *TWR*. Therefore, the *TWR* increases with the increase in *MRR*. The best compromise value for *TWR* achieved by MO-Jaya algorithm lies in the range of 0.00965 mg/s to 25.64 mg/s.

It is observed that *MRR* increases steadily as the current increases from 10 A to 45 A. However, *TWR* is low at lower value of current (10 A) but at a higher value of current (45 A) the tool wear rate increases drastically. As the pulse-on time increases, due to more energy input per pulse *MRR* also increases. However, beyond a limiting value of pulse-on time the *MRR* decreases with further increase in pulse-on time because with in fixed pulse duration the increase in pulse-on time is compensated with decrease in pulse-off time. This results in improper flushing of debris by the electrolyte. The accumulation of debris reduces the arc gap and thus the *MRR* decreases. Furthermore, accumulation of debris in the arc gap causes the formation of arc between workpiece debris and the tool resulting in increase in *TWR* without removal of material from the tool. Further, with increase in pulse-on-time less time is available for cooling of the tool which further increases the *TWR*.

The taper angle increases with increase in pulse on time because the workpiece debris result in abrasive action on the walls of the workpiece during flushing. The increase in input energy increases the taper angle due to secondary discharge caused due to increase in temperature of dielectric fluid and increase in workpiece debris. The best compromised values for taper angle suggested by MO-Jaya algorithm lies in the range of 0.0811 degrees to 3.8046 degrees. The best compromised values for delamination factor suggested by MO-Jaya algorithm lies in the range of 1.0749 to 1.2849.

4.3 Optimization of micro-EDM process

The objective of this work is to improve the performance of micro-EDM milling process by means of process parameter optimization. The regression models for *MRR* (mm³/min) and *TWR* (mm³/min) are developed based on actual data collected by means of experimentation and the same as used as fitness functions for MO-Jaya algorithm in order to obtain multiple trade-off solutions. The experiments are performed at Manufacturing Science Laboratory of IIT Kanpur, India and DT110 high precision, CNC controlled, micro-machining setup with integrated multi-process machine tool was used for the purpose of experimentation. The workpiece is die material EN24, cylindrical tungsten electrode (dia. 500 μ m) is used as tool and conventional EDM oil is used as die electric. The feature shape considered for the study is a μ -channel of width approximately equal to the diameter of the tool, length of cut 1700 μ m, the depth of channel is considered as 1000 μ m.

In the present study the bulk machining approach for μ -EDM milling is used. As the bulk machining approach results in excessive tool wear intermittent tool dressing with block electro-

discharge grinding (EDG) process is used. Review of literature shows that there are a number of process parameters that affect the performance of μ -EDM milling process. Therefore prior to actual experimentation dimensional analysis is performed to identify the most influential parameters of the process such as Energy ' E ' (μ J), feed rate ' F ' (μ m/s), tool rotation speed ' S ' (rpm) and aspect ratio ' A '. The useful levels of these parameters is identified using one factor at a time (OFAT) analysis and 2 levels of energy, 4 levels of feed rate, 3 levels of rotational speed, and 4 levels of aspect ratio are identified. The measurement of MRR and TWR during experimentation is carried out by means of a CAD softwares like Solidworks and AutoCAD along with images of cross section at the entry and exit of the micro channel which are recorded using a USB microscope with a digital scale interface. The amount of re-deposition on the microchannel surface was studied by means of chemical analysis on channel surface using energy dispersive analysis X-ray technique (EDAX).

The regression models for MRR and TWR are formulated by considering a full factorial experimental design, considering all combination of process parameter values a total number of 96 experiments are conducted. The values of MRR (mm^3/min) and TWR (mm^3/min) are measured and recorded as shown in Table 5. The regression models for MRR and TWR are developed using the experimental data, using a logarithmic scale, and are expressed by Eq. 21 and Eq. 22 in the uncoded form of process parameters.

$$\begin{aligned}
 MRR = \exp \{ & 11.15134 - 1.79325 (\log F) - 3.20333 (\log S) - 0.114931 (\log A) \\
 & - 0.072533 (\log E)^2 + 0.06657 (\log F)^2 + 0.251122 (\log S)^2 \\
 & - 0.16314 (\log A)^2 + 0.21496 (\log E \cdot \log F) + 0.099501 (\log E \cdot \log S) \\
 & + 0.16903 (\log E \cdot \log A) + 0.040721 (\log F \cdot \log S) - 0.11206 (\log F \cdot \log A) \\
 & - 0.07489 (\log S \cdot \log A) \}
 \end{aligned} \tag{21}$$

$$(R^2 = 0.94)$$

Table 5 Design of experiments for micro-EDM process and values of MRR and TWR measured after experimentation

S. No.	E (μ J)	F (μ m/s)	S (rpm)	A	MRR ($10^{-3}\text{mm}^3/\text{min}$)	TWR ($10^{-3}\text{mm}^3/\text{min}$)
1	2000	60	100	1	9.16	1.99
2	2000	60	800	1	23.48	5.16
3	500	60	800	1	12.88	3.2
4	500	60	100	1	6.26	0.92
5	500	10	100	1	4.53	0.74
6	2000	10	800	1	12.58	2.29
7	500	10	800	1	8.48	1.48
8	500	10	500	1.5	7.06	1.08
9	500	25	800	1.5	10.14	1.67
10	500	45	500	1.5	9.92	1.55
11	500	45	800	0.5	9.39	1.43
12	500	10	500	2	5.97	1.05
13	500	25	100	0.5	3.6	0.54
14	2000	45	500	2	16	3.66
15	2000	60	500	1	19.01	4.48
16	500	45	100	2	4.05	0.83
17	2000	10	100	2	6.05	1.11
18	500	60	500	1	9.91	2.15
19	500	60	100	1.5	6.57	1.01
20	500	10	800	0.5	7.34	1.19
21	2000	60	800	1.5	28.17	5.87
22	2000	25	800	2	19.68	3.83
23	500	25	800	2	11.69	1.61
24	500	25	500	0.5	6.32	0.81
25	2000	10	100	1	4.24	0.53
26	500	60	100	0.5	5.52	1.27
27	2000	60	100	2	12.08	3.56
28	2000	10	500	1	5.28	1.34
29	500	25	100	1	4.56	0.79
30	2000	25	500	1	10.15	2.45
31	500	60	800	0.5	12.71	2.84
32	500	45	500	1	9.2	1.92
33	2000	60	800	2	25.39	5.14
34	500	45	100	1.5	5.72	1.02
35	2000	10	500	2	7.66	1.87
36	500	10	500	1	6.69	1.23

Table 5 Design of experiments for micro-EDM process and values of *MRR* and *TWR* measured after experimentation (continuation)

37	500	25	800	1	9.86	1.64
38	2000	45	800	2	23.75	5.06
39	2000	25	800	1	21	3.33
40	500	60	800	2	12.02	2.1
41	500	60	100	2	5.62	0.93
42	2000	45	100	2	11.62	3.12
43	500	45	800	2	12.62	1.96
44	500	60	500	0.5	9.26	1.49
45	2000	25	500	1.5	15	3.32
46	2000	25	500	0.5	6.7	1.13
47	2000	10	800	1.5	13.32	2.77
48	500	10	800	1.5	9.03	1.36
49	2000	60	500	0.5	16.12	3.33
50	500	45	500	2	10.63	1.73
51	500	45	100	1	5.55	0.73
52	2000	45	500	1	17.65	4.49
53	2000	60	500	2	17.46	3.84
54	500	10	100	2	4.52	0.73
55	2000	45	800	1.5	29.84	6.4
56	500	60	500	1.5	10.08	2.06
57	2000	45	500	1.5	22.29	5.04
58	2000	60	100	0.5	7.32	1.13
59	2000	45	100	0.5	4.84	0.97
60	2000	45	800	0.5	23.2	3.84
61	500	45	800	1.5	12.7	1.97
62	500	45	100	0.5	5.3	1.02
63	2000	10	800	0.5	9.88	1.79
64	2000	25	100	1	6.13	1.21
65	2000	60	800	0.5	25.64	3.58
66	500	10	100	0.5	3.99	0.63
67	2000	25	800	1.5	25.55	4.23
68	2000	45	100	1	6.93	1.37
69	500	10	500	0.5	6.02	0.97
70	500	10	100	1.5	5.28	0.93
71	2000	25	100	1.5	7.1	1.44
72	2000	60	500	1.5	22.68	5.3
73	500	60	800	1.5	13.8	2.5
74	500	25	500	1.5	7.82	1.19
75	2000	10	500	1.5	7.9	1.73
76	2000	10	500	0.5	3.95	0.64
77	500	25	500	2	8.48	1.33
78	500	45	500	0.5	7.55	1.11
79	2000	60	100	1.5	11.41	3.82
80	2000	10	100	1.5	6.79	0.95
81	2000	45	800	1	24.61	5.82
82	500	25	100	2	4.75	0.78
83	500	45	800	1	11.25	2.33
84	2000	45	100	1.5	9.73	2.14
85	2000	10	800	2	15.46	3.47
86	500	10	800	2	11.33	1.43
87	500	60	500	2	10.34	1.83
88	2000	10	100	0.5	2.73	0.31
89	2000	25	500	2	13.21	3.46
90	500	25	100	1.5	5.31	0.82
91	2000	25	100	0.5	3	0.44
92	2000	25	100	2	7.88	1.86
93	500	25	800	0.5	8.54	1.07
94	2000	45	500	0.5	13.38	1.79
95	500	25	500	1	7.44	1.57
96	2000	25	800	0.5	17.29	1.79

$$\begin{aligned}
 TWR = \exp \{ & 5.68347 - 2.22795 (\log F) - 1.77173 (\log S) - 1.29611 (\log A) \\
 & - 0.07152 (\log E)^2 + 0.175929 (\log F)^2 + 0.13946 (\log S)^2 \\
 & - 0.34761 (\log A)^2 + 0.23781 (\log E \cdot \log F) + 0.1005 (\log E \cdot \log S) \\
 & + 0.380612 (\log E \cdot \log A) - 0.015495 (\log F \cdot \log S) - 0.120799 (\log F \cdot \log A) \\
 & - 0.096066 (\log S \cdot \log A) \} \quad (22)
 \end{aligned}$$

$$(R^2 = 0.933)$$

Now MO-Jaya algorithm is used to maximize the *MRR* and minimize the *TWR*, simultaneously. The regression models for *MRR* and *TWR* expressed by Eq. 21 and Eq. 22, respectively are used

as fitness functions for MO-Jaya algorithms. The process parameter bounds are expressed by Eq. 23 to Eq. 26 as follows.

$$500 \leq E \leq 2000 \quad (23)$$

$$10 \leq F \leq 60 \quad (24)$$

$$100 \leq S \leq 800 \quad (25)$$

$$0.5 \leq A \leq 2.0 \quad (26)$$

The Pareto-efficient set of solutions obtained using MO-Jaya algorithm in a single simulation run is shown Table 6 and the Pareto-front is shown in Fig. 5. The MO-Jaya algorithm required 11 iterations to obtain the Pareto-efficient set of solutions. The MO-Jaya algorithm required 6.086 s to perform 100 iterations.

Table 6 Pareto optimal solution set provided by MO-Jaya algorithm in a single simulation run for micro-EDM process

S. No.	E (μ J)	F (μ m/s)	S (rpm)	A	MRR (10^{-3} mm ³ /min)	TWR (10^{-3} mm ³ /min)
1	2000	10	100	0.5	2.6219	0.3307
2	2000	12.9182	100.0819	0.5	2.9267	0.3709
3	2000	19.5363	100.2894	0.5	3.561	0.4689
4	2000	22.5177	100	0.6364	4.4926	0.6837
5	2000	15.471	100	0.8852	4.6108	0.7671
6	2000	11.1055	525.5919	0.5	5.6157	0.8431
7	2000	14.9048	494.173	0.5018	6.2136	0.9265
8	2000	17.4029	520.7207	0.5028	7.0729	1.0511
9	2000	12.1938	660.3727	0.5	7.2438	1.0534
10	2000	16.9822	648.2183	0.5023	8.5232	1.2308
11	2000	15.3951	800	0.5	9.9806	1.389
12	1999.999	16.3754	800	0.5	10.3308	1.4354
13	2000	18.2665	800	0.5	10.9949	1.5265
14	2000	23.1415	729.9279	0.5	11.4719	1.6347
15	2000	22.9902	800	0.5	12.6004	1.7614
16	2000	25.9902	781.586	0.5	13.2492	1.8773
17	1999.999	26.7446	800	0.5	13.8351	1.9551
18	2000	29.8817	793.8799	0.5	14.7207	2.1072
19	2000	31.589	800	0.5022	15.4229	2.2233
20	2000	33.7982	800	0.5	16.0848	2.3343
21	2000	37.0695	800	0.5	17.1046	2.5167
22	2000	37.6695	800	0.5	17.2904	2.5507
23	2000	40.8566	800	0.5033	18.3284	2.751
24	2000	42.1834	800	0.5	18.6761	2.8103
25	2000	45.1411	800	0.5	19.5745	2.9847
26	2000	48.3518	800	0.5	20.5423	3.1778
27	2000	50.9093	779.8629	0.5	20.7107	3.2622
28	2000	50.6162	800	0.5	21.2207	3.3163
29	2000	52.5044	800	0.5	21.7841	3.4334
30	2000	54.6281	800	0.5	22.4155	3.5667
31	2000	56.967	800	0.5	23.1082	3.7154
32	2000	60	800	0.5	24.0027	3.9115
33	2000	60	800	0.5253	24.5151	4.0939
34	2000	60	800	0.5524	25.0289	4.2814
35	2000	60	800	0.5779	25.4824	4.4508
36	2000	60	794.4076	0.6082	25.7814	4.6148
37	2000	60	800	0.6292	26.3089	4.7687
38	2000	60	800	0.652	26.6441	4.9011
39	2000	60	800	0.6732	26.9399	5.0197
40	2000	60	800	0.686	27.1113	5.0891
41	1999.999	60	800	0.7105	27.4242	5.2172
42	1999.999	60	800	0.7441	27.8258	5.3843
43	2000	60	800	0.8279	28.6992	5.758
44	2000	60	800	0.8464	28.8696	5.8326
45	1999.999	60	800	0.891	29.2525	6.0023
46	2000	60	800	0.9016	29.3378	6.0404
47	2000	60	800	0.9574	29.7536	6.2287
48	2000	60	800	1.0504	30.3372	6.499
49	2000	60	800	1.1582	30.8707	6.7526
50	2000	60	800	1.906	32.1458	7.404

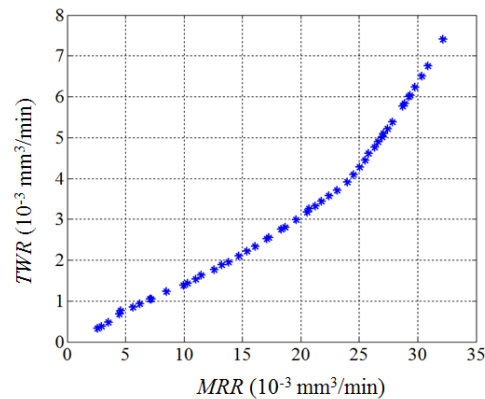


Fig. 5 Pareto-front obtained by MO-Jaya algorithm for micro-EDM process in a single simulation run

The results of MO-Jaya algorithm have revealed that, in order to achieve a trade-off between *MRR* and *TWR* the optimal setting for pulse energy is 2000 μJ and any deviation from this value may result in non-optimal values of *MRR* and *TWR*. With aspect ratio fixed at 0.5 an increase in *MRR* is observed with increase in feed rate and speed. However, at extreme values of feed rate and speed the *MRR* increases with increase in aspect ratio. A low value of feed rate, speed and aspect ratio results in minimum tool wear ($TWR = 0.3307 \times 10^{-3} \text{ mm}^3/\text{min}$, refer solution 1, Table 6). On the other hand, a high value of feed rate, speed and aspect ratio gives a high *MRR* ($32.1458 \times 10^{-3} \text{ mm}^3/\text{min}$, refer solution 50, Table 6) but at the expense of significant increase in *TWR* ($7.040 \times 10^{-3} \text{ mm}^3/\text{min}$).

5. Conclusion

Multi-objective optimization aspects of plasma arc machining, electro-discharge machining, and micro-electro-discharge machining processes are considered in the present work. Mathematical models are developed based on the actual experimental data and these models are used as fitness functions for MO-Jaya algorithm.

In the case of PAM process, the MO-Jaya algorithm is applied to optimize simultaneously the *MRR* and *DFR*. The MO-Jaya algorithm has provided 50 trade-off solutions in 8 iterations. The results of optimization show that in order to achieve a trade-off between *MRR* and *DFR* the process planner should choose the values of current and speed close to their respective upper bounds (45 A and 800 mm/min). However, the values of other parameters such as thickness and arc gap voltage must be selected optimally in the range of 1.58 mm to 2.5 mm and 128 V to 165 V, respectively. The Pareto front obtained by MO-Jaya algorithm is convex in nature with maximum *MRR* equal to 1.0769 (g/s) and minimum *DFR* equal to 0.0004 (g/s).

In the case of EDM process, the MO-Jaya algorithm is applied to optimize the *MRR*, *TWR*, taper angle and *DF*, simultaneously. The MO-Jaya algorithm has obtained 50 trade-off solutions in 20 iterations. The MO-Jaya algorithm could achieve a value of *MRR* as high as 3.10207 (mg/min) and values of *TWR*, taper angle and *DF* as low as 0.00965 (mg/min), 0.0811 (degrees) and 1.0749, respectively.

In the case of micro-EDM process, the MO-Jaya algorithm required 11 iterations to obtain 50 trade-off solutions for *MRR* and *TWR*. The results show that in order to achieve a trade-off between *MRR* and *TWR* a higher value of pulse energy is desired. Therefore, pulse energy may be set to its respective upper bound (2000 μJ) However, the feed rate and rotation speed must be set optimally within their respective ranges. The Pareto front obtained by MO-Jaya algorithm is continuous and convex in nature with the value of *MRR* as high as 0.03214 (mm^3/min) and *TWR* as low as 0.3307×10^{-3} (mm^3/min).

The main advantages of the MO-Jaya algorithm are that: (1) the algorithm does not burden the user with the task of tuning the algorithm-specific parameters, and (2) the algorithm is simple to implement as the solutions are updated in single phase using a single equation and has low computational and time complexities. The effect of the best and worst solutions in the current population are considered simultaneously which gives a high convergence speed to MO-

Jaya algorithm without trapping into local optima. The ranking mechanism based on the concept of non-dominance relation between the solutions helps MO-Jaya algorithm to maintain the good solutions in every generation and guides the search process towards the Pareto-optimal set.

The population size in MO-Jaya algorithm is fixed at the beginning of the algorithm and is maintained constant in every generation throughout the simulation run. However, increasing or reducing the population size adaptively in every generation may save a considerable number of function evaluations which would otherwise be spent in updating a large population.

The Pareto-efficient solutions provided by MO-Jaya algorithm can be used as ready reference by the process engineer in order to set the parameter values at their optimal levels for best performance of machining process with sustainability. Thus the results presented in this work are very useful for real manufacturing environment. The application of MO-Jaya algorithm may be extended to other modern machining processes.

Acknowledgement

The Authors are thankful to the Department of Science and Technology (DST), Ministry of Science & Technology, of the Republic of India and the Slovenian Research Agency (ARRS), Ministry of Education, Science and Sport of the Republic of Slovenia for providing the financial support for the project entitled "Optimization of Sustainable Advanced Manufacturing Processes".

References

- [1] De Wolf, D., Cardon, L., Balic, J. (2010). Parameters effecting the quality of the electrical discharge machining process, *Advances in Production Engineering and Management*, Vol. 5, No. 4, 245-252.
- [2] Aich, U., Banerjee, S. (2016). Application of teaching learning based optimization procedure for the development of SVM learned EDM process and its pseudo Pareto optimization, *Applied Soft Computing*, Vol. 39, 64-83, [doi: 10.1016/j.asoc.2015.11.002](https://doi.org/10.1016/j.asoc.2015.11.002).
- [3] Zhang, T.Y., Owodunni, O., Gao, J. (2015). Scenarios in multi-objective optimization of process parameters for sustainable machining, *Procedia CIRP*, Vol. 26, 373-378, [doi: 10.1016/j.procir.2014.07.186](https://doi.org/10.1016/j.procir.2014.07.186).
- [4] Gupta, M.K., Sood, P.K., Sharma, V.S. (2016). Optimization of machining parameters and cutting fluids during nano-fluid based minimum quantity lubrication turning of titanium alloy by using evolutionary techniques, *Journal of Cleaner Production*, Vol. 135, 1276-1288, [doi: 10.1016/j.jclepro.2016.06.184](https://doi.org/10.1016/j.jclepro.2016.06.184).
- [5] Chandrasekaran, M., Muralidhar, M., Krishna, C.M., Dixit, U.S. (2010). Application of soft computing techniques in machining performance prediction and optimization : A literature review, *The International Journal of Advanced Manufacturing Technology*, Vol. 46, No. 5, 445-464, [doi: 10.1007/s00170-009-2104-x](https://doi.org/10.1007/s00170-009-2104-x).
- [6] Jiang, Z., Zhou, F., Zhang, H, Wang, Y., Sutherland, J.W. (2015). Optimization of machining parameters considering minimum cutting fluid consumption, *Journal of Cleaner Production*, Vol. 108 (part A), 183-191, [doi: 10.1016/j.jclepro.2015.06.007](https://doi.org/10.1016/j.jclepro.2015.06.007).
- [7] Yusup, N., Zain, A.M., Hashim, S.Z.M. (2012). Evolutionary techniques in optimizing machining parameters: Review and recent applications (2007-2011), *Expert Systems with Applications*, Vol. 39, No. 10, 9909-9927, [doi: 10.1016/j.eswa.2012.02.109](https://doi.org/10.1016/j.eswa.2012.02.109).
- [8] Rao, R.V., Kalyankar, V.D. (2014) Optimization of modern machining processes using advanced optimization techniques: A review, *The International Journal of Advanced Manufacturing Technology*, Vol. 73, No. 5, 1159-1188, [doi: 10.1007/s00170-014-5894-4](https://doi.org/10.1007/s00170-014-5894-4).
- [9] Goswami, D., Chakraborty, S. (2015), Parametric optimization of ultrasonic machining process using gravitational search and fireworks algorithms, *Ain Shams Engineering Journal*, Vol. 6, No. 1, 315-331, [doi: 10.1016/j.asej.2014.10.009](https://doi.org/10.1016/j.asej.2014.10.009).
- [10] Saha, A., Mondal, S.C. (2016). Multi-objective optimization in WEDM process of nanostructured hardfacing materials through hybrid techniques, *Measurement*, Vol. 94, 46-59, [doi: 10.1016/j.measurement.2016.07.087](https://doi.org/10.1016/j.measurement.2016.07.087).
- [11] Maity, K.P., Bagal, D.K. (2015). Effect of process parameters on cut quality of stainless steel of plasma arc cutting using hybrid approach, *The International Journal of Advanced Manufacturing Technology*, Vol. 78, No. 1, 161-175, [doi: 10.1007/s00170-014-6552-6](https://doi.org/10.1007/s00170-014-6552-6).
- [12] Rao, R.V., Rai, D.P., Balic, J. (2016). Multi-objective optimization of machining and micro-machining processes using non-dominated sorting teaching-learning-based optimization algorithm, *Journal of Intelligent Manufacturing*, [doi:10.1007/s10845-016-1210-5](https://doi.org/10.1007/s10845-016-1210-5).
- [13] Li, C., Xiao, Q., Tang, Y., Li, L. (2016). A method integrating Taguchi, RSM and MOPSO to CNC machining parameters optimization for energy saving, *Journal of Cleaner Production*, Vol. 35, 263-275, [doi: 10.1016/j.jclepro.2016.06.097](https://doi.org/10.1016/j.jclepro.2016.06.097).
- [14] Rao, R.V. (2016). Jaya: A simple and new optimization algorithm for solving constrained and unconstrained optimization problems, *International Journal of Industrial Engineering Computations*, Vol. 7, No. 1, 19-34, [doi: 10.5267/i.ijiec.2015.8.004](https://doi.org/10.5267/i.ijiec.2015.8.004).

Finite element method for optimum design selection of carport structures under multiple load cases

Özkal, F.M.^{a,*}, Cakir, F.^{b,c}, Arkun, A.K.^d

^aErzincan University, Department of Civil Engineering, Erzincan, Turkey

^bYıldız Technical University, Department of Architecture, İstanbul, Turkey

^cUniversity of California, Pacific Earthquake Engineering Research Center (PEER), Berkeley, California, USA

^dAmasya University, Department of Urban Design and Landscape Architecture, Amasya, Turkey

ABSTRACT

In the field of structural modelling, it is obvious that the number of applicable designs for a particular structural necessity is limitless. Along with the integration of various kinds of available structural materials into this complexity, it gets harder to be able to determine the best design before the production stage. In recent years, with the improvement of computational and structural technology, there have been many studies on the optimal design selection. This study focuses on carport structures and pursuing their best producible shape. For this aim, a performance index formulation was developed to assist the decision of material efficiency as well as structural rigidity. Thereafter, five conceptual models were numerically modelled and finite element analyses (FEA) for multiple load cases were carried out. Reviewing the FEA results, the most appropriate model was determined by the application of this performance qualification method. Results of the analyses show that optimum design of structures under multiple load cases can be determined using finite element method.

© 2016 PEI, University of Maribor. All rights reserved.

ARTICLE INFO

Keywords:

Structural producibility
Performance decision
Multiple load cases
Manufacturing
Finite element method

*Corresponding author:

fmozkal@erzincan.edu.tr
(Özkal, F.M.)

Article history:

Received 26 April 2016
Revised 5 October 2016
Accepted 12 October 2016

1. Introduction

Structures can be designed in many different ways to provide the structural requirements such as performance, economy and appearance. The convenient design of structures is a very important factor for their structural performance. Shape of the structures is a very important factor for their structural behaviour. A poor design might cause fault and quality problems in a structure. It may conduce to decrease quality, performance and to increase cost and unnecessary material usage. Therefore, structural design is a major concern in engineering structures.

Design objectives are generally imprecise real-life situations as well as structural problems and natural idea is to deal directly with these ambiguous objectives. Hence, business experience shows that in many cases, it is beneficial to specify them crispy and then solve the optimization problem [1]. Design of structures depends on not only structural problems, but also knowledge and creativity of the designer. Therefore, design concepts can technically be discussed for a structure and designers seek the best feasible design. However, it is quite difficult to determine which of the designs is more efficient and better than the other ones. In recent years, with improvements of computer and structural technology, one of the ways to achieve an efficient structural design has been mathematical design optimization. Main goal of design optimization is to determine the best producible design for a structure under various constraints. Recently, design

optimization with the finite element method (FEM) has become more popular with significant advances in computer technology. Today many designer and engineers appeal to finite element method and many structural analysis software packages are suitable for FEA.

The design process can be categorized in various ways, but in general, it consists of four main phases [2]. The first stage is to determine the functionality requirements and essential parameters; the second stage is to develop concept models; the third stage is to perform optimization on the developed concept models and the last stage is to compare the optimization results and decide the most suitable design before production. The general flow diagram of the structural design process is shown in Fig. 1. In this study, the best design of carport structures was determined by means of these four steps.

In previous studies, many researchers have investigated the design process and design optimization of many different structures [3-8]. In almost all of the past studies, urban structures have not been completely investigated. Therefore, this study focuses on the carport structures and their best producible design, since they are one of the most common urban structures. The study contributes to the best design of carport structures under multiple load cases in that it develops a performance index formulation, reveals the impact of material efficiency and structural rigidity on the best design. Moreover, this study helps to devise implement strategies and develop actions to improve best design. It is also indicated that the effective optimum design selection contributes to improve efficient structural design.

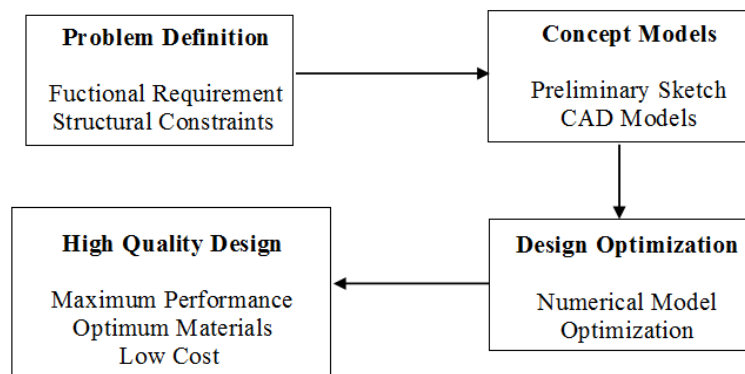


Fig. 1 Flow diagram of the structural design process

2. Carport structures

Carport structures, which are also known as car shelters, parking shades and parking structures, are open sided structures that usually consist of a roof and load bearing parts. Carports are popular all around the world and they are widely used at houses, office buildings, public areas, shopping malls, retail operations and shopping malls. Carports bring many great benefits, such as preventing damage from hailstones, snow and rain, minimizing sun damage, protecting against poorer weather, moisture and corrosion. Carports, which can be freestanding or attached to a building, may have a roofed or canopied form and sides of carports are left wholly or partially open. In other words, carports can be defined as a semi-open space in the context of architecture or space design.

The entrance of a carport is in contrast to a generally open garage. A common variant of the roofing is a corrugated sheet, trapezoidal or their transparent forms corrugated light panels or trapezoidal plates. Open carports without a roof are usually used as an optical setting of outdoor spaces to emphasize this by surrounding open spaces. Increasingly, free areas of the roof are also used for solar systems and as an extensive green roof. A green roof can contribute to decrease temperatures and reduce the heat island effect in the urban environment.

Furthermore, using carports, less materials are needed and the construction time is shorter than garage construction. Carports are assumed to be greener. Moore [9] lists the advantages of carports as serving as a covered main entrance and a place to entertain and do outdoor activi-

ties, in addition to the providing protection and storage for the cars. He also mentions that carports reduce complexity providing more than sufficient shelter, necessitate less construction materials, and accommodate as aesthetically architectural design. Conclusively, he states that people consider the environmental impact of garages compared to carports and choose the cost effective carports due to the rising environmental concerns. These several advantages contribute to widespread use of carports. On the other hand, carports offer no privacy, protection against theft or vandalism. A garage is more secure than a carport.

2.1 Historical background of carport structures

Car ownership has increased very quickly over the past forty years. This increase creates parking space need. Besides open space parking areas, carports which are semi open spaces were emerged especially in a single-detached dwelling setting. Gebhard proposes the older form of the porte cochère as the predecessor for the carports since it serves similarly to carport in terms of sheltering passengers as they exited carriages or automobiles. Gebhard [10] also stated that the architect Walter Burley Griffin used carports in the Sloan House in Elmhurst, Illinois in the early 1900s. By 1913, several Prairie School architects such as the Minneapolis firm of Purcell, Feick&Elmslie also used carports in a home at Lockwood Lake, Wisconsin. According to Fox and Jeffery [11], the expression “carport” was proposed by David Gebhard, an architectural historian, for the way that the term was begun from the component's utilization in 1930s streamline present day structures. Robinson [12] notes that carports were used by American famous architect Frank Lloyd Wright in Usonian Houses design in the 1940s. These carport structures are demonstrated in Fig. 2.

Moreover, Fox and Jeffery [11] points out that carports were accepted as an alternative to garages because of their cost and easy construction after Second World War. According to Moore [9], in the 19th century carports became typical design element of single-family residences and hotels. Today a vast range of sizes and designs of carports are available.



Fig. 2 Porte Cochère (a), Sloan House (b), Usonian (c) [13-15]

2.2 Structural failures of carport structures

Carport structures are exposed to many different external and internal effects throughout their lives. Therefore, a carport structure should be designed to withstand structural loading scenarios. Hence, the accurate estimation of the loads and their combinations on a carport might be the most important and the most difficult task for designers. Loads on carport structures are based on different types and forces, which are dead loads, live loads and lateral loads. Carport structures address the carrying problems of these loads.

Although carport structures are highly durable, some of them in the world unfortunately are deteriorated, damaged, collapsed or failed due to different effects. In general, these structures are destroyed and lost their qualities due to many reasons such as environmental conditions and natural disasters. Therefore, it causes irreversible negative effects on the structure. Observed structural failures occur generally due to the material degradations and poor design. In the past, several carport problems arose because of poor design. If a carport is not well designed, successfully analysed and well-constructed; it may face some problems like collapse, deformation, fracture, fatigue, cracking or failure of fixtures, fittings or partitions and discomfort for occupants. Many carport structures are exposed to destructive vertical loads such as dead load and snow loads, and these loading scenarios can cause damages to the carports (Figs. 3a, 3b). This type of damage is very dangerous since it may cause fatal and destructive crashes and fractures, also causes diversified displacement of the carport components. Therefore, damage risk should be considered and some precautions should be taken against it.

In addition to vertical loads, lateral loads such as earthquake and wind loads may also affect the carports. Lateral loads generally cause to the lateral displacement and irrevocable damage. Wind loads lead to failure of the carport roof and affect the structural stability (Fig. 3c). Moreover, many carport structures are exposed to destructive earthquakes and these earthquakes cause some damages to the structure. Earthquake based damages occur especially on the vertical bearing components of the carport such as cracking and disintegration of the structure (Fig. 3d).



Fig. 3 Structural failure of carport structures due to snow load – (a) and (b), wind load (c), earthquake (d) [16-19]

3. Concept designs

The second part of the design process is to develop conceptual models. In this stage, designer selects the initial forms, type of structures and materials in terms of required structural function. Success at this stage depends on the ability, creativity and engineering approach of designers.

3.1 Material properties

Structural performance and behaviour of a structure technically depend on the construction materials. Moreover, the cost, quality, and design of a structure vary by selected materials. Therefore, selection of the appropriate material type is a crucial and vital process for engineering structures. Today, thousands of materials can be used for the all types of structures. However, not every material may be a correct choice for a structure; therefore, it is very important to select suitable materials.

Carport structures are generally made of steel, wood, plastic and composites. Because of proven properties and significant advantages, steel has been the dominating material for the load bearing parts of structures. Moreover, polymers are widely used for non-bearing parts of structures due to their lightweight, availability, easy usability and corrosion resistance. In this study, load-bearing parts of the carports were designed as structural steel and roofs as polyethylene. Materials properties can be obtained from ANSYS library [20], which are summarized in Table 1.

Table 1 Mechanical properties of the carport materials

Structural materials	Young's modulus (MPa)	Bulk modulus (MPa)	Shear modulus (MPa)	Poisson's ratio	Density (kg/m ³)
Structural steel	2E+5	1.67E+5	0.77E+5	0.30	7,850
Polyethylene	1,100	2,291	387	0.42	950

3.2 Conceptual models

Conceptual models mean to prepare alternative models for a structure. In this part, designers develop various models such as simple and complex shapes. This step is the most interactive section for the design and main aim of developing conceptual models is to consider all possible options. Developed conceptual models depend totally on the imagination, skills and experience of the designers.

In this study, five different conceptual models were developed and it was considered to cover the equal area for all of them. Although there is infinite number of other potential models and some of them surely fit the purpose even better, the fact about optimization approaches is that it is never possible to achieve the global optimum, but just the local optimum result. Since main goal of this study is to investigate the success of finite element method while considering specified structural criteria, it is possible to apply the current design approach on every sort of different models. Moreover, several systems, which are the most popular styles of the carport structures, were used in this study. For model-1 and model-2, a sloping flat roof type was used. On the other hand, a concave roof type was preferred for model-3, model-4 and model-5. These types of roofs were designed in order to provide maximum vehicle coverage and aesthetic. Developed conceptual models in this study are shown in Fig. 4.

4. Numerical models

Numerical models are mathematical expression of a structural member or system and they are used to determine the structural behaviour that might be subjected to multiple load cases. Therefore, numerical modelling is a beneficiary method in terms of the mathematical modelling of the structures. Numerical modelling of structures gets easier owing to the improvements in computer technologies day by day. In the scope of this study, conceptual models were numerically modelled using ANSYS Workbench [20] software. Finite element model was constituted

with SOLID186 elements, which have quadratic 20-noded hexahedrons/10-noded tetrahedrons, and three degrees of freedom per node. Meshing was generated according to the complexity of the designs and adequate refinement was applied on some of the regions, which were determined subsequent to the pre- and post-analysis checking. This is why the number of nodes and elements for some of the designs vary. Fig. 5 shows the numerical model properties of the carport structures with the illustration of the meshed designs.

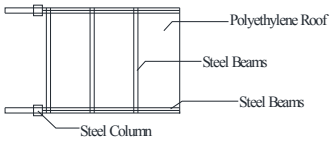
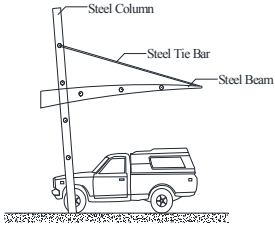
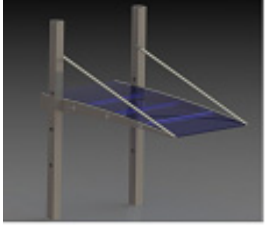
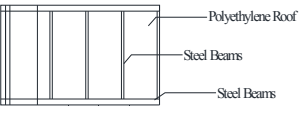
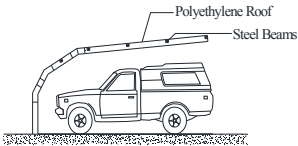
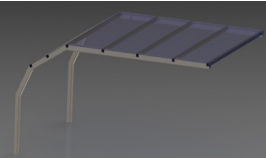
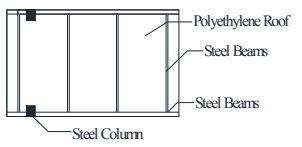
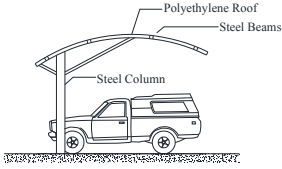
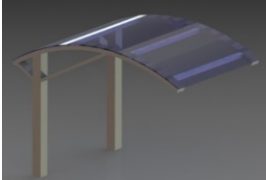
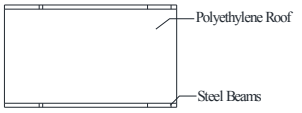
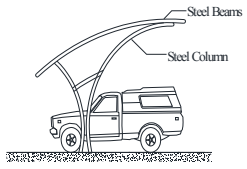
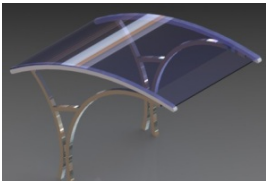
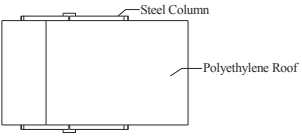
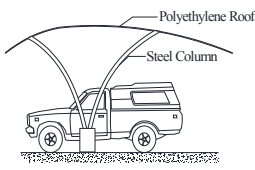
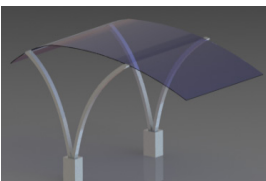
	Plan	Elevation	3D Model
Model - 1			
Model - 2			
Model - 3			
Model - 4			
Model - 5			

Fig. 4 Conceptual carport models

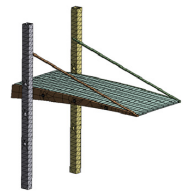
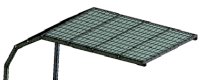
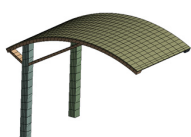

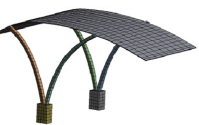
	Model - 1	Model - 2	Model - 3	Model - 4	Model - 5
Elements	20016	21584	3724	7286	1684
Nodes	110963	58192	26332	21765	12943
Numerical Model					

Fig. 5 Finite element parameters of the conceptual models

5. Finite element analysis

Material types were assigned to the structural components of the carport structures from the ANSYS material library. These materials are polyethylene and structural steel for the roof and load carrier parts, respectively. Three types of analyses were performed for each of the models. One of them is the modal analysis that examines the structural behaviour for the first mode, while the others are static structural analyses for snow and wind loadings. According to the assumptions based on international building codes, a snow load of 750 Pa was applied vertically on the roof. Wind load was applied only to the roof because lateral loading to the carrier parts could be neglected owing to their inconsiderable surface areas. Additionally, simplification and rounding off but still based on the international codes were preferred for the calculation of wind load distribution in order to generalize the loading effect for all of the structural designs. Therefore, a positive pressure of 400 Pa to the bottom facet and a suction pressure of 200 Pa to the top facet of the roof were applied in the normal direction of surface elements.

With respect to the determination of the optimum design of conceptual carport structures, volumes of the load carrier parts and total displacement values of the whole structure were recorded and used in the performance index formulation. Moreover, it is difficult and complicated to provide analysis results for each node and element. Therefore, contour pictures and scale tables were used to present the results (Figs. 6, 7). In this study, multiple load cases were considered and the FEA results are discussed within the results and discussions section.

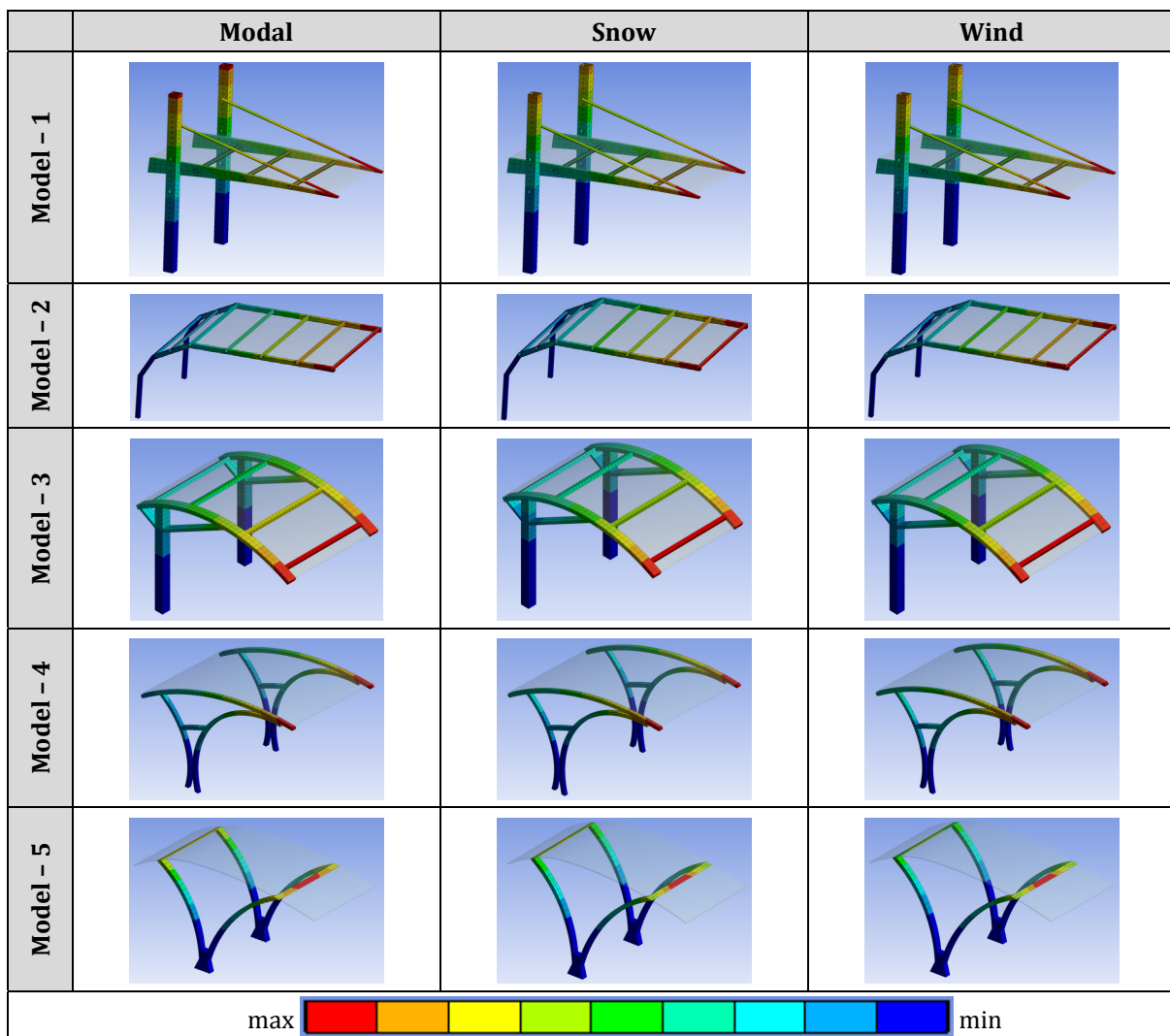


Fig. 6 Total displacement distribution of the steel bearing components

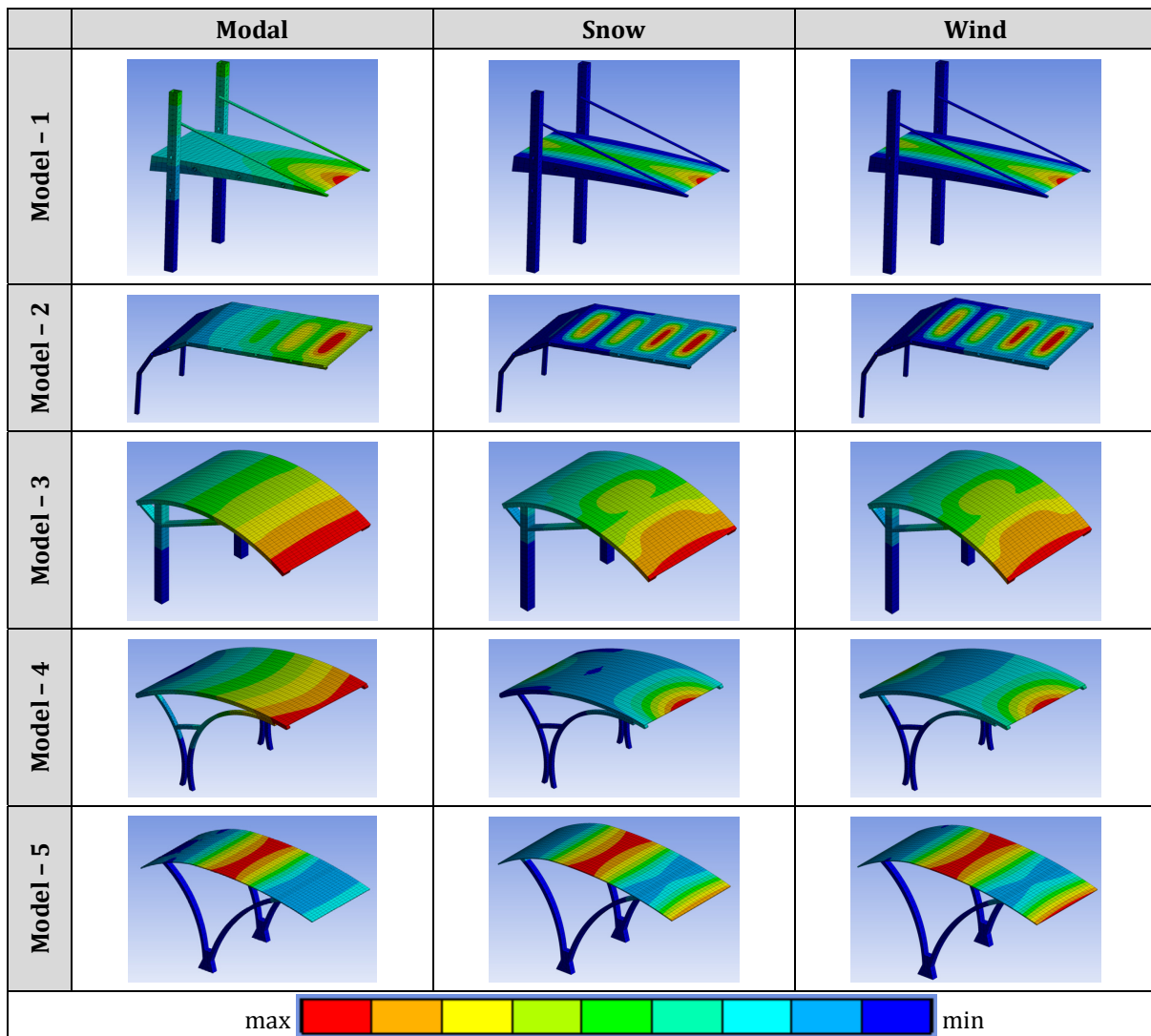


Fig. 7 Total displacement distribution of the all structural components

6. Determination of the optimum design

A structural designer should consider the effective use of materials along with the safety limit and esthetical semblance objectives. Although this point has been investigated in detail by several researchers over the last few decades, manufacturers generally put the semblance forward for the purpose of commercial concerns and push the structural performance of their designs into background.

If a technique is sought in order to answer the question “Which one is the best?”, a performance qualification method is needed to be constituted subsequent to the definition of all the design criterions [21]. In this study, five types of popular carport designs covering equal areas were evaluated. Because expected consumer benefit equality is provided for all of the models, there is no need to consider this factor. Furthermore, it should be noted that each product, including carport structures, must be optimized not only based on material concerns or structural behaviour, but also by considering the easy-for-manufacture and easy-for-assembly paradigms. The most suitable design is usually a compromise among the above mentioned requirements. Because current study deals with the rough design at the pre-production stage, it has also been neglected for the aim of obtaining optimum result. For instance, a stability analysis incorporating structural assembly details that was studied by Manifold [22] or a geotechnical investigation that was studied by Hrestak et al. [23] could be integrated as a post-verification stage to the design process in order to make sure every constraint is satisfied before the production.

Design objective for a carport structure could be summarized as satisfying material efficiency objective while maintaining a rigid behaviour against various possible load cases. Although uniform stress levels for the whole structure will assist material efficiency, size and shape dissimilarity of finite elements prevent an accurate calculation. Hence, a new modified performance index formulation, based generally on the nodal displacement levels, should be built according to the following problem definition:

$$\begin{aligned} \text{minimize} \quad & W = \sum_{e=1}^t \rho V_e \\ \text{subject to} \quad & u_{max} \leq u_{max}^* \Rightarrow \frac{u_{max}}{u_{max}^*} \geq 1 \\ & u_{avg} \geq u_{avg}^* \Rightarrow \frac{u_{avg}}{u_{avg}^*} \geq 1 \end{aligned}$$

where W is the weight of the structure, ρ is the material density, V_e is the volume of the e th element, t is the total number of elements, u_{max} is the absolute value of the maximum nodal displacement, u_{avg} is the absolute value of the average nodal displacement value while u_{max}^* and u_{avg}^* are the upper and lower bound limits of the displacement constraints, respectively.

For the determination of the optimality of carport designs, a performance index, which could be applied in a general scope and considers all the load cases, should be developed step by step. In order to constitute a rigid structure, structural performance level based on the maximum displacement value of the i th model for the j th load case is firstly defined.

$$\chi_i^I = \sum_{j=1}^n \left(\frac{u_{max}^{ij}}{u_{max}^*} \right) \quad (1)$$

Secondly, the average nodal displacement value should be added to the formulation for the purpose of assisting material efficiency qualification.

$$\chi_i^{II} = \sum_{j=1}^n \left(\frac{u_{max}^{ij}}{u_{max}^*} \frac{u_{avg}^{ij}}{u_{avg}^*} \right) \quad (2)$$

The mathematical definition of structural performance level is finalized by implementing the weight value as follows.

$$\chi_i = \frac{1}{W_i} \sum_{j=1}^n \left(\frac{u_{max}^{ij}}{u_{max}^*} \frac{u_{avg}^{ij}}{u_{avg}^*} \right) \quad (3)$$

However, there is a need to define a reference performance level in order to compare the designs with each other. Considering a certain number of models are evaluated in this study, this reference level could be formulated as the mean performance level of all models.

$$\chi_{ref} = \frac{1}{m} \sum_{i=1}^m \left[\frac{1}{W_i} \sum_{j=1}^n \left(\frac{u_{max}^{ij}}{u_{max}^*} \frac{u_{avg}^{ij}}{u_{avg}^*} \right) \right] \quad (4)$$

Finally, a performance index formulation is generated by the proportion of the i th model's and reference performance level values. It is named as PI_{rd} because of the aim to attain a rigid design while minimizing the material weight of the structure; in other words, while maximizing the material efficiency.

$$PI_{rd} = \frac{\chi_i}{\chi_{ref}} = \frac{\frac{1}{W_i} \sum_{j=1}^n \left(\frac{u_{avg}^{ij}}{u_{max}^*} \right)}{\frac{1}{m} \sum_{i=1}^m \left[\frac{1}{W_i} \sum_{j=1}^n \left(\frac{u_{avg}^{ij}}{u_{max}^*} \right) \right]} \quad (5)$$

This performance index is suitable to be used for any type of design optimization or comparison problem in order to determine the optimum structure that achieves a rigid structural behaviour with the efficient material use under multiple load cases. Optimum design selection could be practiced simply by choosing the model that has the greatest performance index.

7. Results and discussions

Five conceptual models of carport structures were analysed and investigated in this study. Expected consumer benefit equality is provided for all of the models because they have equal cover area. Modal analysis and static analyses of snow and wind loadings have been performed for each of the models. Weights of the models were calculated according to the solid volume of geometrical designs and material density of the structural parts. Subsequent to the analyses, maximum displacement and average displacement values of the structural nodes were recorded for the calculation of performance index (PI_{rd}). However, an important decision is needed to be made for the calculation of PI_{rd} . Because carport structures consist of a roof and load bearing parts, which are made of different kinds of material, it would not be completely appropriate to calculate PI_{rd} for the whole model. It should be noted that the maximum displacement was confirmed to occur on the roof part for all of the models and analyses. It is possible to decrease the displacement value of roof parts with the aid of little design modifications that would not substantially affect the structural performance in either a positive nor negative way. Since the structural behaviour of load bearing parts is more important in order to design a rigid model; PI_{rd} , which is calculated just for the load bearing parts, should be considered for the optimum design selection. Performance index values of the whole structure for all of the models are also given in this study for the purpose of providing insight into the performance decision concept. Geometrical properties (volume and weight) of the models, average-maximum displacement values for the multiple load cases (modal, snow and wind loadings) and performance index values are presented in Table 2.

Table 2 Structural analysis results of the conceptual models

	Structural parts	Volume (m ³)	Weight (kg)	Modal		Snow		Wind		PI_{rd}
				u_{avg} (mm)	u_{max} (mm)	u_{avg} (mm)	u_{max} (mm)	u_{avg} (mm)	u_{max} (mm)	
Model - 1	Bearing	0.550	4,318	15.09	26.99	1.56	3.03	1.29	2.50	0.31
	Total	0.909	4,659	15.28	49.97	1.86	27.77	1.53	22.13	0.18
Model - 2	Bearing	0.037	291	41.20	103.27	28.96	69.97	24.90	58.93	3.55
	Total	0.075	326	44.56	160.13	40.54	358.99	34.27	290.77	2.94
Model - 3	Bearing	0.516	4,053	9.84	28.76	1.56	5.13	1.28	4.18	0.20
	Total	1.000	4,512	12.43	29.30	2.05	5.64	1.69	4.59	0.48
Model - 4	Bearing	0.179	1,408	14.13	45.77	3.51	11.78	5.01	15.19	0.56
	Total	0.611	1,818	17.62	45.84	6.89	47.26	8.34	42.63	0.75
Model - 5	Bearing	0.312	2,445	6.28	15.09	6.32	17.35	4.80	13.70	0.39
	Total	0.801	2,910	27.75	92.90	29.36	82.93	22.57	63.07	0.65

According to the performance index values of their load bearing parts, the best carport structure throughout the five conceptual models is model-2. It is seen in Table 2 that PI_{rd} value of model-2 is the highest one by a wide margin in comparison to the other models'. Its PI_{rd} value is 3.55 while the second best model's is 0.56 and the last model's is 0.20. Even though the maximum displacement of the respective model is much higher as well, the closeness of the average displacement values to the maximum and particularly the lowest material weight, suggests that this model to have the best structural performance.

When the differences of PI_{rd} values, which were calculated for the whole of any structural models, are investigated, structural performances of the roof parts should be evaluated carefully. PI_{rd} values for the whole structure of models -1 and -2 are lower than the PI_{rd} values for the bearing parts, while this relation is inverse for the other models. Because the material amount is equal for all the models, one can assume that maximum displacement values of the roof parts of these two models are excessively higher than the values at bearing parts. It is true that maximum displacement values are higher but the reason why PI_{rd} value is higher for models -3, -4 and -5 is that average displacement value increased, as did the maximum displacement value. Therefore, when the structural behaviour of these five carport structures are evaluated by the performance index concept, this method indicates that model-2 has the best structural performance, regardless of having higher displacement values. However, this model can be improved in order to decrease the maximum displacement value by little modifications at lower levels. Magnification of cross-sections or supplementation of new bearing members especially at the most stressed regions will verify this objective without increasing the material weight too much. These modelling modifications should depend on designer's choice or consumer's necessity, also any appropriate geometrical optimization method could be employed as an alternative way.

8. Conclusion

A structural design problem prior to the production stage comes with many questions. These are revision of previous similar solutions, selection of the materials to be used, geometrical modelling method to be performed and determination of the best design throughout the possible designs, respectively. In case there is a need to consider multiple load cases, the complexity of the problem gets bigger. This study seeks the answer to the last question and evaluates five conceptual carport structures depending on a structural performance qualification approach. The main contribution of this research is to develop a performance index formulation in order to determine the best design before the production stage. The study intended to investigate effects of material efficiency and structural rigidity on the design of carport structures by using finite element analysis. For this aim, a performance index formulation was developed to assist the decision of material efficiency as well as structural rigidity, that is called as PI_{rd} . Formulation steps consider the influence of the geometrical properties and finite element analysis results that exhibit the structural behaviour collectively.

Subsequent to the finite element analyses of the conceptual models, which are subjected to multiple load cases, their PI_{rd} values have been calculated and commented with respect to the analysis results. Actually, the best model could have been evaluated as inadequate without any qualification method but the performance index concept leads the way by numerical results and facilitates one of the most important steps of a structural design problem.

Additionally, the production process of any type of structure involves not only materials from which the product is made of, but also the manufacturing processes, machine tools, tools, fixtures, assembly process, environment requirements etc. Integrating also esthetical semblance will make the optimum design problem more complex, however, conducting a questionnaire throughout the sectoral experts to attain a sensitivity degree is possible. In order to overcome manufacturing related concerns, modification of performance index formulation using that sensitivity degree or consulting some other optimization methods such as fuzzy logic could be considered in future studies.

References

- [1] Kosheleva, O., Kreinovich, V., Nguyen, H.T. (2015). Why it is important to precisiatate goals. *Departmental Technical Reports (CS)*, Technical Report: UTEP-CS-15-25, Paper 920.
- [2] Kirsch, U. (1981). *Optimum structural design*, McGraw Hill, New York, USA.
- [3] Cash, P., Hicks, B., Culley, S. (2015). Activity Theory as a means for multi-scale analysis of the engineering design process: A protocol study of design in practice. *Design Studies*, Vol. 38, 1-32, doi: [10.1016/j.destud.2015.02.001](https://doi.org/10.1016/j.destud.2015.02.001).
- [4] Haldankar, M., Shirahatti, A.M. (2014). Finite element analysis and optimization of commercial bus body structure, *International Journal of Engineering and Technical Research*, Vol. 2, No. 12, 175-178.
- [5] Jain, R., Tandon, P., Kumar, M.V. (2014). Optimization methodology for beam gauges of the bus body for weight reduction, *Applied and Computational Mechanics*, Vol. 8, No. 1, 47-62.
- [6] Srihari, P., Azad, D., Sreeramulu, D. (2014). Optimization of rail inserts using finite element analysis. *International Journal of Engineering, Science and Technology*, Vol. 6, No. 2, 65-75, doi: [10.4314/ijest.v6i2.5](https://doi.org/10.4314/ijest.v6i2.5).
- [7] Marczak, R.J. (2007). Optimization of elastic structures using boundary elements and a topological-shape sensitivity formulation, *Latin American Journal of Solids and Structures*, Vol. 5, No. 2, 99-117.
- [8] Rajan, S.D., Belegundu, A.D., Lee, D., Damle, A.S., St Ville, J. (2004). Finite element analysis & design optimization in a distributed computing environment, In: *Collection of Technical Papers – 10th AIAA/ISSMO Multidisciplinary Analysis and Optimization Conference*, Albany, NY, USA, Vol. 3, 1716-1726.
- [9] Moore, A. Carport History, from <https://www.versatube.com/news/carport-history>, accessed January 30, 2016.
- [10] Gebhard, D. (1992). The suburban house and the automobile, In: Wachs, M., Crawford, M. (ed.), *The car and the city: the automobile, the built environment and daily urban life*, Ann Arbor, University of Michigan Press, Michigan, USA, 106-123.
- [11] Fox, J., Jeffery, R.B. (2005). *Carport Integrity Policy*, Arizona State Historic Preservation Office, Preservation Studies, University of Arizona, USA, 1-9.
- [12] Robinson, M. (2000). Taj Mahal on a Cul de Sac: Concrete blocks, carports and architectural appropriation, *Arris – The Journal of the Southeast Chapter of the Society of Architectural Historians*, Vol. 11, 71-83.
- [13] Anonymous. Vintage Designs, Gaineswood, from <http://vintagedesigns.com/architecture/gkrev/gwd/index.htm>, accessed January 29, 2016.
- [14] Anonymous. Auto Space, *The Garage Journal*, from <http://www.garagejournal.com/2009/03/auto-space>, accessed January 29, 2016.
- [15] Anonymous. Affordable, Modern, Sustainable Homes, http://www.archdaily.com/238195/connecthomes-offers-affordable-modern-sustainable-homes/4series_carport, accessed January 29, 2016.
- [16] Anonymous. Carport Collapse (Spokane), from http://images.fanpop.com/images/image_uploads/Winter-in-the-Inland-Northwest-winter-708370_450_299.jpg, accessed January 21, 2016.
- [17] Anonymous. Imgarcade, Homemade Carport Collapse, from <http://imgarcade.com/1/homemade-carport>, accessed January 21, 2016.
- [18] Stickney, R., NBC San Diego, Collapsed Carport Crushes Cars in Alpine, from <http://www.nbcsandiego.com/news/local/Carport-Collapse-Alpine-Arnold-Way-San-Diego-Heartland--234238281.html>, accessed January 21, 2016.
- [19] Anonymous. Oxu.az, A powerful earthquake in California: There's destruction, from <http://ru.oxu.az/world/39156>, accessed January 21, 2016.
- [20] ANSYS (2014). Releases 14.0, Finite element analysis software, USA.
- [21] Özkal, F.M., Uysal, H. (2012). A fully stressed design method to determine the optimum strut-and-tie model for beam-column connections. *International Journal of Computational Methods*, Vol. 9, No. 3, 1250035, doi: [10.1142/S0219876212500351](https://doi.org/10.1142/S0219876212500351).
- [22] Manifold, S.M. (2014). Stability analysis and finite element stress analysis of a solarwing carport structure and solar panel array, Technical Report: Concurrent Design, Inc., from <http://www.concurrentdesign.com/engineering-analysis.htm>, accessed September 28, 2016.
- [23] Hrestak, T., Lazarević, A.J., Frgić, L. (2015). Stress and strain analysis during the Sleme tunnel excavation, *Technical Gazette – Tehnički Vjesnik*, Vol. 22, No. 3, 703-709, doi: [10.17559/TV-20140530103847](https://doi.org/10.17559/TV-20140530103847).

Applying multi-phase particle swarm optimization to solve bulk cargo port scheduling problem

Tang, M.^{b,c}, Gong, D.^{a,b,c,*}, Liu, S.^{b,c}, Zhang, H.^{b,c}

^aSchool of Economics & Management, Tsinghua University, China

^bSchool of Economics & Management, Beijing Jiaotong University, China

^cInternational Center for Informatics Research, Beijing Jiaotong University, China

ABSTRACT

Factors related to bulk cargo port scheduling are very complex and peculiar. Changes in the factors will affect the reusability of a model, so establishing a reliable scheduling model for bulk cargo ports is particularly important. This paper sorts the factors affecting bulk cargo port scheduling, such as the number of vessels, the number of berths, vessel-berthing constraints (basic factors), the service priority, and the makespan (special factors), and then establishes the non-deterministic polynomial (NP) model, which aims to minimize the total service time and makespan. Lastly, it solves the model based on the multi-phase particle swarm optimization (MPPSO) algorithm and Matlab. Some important conclusions are obtained. (1) For the model neglecting priority, the total service time is the smallest, whereas the maximum waiting time and maximum operating time are relatively large, and the makespan is the latest. (2) For the model considering priority, the total service time is relatively large, whereas the maximum waiting time and maximum operating time are relatively small, and the makespan is relatively early. (3) For the model considering the makespan, the total service time is the mostlargest, whereas the maximum waiting time and especially the maximum operating time are the smallest, and the makespan is the earliest. We can choose different models according to different situations in bulk cargo port scheduling.

© 2016 PEI, University of Maribor. All rights reserved.

ARTICLE INFO

Keywords:

Bulk cargo
Scheduling
Priority
Makespan
Multi-phase particle swarm optimization (MPPSO)

*Corresponding author:
gongtuipigua@163.com
(Gong, D.)

Article history:

Received 7 October 2016
Revised 9 November 2016
Accepted 10 November 2016

1. Introduction

Berths are scarce resources in bulk cargo ports, and due to the increased throughput of vessels, the berth allocation problem (BAP) is inevitable. Additionally, the uncertainty of vessels at a port, the specific demand for different vessels, the time lag of vessels leaving a port and vessel-berthing constraints will all affect the scheduling of bulk cargo ports. The berth scheduling problem deals with the assignment of vessels to berths in a marine terminal, with the objective of maximizing the ocean carriers' satisfaction (minimize delays) and/or minimizing the terminal operator's costs [1].

The vessels differ with each other in many aspects, such as loaded cargoes, freight volume, and transport types, so ports must provide different processes, facilities, resources, etc. Experience, rather than standards, is needed in bulk cargo port scheduling, and the actual work takes considerable personal time and effort [2, 3]. Due to the disadvantages of experience, scholars began to study the factors related to scheduling [4, 5]; also, the setting of a scheduling goal can play an important role in the scheduling process [6, 7], and heuristics algorithms, simulation

technology and artificial intelligence are introduced to solve the scheduling problem [8]. Factors related to bulk cargo port scheduling are very complex and peculiar, and changes in the factors will affect the reusability of a model. Existing research has not paid enough attention to special factors such as the service priority and makespan. This paper establishes the NP model, which aims to minimize the total service time and makespan, and solves the model based on the MPPSO algorithm. We organize this paper as following: In the following section, we present the literature review. In section 3, we propose the mathematical model, which forms the theoretical foundation of this study. In section 4, we solve the model based on the MPPSO algorithm, which provides the basis for our analysis. Finally, in the last section, we conclude the study.

2. Literature review

Due to the disadvantage of experience, scholars began to study the factors related to scheduling. For example, Xu considered the BAP in container terminals in which the assignment of vessels to berths was limited by water depth and tidal conditions [4]. Raa et al. dealt with the quay crane assignment problem (CAP) when scheduling vessels [5]. Meisel and Bierwirth investigated the combined problem of berth allocation and crane assignment in container terminals, and their proposed model considered the decrease of marginal productivity of quay cranes assigned to a vessel and the increase in handling time if vessels were not berthed at their desired position at the quay [10]. Cheong et al. considered a BAP that required the determination of exact berthing times and positions of incoming vessels in a container port. The proposed algorithm was developed to concurrently minimize the three objectives of makespan, waiting time, and degree of deviation from a predetermined priority schedule [1]. Golias et al. presented a berth-scheduling policy to minimize delayed departures of vessels and indirectly reduce fuel consumption and emissions produced by vessels. Vessel arrival times were considered as a variable and were optimized to accommodate the objectives of the proposed policy [11]. Türkoğulları et al. focused on the integrated planning of problems faced at container terminals. The problem included berth allocation, quay crane assignment, and quay crane assignment [12].

For the BAP, the mathematical model cannot cover all the factors, and the objective function can influence the scheduling results greatly. For example, Imai et al. minimized the waiting time to a dynamic berth assignment for vessels in the public berth system [6]. Guan et al. considered a scheduling model in which the objective was to minimize the total weighted completion time of the jobs, and this problem was motivated by the operation of berth allocation [7]. Imai et al. discussed two typical schemes for berth allocation: one in discrete locations and the other in continuous locations. The former had the advantage of being easy to schedule, and the latter exhibited the complete opposite characteristics [13]. Legato et al. presented a queuing network model of logistic activities related to the arrival, berthing, and departure processes of vessels at a container terminal, and argued that non-standard service stations, time-dependent priority mechanisms, and complex resource allocation policies could prevent the use of analytical approaches to the solution [14]. Robenek proposed an exact solution algorithm based on a branch and price framework to solve the BAP. The objective was to minimize the total service time of vessels berthing at the port [15]. Arango et al. put forward allocation planning aimed at minimizing the total service time for each vessel and considered a first-come-first-served allocation strategy [8].

A variety of heuristics algorithms, simulation technology and artificial intelligence has been introduced to solve the scheduling problem. For example, Arango et al. proposed a mathematical model and developed a heuristic procedure based on a genetic algorithm to solve non-linear problems, and Arena software computational experiments showed that the proposed model could improve the current berth management strategy [8]. Galzina et al. proposed a novel adaptive model with fuzzy particle swarm optimization to solve flow-shop scheduling problem, benchmark examples were utilized to evaluate the proposed model which is applied on flow production problem [9]. Nishimura et al. developed a heuristic procedure based on a genetic algorithm to obtain a good solution with considerably small computational effort, and experiments showed that the proposed algorithm was adaptable to real world applications [16]. Imai et al. addressed a two-objective berth allocation problem: the vessel service quality, expressed

by the minimization of delay in vessels' departure, and berth utilization, expressed by the minimization of the total service time. A genetic algorithm was proposed to solve this problem. The numerical experiments showed that the genetic algorithm outperformed subgradient optimization [17]. Fu et al. presented a genetic algorithm to analyze the integrated quay crane assignment and scheduling problem due to its complexity, and the computational results validated the performance of the proposed algorithm [18]. To optimize the process plans generated from complex parts, Wang et al. modified the traditional particle swarm optimization (PSO) algorithm [19]. Mocnik et al. put forward the modeling of dimensional deviation of workpiece using regression, ANN and PSO models [20]. Ting et al. focused on the discrete and dynamic berth allocation problem, assigning vessels to discrete berth positions and minimizing the total waiting times and handling times for all vessels. The particle swarm optimization approach was developed to solve the BAP [21].

The current studies mainly focus on influencing factors, objective functions and algorithms. Factors such as the priority service and makespan are not considered in these models, and any changes in factors will affect the model reusability. Therefore, the following research problem arises: how do specific factors affect model reusability, and what are the differences among different models? No related work solves this problem. Based on the analysis of scheduling factors, combined with the MPPSO algorithm, bulk cargo port scheduling model is formed and solved considering the priority and makespan. The models can make sense of bulk cargo port scheduling.

3. Mathematical model

In this paper, four main assumptions are made regarding the status of a vessel: (a) all vessels to be served are already in the port before the planning period starts, (b) the vessels are scheduled to arrive after the planning period starts, (c) the vessels cannot move to other berths if the berth allocation is finished, and (d) the time of vessels moving is ignored.

3.1 The standard model

There are two kinds of vessel-berthing constraints in the process of berth allocation: the physical conditions and the operating conditions. The constraints can be set as follows:

$$\sum_{i=1}^n v_i = V \text{ and } \sum_{j=1}^m b_j = B$$

$$cargo(v_i) = V_{cargo}$$

$$\sum V_{cargo} = \sum B_{type}$$

$$V_{cargo} = B_{type} = (V_{cargo}^1, V_{cargo}^2, V_{cargo}^3) \rightarrow berth(v_i) = b_j \tag{1}$$

where v_i is the vessel, b_j is the berth, V is the vessels set, B is the berth set, $cargo(v_i)$ is the cargo, V_{cargo} is the cargo type set, and B_{type} is the berth type set. Only if the cargo type is in accordance with the berth type can the job start in the berth. $berth(v_i)$ indicates berth j provides service for vessel i . Therefore, the matrix of vessel-berthing constraints can be set as follows:

$$A = \begin{bmatrix} y_{11} & \cdots & y_{1n} \\ \vdots & \ddots & \vdots \\ y_{m1} & \cdots & y_{mn} \end{bmatrix} \tag{2}$$

where $0 < i \leq m, 0 < j \leq m, i \leq m, y_{ij} = (0,1)$

The scheduling model should comprehensively consider the specific needs of different vessels, so the priority factor is included in the model:

$$P_i = \alpha v_i^{customer} + \beta v_i^{cargo} + \gamma v_i^{trade} \quad (3)$$

where α , β , and γ are the coefficients and $v_i^{customer}$, v_i^{cargo} , and v_i^{trade} are the weights of factors (vessel, its cargo and trade type), respectively. Therefore, priority X_{ijk} can be generated by P_i .

There are many variables and parameters included in the bulk cargo port scheduling model, such as the number of vessels, the number of berths, vessel-berthing constraints, the service priority, the operating time and the waiting time. Therefore, scheduling can be affected by the following multi-tuple:

$$Cap_service(V_n, B_n, W_{S_i}, T_{f_i}, T_{S_i}, T_{e_i}, T_{w_i}, B_{V_j}, B_{e_j}, X_{ijk}, y_{ij}) \quad (4)$$

where V_n is the number of vessels, B_n is the number of berths, W_{S_i} is the outturn for vessel i , T_{f_i} is the arrival time for vessel i , T_{S_i} is the job starting time for vessel i , T_{e_i} is the job finishing time for vessel i , T_{w_i} is the waiting time for vessel i , B_{V_j} is the job velocity for berth j , B_{e_j} is the job finished time for vessel in berth j , X_{ijk} is the job sequence k for vessel i in berth j , and y_{ij} is the vessel-berthing constraints.

The multi-tuple can be prolonged if more factors and parameters are added in the model, and the multi-tuple can affect the model reusability. Scheduling should pay attention to the job efficiency of berths. Therefore, the objective of the model can be minimizing the makespan, that is $Min(Max(T_{e_i}))$. The paper will analyze the standard model firstly.

To minimize the total service time (waiting time and operating time) for vessel i , that is

$$T_{S_i} - T_{f_i} + W_{S_i}/B_{V_j} \quad (5)$$

The objective of standard model is

$$Min \sum_{i=0}^{V_n} \sum_{j=0}^{B_n} (T_{S_i} - T_{f_i} + W_{S_i}/B_{V_j}) X_{ijk} \quad (6)$$

subjected to

$$\sum_{i=0}^{V_n} \sum_{j=0}^{B_n} X_{ijk} = 1, \text{ where } i = 1, 2, \dots, V_n \quad (7)$$

Each vessel should be allocated by berth, where they can be allocated only one time:

$$\sum_{i=0}^{V_n} X_{ijk} \leq 1, \text{ where } j = 1, 2, \dots, B_n \quad (8)$$

Each berth can provide service for only one vessel at a time:

$$X_{ijk} \leq y_{ij} \quad (9)$$

y_{ij} is the vessel-berthing constraints that the job must obey.

$T_{f_i} \leq T_{S_i}$ if the vessel arrival time is earlier than the job starting time, and $B_{e_j} \leq T_{S_i}$ if the job starting time of vessel i is later than the job finishing time of vessel j in berth j .

3.2 The improved model

Priority P_i is an important factor affecting scheduling, so P_i is added in the standard model. The waiting time or operating time is given the weight):

$$Min \sum_{i=0}^{V_n} \sum_{j=0}^{B_n} (T_{S_i} - T_{f_i} + W_{S_i}/B_{V_j}) X_{ijk} P_i \quad (10)$$

$$\text{Min} \sum_{i=0}^{Vn} \sum_{j=0}^{Bn} ((Ts_i - Tf_i)P_i + Ws_i/BV_j) X_{ijk} \tag{11}$$

In Eq. 10, the waiting time and operating time are given weights, and in Eq. 11, the waiting time is given the weight.

$$\text{Min}(\text{Max}(Te_i)), i \in V \tag{12}$$

$$\text{Max}(Te_i) \geq Ts_i - Tf_i + Ws_i/BV_j \tag{13}$$

$$(Ts_i - Tf_i + Ws_i/BV_j) - (Ts_{i+1} - Tf_{i+1} + Ws_{i+1}/BV_{j+1}) \geq 0 \tag{14}$$

Eq. 12 minimizes the makespan.

4. MPPSO for BAP and computational experiments

4.1 Algorithm design

MPPSO is developed to solve the BAP for a bulk cargo port.

(1) Position coding

Each vessel has information about the job berths and job sequence, so each particle has two-dimensional information about the job berths and job sequence. Job berths are affected by a vessel's own properties and berth conditions. Thus, we need to obtain the berths arrays firstly. For example, if berths 1, 3, and 6 are available for each vessel, the berths array is [1 3 6 0 0 0] (assuming six berths). The job sequence of particles can be explained by the continuous value; the smaller the value is, the earlier the vessel will obtain service (more details in Table 1).

Table 1 Example of position coding

Dimension	1	2	3
Berths	[1 3 6 0 0 0]	[1 3 0 0 0 0]	[6 0 0 0 0 0]
Sequence	2 0.6173	2 0.3214	1 0.4142

In Table 1, we can obtain the job berths and job sequence through the position decoding; that is, vessels 1 and 2 obtain service in berth 3, where berth 3 provides service for vessel 2 firstly, and vessel 3 obtains service in berth 6.

(2) Position renewal

The parameter setting of MPPSO is as follows:

- T : maximum iterations
- N : number of particle swarms
- D : dimension
- $v_{id}(t)$: velocity of the i -th particle with the d -th dimension at time t
- $x_{id}(t)$: position of the i -th particle with the d -th dimension at time t
- $g_d(t)$: best positions discovered by all particles at time t or earlier, with d -th dimension
- ph : number of phases
- pcf : phase change frequency
- g : number of groups within each phase
- C_v, C_x , and C_g : coefficient value in each group within each phase
- sl : sub-length of the dimension
- VC : velocity change variable

Therefore, the renewal process of velocity and position is expressed as follows:

$$v_{id1}(t + 1) = C_v v_{id1}(t) + C_x x_{id1}(t) + C_g g_{d1}(t) \tag{15}$$

$$x_{id1}(t + 1) = x_{id1}(t) + v_{id1}(t + 1) \tag{16}$$

$$v_{id2}(t+1) = C_v v_{id2}(t) + C_x x_{id2}(t) + C_g g_{d2}(t) \quad (17)$$

$$x_{id2}(t+1) = x_{id2}(t) + v_{id2}(t+1) \quad (18)$$

The pseudo-code for MPPSO is shown in Table 2:

Table 2 Pseudo-code for MPPSO

```

Step 0 read data: Vn and Bn
Step 1 get the berths arrays based on data
Step 2 T D N ph pcf g VC
Step 3 initialize the velocity and position for particles, get the best of positions Pgx and the best
        fitness value Pg
Step 4 iteration
for t = 1 : T
    if t is a multiple of VC reinitiate velocity
        determine its phase
        for i = 1 : N
            determine its group
            choose sl randomly from [1,min(10,n)]
            sl = roundn(rand*(min(10,D)-1)+1,0);
            deal with each dimension of particle
            d = 1;
            initialize the current dimension
            dimension limited
            while ( d <= D )
                Cache the initial position of particle
                temp (1,:,:) = x(i,:,:)
                deal with the sub dimension of particle
                for j = 0 : sl
                    updating dimension
                    d_temp = d + j;
                    if d_temp > D, break
                        Step 4.1 updating the berth
                        get the coefficient of velocity formula
                        update the velocity of berth based on formula(12)
                        update the position of berth based on formula(13)
                        if out of berth array scope, reinitiate position
                            Step 4.2 updating the sequence
                            get the coefficient of velocity formula
                            update the velocity of vessel based on formula(14)
                            update the position of vessel based on formula(15)
                end
                judge the fitness
                if fitness(temp) < fitness(x(i,:,:))
                    accept the updating
                    x(i,:,:) = temp(1,:,:)
                end
            end
            update the best of positions in particle swarm
            if fitness(x(i,:,:)) < Pg
                Pgx = x(i,:,:)
                Pg = f;
            end
        end
    end
end
Step 5 decoding

```

4.2 Computational experiments

Table 3 and Table 4 provide the data for vessels in the bulk cargo port and the data for berths, respectively.

Table 3 Data of vessels

ID	Length	Width	Trade type	Arrival time	Draft	Cargo	Cargo weight	Rating
1	224	32	foreign	2014-8-13 1:00	14.6	coal	73900	9
2	228	38	foreign	2014-8-13 19:00	13.7	bean	77000	7
3	98	14	foreign	2014-8-13 9:30	6.25	fishmeal	2600	8
4	228	32	foreign	2014-8-13 12:00	12.3	coal	64400	7
5	201	27	domestic	2014-8-13 5:00	11.6	coal	39500	8
6	191	31	domestic	2014-8-13 20:00	12.4	coal	18000	9
7	214	32	domestic	2014-8-13 7:00	12	coal	49600	3
8	201	32	domestic	2014-8-13 18:00	12.5	coal	56100	7
9	200	32	domestic	2014-8-13 23:00	12	coal	54200	8
10	226	32	domestic	2014-8-13 5:00	12.5	coal	63400	5
11	201	32	domestic	2014-8-13 17:00	12.5	coal	54500	8
12	226	32	domestic	2014-8-13 19:00	12.5	coal	61600	6
13	224	32	foreign	2014-8-13 0:00	13.2	coal	60000	9
14	224	32	foreign	2014-8-13 0:00	13.4	bean	66400	8

Note: the unit of the vessel length, vessel width and draft is meters; the unit of the cargo weight is tons.

Table 4 Data of berths

ID	Depth	Length	Velocity	Type	The finished time of operating vessel
1	15.5	250	5000	Coal	2014-08-12 20:00
2	13.5	230	4000	Coal	2010-08-12 11:00
3	12.5	165	3500	general	2014-08-12 23:00
4	12	231	2000	Coal	2014-08-12 17:00
5	13	215	5000	Coal	2014-08-13 05:00
6	14	230	4000	Bulk grain	2014-08-12 19:00

Note: the units of berths depth, berth length, and velocity are meters, and tons per hour, respectively.

The weights of coal, bean, and fishmeal are 4, 4, and 8, respectively; the weights of foreign trade and domestic trade are 10 and 2, respectively, and $\alpha = 0.5$, $\beta = 0.3$, and $\gamma = 0.2$, so the priority index can be calculated (Table 5). The larger the priority index is, the earlier the vessel will receive service. A comparative analysis of the four model proposed in Section 3 is carried out below: $ph = 2$; $pcf = 5$; $g = 2$; $sl \in [1, \min(10, D)]$; $VC = 10$; $Cv = \text{rand}$; $T = 500$; $D = 14$; $N = 30$; $Cx = \text{rand}$; $Cg = -\text{rand}$ (particle 1 is in phase 1 or particle 2 is in phase 2); $Cx = -\text{rand}$, $Cg = \text{rand}$ (particle 1 is in phase 2 or particle 2 is in phase 1).

Table 5 The priority index

ID	Value	ID	Value
1	7.7	8	5.1
2	6.7	9	5.6
3	8.4	10	4.1
4	6.7	11	5.6
5	5.6	12	4.6
6	6.1	13	7.7
7	3.1	14	7.2

(1) Model 1 – Eq. 6

The priority and makespan are not considered in this model. We use the setting as shown in Table 6. MPPSO is used to solve the model. The program runs approximately 900 times to achieve the optimal results when the objective function becomes stable and convergent, Fig. 1(a). The results are shown in Table 10. In Table 10, vessels 1, 4, and 12 obtain service in berth 1; vessels 13, 10, and 9 obtain service in berth 2; vessel 3 obtains service in berth 3; vessel 5 obtains service in berth 4; vessel 7, 11, 6, and 8 obtain service in berth 5; and vessels 14 and 2 obtain service in berth 6. The total service time is 9.55 days, and the makespan is 2014-08-14 20:24.

Table 6 Model 1 setting

berths_ships(i,4) = arrivedTime; berths_ships(i,5) = startTime; waitingTime = startTime-arrivedTime; berths_ships(i,6) = waitingTime; workingTime = ceil(weight*60/effeciency)/60/24; sum = sum + (waitingTime + workingTime).

(2) Model 2 – Eq. 10

Priority is added in this model, and the waiting time and operating time are given weights. We use the setting as shown in Table 7. MPPSO is used to solve the model, the program runs approximately 190 times to achieve the optimal results, when the objective function becomes stable and convergent, Fig. 1(b). The results are shown in Table 10. In Table 10, vessel 1, 11, 12 obtain service in berth 1; vessel 13,4, 10 obtain service in berth 2; vessel 3 still obtains service in berth 3; vessel 7 obtains service in berth 4; vessel 5,6,9,8 obtain service in berth 5; vessel 14, 2 still obtain service in berth 6; the total service time is 9.79 days; the makespan is 2014-08-14 22:57.

Table 7 Model 2 setting

berths_ships(i,4) = arrivedTime; berths_ships(i,5) = startTime; waitingTime = startTime-arrivedTime; berths_ships(i,6) = waitingTime; workingTime = ceil(weight*60/effeciency)/60/24; sum = sum + (waitingTime + workingTime)*priorityIndex.

(3) Model 3 – Eq. 11

Priority is added in this model, and the waiting time is given a weight. We use the setting as shown in Table 8. MPPSO is used to solve the model. The program runs approximately 50 times to achieve the optimal results, when the objective function becomes stable and convergent, Fig. 1(c). The results are shown in Table 10. In Table 10, vessels 1, 4, and 10 obtain service in berth 1; vessels 13, 6, and 12 obtain service in berth 2; vessel 3 still obtains service in berth 3; vessels 5 and 9 obtain service in berth 4; vessels 7, 11, and 8 obtain service in berth 5; and vessels 14 and 2 still obtain service in berth 6. The total service time is 9.81 days; and the makespan is 2014-08-15 03:51.

Table 8 Model 3 setting

berths_ships(i,4) = arrivedTime; berths_ships(i,5) = startTime; waitingTime = startTime-arrivedTime; berths_ships(i,6) = waitingTime; workingTime = ceil(weight*60/effeciency)/60/24; sum = sum + (waitingTime*priorityIndex + workingTime).

(4) Model 3 – Eq. 12

This model will minimize the makespan neglecting the priority. We use the setting as shown in Table 9. MPPSO is used to solve the model. The program runs 120 times to achieve the optimal results when the objective function becomes stable and convergent, Fig. 1(d). The results are

shown in Table 10. In Table 10, vessels 1, 12, and 4 obtain service in berth 1; vessels 13, 10, and 9 obtain service in berth 2; vessel 5 obtains service in berth 4; vessels 7, 8, 11, and 6 obtain service in berth 5; vessels 14, 3, and 2 obtain service in berth 6; and berth 3 is idle. The total service time is 10.54 days, and the makespan is 2014-08-14 20:24.

Table 9 Model 4 setting

```

Sum = sum + (waitingTime + workingTime);
start_time = start_time + workingTime;
berths_ships(i,7) = start_time;
if berths_ships(i,7) > max_finish_time
    max_finish_time = berths_ships(i,7);
end
    
```

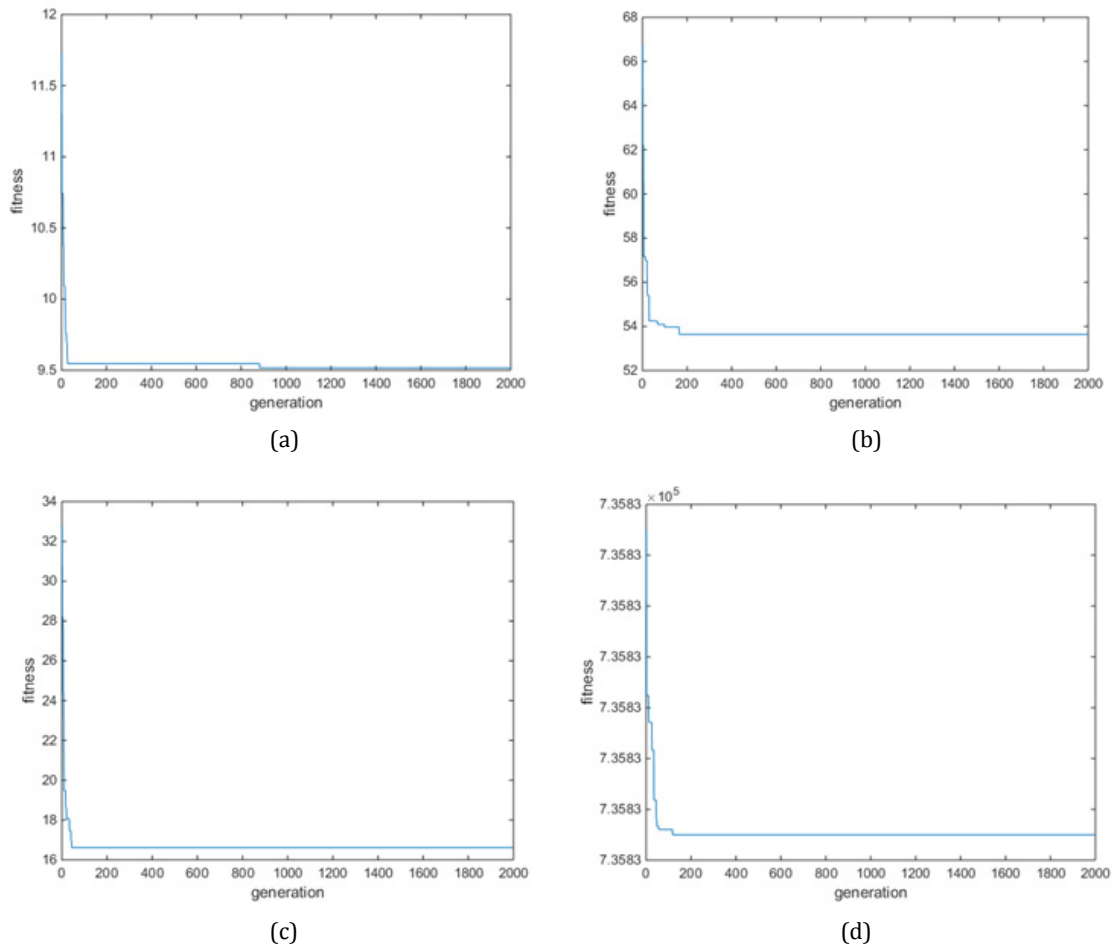


Fig. 1 Iteration process and fitness value

Table 10 MPPSO results

Model	Berth ID	Vessel ID	Starting time	Waiting time	Finishing time	Operating time
1	1	1	2014-08-13 01:00	0.00	2014-08-13 15:47	0.62
		4	2014-08-13 15:47	0.16	2014-08-14 04:40	0.54
		12	2014-08-14 04:40	0.40	2014-08-14 17:00	0.51
	2	13	2014-08-13 00:00	0.00	2014-08-13 15:00	0.63
		10	2014-08-13 15:00	0.42	2014-08-14 06:51	0.66
		9	2014-08-14 06:51	0.33	2014-08-14 20:24	0.56
	3	3	2014-08-13 09:30	0.00	2014-08-13 10:15	0.03
	4	5	2014-08-13 05:00	0.00	2014-08-14 00:45	0.82

Table 10 MPPSO results (continuation)

	7	2014-08-13 07:00	0.00	2014-08-13 16:56	0.41
	11	2014-08-13 17:00	0.00	2014-08-14 03:54	0.45
5	6	2014-08-14 03:54	0.33	2014-08-14 07:30	0.15
	8	2014-08-14 07:30	0.56	2014-08-14 18:44	0.47
	14	2014-08-13 00:00	0.00	2014-08-13 16:36	0.69
6	2	2014-08-13 19:00	0.00	2014-08-14 14:15	0.80
	1	2014-08-13 01:00	0.00	2014-08-13 15:47	0.62
	11	2014-08-13 17:00	0.00	2014-08-14 03:54	0.45
1	12	2014-08-14 03:54	0.37	2014-08-14 16:14	0.51
	13	2014-08-13 00:00	0.00	2014-08-13 15:00	0.63
	4	2014-08-13 15:00	0.13	2014-08-14 07:06	0.67
2	10	2014-08-14 07:06	1.09	2014-08-14 22:57	0.66
	3	2014-08-13 09:30	0.00	2014-08-13 10:15	0.03
2	4	2014-08-13 07:00	0.00	2014-08-14 07:48	1.03
	5	2014-08-13 05:00	0.00	2014-08-13 12:54	0.33
	6	2014-08-13 20:00	0.00	2014-08-13 23:36	0.15
	9	2014-08-13 23:36	0.03	2014-08-14 10:27	0.45
	8	2014-08-14 10:27	0.69	2014-08-14 21:41	0.47
	14	2014-08-13 00:00	0.00	2014-08-13 16:36	0.69
6	2	2014-08-13 19:00	0.00	2014-08-14 14:15	0.80
	1	2014-08-13 01:00	0.00	2014-08-13 15:47	0.62
	4	2014-08-13 15:47	0.16	2014-08-14 04:40	0.54
1	10	2014-08-14 04:40	0.99	2014-08-14 17:21	0.53
	13	2014-08-13 00:00	0.00	2014-08-13 15:00	0.63
	6	2014-08-13 20:00	0.00	2014-08-14 00:30	0.19
2	12	2014-08-14 00:30	0.23	2014-08-14 15:54	0.64
	3	2014-08-13 09:30	0.00	2014-08-13 10:15	0.03
3	4	2014-08-13 05:00	0.00	2014-08-14 00:45	0.82
	9	2014-08-14 00:45	0.07	2014-08-15 03:51	1.13
	7	2014-08-13 07:00	0.00	2014-08-13 16:56	0.41
	11	2014-08-13 17:00	0.00	2014-08-14 03:54	0.45
5	8	2014-08-14 03:54	0.41	2014-08-14 15:08	0.47
	14	2014-08-13 00:00	0.00	2014-08-13 16:36	0.69
6	2	2014-08-13 19:00	0.00	2014-08-14 14:15	0.80
	1	2014-08-13 01:00	0.00	2014-08-13 15:47	0.62
	12	2014-08-13 19:00	0.00	2014-08-14 07:20	0.51
1	4	2014-08-14 07:20	0.81	2014-08-14 20:13	0.54
	13	2014-08-13 00:00	0.00	2014-08-13 15:00	0.63
	10	2014-08-13 15:00	0.42	2014-08-14 06:51	0.66
2	9	2014-08-14 06:51	0.33	2014-08-14 20:24	0.56
	5	2014-08-13 05:00	0.00	2014-08-14 00:45	0.82
4	7	2014-08-13 07:00	0.00	2014-08-13 16:56	0.41
	8	2014-08-13 18:00	0.00	2014-08-14 05:14	0.47
	11	2014-08-14 05:14	0.51	2014-08-14 16:08	0.45
5	6	2014-08-14 16:08	0.84	2014-08-14 19:44	0.15
	14	2014-08-13 00:00	0.00	2014-08-13 16:36	0.69
	3	2014-08-13 16:36	0.30	2014-08-13 17:15	0.03
6	2	2014-08-13 19:00	0.00	2014-08-14 14:15	0.80

Note: the unit of the waiting time and operating time is days.

4.3 Discussion

On the condition of small samples ($V_n = 14$, $B_n = 6$), for Model 1, the total service time, the maximum waiting time and the maximum operating time are minimal, and the makespan is the earliest. For Model 2 and Model 3, the total service time, the maximum waiting time and the maximum operating time will be increased slightly, and the makespan can be delayed. For model 4, the total service time is the highest, but the maximum waiting time and the maximum operating time are relatively small. The makespan is also the earliest (Table 11).

On the condition of big samples ($V_n = 24$, $B_n = 6$), for Model 1, the total service time is still the smallest, but the maximum waiting time and the maximum operating time are increased. Additionally, the makespan is the latest. For Model 2 and Model 3, the total service time is still large, but the maximum waiting time and the maximum operating time are relatively small, and the makespan is competitive compared with Model 1. For model 4, the total service time is still the highest, but the maximum operating time, especially the maximum waiting time, is the lowest. The makespan is the earliest (Table 11).

On one hand, the total service time of berth needs to be decreased to satisfy the general requirements, so the model considering priority offers a great advantage. On the other hand, the total service time of berths reflects the capacity; the longer the service time is, the higher the berth service capacity will be. The departure time of the last vessel needs to be considered, so the model minimizing makespan offers a great advantage. In short, we can choose a suitable model according to the actual situation in bulk cargo port scheduling.

Table 11 Comparative results of four models

Model	Total service time		Maximum waiting time		Maximum operating time		Makespan	
	Small samples	Big samples	Small samples	Big samples	Small samples	Big samples	Small samples	Big samples
1	9.55	24.01	0.56	2.20	0.82	1.04	2014-08-14 20:24	2014-08-16 00:25
2	9.79	24.39	1.09	2.09	1.03	1.09	2014-08-14 22:57	2014-08-15 19:18
3	9.81	24.30	0.99	2.08	0.82	1.09	2014-08-15 03:51	2014-08-15 19:18
4	10.54	27.54	0.84	1.52	0.82	1.09	2014-08-14 20:24	2014-08-15 17:49

5. Conclusion

Social and economic progress drives the development of bulk cargo port transportation, so the transportation demand is also growing. However, scheduling management and efficiency are incompatible with its development. The problems are as follows: (1) The scheduling is dispersed. Due to multi-level allocation, vessel scheduling is cumbersome, and much repetitive work is done, thereby affecting the efficiency of scheduling. (2) The management mode lags behind. People basically rely on experience to manage berth scheduling. Therefore, reducing the total service time of berths and maximizing their operational capabilities (minimizing the makespan) are of great importance to improving the efficiency and management of bulk cargo port scheduling.

This paper sorts the factors affecting bulk cargo port scheduling, such as the number of vessels, the number of berths, vessel-berthing constraints, the service priority, and the makespan, and establishes the NP model, which aims to minimize the total service time and makespan, and solves the model based on the MPPSO algorithm. Through computational experiments, we obtain information not only about the berth allocation (the starting time, finishing time, waiting time, and operating time) but also the comparative results of different modes (the total service time, maximum waiting time, maximum operating time, and makespan). We can choose a suitable model according to the actual situation in bulk cargo port scheduling.

Of course, like all studies, this paper has certain limitations and deficiencies. To guarantee the computability of the model, this paper assumes that the vessels cannot move to other berths if the berth allocation is complete, and the time of vessels moving is ignored. We should further study these topics.

Acknowledgement

The study is supported by a project funded by the China Postdoctoral Science Foundation (2016M591194) and the National Natural Science Foundation (71132008,71390334). We appreciate their support very much.

References

- [1] Cheong, C.Y., Tan, K.C., Liu, D.K., Lin, C.J. (2010). Multi-objective and prioritized berth allocation in container ports, *Annals of Operations Research November*, Vol. 180, No. 1, 63-103, [doi: 10.1007/s10479-008-0493-0](https://doi.org/10.1007/s10479-008-0493-0).
- [2] Conway, R.W., Maxwell, W.L., Miller, L.W. (2003). *Theory of scheduling*, Dover publication, New York, USA.
- [3] Gantt, H. (1919). *Organization for Work*, Allen and Unwin, London, UK.
- [4] Xu, D., Li, C.L., Leung, J.Y.-T. (2012). Berth allocation with time-dependent physical limitations on vessels, *European Journal of Operational Research*, Vol. 216, No. 1, 47-56, [doi: 10.1016/j.ejor.2011.07.012](https://doi.org/10.1016/j.ejor.2011.07.012).
- [5] Raa, B., Dullaert, W., Van Schaeren, R. (2011). An enriched model for the integrated berth allocation and quay crane assignment problem, *Expert Systems with Applications*, Vol. 38, No. 11, 14136-14147, [doi: 10.1016/j.eswa.2011.04.224](https://doi.org/10.1016/j.eswa.2011.04.224).
- [6] Imai, A., Nishimura, E., Papadimitriou, S. (2001). The dynamic berth allocation problem for a container port, *Transportation Research Part B: Methodological*, Vol. 35, No. 4, 401-417, [doi: 10.1016/S0191-2615\(99\)00057-0](https://doi.org/10.1016/S0191-2615(99)00057-0).
- [7] Guan, Y., Xiao, W.Q., Cheung, R.K., Li, C.L. (2002). A multiprocessor task scheduling model for berth allocation: Heuristic and worst-case analysis, *Operations Research Letters*, Vol. 30, No. 5, 343-350, [doi: 10.1016/S0167-6377\(02\)00147-5](https://doi.org/10.1016/S0167-6377(02)00147-5).
- [8] Arango, C., Cortés, P., Muñuzuri, J., Onieva, L. (2011). Berth allocation planning in Seville inland port by simulation and optimization, *Advanced Engineering Informatics*, Vol. 25, No. 3, 452-461, [doi: 10.1016/j.aei.2011.05.001](https://doi.org/10.1016/j.aei.2011.05.001).
- [9] Galzina, V., Lujić, R., Šarić, T. (2012). Adaptive fuzzy particle swarm optimization for flow-shop scheduling problem, *Technical Gazette – Tehnički vjesnik*, Vol. 19, No. 1, 151-157.
- [10] Meisel, F., Bierwirth, C. (2009). Heuristics for the integration of crane productivity in the berth allocation problem, *Transportation Research Part E: Logistics and Transportation Review*, Vol. 45, No. 1, 196-209, [doi: 10.1016/j.tre.2008.03.001](https://doi.org/10.1016/j.tre.2008.03.001).
- [11] Golias, M.M., Saharidis, G.K., Boile, M., Theofanis S., Ierapetritou M.G. (2009). The berth allocation problem: Optimizing vessel arrival time, *Maritime Economics & Logistics*, Vol. 11, No. 4, 358-377, [doi: 10.1057/mel.2009.12](https://doi.org/10.1057/mel.2009.12).
- [12] Türkoğulları, Y.B., Taşkın, Z.C., Aras, N., Altinel, İ.K. (2014). Optimal berth allocation and time-invariant quay crane assignment in container terminals, *European Journal of Operational Research*, Vol. 235, No. 1, 88-101, [doi: 10.1016/j.ejor.2013.10.015](https://doi.org/10.1016/j.ejor.2013.10.015).
- [13] Imai, A., Sun, X., Nishimura, E., Papadimitriou, S. (2005). Berth allocation in a container port: Using a continuous location space approach, *Transportation Research Part B: Methodological*, Vol. 39, No. 3, 199-221, [doi: 10.1016/j.trb.2004.04.004](https://doi.org/10.1016/j.trb.2004.04.004).
- [14] Legato, P., Mazza, R.M. (2001). Berth planning and resources optimization at a container terminal via discrete event simulation, *European Journal of Operational Research*, Vol. 133, No. 3, 537-547, [doi: 10.1016/S0377-2217\(00\)00200-9](https://doi.org/10.1016/S0377-2217(00)00200-9).
- [15] Robenek, T., Umang, N., Bierlaire, M., Ropke, S. (2014). A branch-and-price algorithm to solve the integrated berth allocation and yard assignment problem in bulk ports, *European Journal of Operational Research*, Vol. 235, No. 2, 399-411, [doi: 10.1016/j.ejor.2013.08.015](https://doi.org/10.1016/j.ejor.2013.08.015).
- [16] Nishimura, E., Imai, A., Papadimitriou, S. (2001). Berth allocation planning in the public berth system by genetic algorithms, *European Journal of Operational Research*, Vol. 131, No. 2, 282-292, [doi: 10.1016/S0377-2217\(00\)00128-4](https://doi.org/10.1016/S0377-2217(00)00128-4).
- [17] Imai, A., Zhang, J.T., Nishimura, E., Papadimitriou, S. (2007). The berth allocation problem with service time and delay time objectives, *Maritime Economics & Logistics*, Vol. 9, No. 4, 269-290, [doi: 10.1057/palgrave.mel.9100186](https://doi.org/10.1057/palgrave.mel.9100186).
- [18] Fu, Y.M., Diabat, A., Tsai, I-T. (2014). A multi-vessel quay crane assignment and scheduling problem: Formulation and heuristic solution approach, *Expert Systems with Applications*, Vol. 41, No. 15, 6959-6965, [doi: 10.1016/j.eswa.2014.05.002](https://doi.org/10.1016/j.eswa.2014.05.002).
- [19] Wang, J.F., Kang, W.L., Zhao, J.L., Chu, K.Y. (2016). A simulation approach to the process planning problem using a modified particle swarm optimization, *Advances in Production Engineering & Management*, Vol. 11, No. 2, 77-92, [doi: 10.14743/apem2016.2.211](https://doi.org/10.14743/apem2016.2.211).
- [20] Mocnik, D., Paulic, M., Klančnik, S., Balic, J. (2014) Prediction of dimensional deviation of workpiece using regression, ANN and PSO models in turning operation, *Technical Gazette – Tehnički vjesnik*, Vol. 21, No. 1, 55-62.
- [21] Ting, C.J., Wu, K.C., Chou, H. (2014). Particle swarm optimization algorithm for the berth allocation problem, *Expert Systems with Applications*, Vol. 41, No. 4 (Part 1), 1543-1550, [doi: 10.1016/j.eswa.2013.08.051](https://doi.org/10.1016/j.eswa.2013.08.051).

A case-based reasoning approach for non-traditional machining processes selection

Boral, S.^a, Chakraborty, S.^{a,*}

^aDepartment of Production Engineering, Jadavpur University, Kolkata, West Bengal, India

ABSTRACT

To sustain in the modern era of rapid manufacturing development, it becomes necessary to generate complex shapes on materials which are highly temperature and corrosion resistant, hard to machine, and have high strength-to-weight ratio. Generation of complex shapes on those materials using conventional machining processes ultimately affects surface finish, material removal rate, accuracy, cost, safety etc. Non-traditional machining (NTM) processes have the capability to machine those advanced engineering materials with satisfactory results. But, selection of the most appropriate NTM process for a particular machining application is often a complicated task. Case-based reasoning (CBR), a domain of artificial intelligence, is a paradigm for reasoning new problems from the past experience. In CBR, a memory model is assumed for representing, indexing and organizing past similar cases, and a process model is supposed for retrieving and modifying the past cases and assimilating the new ones. This paper primarily focuses on the application of CBR approach for NTM process selection. Based on different process characteristics and process parameter values, the past similar cases are retrieved and reused to solve a current NTM process selection problem. For this, a software prototype is developed and three real time examples are cited to illustrate the application potentiality of CBR system.

© 2016 PEI, University of Maribor. All rights reserved.

ARTICLE INFO

Keywords:

Non-traditional machining processes
Process selection
Artificial intelligence
Case-based reasoning

*Corresponding author:

s_chakraborty00@yahoo.co.in
(Chakraborty, S.)

Article history:

Received 7 June 2016
Revised 25 October 2016
Accepted 12 November 2016

1. Introduction

With the development of newer materials having improved thermal, mechanical and chemical properties, it has now become quite difficult to machine those materials using conventional machining processes. These processes, generally based on cutting and abrasion mechanism, incur higher machining cost while generating complex shape features on composites, ceramics and other advanced engineering materials. The achieved surface quality and dimensional accuracy of the machined components are also not satisfactory, and often fail to meet the desired target. In these machining processes, unwanted material from the parent workpiece is generally removed employing mechanical energy. This energy is supplied by means of a cutting tool kept in contact with the workpiece, causing shear deformation along the shear plane, leading to chip formation. New exotic work materials and complex geometrical shapes on those materials have been putting more pressure on the capabilities of the conventional machining processes. This leads to the development and deployment of a new set of machining processes, popularly known as non-traditional machining (NTM) processes. In these processes, unwanted material is removed from the parent workpiece using various forms of energy, like chemical, thermal, mechanical, electrical or combination of those energies. In an NTM process, there is no direct contact between the

cutting tool and the workpiece. In abrasive jet machining process, excess material is removed by means of microscopic chips and in electrochemical machining process by electrolytic dissolution. In laser beam machining process, there is even no need of any cutting tool. It is also not necessary that the cutting tool should be harder than the workpiece material in an NTM process. Now-a-days, it has become easier to generate complex shapes on materials, like steel, carbide, titanium and its alloys, ceramics, superalloys (Inconel 718, hastelloy) etc. employing NTM processes [1,2]. Till date, there have been approximately 20 NTM processes developed and applied in modern manufacturing industries. Selection of the best suitable NTM process for a particular work material and shape feature combination is generally made by a domain expert on the basis of various factors, such as workpiece material, shape feature to be generated, material removal rate, surface finish, surface damage, corner radii, tolerance, cost, safety, power requirement etc. Thus, an expert in this domain must have a vast and in-depth knowledge about the characteristics and capabilities of different available NTM processes. But, in the present manufacturing scenario, most of the process engineers lack the requisite domain knowledge and availability of experts is also sometimes constrained.

Usually, a domain expert acquires knowledge from the past experience as well as from other reliable sources. Taking this concept as a plinth, when an expert attempts to select an NTM process for a given machining application, he/she just recalls the similar past situations and their solutions. Thus, based on the similar past problems and their solutions, new NTM process selection cases are solved. This entire cognitive process of a domain expert's thinking has given birth to a new branch of artificial intelligence (AI) technique, known as case-based reasoning (CBR) approach. This CBR approach is applied here for NTM process selection. In this paper, in order to choose the most suitable NTM process for a specific machining application, an exhaustive case-base containing the machining characteristics of various available NTM processes and their pertinent process parameters is first created. These machining characteristics and process parameter data are later used to select the feasible NTM processes according to the end requirements. The selection procedure is based on retrieval of the best matched case from the case-base using the nearest neighbourhood technique, while calculating the similarity score between two cases. The best matched case, which is retrieved from the case-base according to the values of different process characteristics as set by the process engineer/end user, has the similarity score greater than the other cases. To automate and simplify the application of CBR approach in NTM process selection, a software prototype having a graphical user interface (GUI) is designed and developed in Visual Basic 6.0. The developed system simultaneously considers both the user requirements (product characteristics) and technical requirements (process characteristics) for a given NTM process selection problem.

2. Literature review

Using two multi-attribute decision making (MADM) tools, i.e. analytic hierarchy process (AHP) and technique for order preference by similarity to ideal solution (TOPSIS), Yurdakul and C¸ogun [3] attempted to simplify the NTM process selection procedure for the manufacturing personnel. A list of feasible NTM processes satisfying the users' requirements was first generated and those processes were then ranked based on their suitability to meet the desired machining operation. An expert system was developed by Chakraborty and Dey [4] for selecting the best NTM process under constrained material and machining conditions. It would rely on the priority values of different criteria and sub-criteria for a specific NTM process selection problem, and the NTM process with the highest acceptability index was finally identified. Chakraborty and Dey [5] developed a quality function deployment (QFD)-based expert system for NTM process selection. An overall score for each of the NTM processes was estimated using the weights extracted from the house of quality matrix for various process characteristics. The overall scores of some of the NTM processes simultaneously satisfying certain critical criteria requirements were again compared and the NTM process having the maximum score was finally selected as the optimal choice. A web-based knowledge base system was proposed by Edison Chandraseelan et al. [6] for identifying the most suitable NTM process to meet some input parametric requirements,

like type of the work material, shape application, process economy, and other process capabilities, like surface finish, corner radii, width of cut, tolerance etc. Sadhu and Chakraborty [7] applied an input minimized Charnes, Cooper and Rhodes (CCR) model of data envelopment analysis for NTM process selection. Employing weighted-overall efficiency ranking method of MADM theory, the efficient NTM processes were ultimately ranked in descending order of their priorities. Temuçin et al. [8] designed a fuzzy decision support model for NTM process selection while assessing the potentials of some distinct NTM processes. Chatterjee and Chakraborty [9] proved the application potentiality of evaluation of mixed data (EVAMIX) method for solving NTM process selection problems using three demonstrative examples. Roy et al. [10] integrated fuzzy AHP and QFD techniques for selection of NTM processes based on some predefined customers' perspectives. Temuçin et al. [11] solved the NTM process selection problem under fuzzy and crisp environment, and proposed a decision support model to guide the process engineers to explore the potentials of some distinct NTM processes. The applicability of the proposed model was also validated. Khandekar and Chakraborty [12] applied fuzzy axiomatic design principles for selection of NTM processes. Madić et al. [13] demonstrated the applicability, suitability and computational procedure of operational competitiveness ratings analysis (OCRA) method for solving NTM process selection problems.

Nowadays, CBR as a part of cognitive science, has been emerged out as an interesting research topic. Amen and Vomacka [14] employed CBR approach as a tool for selection of material and heat treatment process from an exhaustive database to simplify the task of a designer. Khemani et al. [15] applied CBR approach in fused cast refractory manufacturing industry. Fang and Wong [16] applied a hybrid CBR approach in agent-based negotiation for effective supply chain management. Armaghan and Renaud [17] adopted CBR approach to prove the complementary nature of multi-criteria decisions and CBR approach. Although the past researchers applied numerous MADM methods and developed different distinct decision aids for selection of NTM processes for varying machining applications, but till date, no attempt has been put forward on selection of NTM processes using CBR approach. This paper thus proposes development of a decision making model based on CBR approach for selecting the best suited NTM process for a given machining application. It is observed that CBR is the correct and simplest approach in this domain where availability of experts is sometimes constrained. In CBR approach, a set of feasible NTM processes is first retrieved from the case-base satisfying the work material and shape feature combination. Based on the user and technical requirements, it then identifies the best matched NTM process from the stored similar cases. The past cases are just reused here for NTM process selection for providing the optimal solution.

3. CBR approach

Intelligence, being a part of cognitive science, can be defined as the process involving rational and abstract thinking. It is often goal oriented and purposeful. It consists of knowledge and feats, both conscious and unconscious, which are acquired through continuous study and experience. The AI is actually the intelligence in machines. Intelligent system is the basement of knowledge engineering. It involves several tasks, like knowledge acquisition, creation of a knowledge base, knowledge representation and use of the acquired knowledge. The represented knowledge is basically used for reasoning or inference. In AI, knowledge is represented using symbols along with heuristics or rules of thumb. While using these heuristics, one should not have to rethink when a similar problem is encountered. The expert system can be defined as an intelligent computer program that uses knowledge and inference procedures to solve problems that are difficult enough requiring significant human expertise for their solution. Basically in expert system, knowledge is represented using 'if-then' rules.

The CBR approach is a part of AI technique that utilizes information stored in the knowledge base, when similar past problems are encountered again. It provides solution to the present problem that is almost similar to the past. In CBR approach, a problem is represented as an input in the present situation. It just retrieves the most similar case to the new one from its case-base while calculating the similarity score over the defined parameters. It first searches the case history

and chooses that case having the closest similarity to the current problem. In CBR system, the case-base is well structured and documented. The case representation may be flat, where all cases are represented at the same level, or it can be hierarchical, expressing relationship between cases and sub-cases.

There are four major steps that constitute a CBR system, i.e. retrieve, reuse, revise and retain. Thus, it is also called as 4-R cycle or CBR cycle, as shown in Fig. 1. When a problem occurs in the current situation, similar past situations are retrieved from the case-base. Reusing the past cases, a predictable solution to the current problem is thus provided. If there is a need of any revision, the retrieved data are revised and retained as a new case in the case-base for future use [18-21].

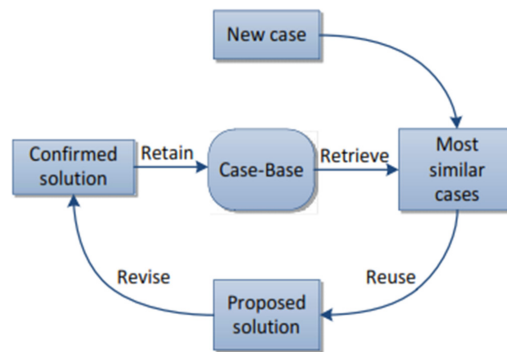


Fig. 1 A CBR cycle or 4-R cycle

Retrieving the most similar case along with the solution is based on some logical expressions. The similarity between two cases is usually measured with respect to each parameter. It also depends on the type of parameter (beneficial or non-beneficial) being used. The followings are the most common methods for calculating similarity between two cases:

a) Numeric:

$$\text{Sim}(a,b) = |a - b|/\text{Range} \quad (1)$$

where *Range* is the difference between the upper and lower boundaries of a set.

b) Symbolic:

$$\begin{aligned} \text{Sim}(a,b) &= 1 \text{ if } a = b \\ &= 0 \text{ if } a \neq b \end{aligned} \quad (2)$$

c) Multi-valued:

$$\text{Sim}(a,b) = \frac{\text{Card}(a) \cap \text{Card}(b)}{\text{Card}(a) \cup \text{Card}(b)} \quad (3)$$

where *Card* is the cardinality (size) of a set.

d) Taxonomy:

$$\text{Sim}(a,b) = \frac{h(\text{common node}(a,b))}{\min(h(a), h(b))} \quad (4)$$

where *h* is the height (number of levels) of the specified taxonomy tree.

The procedural steps of a CBR approach are presented as below:

- A solution is first defined using several parameters. One of the parameters should be chosen carefully so that it would remain unique throughout the documentation procedure, e.g. case number.
- A huge set of known solutions is put into the case-base of CBR system. An existing database can also be used for this purpose.
- The CBR system generally reads the database and organizes a copy of its own.

- d) The user generally formulates a query according to the end requirements. All the available variables are first displayed. The user has the option to choose all or few variables based on the problem statement. The query includes those variables as set by the user. The user also has the option to allocate different priority weights to the considered variables.
- e) As a result of the user-defined query, CBR system may display a number of cases or the best matched case. It may also be possible that none of the cases would match the query exactly.

Favouring CBR technique as the most efficient tool for NTM process selection is a challenging task, as several other approaches have already been available for the same purpose. It is observed from the available literature that none of the MADM methods, like AHP, EVAMIX, TOPSIS etc. can provide complete solution when the domain is ill-structured and murky. The working principle of CBR is based on some available specific experiences instead of abstracted rules. It is considered as a useful tool if the utilization of prior experience is more vital than to produce a thoroughly optimized solution according to the specifications. The CBR approach has no optimizing potentiality, but it can be used for searching, not for calculations. Its efficiency is determined by fast retrieval of the most similar cases from the case-base. The principle of CBR also states that it can find the similarities between cases but not reasons. So, it is unable to judge how important the encountered departures are that can be determined only by an experienced user.

A comparison between the existing search techniques and the adopted CBR approach is elucidated in Table 1.

Table 1 Comparison between different search techniques and CBR approach

Method	Flexibility	Operational approach	Computational time	Programming complexity	Decision maker's involvement	Type of data
Genetic algorithm	Medium (lack of learning ability)	Population based probabilistic search and optimization technique	High (based on the desired accuracy and termination criterion)	High	High	Numerical
Artificial neural network	High	Mimics the working principle of biological neurons	High	Medium	Medium	Numerical
Simulated annealing	Medium	Cooling process of molten metal is modeled artificially to construct an optimization algorithm	Medium (based on the desired accuracy and termination criterion)	High	High	Numerical
Expert system	Medium	Exact matching of input and stored data producing several 'if-then' rules for inference	Medium	Medium	High	Both numerical and textual
CBR	High	Notion of similarity between present and prior stored cases	Low	Low	Medium	Both numerical and textual

4. CBR-based approach for NTM processes selection

Although CBR approach has already been successfully applied in various fields of mechanical engineering, such as material selection, design selection, parts selection for automobile industries etc., no attempt has still been made for its application in the domain of NTM process selection. The CBR approach has the potential to provide complete information about a case where minimum information is available to the user. It yields the best results when the user provides detailed query information.

While selecting the most suitable NTM process for a particular machining application, the process engineer has to consider several machining characteristics of the available NTM processes. In the developed CBR approach-based decision making model, nine NTM processes, i.e. abrasive jet machining (AJM), abrasive water jet machining (AWJM), electric discharge machining (EDM), laser beam machining (LBM), ultrasonic machining (USM), electrochemical machining (ECM), electrochemical discharge machining (ECDM), plasma arc machining (PAM) and wire electric discharge machining (WEDM) are taken into consideration. As the process characteristics, type of the workpiece material, shape feature to be generated, material removal rate (MRR) (in mg/min), surface roughness (SR) (in μm), surface damage (SD) (in μm), tolerance (Tol) (in mm), overcut (OC) (in mm), corner radii (CR) (in mm), taper (TP) (in mm/mm), cost (C) (in relative (R) priority scale), power (P) (in kW) and safety (S) (in R scale) are considered. For cost, the R scale is set as 1 - lowest, 2 - very low, 3 - low, 4 - medium, 5 - high, 6 - very high and 7 - highest. On the other hand, for safety, the R scale is set as 1 - highly safe, 2 - safe and 3 - attention required. As work materials, a) aluminium, b) aluminium alloys, c) ceramics, d) composites, e) glass, f) steel, g) superalloys and h) titanium are considered in this model. The above-mentioned NTM processes can generate a) hole (precision) ($0.03 \text{ mm} \leq D < 0.13 \text{ mm}$), b) hole (standard) ($L/D \leq 20$), c) hole (standard) ($L/D > 20$), d) through cut (shallow) ($t/w \leq 2$), e) through cut (deep) ($t/w > 2$), f) through cavity (standard) ($t/w > 10$), g) through cavity (precision) ($t/w \leq 10$), h) pocket (shallow) ($t \leq 1 \text{ mm}$), i) pocket (deep) ($t > 1 \text{ mm}$) and j) surface of revolution feature on the work material (where L is the length of the hole, D is the diameter of the hole, t is the thickness and w is the width of the machined feature). The relevant machining characteristics data for different NTM processes are accumulated from experimentations, machining data handbooks and other reliable resources to create the corresponding case-base. The collected data are then organized in a structured manner in MS Access. The step-wise operational procedures of the developed CBR system for selecting the best suited NTM process for a particular machining application are depicted as follows:

Step 1: When the developed CBR system starts to run, the first screen, as shown in Fig. 2, appears to the end user where the type of the work material to be machined and type of the shape feature to be generated can be chosen from the given options as the primary inputs to the system.

Step 2: After clicking 'OK' button, a list of feasible NTM process(es) capable of generating the desired shape on the specified work material is displayed. For this, Eqn. (2) is utilized for filtering and retrieving the data.

Step 3: When the user presses 'Next' button, another screen, as shown in Fig. 3, is displayed to identify the most suitable NTM process from the list of feasible processes while satisfying the set machining requirements.

Step 4: In this screen, the end user has to choose the desired process characteristics based on which the final NTM process selection is made.

Step 5: When 'Enter range' functional key is clicked, the required number of empty cells are automatically generated where the input ranges for the selected NTM process characteristics can be provided.

Step 6: After inputting the desired ranges of values, pressing of 'Best NTM process' button identifies the most suitable NTM process for the specified machining application while satisfying the set criteria values. For retrieving the best NTM process in this step, Eqn. (1) is employed.

Step 7: The actual retrieved values of all the technical characteristics for the best matched NTM process are also displayed.

Step 8: When 'Best NTM process' button is clicked, the technical details (tentative settings of the associated process parameters) of the best matched NTM process are also available, as shown in Fig. 4.

Although in step 5, there is an option for entering ranges of process characteristic values, but if the developed CBR system does not find any data within those ranges from the case-base, it would retrieve the possible data nearest to the query set. For a particular NTM process selection problem, MRR is the sole beneficial attribute where its value is always required to be maximized. On the other hand, SR, SD, Tol, TP, OC, CR, C, P and S are non-beneficial attributes requiring their minimum values. The best matched case should have the highest similarity score, which is calculated with respect to each of the process characteristics. After summing up these similarity scores for the set process characteristics for each case, the NTM process having the highest similarity score is chosen as the most suitable option.

5. Illustrative examples

5.1 Example 1: Standard hole on composite material

In this example, standard holes are to be generated on a composite material. After providing the inputs of composite as the work material and hole (standard) as the shape feature options in the primary selection window of Fig. 2, a set of feasible NTM processes consisting of AJM, AWJM, ECDM, ECM, EDM, LBM and USM is displayed, when 'OK' button is clicked. All the processes can generate standard holes on composite materials. In the next window of Fig. 3, MRR, SR, Tol, OC, CR and C are opted as the most important process characteristics based on which the final NTM process selection is to be made. In this example, the desired input ranges for those process characteristics are set as MRR 100-1000 mg/min, SR 2-12 μm , Tol 0-0.5 mm, OC 0-0.05 mm, CR 0-0.5 mm and C 1-4 (in R scale). Now, when 'Best NTM process' functional button is clicked, LBM process is identified as the best matched case, capable of meeting the set process characteristic values. It is interesting to observe that apart from the set process characteristics, values of the other process characteristics are also available for the best matched NTM process. In this example, the selected LBM process can achieve values of MRR as 286.08 mg/min, SR as 2.63 μm , SD as 102 μm , Tol as 0.02 mm, OC as 0.001 mm, CR as 0.5 mm, TP as 0.05 mm/mm, C as 1 (in R scale), P as 0.23 kW and S as 3 (in R scale).

In Fig. 4, the process engineer can also have an idea about the settings of different machining parameters of LBM process. These are the tentative process parametric settings and for achieving the maximum machining performance, fine-tuning of these settings is often necessary. A real time photograph of LBM process is also available in Fig. 4.

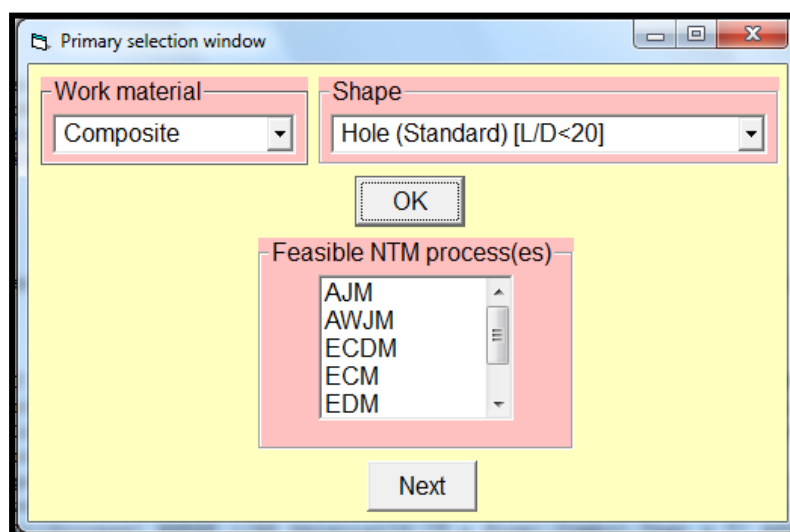


Fig. 2 Primary selection window for Example 1

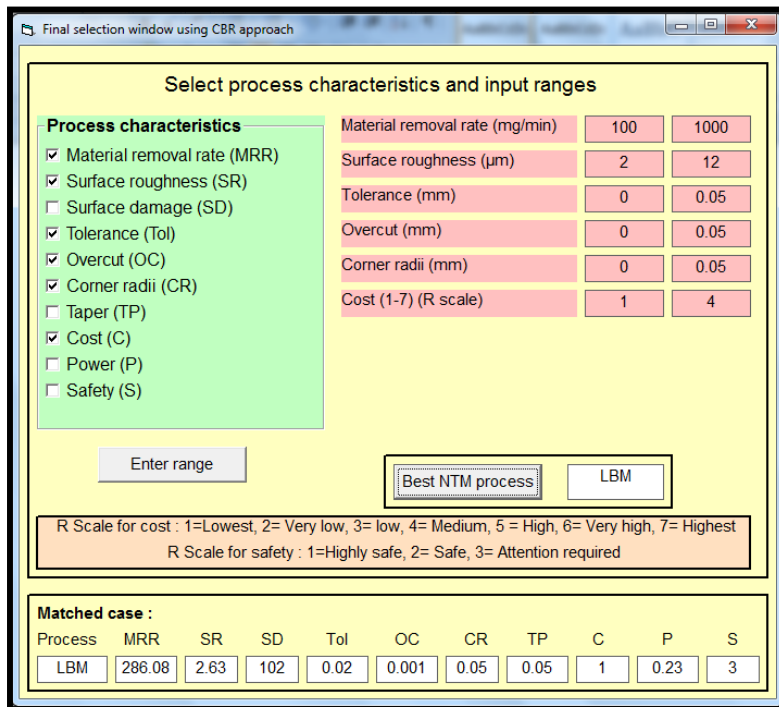


Fig. 3 Best NTM process for Example 1

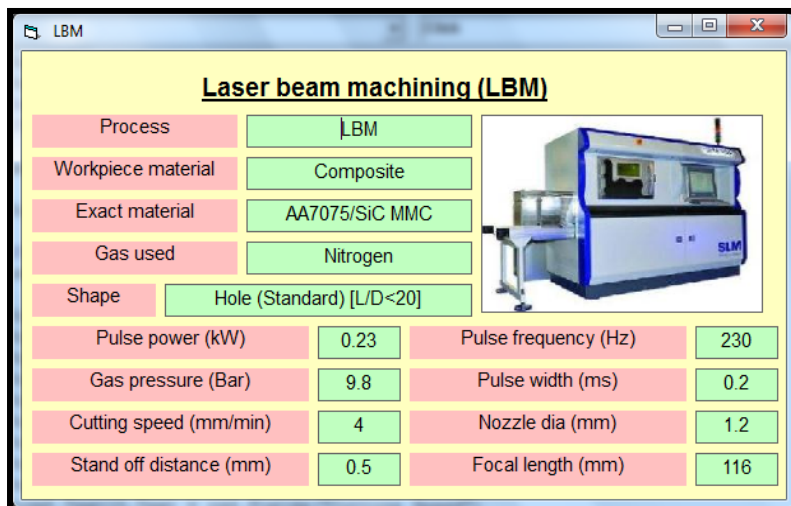


Fig. 4 Details of LBM process

5.2 Example 2: Standard through cavity on ceramics

Here, the process engineer wants to generate a standard through cavity on a ceramic work material. In the primary selection window, as shown in Fig. 5, the developed CBR approach first extracts five NTM processes, i.e. AJM, AWJM, EDM, USM and WEDM as the feasible options satisfying the said work material and shape feature combination requirement.

In Fig. 6, MRR, SR, Tol, OC, CR, C and S are chosen as the most important process characteristics based on which the final NTM process needs to be selected. Based on the ranges of values for these process characteristics, USM process is identified as the best matched case for this machining application. For USM process, the attainable process characteristics are MRR as 131.96 mg/min, SR as 0.66 µm, SD as 25 µm, Tol as 0.014 mm, OC as 0.15 mm, CR as 0.08 mm, TP as 0.005 mm/mm, C as 5 (in R scale), P as 0.4 kW and S as 1 (in R scale).

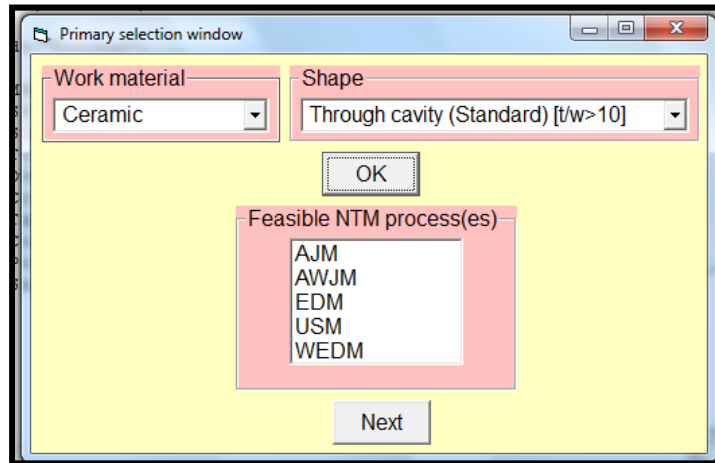


Fig. 5 Primary selection window for Example 2

In Fig. 7, the tentative parametric settings and the technical specifications of USM process along with its actual photograph are displayed to guide the process engineer to achieve the best machining performance.

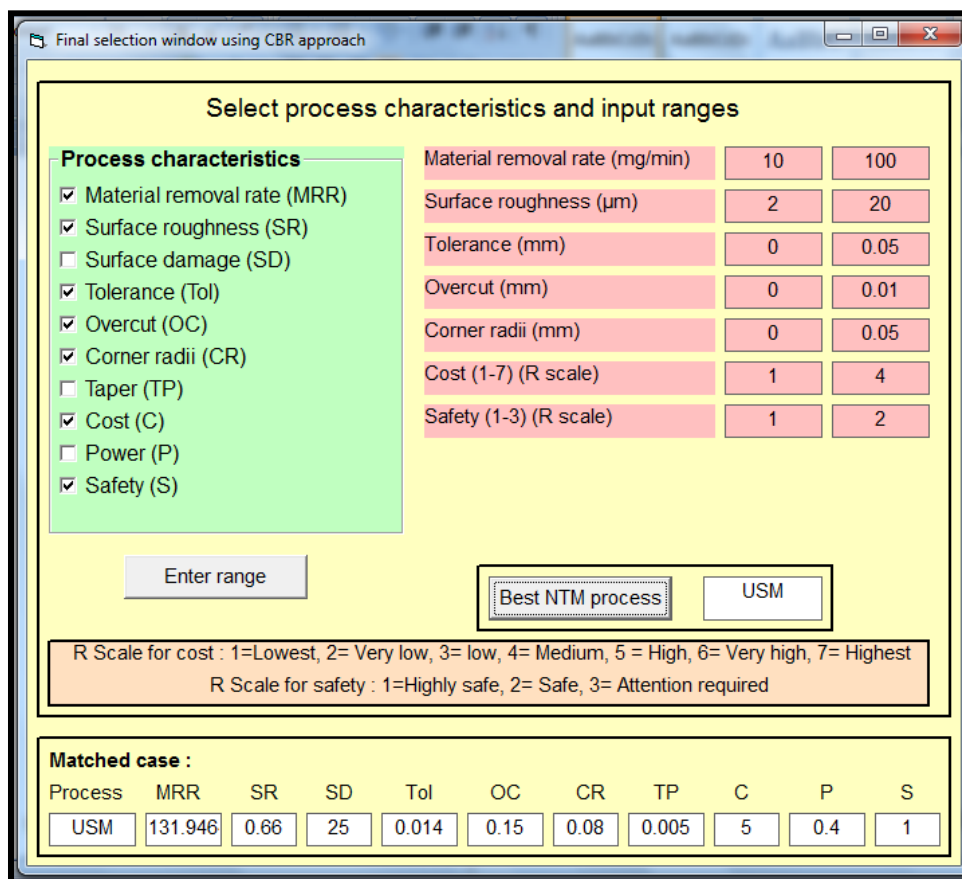


Fig. 6 Best NTM process for Example 2

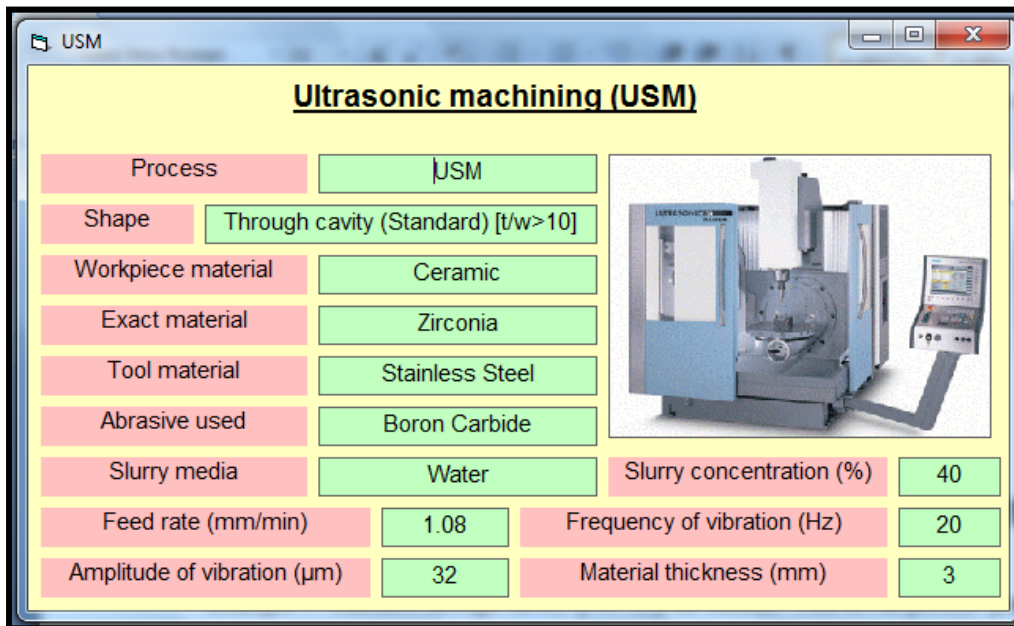


Fig. 7 Details of USM process

5.3 Example 3: Shallow through cutting on steel

In this example, a shallow through cutting operation needs to be performed on a standard steel plate. For this work material and shape feature combination, the CBR system first recognizes AJM, AWJM, ECM, EDM, LBM and PAM as the six feasible NTM processes, as shown in Fig. 8. Then, in Fig. 9, seven process characteristics, i.e. MRR, SR, SD, Tol, OC, CR and C are identified by the process engineer for the final selection of the most suited NTM process for the considered machining application. In this window, the ranges of values of the set process characteristics are also provided.

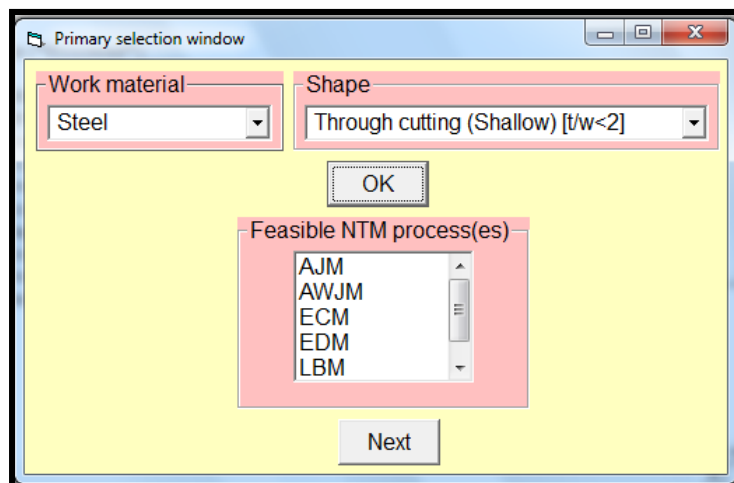


Fig. 8 Primary selection window for Example 3

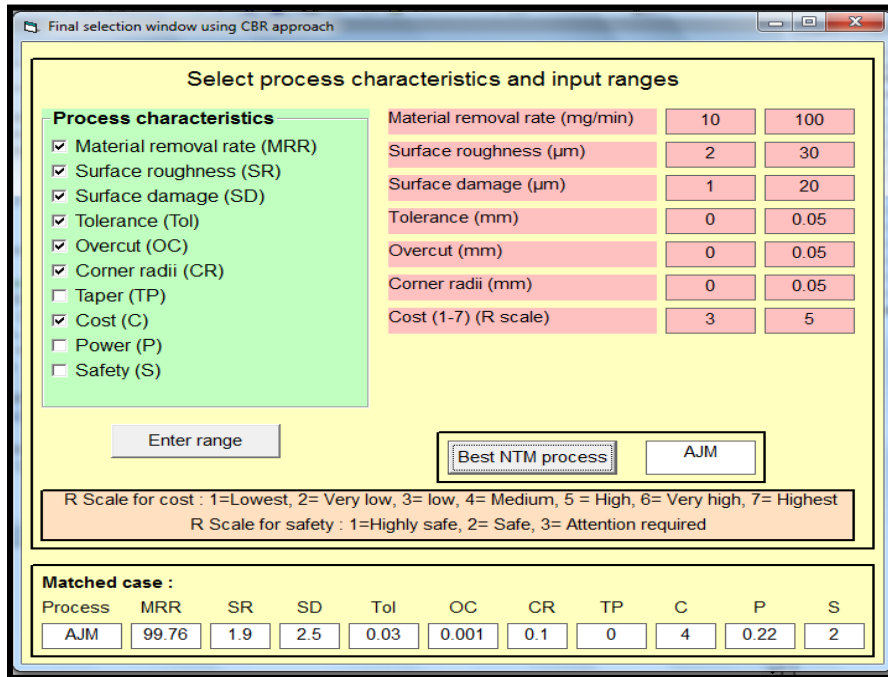


Fig. 9 Best NTM process for Example 3

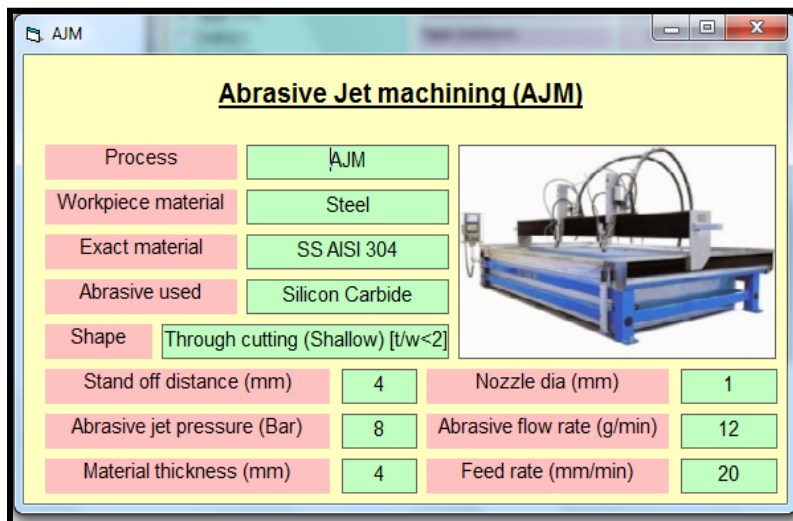


Fig. 10 Details of AJM process

The developed CBR system identifies AJM as the most appropriate NTM process for generating a shallow through cut on steel material. In Fig. 9, values of various process characteristics of AJM process are provided as MRR - 99.76 mg/min, SR - 1.9 μm , SD - 2.5 μm , Tol - 0.03 mm, OC - 0.001 mm, CR - 0.1 mm, TP - 0.005 mm/mm, C - 4 (in R scale), P - 0.22 kW and S - 2 (in R scale). In Fig. 10, this CBR system also guides the process engineer in setting the most desired values of various AJM process parameters for achieving the optimal machining performance. But, depending on the end requirements and availability of the machining setup, those AJM process parameters need to be accurately adjusted.

In CBR approach, all the cases, along with the relevant parameters, are well-structured in the case-base. They are collected from real time experiments, machining handbooks and expert's opinions. Hence, when a case is retrieved by CBR system, it is likely to be closely matched with the expert's opinion. Moreover, CBR is a technique that can provide the closest solution to the input problem. In all these three examples, the final results provided by CBR system are well validated by the experts who have a vast capability of understanding and years of experience.

In CBR approach, as the selection procedure is entirely based on similarity score calculation over several process characteristics for an efficient case retrieval, there is almost negligible probability that two cases have exactly the same similarity score. Moreover, in the developed CBR approach-based software prototype, the data type for the similarity score is considered as 'double'. Thus, two NTM processes may be apparently same from the logical as well as application point of view, but they are always slightly different based on the calculated similarity scores over several process characteristics by CBR system.

6. Conclusion

In this paper, based on CBR approach, a decision making model is developed for selecting the most appropriate NTM process for a given work material and shape feature combination. The functional mechanism of CBR approach is based on retrieving and reusing the past similar cases from the case-base. In the case-base, numerous cases are stored from the real time experimental data which are later utilized to extract the case nearest to the given query set. It is observed that the CBR system can provide a reasonable solution to a given machining problem where there is a lack of expert knowledge. The developed model can be a pathway towards new research in the direction of NTM process selection. Its potentiality and solution accuracy are validated using three real time demonstrative examples. It can also guide a process engineer in setting various NTM process parameters for a specific machining operation, although fine-tuning of those parametric settings may sometimes be required. Its accuracy can further be increased while developing a hybrid CBR system, incorporating more cases in the case-base or providing more options with respect to work material and shape feature choices. A validation of the results derived using the CBR approach against the existing search mechanisms, like genetic algorithm, simulated annealing, artificial neural network etc. may be the future scope of this research paper.

References

- [1] El-Hofy, H. (2005). *Advanced machining processes: Nontraditional and hybrid machining processes*, The McGraw-Hill Companies, New York, USA.
- [2] Pandey, P.C., Shan, H.S. (1981). *Modern machining processes*, Tata McGraw-Hill Publishing Com. Ltd., New Delhi.
- [3] Yurdakul, M., Çogun, C. (2003). Development of a multi-attribute selection procedure for non-traditional machining processes, *Proceedings of the Institution of Mechanical Engineers, Part B: Journal of Engineering Manufacture*, Vol. 217, No. 7, 993-1009.
- [4] Chakraborty, S., Dey, S. (2006). Design of an analytic-hierarchy-process-based expert system for non-traditional machining process selection, *The International Journal of Advanced Manufacturing Technology*, Vol. 31, No. 5, 490-500, doi: [10.1007/s00170-005-0216-5](https://doi.org/10.1007/s00170-005-0216-5).
- [5] Chakraborty, S., Dey, S. (2007). QFD-based expert system for non-traditional machining processes selection, *Expert Systems with Applications*, Vol. 32, No. 4, 1208-1217, doi: [10.1016/j.eswa.2006.02.010](https://doi.org/10.1016/j.eswa.2006.02.010).
- [6] Edison Chandrasselan, R., Jehadeesan, R., Raajenthiren, M. (2008). Web-based knowledge base system for selection of non-traditional machining processes, *Malaysian Journal of Computer Science*, Vol. 21, No. 1, 45-56.
- [7] Sadhu, A., Chakraborty, S. (2011). Non-traditional machining processes selection using data envelopment analysis (DEA), *Expert Systems with Applications*, Vol. 38, No. 7, 8770-8781, doi: [10.1016/j.eswa.2011.01.088](https://doi.org/10.1016/j.eswa.2011.01.088).
- [8] Temuçin, T., Tozan, H., Vayvay, Ö., Harničárová, M., Valčík, J. (2014). A fuzzy based decision model for nontraditional machining process selection, *The International Journal of Advanced Manufacturing Technology*, Vol. 70, No. 9, 2275-2282, doi: [10.1007/s00170-013-5474-z](https://doi.org/10.1007/s00170-013-5474-z).
- [9] Chatterjee, P., Chakraborty, S. (2013). Nontraditional machining processes selection using evaluation of mixed data method, *The International Journal of Advanced Manufacturing Technology*, Vol. 68, No. 5, 1613-1626, doi: [10.1007/s00170-013-4958-1](https://doi.org/10.1007/s00170-013-4958-1).
- [10] Roy, M.S., Ray, A., Pradhan, B.B. (2014). Non-traditional machining process selection using integrated fuzzy AHP and QFD techniques: A customer perspective, *Production & Manufacturing Research*, Vol. 2, No. 1, 530-549.
- [11] Temuçin, T., Tozan, H., Valčík, J., Harničárová, M. (2013). A fuzzy based decision support model for non-traditional machining process selection, *Tehnički vjesnik – Technical Gazette*, Vol. 20, No. 5, 787-793.
- [12] Khandekar, A.V., Chakraborty, S. (2016). Application of fuzzy axiomatic design principles for selection of non-traditional machining processes, *The International Journal of Advanced Manufacturing Technology*, Vol. 83, No. 1, 529-543. doi: [10.1007/s00170-015-7608-y](https://doi.org/10.1007/s00170-015-7608-y).
- [13] Madić, M., Petković, D., Radovanović, M. (2015). Selection of non-conventional machining processes using the OCRA method, *Serbian Journal of Management*, Vol. 10, No. 1, 61-73, doi: [10.5937/sjm10-6802](https://doi.org/10.5937/sjm10-6802).

- [14] Amen, R., Vomacka, P. (2001). Case-based reasoning as a tool for materials selection, *Materials & Design*, Vol. 22, No. 5, 353-358, doi: [10.1016/S0261-3069\(00\)00105-9](https://doi.org/10.1016/S0261-3069(00)00105-9).
- [15] Khemani, D., Selvamani, R.B., Dhar, A.R., Michael, S.M. (2002). InfoFrax : CBR in fused cast refractory manufacture, *Advances in Case-Based Reasoning*, 2416, 560-574, doi: [10.1007/3-540-46119-1_41](https://doi.org/10.1007/3-540-46119-1_41).
- [16] Fang, F., Wong, T.N. (2010). Applying hybrid case-based reasoning in agent-based negotiations for supply chain management, *Expert Systems with Applications*, Vol. 37, No. 12, 8322-8332, doi: [10.1016/j.eswa.2010.05.052](https://doi.org/10.1016/j.eswa.2010.05.052).
- [17] Armaghan, N., Renaud, J. (2012). An application of multi-criteria decision aids models for case-based reasoning, *Information Sciences*, Vol. 210, 55-66, doi: [10.1016/j.ins.2012.04.033](https://doi.org/10.1016/j.ins.2012.04.033).
- [18] Slade, S. (1991). Case-based reasoning: A research paradigm, *AI Magazine*, Vol. 12, No. 1, 42-55.
- [19] Kolodner, J.L. (1992). An introduction to case-based reasoning, *Artificial Intelligence Review*, Vol. 6, No. 1, 3-34, doi: [10.1007/BF00155578](https://doi.org/10.1007/BF00155578).
- [20] Aamodt, A., Plaza, E. (1994). Case-based reasoning: Foundational issues, methodological variations, and system approaches, *AI Communications*, Vol. 7, No. 1, 39-59.
- [21] Watson, I. (1999). Case-based reasoning is a methodology not a technology, *Knowledge-Based Systems*, Vol. 12, No. 5-6, 303-308, doi: [10.1016/S0950-7051\(99\)00020-9](https://doi.org/10.1016/S0950-7051(99)00020-9).

Dimensional accuracy of camera casing models 3D printed on Mcor IRIS: A case study

Mandić, M.^a, Galeta, T.^{a,*}, Raos, P.^a, Jugović, V.^a

^aMechanical Engineering Faculty in Slavonski Brod, J.J. Strossmayer University of Osijek, Slavonski Brod, Croatia

ABSTRACT

The main objective of this research was to determine the deviations and evaluate the dimensional accuracy of 3D printed camera casing models compared to the original models in the STL format. The study sample consisted of the 3D printed camera casing models and the same models in the STL format. The STL format came from Mcor in a set of sample models shipped with the 3D printer. The models were 3D printed on Mcor IRIS and then scanned with ATOS 3D scanner. A comparison between the scanned and original STL models was made in the GOM Inspect software. The results indicate that the maximum deviation occurred on the scanned front camera cover and it is 0.82 mm in the direction z. The average deviation of scanned front camera cover is 0.0845 mm and the average deviation of scanned back camera cover is 0.0722 mm. The analysis of the results proves that the three-dimensional printed paper-based parts have the dimensions close to the original CAD models.

© 2016 PEI, University of Maribor. All rights reserved.

ARTICLE INFO

Keywords:
Additive manufacturing
3D printing
Mcor IRIS
3D scanning
Accuracy

**Corresponding author:*
tgaleta@sfsb.hr
(Galeta, T.)

Article history:
Received 14 April 2016
Revised 6 October 2016
Accepted 10 October 2016

1. Introduction

One of the most important specifications of three-dimensional printing machines is the ability of a machine to print accurate parts in comparison to the designed models. The dimensional accuracy of a component part represents the degree of agreement between the manufactured dimension and its designed specification. According to current dimensioning and tolerating standards, the dimensional accuracy of a part is evaluated through its size and shape by changing the printing parameters [1]. The determination of dimensional accuracy is the topic of many researches, which is evident in the number of published papers [2-9]. The main material in this research used for printing parts is paper. Paper is subject to the influence of humidity. Furthermore, paper can absorb glue potentially causing the paper parts to shrink and change dimensions. The question is whether the paper based parts that absorb moisture and glue can have considerable dimensional accuracy compared to the original model. Therefore, determining the deviation between the paper based parts and the original STL model is the main objective of this research.

2. Method

The dimensional accuracy of 3D printed camera casing is evaluated in a few steps:

1. Printing of 3D models of camera casing,
2. Scanning of 3D models of camera casing,
3. Determination of deviation between the original STL and 3D printed models of camera casing.

The camera casing models are one of the samples shipped with the 3D printer. Model is delivered as an STL file and is considered as a reference model for further analysis. The 3D printer used in this research was model Mcor IRIS, product of Mcor Technology. It is a 360° high definition color paper-based printer, that uses standard A4 format paper (80 g/m²) as building material [10]. The STL models were aligned and prepared in the printer software SliceIT, version 6.6.02. The aligned STL camera casing model in SliceIT is shown in Fig. 1. After that, the camera casing was 3D printed. The printed models were composed of 134 built layers. Time needed for printing was 5h 51' 35". The 3D printed models of camera casing are shown in Fig. 2. Moreover, the printed models were measured with digital caliper Lux Profi model 572587, with the measurement range 1-150 mm and accuracy 0.01 mm. The measured dimensions on the front camera cover are shown at Fig. 3 i.e. on the back camera cover at Fig. 4.

After 3D printing, the camera casing models were stored inside the plastic bag in order to avoid the influence of humidity on dimensions. Furthermore, the models were kept inside the firm paper box to avoid any mechanical damage during transportation.

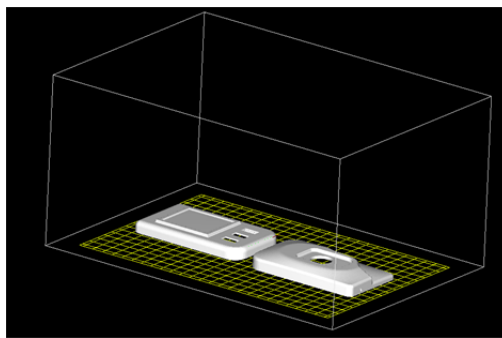


Fig. 1 STL models of camera casing aligned in Slice-IT



Fig. 2 3D printed models of camera casing

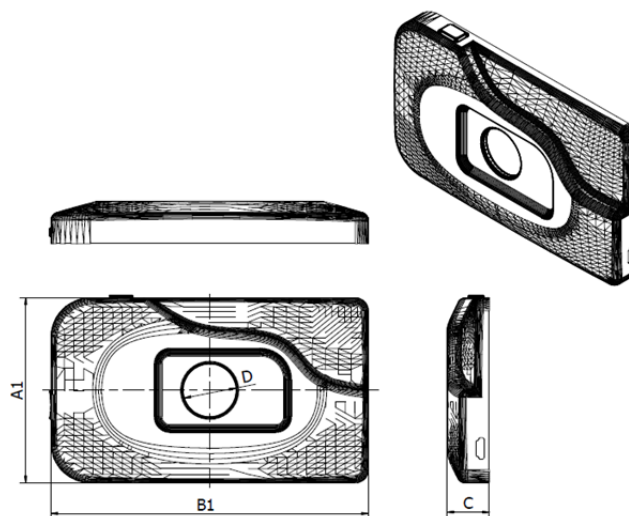


Fig. 3 Measured dimensions of original front cover

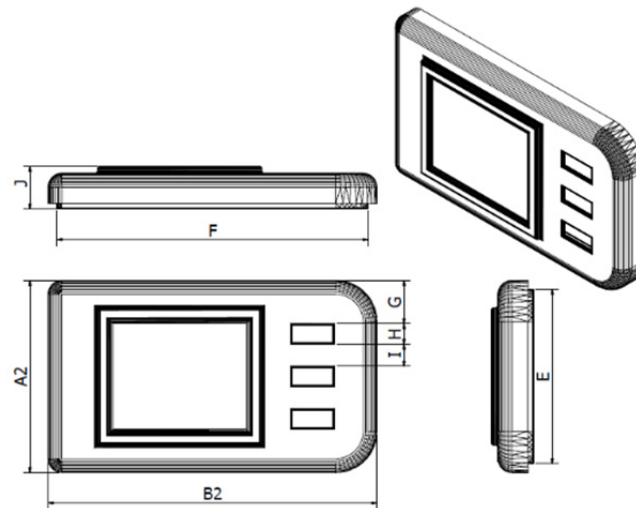


Fig. 4 Measured dimensions of original back camera cover

The printed models were scanned with 3D scanner ATOS Compact Scan 2M, product of GOM company, similar to those used in [11]. The parameters of ATOS Compact Scan 2M are as follows: Camera Pixels – $2 \times 2\,000\,000$, Measuring Area from 35×30 up to 1000×750 mm (model dimensions: $108 \times 63 \times 14.4$), Point Spacing – 0.021-0.615 mm, Working Distance – 450-1200 mm [12]. The printed camera casing was scanned and two models were obtained, the first one for the front cover and the second for the back cover. For easier comparison, the original single STL file of camera casing was separated in two files, the original front cover and the original back cover. The camera casing was separated in Autodesk Meshmixer software, version 10.9.297 [13]. Details of original, scanned and printed front cover are shown side-by-side illustrating clearly visible deviations in Fig. 5.

Furthermore, the scanned parts and the original STL parts, the front and back covers were compared in GOM Inspect software, version 8.0 [14]. In GOM Inspect, the maximum, minimum and average deviations were obtained. The original STL and scanned camera casing aligned in GOM Inspect are presented in Fig. 6. The original STL model is marked with blue color and the scanned model is marked with grey color. Obtaining the dimensions of original camera case was conducted in Autodesk Inventor 2015 using add-in Mesh Enabler version 1.0.4. Using Mesh Enabler, the STL mesh model was changed to a solid model. Fig. 3 presents the measured dimensions of original front camera cover, while the measured dimensions of original back camera cover are shown in Fig. 4. The values are listed in Table 1.



Fig. 5 Detail of original (left), scanned (middle) and printed (right) front camera cover

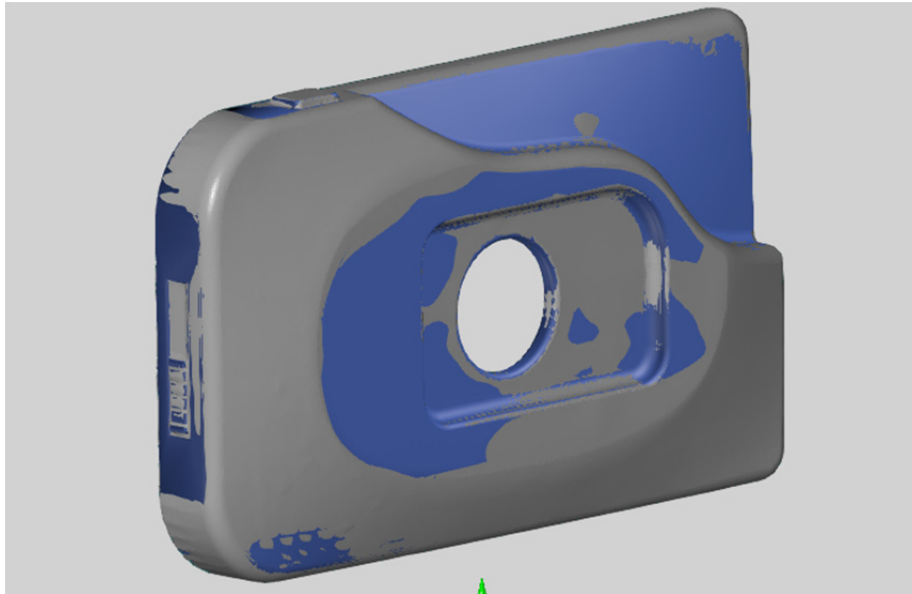


Fig. 6 Original STL (blue) and scanned front cover (grey) aligned in GOM Inspect

3. Results

The measurement results of the camera case are presented in Table 1. The nominal value of dimensions and common statistical calculated values are presented in table rows, grouped by measured dimensions. Calculated values are: arithmetic mean (\bar{x}); standard deviation (S); relative standard deviation (RSD); average error (Δx). The relative standard deviation adequately expresses the precision of a particular experiment combination regarding the measured dimensions. It is the absolute value of the coefficient of variation, usually expressed as a percentage and calculated by:

$$RSD = \frac{S}{\bar{x}} \cdot 100 \quad (1)$$

Table 1 Camera case measurements for controlled dimensions

	A1	B1	C	D	A2	B2	E	F	G	H	I	J
Nominal value	63	108	14.4	18	63	108	57.24	102.24	14.58	5.85	8.1	13.95
\bar{x}	63.1	108.06	14.46	17.94	62.98	108.05	57.22	102.24	14.49	5.94	8.11	13.58
S	0.045	0.107	0.108	0.133	0.031	0.031	0.041	0.046	0.058	0.018	0.029	0.017
RSD, %	0.072	0.099	0.747	0.742	0.049	0.028	0.071	0.045	0.397	0.302	0.354	0.126
Δx	0.10	0.06	0.06	0.06	0.02	0.05	0.02	0.00	0.09	0.09	0.01	0.37

If average error for every measured dimension on camera case are presented in a single chart, it can be noticed that the "J" dimension have significant average error compared to other dimensions (Fig. 7).

A comparison of the original STL file containing the front and back camera covers with the 3D scanned models produced on the 3D printer provided the resulting deviations for the analysis. The dimensions of original camera casing from the STL files are authoritative, considered as a reference geometry for the evaluation. The deviations with positive values mean that the scanned model is above the surface of original model and the negative deviation values are under the surface of original model. The colors on the 3D scanned model show the distribution of deviation starting with the green color for the deviations near the zero value. As deviations get more positive, the model colors are yellow, followed by red for the maximum positive value. As deviations get more negative, the colors of model are cyan, followed by blue for the maximum negative value.

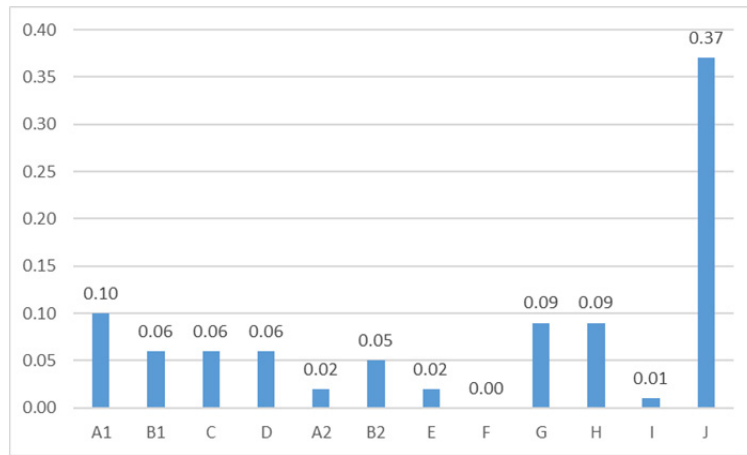


Fig. 7 Average error of camera casing

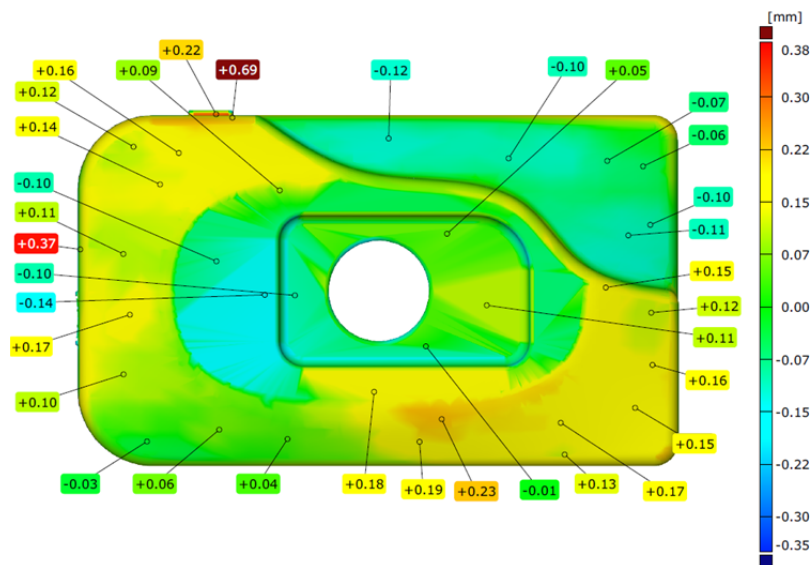


Fig. 8 Deviations of front camera cover – front view

In Fig. 8, the deviations of front camera cover from the front view are shown. The deviations are uniformed, only tenths of millimeters around zero. Maximum deviations occur on the top side of the front camera cover model: +0.69 mm. In order to investigate those deviations more closely, the top side view of the front camera cover is thoroughly examined, Fig. 9. The top side view reveals grey area on a groove for the camera switch.

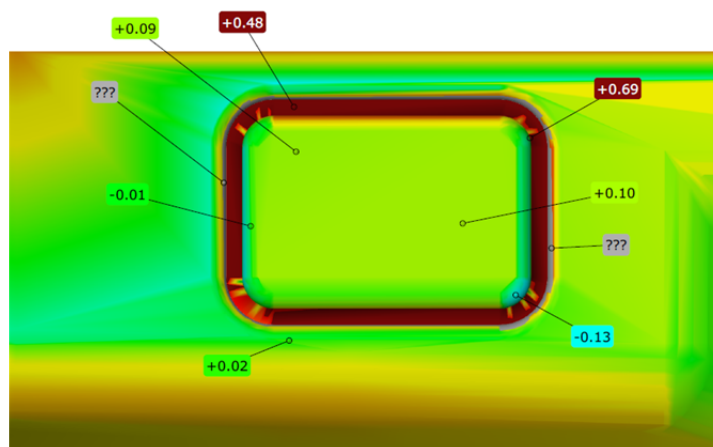


Fig. 9 Deviations of front camera cover – detail of top side view

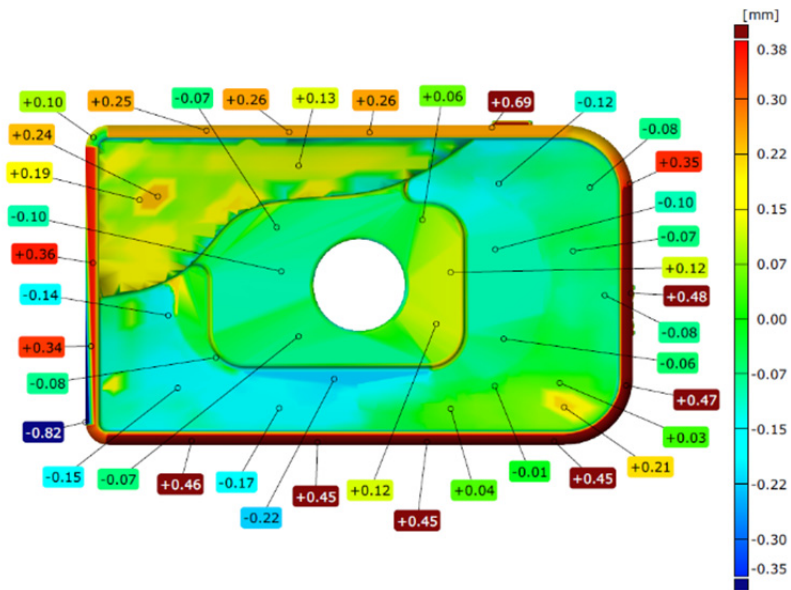


Fig. 10 Deviations of front camera cover – rear view

The deviations of front camera cover examined in the rear view (Fig. 10) reveal similar distribution. On the edge of positioning surface for the camera lens, the minimum value is -0.82 mm. These deviations must be additionally verified and further analyzed with the purpose of determining the probable causes.

Fig. 11 reveals that the deviations of back camera cover in the front view are uniformed. No significant deviations occur on a front side of the back camera cover model.

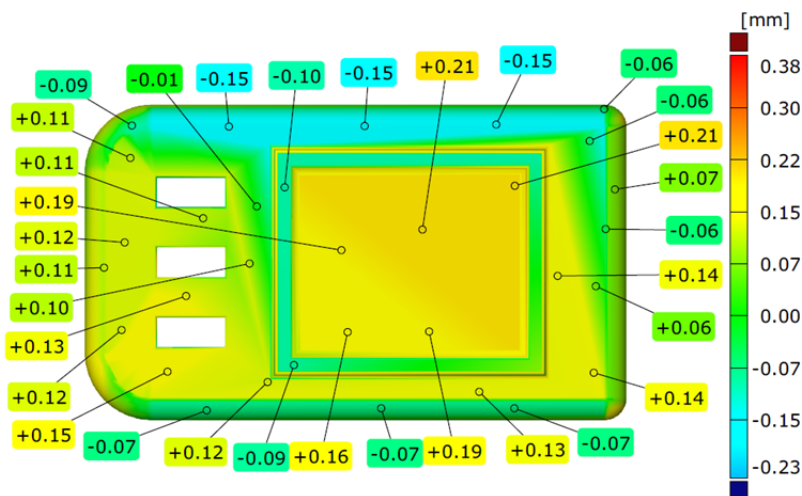


Fig. 11 Deviations of back camera cover – front view

The rear view of deviations of back camera cover presented in Figure 12 reveals maximum deviation alongside the fitting surface for joining the front and back camera cover. The maximum deviation of the fitting surface is +0.38 mm. The minimum deviation occur on the lower left edge of the bottom opening with value: -0.23 mm.

Finally, the overall average deviation of the scanned front camera cover is 0.0845 mm and the deviation of the scanned back camera cover is 0.0722 mm.

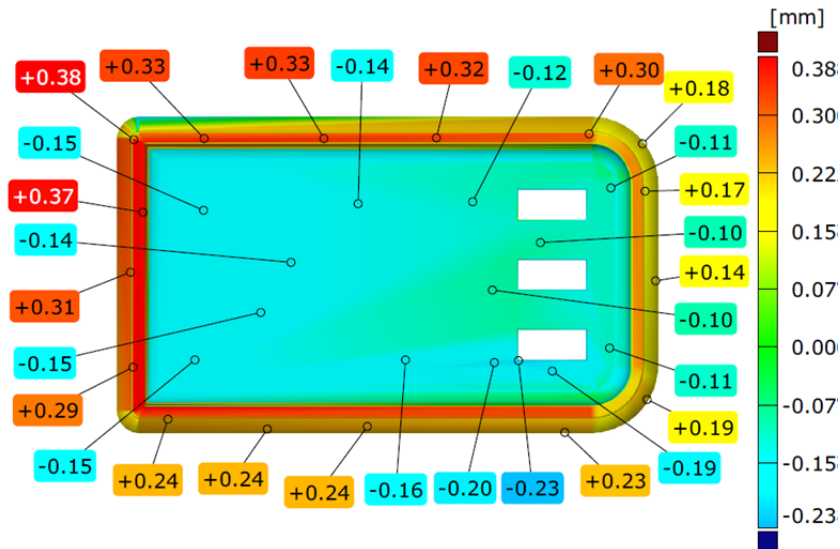


Fig. 12 Deviations of back camera cover – rear view

4. Analysis

A review of the deviations for the camera cover reveals that the maximum deviations occurred on the top side of the front case (Fig. 9). The minimum deviation occur in rear view of front case, at the edge of positioning surface for the camera lens (Fig. 10). However, no similar deviations appeared on other investigated surfaces.

In Fig. 13, the maximum deviation of the scanned camera casing model is shown. A detailed look at the critical section in GOM Inspect reveals the maximum deviation of +0.67 mm. Analysis of the average errors for measured values in Table 1, reveals the maximum value of 0.37 mm. Based on that, the upper deviation limit in GOM inspect is set to 1 mm so every deviation above 1 mm is colored grey i.e. ignored. Due to the light reflection, scanner software is interpolating surface in shape as shown at Fig. 14.

Detail section analysis of minimum deviation on front camera case (Fig. 10) did not reveal deviation of -0.82 mm (Fig. 15). Furthermore, analysis of this section show large sized triangles (Fig. 16) most probably generated during conversion of original CAD model to STL. The effect of large deviation can be compared with hang glider and pilot: if observer look at the side view, he will notice only small distance between pilot and glider's large kite. However, if observer looks from the top, he can clearly see large distance between tips of the kite and the pilot. In the same way, cross-section here does not reveal present big distance. The whole model of camera case verified the deviations only in the range of tenths of millimeters.

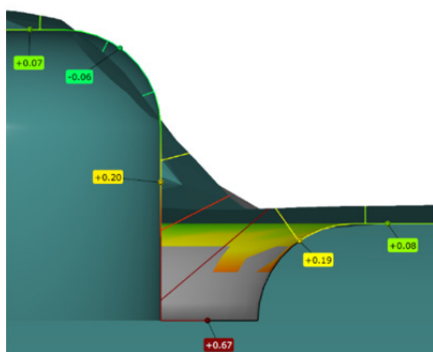


Fig. 13 Detail of section with maximum deviation of scanned camera casing model

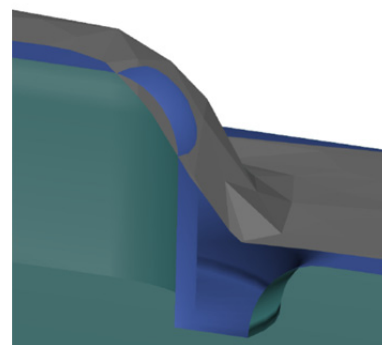


Fig. 14 Generated model (blue) and scanned model (grey)

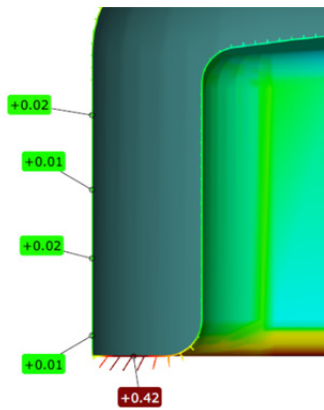


Fig. 15 Detail of section with minimum deviation of scanned camera casing model

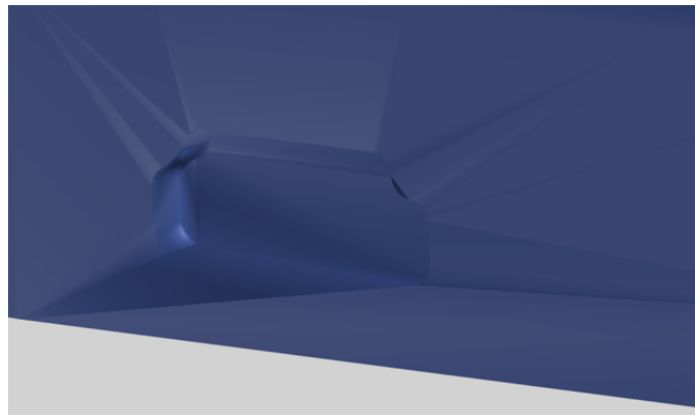


Fig. 16 Large size triangles on section with minimum deviation of scanned camera casing model

5. Conclusion

The results obtained in this research confirmed that the paper-based model has satisfactory accuracy, with the average deviation within only tenths of millimeters. Such low deviations confirm the accuracy of Mcor IRIS specified by manufacturer.

Selected long shell models enable special observation of accuracy in Z direction. Z direction in long thin models might be more affected by cutting force, humidity, gluing and post-processing. However, 3D scanning results did not reveal significant neither concave nor convex deviations in Z direction, thus confirming that glued papers successfully withstand 3D printing process and deliver sufficient rigidity.

Moreover, since we printed two parts, we were able to test mating and relative insertion of parts. It is additional verification of assembling capabilities for this particular technology, valuable to design engineers.

Paper changes due to absorbing of glue during the gluing process and removing of excess paper result in slight deviations in both positive and negative directions. High deviations that occurred in some sections of the camera casing were caused by the light noise and reflection during the 3D scanning process.

Since the accuracy of paper-based 3D printing is mainly constrained by the paper thickness and cutting methods, in order to improve the accuracy, researchers and manufacturers could devote some additional effort in this direction. The adjustable cutting angle of the knife might reduce the stair-look of sloped surface. The following experimental analysis of measured surface roughness similar to the conventional processes should verify the method [15]. However, the adjustable cutting angle will certainly result in a more complicated tool holder and controlling logic. It could furthermore increase time for 3D printing, so it should be very carefully balanced. The tests with thinner paper could also be considered to improve the accuracy, although it might require some greater changes of the actual 3D printer's components.

Acknowledgement

The authors wish to thank Industrial Park Nova Gradiška (IPNG) for assistance and 3D scanning of printed model and to Professor Željka Rosandić for proofreading the manuscript. The work presented in this paper was financially supported by the Ministry of Science, Education and Sports, Republic of Croatia and by the European Union through the project IPA2007/HR/16IPO/001-040504.

References

- [1] Farzadi, A., Waran, V., Solati-Hashjin, M., Rahman, Z.A.A., Asadi, M., Osman, N.A.A. (2015). Effect of layer printing delay on mechanical properties and dimensional accuracy of 3D printed porous prototypes in bone tissue engineering, *Ceramics International*, Vol. 41, No. 7, 8320-8330, doi: [10.1016/j.ceramint.2015.03.004](https://doi.org/10.1016/j.ceramint.2015.03.004).
- [2] Farzadi, A., Solati-Hashjin, M., Asadi-Eydivand, M., Abu Osman, N.A., (2014). Effect of layer thickness and printing orientation on mechanical properties and dimensional accuracy of 3D printed porous samples for bone tissue engineering, *PLoS ONE*, Vol. 9, No. 9, e108252, doi: [10.1371/journal.pone.0108252](https://doi.org/10.1371/journal.pone.0108252).
- [3] Galantucci, L.M., Bodi, I., Kacani, J., Lavecchia, F. (2015). Analysis of dimensional performance for a 3D open-source printer based on fused deposition modeling technique, *Procedia CIRP*, Vol. 28, 82-87, doi: [10.1016/j.procir.2015.04.014](https://doi.org/10.1016/j.procir.2015.04.014).
- [4] Galeta, T., Kljajin, M., Karakasic, M. (2008). Geometric Accuracy by 2-D Printing Model, *Strojniški Vestnik – Journal of Mechanical Engineering*, Vol. 54, No. 10, 725-733.
- [5] Daneshmand, S., Aghanajafi, C., Shahverdi, H. (2013). Investigation of rapid manufacturing technology effect on aerodynamics properties (Istraživanje utjecaja tehnologije brze izrade na aerodinamička svojstva), *Tehnički vjesnik – Technical gazette*, Vol. 20, No. 3, 425-433.
- [6] Scuzs, T.D., Brabazon, D. (2007). Analysis of the Effects of 3DP Parameters on Part Feature Dimensional Accuracy, In: *Proceedings of the Solid Freeform Fabrication Symposium*, Austin, Texas, USA, 20-31.
- [7] Asadi-Eydivand, M., Solati-Hashjin, M., Farzad, A., M., Osman, N.A.A. (2016). Effect of technical parameters on porous structure and strength of 3D printed calcium sulfate prototypes, *Robotics and Computer-Integrated Manufacturing*, Vol. 37, 57-67, doi: [10.1016/j.rcim.2015.06.005](https://doi.org/10.1016/j.rcim.2015.06.005).
- [8] Islam, M.N., Boswell, B., Pramanik, A. (2013). An investigation of dimensional accuracy of parts produced by three-dimensional printing, In: *Proceedings of the World Congress on Engineering*, London, United Kingdom, 522-525.
- [9] Fahad, M., Hopkinson, N. (2012). A new benchmarking part for evaluating the accuracy and repeatability of additive manufacturing (AM) processes, In: *2nd International Conference on Mechanical, Production and Automobile Engineering*, Singapore, 234-238.
- [10] Mcor Technologies, Mcor IRIS HD Features & Specs, from <http://mcor technologies.com/3d-printers/iris/>, accessed August 1, 2015.
- [11] Tomasiak, J. (2012). Rapid technology in industrial fitting, In: *Annals of DAAAM for 2012 & Proceedings of the 23rd International DAAAM Symposium*, Vol. 23, No. 1, 433-436.
- [12] GOM, ATOS Compact Scan, from <http://www.gom.com/metrology-systems/system-overview/atos-compact-scan.html>, accessed August 4, 2015.
- [13] Meshmixer., MeshmixerManual, from <http://meshmixer.com/help/manual/MeshmixerManual.pdf>, accessed August 4, 2015.
- [14] GOM, GOM Inspect Software, from <http://www.gom.com/3d-software/gom-inspect.html>, accessed August 4, 2015.
- [15] Krolczyk, G.M., Legutko, S. (2014). Experimental analysis by measurement of surface roughness variations in turning process of duplex stainless steel, *Metrology and Measurement Systems*, Vol. 21, No. 4, doi: [10.2478/mms-2014-0060](https://doi.org/10.2478/mms-2014-0060).

Effect of delayed differentiation on a multiproduct vendor-buyer integrated inventory system with rework

Chiu, Y.-S.P.^a, Kuo, J.-S.^a, Chiu, S.W.^{b,*}, Hsieh, Y.-T.^a

^aDepartment of Industrial Engineering and Management, Chaoyang University of Technology, Wufong, Taichung, Taiwan

^bDepartment of Business Administration, Chaoyang University of Technology, Wufong, Taichung, Taiwan

ABSTRACT

This study explores the effect of delayed differentiation on a multiproduct vendor-buyer integrated inventory system with rework to identify its potential benefits and provide managers with in-depth information for operational decision-making. The main considerations of the proposed study include a multiproduct fabrication plan to increase machine utilization, a rework process to ensure product quality, and a multi-shipment policy to distribute the end products. In addition, these products sharing an intermediate part for which a two-stage fabrication scheme is adopted, wherein the common parts are produced at the first stage and the end products are manufactured at the second stage. The aim is to reduce the overall system costs and shorten the replenishment cycle time. Mathematical modeling and optimization methods were employed to derive the closed-form optimal replenishment cycle time and delivery decisions. We demonstrated the applicability of our research results through numerical examples and revealed that for both linear and nonlinear relationships between the common intermediate part's completion rate α and its practical value at α , our proposed two-stage production scheme with delayed differentiation is considerably beneficial vis-à-vis single-stage schemes in saving overall system costs and reducing the replenishment cycle time.

© 2016 PEI, University of Maribor. All rights reserved.

ARTICLE INFO

Keywords:

Multi-product vendor-buyer system
Production-shipment decision
Rework
Common intermediate part
Delayed differentiation

*Corresponding author:

swang@cyut.edu.tw
(Chiu, S.W.)

Article history:

Received 31 May 2016
Revised 15 November 2016
Accepted 18 November 2016

1. Introduction

Conventional economic production quantity (EPQ) model considers a single product fabrication with all items produced are of perfect quality and customer's demand satisfied by a continuous inventory issuing policy [1–3]. However, in real world supply chain systems, vendors usually adopt a *multi-product* production plan to get the most out of machine utilization and consider reworking of nonconforming items to lower their production cost. Aggarwal [4] presented a simple grouping idea under a common order cycle to resolve the multi-product inventory system. A computation procedure was also presented to derive optimal values of common order cycle. Rosenblatt and Rothblum [5] studied the multi-item inventory systems under a single-resource capacity constraint. Two solution procedures were proposed to derive optimal capacity policy. A numerical example is used to show that their solution procedures can be applied to different types of cost functions. Aliyu and Andijani [6] examined a multi-item production-inventory system with shortages, deterministic demand, deterioration, and capacity and budget constraints. Linear quadratic theory was used to solve the optimal control policy. Balkhi and Foul [7] studied a multi-product inventory model with deterministic demand, production, and deterioration rates for each product in finite time periods. Shortage is allowed and backordered

for each product. For each product, they derived the optimal production and restarting times in each period that minimize the total inventory costs. Rahmani et al. [8] investigated a two-stage real capacitated production system with uncertain demand and production costs. A mixed-integer programming model was developed to the problem. An initial robust schedule was obtained and it can be improved against any possible occurrences of uncertain parameters. They provided a real case to demonstrate the practical use of their model. Chiu et al. [9] developed an exact mathematical model to simultaneously derive the production and shipment decisions for a multi-product inventory system with a rework process. A single-stage production process is considered without involving the common intermediate part. Their results enable managers of such a specific system to better understand and control over the effects of variations in different system parameters on the optimal production-shipment policy and on the expected system costs. Additional studies related to the multi-product inventory systems can also be found elsewhere [10-14].

In multi-item production planning, if multiple products share a *common intermediate part*, vendors would always be interested in evaluating a two-stage fabrication scheme with the first stage making common intermediate parts for all products, and the second stage producing the end products to reduce overall system costs and shorten the replenishment cycle time. Gerchak et al. [15] developed a model for an arbitrary number of products with general joint demand distribution. They discussed the case of using a service-level measure where rationing of common components might be required and characterized the implied rationing rule. Garg and Tang [16] stated that practically most product families have a number of points of differentiation. They developed two models to investigate products with more than one point of differentiation. Benefits of delayed differentiation at each point in each model are examined. Necessary conditions are decided when one type of delayed differentiation is more beneficial than the other. They found that variations in demand and lead times have significant effects on determining which point of differentiation should be delayed. Graman [17] developed a two-product, single-period, order-up-to cost model to assist in deciding the inventory levels of end products and postponement capacity. A non-linear programming was used to determine the optimal solutions to inventory levels and capacity that minimize the total system cost. He indicated that altering product value, holding cost, cost of postponement, packaging cost, and fill rate can reduce expected total cost and increase postponement capacity. Other studies addressed various aspects of multi-product systems with *delayed product differentiation* can also be found elsewhere [18-21]. Also, in real manufacturing environments, due to various uncontrollable factors during production process, generation of defective items is inevitable. Quality assurances, such as inspection of product quality, rework of all repairable items, and scrapped of defective items, have been extensively studied in past decades [22-28]. Also, in contrast to the assumption of continuous issuing policy in conventional EPQ model, most nowadays supply chain systems practically adopt a periodic multi-shipment policy to distribute end products to their customers. Studies of various aspects of periodic or multi-delivery issues of vendor-buyer integrated systems have been extensively carried out during past decades [29-44].

Inspired by the potential benefits derived from applying delayed differentiation to multi-product systems, and seeking to provide managers of transnational enterprises with information to assist them in achieving the key operational goals such as maximizing machine utilization, ensuring product quality, lowering overall operating costs, and shortening response time, this study extends a prior work [9] and explores the effect of delayed differentiation on a multi-product vendor-buyer integrated inventory system with rework. Since little attention has been paid to this specific research area, the present study is intended to bridge the gap.

2. Model description and mathematical analysis

Description of the proposed multi-product vendor-buyer integrated inventory system with delayed differentiation strategy and rework using a single-machine production scheme is as follows. Consider a vendor has annual demand λ_i for L different products (where $i = 1, 2, \dots, L$) that must be satisfied. These L customized end items share a *common intermediate part* and are

manufactured using a two-stage process. The first stage produces only the common intermediate components, and the second stage fabricates in sequence L different customized end products under the common production cycle time policy. The objectives of the proposed production plan are to maximize machine utilization, shorten the replenishment cycle time, and minimize total production-inventory-delivery costs. The common intermediate part is manufactured at a rate of $P_{1,0}$ in stage one. After that, L different customized end products are produced in order under a common cycle time policy in stage two (see Fig. 1), at a rate of $P_{1,i}$.

All items made are screened and unit inspection cost is included in unit production cost C_i . The production processes in each stage (either for *common intermediate part* or for customized end products) may randomly produce x_i portion of defective items at a rate of $d_{1,i}$ and $d_{1,i} = P_{1,i}x_i$ (where $i = 0, 1, 2, \dots, L$; with $i = 0$ denotes that it is for the production of *common intermediate part* in the stage 1). Under the ordinary assumption of the EPQ model without shortages, the constant production rate $P_{1,i}$ must be larger than the sum of demand rate λ_i and production rate of defective items $d_{1,i}$. That is: $(P_{1,i} - d_{1,i} - \lambda_i) > 0$ or $(1 - x_i - \lambda_i/P_{1,i}) > 0$. It is further assumed that all defective items can be reworked and repaired. The rework processes starts immediately after the end of regular production processes in each production cycle (see Fig. 2), at a rate of $P_{2,i}$.

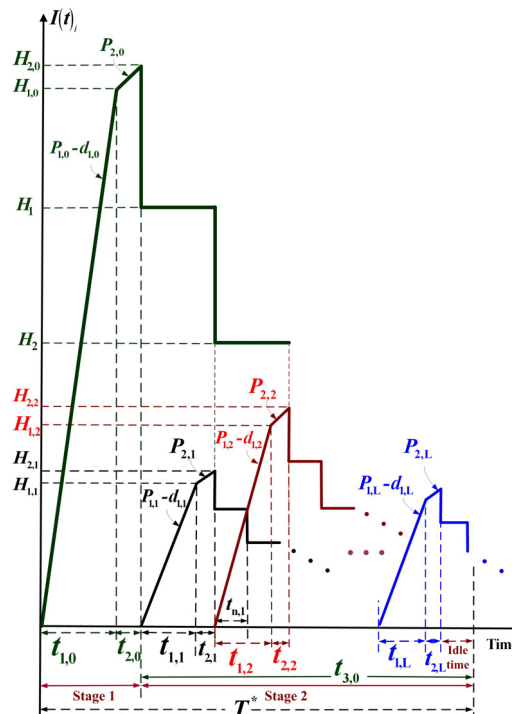


Fig. 1 Inventory level of perfect quality common intermediate parts and customized final products in the proposed two-stage multi-product vendor-buyer integrated inventory system with rework

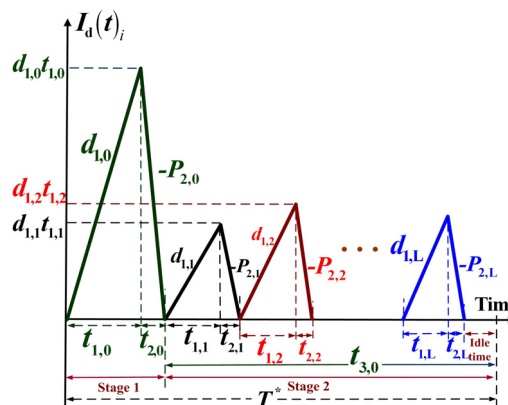


Fig. 2 Inventory level of defective items in both stages of the proposed two-stage multi-product system

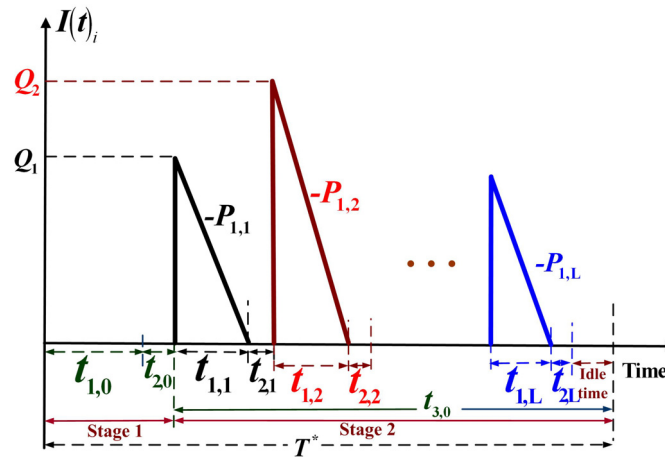


Fig. 3 Inventory level of common intermediate parts waiting to be fabricated into customized final products in the stage 2 of the proposed two-stage multi-product system

Upon completion of the production in stage 1, L different lots of *common intermediate parts* are made ready for the production in stage 2. They are fabricated in sequence into customized end products under the common production cycle time policy. The inventory level of common intermediate parts waiting to be fabricated in stage 2 is depicted in Figure 3.

In stage 2, after the completion of rework process ($t_{2,i}$) of each end product i , fixed quantity n installments of the finished batch are transported to customers at a fixed interval of time in the delivery time $t_{3,i}$ (see Fig. 1). The inventory level of end products at the buyers' side during a production cycle is depicted in Figure 4 (which is similar to Fig. 3 in [9]).

The following are additional notation used in this study (where $i = 1, 2, \dots, L$, represents L different products in stage 2; and $i = 0$ denotes the *common intermediate part* in stage 1):

- T – Production cycle length, one of the decision variables,
- n – Number of fixed quantity installments of the finished batch to be delivered in each cycle, the other decision variable,
- α – Completion rate of common intermediate part as compared to the finished product,
- Q_i – Production lot size for product i ,
- K_i – Production setup cost for product i in a production cycle,
- C_i – Unit production cost for product i ,
- $h_{1,i}$ – Unit holding cost for product i ,
- $h_{2,i}$ – Holding cost per reworked item for product i ,

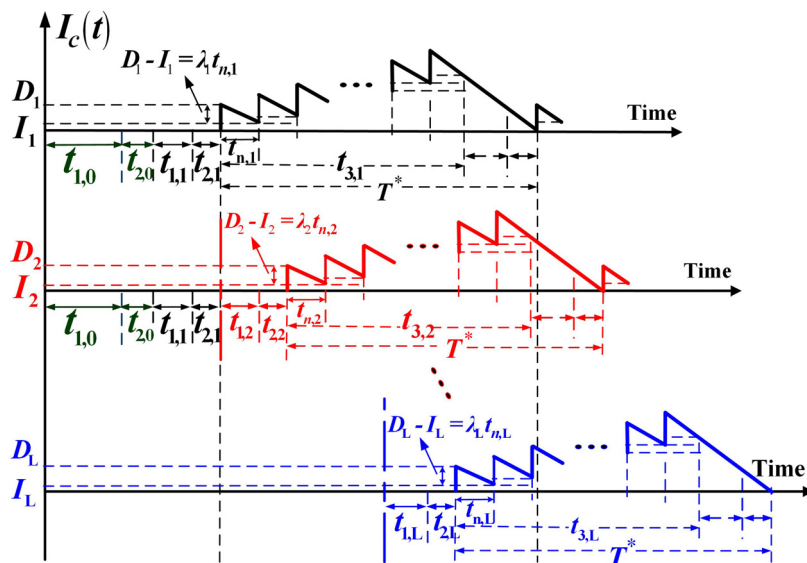


Fig. 4 Inventory level of customized final products at the buyers' side during a production cycle [9]

- $h_{3,i}$ – Unit holding cost for stocks stored at customer’s side,
- $h_{4,i}$ – Unit holding cost for safety stocks stored at producer’s side,
- $C_{R,i}$ – Unit reworking cost for product i ,
- $t_{1,i}$ – Production uptime for product i in a production cycle,
- $t_{2,i}$ – The reworking time for product i in a production cycle,
- $t_{3,i}$ – Delivery time for product i in a production cycle,
- H_i – Inventory level of common intermediate part at the time of producing end product i ,
- $H_{1,i}$ – Maximal level of perfect quality items i in the end of regular production,
- $H_{2,i}$ – Maximal level of perfect quality items i in the end of rework process before delivery,
- $K_{1,i}$ – Fixed delivery cost per shipment for product i ,
- $C_{T,i}$ – Unit delivery cost for product i ,
- $t_{n,i}$ – A fixed interval of time between each installment of finished items of product i to be delivered to customer during downtime $t_{3,i}$,
- $I(t)_i$ – On-hand inventory level of perfect quality items i at time t ,
- $I_d(t)_i$ – On-hand inventory level of defective items i at time t ,
- $I_c(t)_i$ – On-hand inventory level of finished product i at time t , at customer’s side,
- I_i – The left-over number of finished items of product i in each $t_{n,i}$, at customer’s side,
- D_i – Number of finished items of product i to be transported to customer in each shipment,
- $TC(T, n)$ – Total production-inventory-delivery cost per cycle,
- $E[T]$ – The expected production cycle length,
- $E[TC(T, n)]$ – The expected production-inventory-delivery cost per cycle,
- $E[TCU(T, n)]$ – The long-run average costs per unit time for the proposed model.

2.1 Modeling and analysis

A two-stage EPQ-based production plan considering the postponement is proposed to satisfy annual demand λ_i of L different customized products. From Figure 1, we observe the production cycle time as

$$T = t_{1,i} + t_{2,i} + t_{3,i} = \frac{Q_i}{\lambda_i} \text{ for } i = 0, 1, 2, \dots, L \tag{1}$$

In stage 1, the production lot-size of *common intermediate parts* Q_0 , depends on the sum of production lot sizes Q_i of L different products to be made in the stage 2. Therefore, we obtain the following equations (refer to Fig. 1):

$$Q_i = \lambda_i T \text{ for } i = 1, 2, \dots, L \tag{2}$$

$$Q_0 = \sum_{i=1}^L Q_i = \lambda_0 T \tag{3}$$

$$t_{1,0} = \frac{Q_0}{P_{1,0}} = \frac{H_{1,0}}{P_{1,0} - d_{1,0}} \tag{4}$$

$$H_{1,0} = t_{1,0} (P_{1,0} - d_{1,0}) \tag{5}$$

$$H_{2,0} = H_{1,0} + P_{2,0} t_{2,0} = \sum_{i=1}^L Q_i \tag{6}$$

$$t_{2,0} = \frac{x_0 Q_0}{P_{2,0}} = \frac{d_{1,0} t_{1,0}}{P_{2,0}} = \frac{H_{2,0} - H_{1,0}}{P_{2,0}} \tag{7}$$

$$H_1 = H_{2,0} - Q_1 \tag{8}$$

$$H_i = H_{(i-1)} - Q_i \text{ for } i = 2, 3, \dots, L \tag{9}$$

$$H_L = H_{(L-1)} - Q_L = 0 \tag{10}$$

In stage 2, for fabrication of L different products we obtain the following equations directly from Figs. 1 to 4 (where $i = 1, 2, \dots, L$):

$$t_{1,i} = \frac{Q_i}{P_{1,i}} = \frac{H_{1,i}}{P_{1,i} - d_{1,i}} \tag{11}$$

$$H_{1,i} = (P_{1,i} - d_{1,i}) t_{1,i} \tag{12}$$

$$H_{2,i} = H_{1,i} + P_{2,i} t_{2,i} \tag{13}$$

$$t_{2,i} = \frac{x_i Q_i}{P_{2,i}} = \frac{d_{1,i} t_{1,i}}{P_{2,i}} = \frac{H_{2,i} - H_{1,i}}{P_{2,i}} \tag{14}$$

$$t_{3,i} = nt_{n,i} \tag{15}$$

$$D_i = \frac{H_{2,i}}{n} \tag{16}$$

$$I_i = D_i - \lambda_i t_{n,i} \tag{17}$$

$$nI_i = \lambda_i(t_{1,i} + t_{2,i}) \tag{18}$$

2.2 Cost analysis

Inventory holding costs for *common intermediate parts* (including perfect and imperfect quality items) during $t_{1,0}$, $t_{2,0}$, and $t_{3,0}$, are (see Figs. 1 and 2)

$$h_{1,0} \left[\frac{H_{1,0}t_{1,0}}{2} + \frac{(H_{2,0}+H_{1,0})t_{2,0}}{2} + \sum_{i=1}^L H_i(t_{1,i} + t_{2,i}) \right] + h_{1,0} \left[\frac{(d_{1,0}t_{1,0})t_{1,0}}{2} \right] \tag{19}$$

In stage 2, inventory holding cost for *common intermediate parts* waiting to be fabricated into customized end products (see Fig. 3) is

$$\sum_{i=1}^L \left\{ h_{1,i} \left[\frac{Q_i}{2} (t_{1,i}) \right] \right\} \tag{20}$$

Inventory holding costs for imperfect quality items waiting to be reworked in both stages are

$$h_{2,0} \left[\frac{d_{1,0}t_{1,0}}{2} (t_{2,0}) \right] + \sum_{i=1}^L \left[h_{2,i} \left(\frac{P_{2,i}t_{2,i}}{2} \right) (t_{2,i}) \right] \tag{21}$$

In stage 2, fixed and variable delivery costs and inventory holding cost for finished product i waiting to be distributed in $t_{3,i}$ are

$$\sum_{i=1}^L [nK_{1,i} + C_{T,i}Q_i] + \sum_{i=1}^L \left\{ h_{1,i} \left(\frac{n-1}{2n} \right) H_{2,i}t_{3,i} \right\} \tag{22}$$

The stock holding cost for end product i stored at customers' sides (see Fig. 4) is

$$\sum_{i=1}^L \left\{ h_{3,i} \left[\frac{n(D_i-I_i)t_{n,i}}{2} + \frac{n(n+1)}{2} I_i t_{n,i} + \frac{nI_i(t_{1,i}+t_{2,i})}{2} \right] \right\} \tag{23}$$

The overall cost per cycle $TC(T, n)$ for the proposed system, includes production setup cost, variable production cost, reworking cost, holding cost, and safety stock cost in both stages; and fixed and variable delivery costs and holding costs for stocks stored at customers' side in stage 2. Hence, $TC(T, n)$ is

$$TC(T, n) = \left\{ K_0 + C_0Q_0 + C_{R,0}x_0Q_0 + h_{2,0} \left(\frac{d_{1,0}t_{1,0}}{2} \right) (t_{2,0}) + h_{4,0}(x_0Q_0)T \right. \\ \left. + h_{1,0} \left[\frac{H_{1,0}t_{1,0}}{2} + \frac{H_{2,0}+H_{1,0}}{2} (t_{2,0}) + \frac{d_{1,0}t_{1,0}}{2} (t_{1,0}) + \sum_{i=1}^L H_i(t_{1,i} + t_{2,i}) \right] \right\} + \\ \sum_{i=1}^L \left\{ \begin{aligned} &K_i + C_iQ_i + C_{R,i}x_iQ_i + nK_{1,i} + C_{T,i}Q_i + h_{2,i} \left(\frac{P_{2,i}t_{2,i}}{2} \right) (t_{2,i}) \\ &+ h_{1,i} \left[\frac{Q_i}{2} (t_{1,i}) + \frac{H_{1,i}t_{1,i}}{2} + \frac{H_{2,i}+H_{1,i}}{2} (t_{2,i}) + \left(\frac{n-1}{2n} \right) H_{2,i}t_{3,i} + \frac{d_{1,i}t_{1,i}}{2} (t_{1,i}) \right] \\ &+ h_{3,i} \left[\frac{n(D_i-I_i)t_{n,i}}{2} + \frac{n(n+1)}{2} I_i t_{n,i} + \frac{nI_i(t_{1,i}+t_{2,i})}{2} \right] + h_{4,i}(x_iQ_i)T \end{aligned} \right\} \tag{24}$$

Substituting Eqs. 1 to 18 in Eq. 24 and taking randomness of defective rate into account, and the long-run average system costs $E[TCU(T, n)]$ can be derived as follows:

$$E[TCU(T, n)] = \frac{E[TC(T,n)]}{E[T]} = \\ \left\{ \frac{K_0}{T} + C_0\lambda_0 + C_{R,0}\lambda_0 E[x_0] + z_0T \right\} + \\ \sum_{i=1}^L \left\{ \begin{aligned} &\left[\frac{K_i}{T} + C_i\lambda_i + C_{R,i}\lambda_i E[x_i] + \frac{nK_{1,i}}{T} + C_{T,i}\lambda_i \right] + \frac{h_{1,i}T\lambda_i^2}{2} \left\{ \delta_{2,i} - \frac{\delta_{1,i}}{n} \right\} \\ &+ \frac{h_{2,i}T\lambda_i^2 E[x_i]^2}{2P_{2,i}} + \frac{h_{3,i}T\lambda_i^2}{2} \left[\frac{1}{P_{1,i}} + \frac{E[x_i]}{P_{2,i}} + \frac{\delta_{1,i}}{n} \right] + Th_{4,i}\lambda_i E[x_i] \end{aligned} \right\} \tag{25}$$

where

$$z_0 = \left\{ \begin{aligned} & \frac{h_{1,0}\lambda_0^2}{2} \left[\frac{1}{P_{1,0}} + \frac{2E[x_0]}{P_{2,0}} - \frac{E[x_0]^2}{P_{2,0}} \right] + \frac{h_{2,0}\lambda_0^2 E[x_0]^2}{2P_{2,0}} \\ & + h_{1,0} \sum_{i=1}^L \left\{ \left(\frac{\lambda_i}{P_{1,i}} + \frac{\lambda_i E[x_i]}{P_{2,i}} \right) \left[\sum_{i=1}^L (\lambda_i) - \sum_{j=1}^i (\lambda_j) \right] \right\} + h_{4,0}\lambda_0 E[x_0] \end{aligned} \right\};$$

$$\delta_{1,i} = \left[\frac{1}{\lambda_i} - \frac{1}{P_{1,i}} - \frac{E[x_i]}{P_{2,i}} \right]; \text{ and } \delta_{2,i} = \left[\frac{1}{\lambda_i} - \frac{E[x_i]^2}{P_{2,i}} + \frac{1}{P_{1,i}} + \frac{E[x_i]}{P_{2,i}} \right] \text{ for } i = 1, 2, \dots, L \quad (26)$$

3. Convexity and the optimal decision

Upon obtaining the long-run average system costs $E[TCU(T, n)]$, we then prove it is a convex function by applying the Hessian matrix equations [45] to verify that Eq. 27 holds.

$$[T \ n] \cdot \begin{pmatrix} \frac{\partial^2 E[TCU(T, n)]}{\partial T^2} & \frac{\partial^2 E[TCU(T, n)]}{\partial T \partial n} \\ \frac{\partial^2 E[TCU(T, n)]}{\partial T \partial n} & \frac{\partial^2 E[TCU(T, n)]}{\partial n^2} \end{pmatrix} \cdot \begin{bmatrix} T \\ n \end{bmatrix} > 0 \quad (27)$$

From Eq. 25 we obtain

$$\frac{\partial E[TCU(T, n)]}{\partial T} = \left(\frac{-K_0}{T^2} + z_0 \right) + \sum_{i=1}^L \left\{ \begin{aligned} & \left[\frac{-K_0}{T^2} - \frac{nK_{1,i}}{T^2} \right] + \frac{h_{1,i}\lambda_i^2}{2} \left\{ \delta_{2,i} - \frac{\delta_{1,i}}{n} \right\} \\ & + \frac{h_{2,i}\lambda_i^2 E[x_i]^2}{2P_{2,i}} + \frac{h_{3,i}\lambda_i^2}{2} \left[\frac{1}{P_{1,i}} + \frac{E[x_i]}{P_{2,i}} + \frac{\delta_{1,i}}{n} \right] + h_{4,i}\lambda_i E[x_i] \end{aligned} \right\} \quad (28)$$

$$\frac{\partial E[TCU(T, n)]}{\partial T^2} = \frac{2K_0}{T^3} + \sum_{i=1}^L \left\{ \frac{2K_i}{T^3} + \frac{2nK_{1,i}}{T^3} \right\} \quad (29)$$

$$\frac{\partial E[TCU(T, n)]}{\partial n} = \sum_{i=1}^L \left\{ \frac{K_{1,i}}{T} + \frac{T\lambda_i^2}{2n^2} [(h_{1,i} - h_{3,i})\delta_{1,i}] \right\} \quad (30)$$

$$\frac{\partial E[TCU(T, n)]}{\partial n^2} = \sum_{i=1}^L \left\{ \frac{T\lambda_i^2}{n^3} [(h_{3,i} - h_{1,i})\delta_{1,i}] \right\} \quad (31)$$

$$\frac{\partial^2 E[TCU(T, n)]}{\partial T \partial n} = \sum_{i=1}^L \left\{ -\frac{K_{1,i}}{T^2} + \frac{T\lambda_i^2}{2n^2} [(h_{1,i} - h_{3,i})\delta_{1,i}] \right\} \quad (32)$$

Substituting Eqs. 29, 31, and 32 in Eq. 27, we obtain

$$[T \ n] \cdot \begin{pmatrix} \frac{\partial^2 E[TCU(T, n)]}{\partial T^2} & \frac{\partial^2 E[TCU(T, n)]}{\partial T \partial n} \\ \frac{\partial^2 E[TCU(T, n)]}{\partial T \partial n} & \frac{\partial^2 E[TCU(T, n)]}{\partial n^2} \end{pmatrix} \cdot \begin{bmatrix} T \\ n \end{bmatrix} = \frac{2K_0}{T} + \sum_{i=1}^L \frac{2K_i}{T} > 0 \quad (33)$$

Because K_0 , K_i , and T are all positive, we find Eq. 33 is positive. Hence, $E[TCU(T, n)]$ is a strictly convex function for all T and n different from zero. In order to simultaneously determine production-shipment decision for the proposed system, we can solve the linear system of first derivatives of $E[TCU(T, n)]$ with respect to T and n , respectively, by setting these partial derivatives equal to zero. With further derivations we find

$$T^* = \sqrt{\frac{K_0 + \sum_{i=1}^L (K_i + nK_{1,i})}{z_0 + \sum_{i=1}^L \left\{ \begin{aligned} & \frac{h_{1,i}\lambda_i^2}{2} \left\{ \delta_{2,i} - \frac{\delta_{1,i}}{n} \right\} + \frac{h_{2,i}\lambda_i^2 E[x_i]^2}{2P_{2,i}} \\ & + \frac{h_{3,i}\lambda_i^2}{2} \left[\frac{1}{P_{1,i}} + \frac{E[x_i]}{P_{2,i}} + \frac{\delta_{1,i}}{n} \right] + h_{4,i}\lambda_i E[x_i] \end{aligned} \right\}}} \quad (34)$$

and

$$n^* = \sqrt{\frac{(K_0 + \sum_{i=1}^L K_i) \sum_{i=1}^L \left[\frac{\lambda_i^2}{2} (h_{3,i} - h_{1,i}) (\delta_{1,i}) \right]}{\left(\sum_{i=1}^L K_{1,i} \right) \left\{ z_0 + \sum_{i=1}^L \left(\frac{h_{1,i}\lambda_i^2}{2} (\delta_{2,i}) + \frac{h_{2,i}\lambda_i^2 E[x_i]^2}{2P_{2,i}} + h_{4,i}\lambda_i E[x_i] \right) \right\} + \sum_{i=1}^L \left(\frac{h_{3,i}\lambda_i^2}{2} \left[\frac{1}{P_{1,i}} + \frac{E[x_i]}{P_{2,i}} + \frac{\delta_{1,i}}{n} \right] \right) \right\}}} \quad (35)$$

4. Numerical example and discussion

The following numerical example is used to show the practical uses of research results obtained in the previous section. Consider a manufacturer must fabricate five different products and they share a *common intermediate part* that has completion rate $\alpha = 0.5$ (i.e., halfway done). To ease comparison efforts for readers, we reconsider a numerical example used in a prior study [9] regarding optimization of a single-stage multi-product system without adopting postponement in its production. Annual production rates of five end products $P_{1,i} = 58,000, 59,000, 60,000, 61,000,$ and $62,000$ units, respectively; annual demands $\lambda_i = 3,000, 3,200, 3,400, 3,600,$ and $3,800$ units, respectively; annual reworking rates $P_{2,i} = 46,400, 47,200, 48,000, 48,800,$ and $49,600$ units, respectively; setup costs $K_i = \$17,000, \$17,500, \$18,000, \$18,500,$ and $\$19,000$, respectively; unit fabrication costs $C_i = \$80, \$90, \$100, \$110,$ and $\$120$, respectively; the defective rates x_i follow uniform distribution over the intervals $[0, 0.05], [0, 0.10], [0, 0.15], [0, 0.20],$ and $[0, 0.25]$, respectively; and unit reworking costs $C_{R,i} = \$50, \$55, \$60, \$65,$ and $\$70$, respectively. Based on *common intermediate part's* completion rate $\alpha = 0.5$, a straightforward relationship $1/\alpha$ is assumed for its relevant production rates. Hence, in the proposed two-stage single-machine production scheme we have $P_{1,0} = (1/\alpha) * (\text{the mean of } P_{1,i}'\text{s}) = 120,000$ and $P_{2,0} = (1/\alpha) * (\text{the mean of } P_{2,i}'\text{s}) = 96,000$.

The relationship between *common intermediate part's* relevant costs and its completion rate α can either be linear or nonlinear. Both cases are investigated in the following subsections.

4.1 Case 1: Analysis of linear relationship of cost relevant variables

If the relationship between practical fabrication related cost of *common intermediate part* (or called 'the value' of common part) and its completion rate α is linear, then for $\alpha = 0.5$ we have the following linear-based relevant values of variables in our proposed system:

- C_0 – \$40, unit fabrication cost for common intermediate part,
- K_0 – \$8,500, setup cost for common intermediate part,
- $C_{R,0}$ – \$25, unit reworking cost for common intermediate part,
- $h_{1,0}$ – \$5, unit holding cost for common intermediate part,
- $h_{4,0}$ – \$5, unit safety stock cost for common intermediate part,
- $h_{2,0}$ – \$15, unit holding cost for common intermediate part during the reworking processes,
- K_i – Setup costs of end products are \$8,500, \$9,000, \$9,500, \$10,000, and \$10,500 respectively,
- x_0 – $[0, 0.04]$, the interval uniformly distributed defective rate in the production of common intermediate part,
- C_i – Unit production costs of end products are \$40, \$50, \$60, \$70, and \$80, respectively,
- $h_{1,i}$ – Unit holding costs of end products are \$10, \$15, \$20, \$25, and \$30, respectively,
- $P_{1,i}$ – Annual production rates of five end products are 112,258, 116,066, 120,000, 124,068, and 128,276 units, respectively; they are simply calculated by $P_{1,i} = 1/(1/P_{1,i} - 1/P_{1,0})$,
- x_i – End items' defective rates follow the uniform distribution over the intervals $[0, 0.01], [0, 0.06], [0, 0.11], [0, 0.16],$ and $[0, 0.21]$, respectively,
- $C_{R,i}$ – Unit reworking costs of end products are \$25, \$30, \$35, \$40, and \$45, respectively,
- $P_{2,i}$ – Annual reworking rates of five end products are 89,806, 92,852, 96,000, 99,254, and 102,621 units, respectively; they are simply calculated by $P_{2,i} = 1/(1/P_{2,i} - 1/P_{2,0})$,
- $h_{2,i}$ – Unit holding cost per reworked items of end products are \$30, \$35, \$40, \$45, and \$50, respectively,
- $K_{1,i}$ – Fixed delivery costs per shipment: \$1,800, \$1,900, \$2,000, \$2,100, and \$2,200, respectively,
- $C_{T,i}$ – Unit delivery costs of end items are \$0.1, \$0.2, \$0.3, \$0.4, and \$0.5, respectively,
- $h_{3,i}$ – Unit holding costs at the customer's side are \$70, \$75, \$80, \$85, and \$90, respectively,
- $h_{4,0}$ – Unit safety stock costs of end products are \$10, \$15, \$20, \$25, and \$30, respectively.

First, the annual demand for *common intermediate parts* $\lambda_0 = 17,000$ can be obtained by applying Eqs. 2 and 3. Then, by calculating Eqs. 34, 35, and 25, we derive the optimal number of deliveries $n^* = 3$, optimal production cycle time $T^* = 0.4614$ (years), and the expected system costs per unit time $E[TCU(T^*, n^*)] = \$2,145,834$. Figure 5 depicts the effects of variations of the production cycle time T on the expected system costs $E[TCU(T, n)]$.

The behavior of $E[TCU(T, n)]$ with respect to the common intermediate part's completion rate α is exhibited in Figure 6. It can be seen that as the completion rate α increases, the long-run expected system costs $E[TCU(T, n)]$ decreases, and the proposed model realizes a system cost savings of 3.76 % at $\alpha = 0.5$ (i.e., system costs decreased from \$2,229,658 [9] to \$2,145,834) as compared to that in prior study which used a single-stage production scheme. This analytical result demonstrates that the proposed two-stage multi-item production scheme with delayed differentiation is a considerably beneficial model for manufacturers who must meet demands for multiple products that share a common intermediate part.

Figure 7 shows the effects of variations of common part's completion rate α on the optimal production cycle time T^* . As the completion rate α increases, the optimal cycle time T^* decreases significantly, and in the proposed model optimal cycle time T^* is reduced by 25.5 % at $\alpha = 0.5$ (i.e., it decreases from 0.6193 [9] to 0.4614 (years)) as compared to that in prior study which used a single-stage production scheme. Such an analytical result indicates our proposed two-stage multi-item production scheme with delayed differentiation provides a shorter cycle time (or faster response time) than that in a conventional one-stage multi-item system [9].

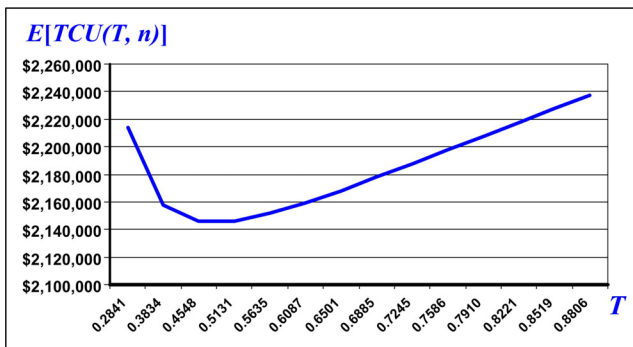


Fig. 5 The effects of variations of the production cycle time T on the expected system costs $E[TCU(T, n)]$

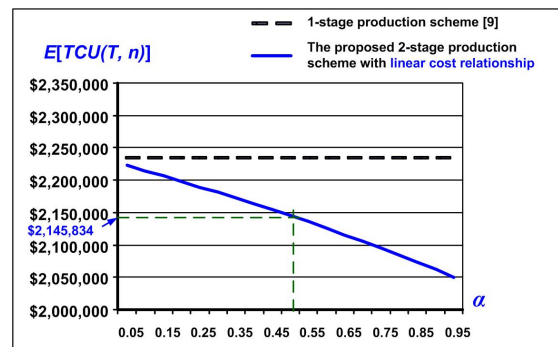


Fig. 6 The behavior of $E[TCU(T, n)]$ with respect to the common intermediate part's completion rate α

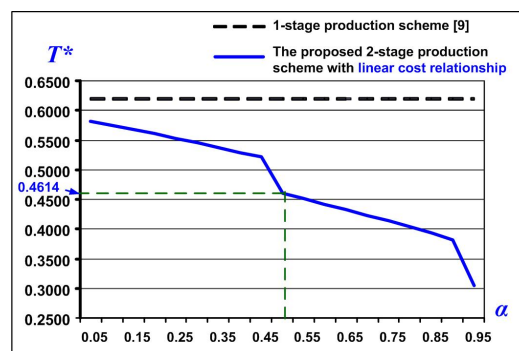


Fig. 7 The effects of variations of common part's completion rate α on the optimal production cycle time T^*

4.2 Case 2: Analysis of nonlinear relationship of cost relevant variables

In this section, we demonstrate that the proposed model is capable of analyzing any given nonlinear relationship between the *common part's* relevant costs and its completion rate α . For instance, if a nonlinear relationship of ' $\alpha^{(1/3)}$ ' between *common part's* relevant costs and α is known, then $C_0 = [\alpha^{(1/3)}]C_1 = [(0.5)^{(1/3)}]\$80 = \$63$, so it obviously has higher production

cost (or called value) than that in the linear relationship case (which is \$40). Apply the similar computation we have the following values of other relevant parameters: $C_{R,0} = \$40$, $K_0 = \$13,493$, $h_{1,0} = h_{4,0} = \$8$, and $h_{2,0} = \$24$. Assume the following parameters' values remain the same as stated in subsection 4.1: $P_{1,0} = 120,000$, $P_{2,0} = 96,000$, and $x_0 = [0, 0.04]$. Accordingly, in stage 2 we obtain the values of other variables as follows: $C_i = \$17, \$27, \$37, \47 , and $\$57$, respectively; $K_i = \$3,507, \$4,007, \$4,507, \$5,007$, and $\$5,507$, respectively; $C_{R,i} = \$10, \$15, \$20, \25 , and $\$30$, respectively; and x_i follows the uniform distribution over the intervals $[0, 0.01]$, $[0, 0.06]$, $[0, 0.11]$, $[0, 0.16]$, and $[0, 0.21]$, respectively

We apply Eqs. 34, 35, and 25 to obtain the optimal number of shipments $n^* = 3$, the optimal production cycle time $T^* = 0.4005$ (years), and the expected system costs $E[TCU(T^*, n^*)] = \$2,093,253$. Figure 8 depicts the behavior of $E[TCU(T, n)]$ with respect to the common part's completion rate α under both linear and nonlinear relationships. In nonlinear relationship case, as the common part's completion rate α increases, the expected system costs $E[TCU(T, n)]$ decreases, and it indicates that $E[TCU(T, n)]$ is decreased by 2.45 % at $\alpha = 0.5$ (i.e., system costs declined from \$2,145,834 to \$2,093,253) compared to that in the earlier linear case. The analytical results demonstrate that the proposed two-stage multi-item production scheme with delayed differentiation is a greatly beneficial model to manufacturers who have to meet demands for multiple products that share a common intermediate part.

Figure 9 illustrates the behavior of the optimal production cycle time T^* with respect to the common part's completion rate α under both linear and nonlinear relationships. As completion rate α increases, the optimal production cycle time T^* decreases significantly, and in the nonlinear case, the optimal cycle time T^* is shortened by 13.20 % at $\alpha = 0.5$ (i.e., it reduces from 0.4614 to 0.4005) compared to that in the earlier linear case. Therefore, it demonstrates that the proposed two-stage multi-item production scheme with delayed differentiation is a considerably beneficial model (in terms of faster response cycle time) for manufacturers who have to meet demands for multiple products that share a common intermediate part.

Furthermore, the analytical results reveals that if the *common part's* relevant costs are higher (e.g., having a nonlinear relationship $\alpha^{1/3}$ rather than the linear one), then the optimal cycle time T^* reduces significantly compared to that in the linear case.

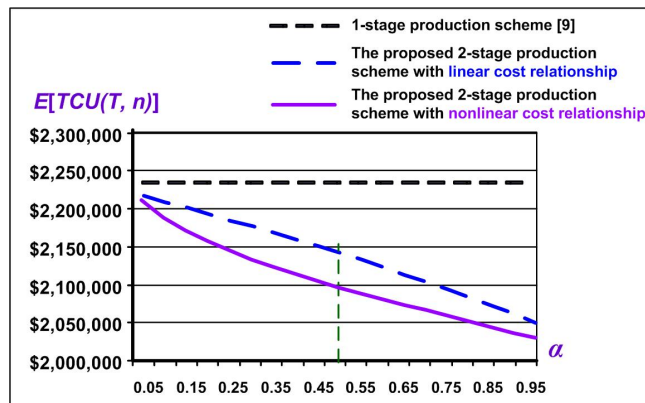


Fig. 8 The behavior of $E[TCU(T, n)]$ with respect to the common intermediate part's completion rate α under both linear and nonlinear relationships

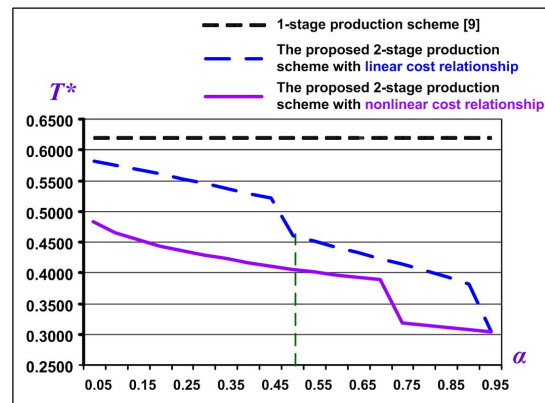


Fig. 9 The behavior of the optimal production cycle time T^* with respect to the common intermediate part's completion rate α under both linear and nonlinear relationships

5. Conclusion

Inspired by the potential benefits derived from applying delayed differentiation to multi-product systems, and with the aim of providing managers of transnational enterprises with information to assist them in achieving the key operational goals such as maximizing machine utilization, ensuring product quality, lowering overall operating costs, and shortening response time, this

study explores the effect of delayed differentiation on a multi-product vendor-buyer integrated inventory system with rework, using a single machine production scheme.

Using mathematical modeling and optimization methods, we derive the closed-form optimal replenishment cycle time and delivery decisions and demonstrate the practical use of our results through a numerical example. The results reveal that our proposed multi-product fabrication scheme with delayed differentiation strategy is considerably beneficial in saving expected system costs and reducing replenishment cycle time. Further analysis also indicates that when the *common intermediate part's* value is higher (e.g., having a nonlinear relationship $\alpha^{1/3}$ rather than the linear one), both the expected system costs and production cycle time reduces significantly compared to that in the linear case. For future study, to explore and compare the effects of the dual-machine production scheme on the optimal operating policies of the same system would be an interesting direction.

Acknowledgement

Authors would like to express their gratefulness to the Ministry of Science and Technology of Taiwan for sponsor of this research (under grant no.: MOST 102-2410-H-324-015-MY2).

References

- [1] Hadley, G., Whitin, T.M. (1963). *Analysis of Inventory Systems*, Prentice-Hall, New Jersey, USA.
- [2] Silver, E.A., Pyke, D.F., Peterson, R. (1998). *Inventory Management and Production Planning and Scheduling*, John Wiley & Sons, New York, USA.
- [3] Nahmias, S. (2009). *Production & Operations Analysis*, McGraw-Hill, New York, USA.
- [4] Aggarwal, V. (1984). Grouping multi-item inventory using common cycle periods, *European Journal of Operational Research*, Vol. 17, No. 3, 369-372, doi: [10.1016/0377-2217\(84\)90132-2](https://doi.org/10.1016/0377-2217(84)90132-2).
- [5] Rosenblatt, M.J., Rothblum, U.G. (1990). On the single resource capacity problem for multi-item inventory systems, *Operations Research*, Vol. 38, No. 4, 686-693, doi: [10.1287/opre.38.4.686](https://doi.org/10.1287/opre.38.4.686).
- [6] Aliyu, M.D.S., Andijani, A.A. (1999). Multi-item-multi-plant inventory control of production systems with shortages/backorders, *International Journal of Systems Science*, Vol. 30, No. 5, 533-539, doi: [10.1080/002077299292272](https://doi.org/10.1080/002077299292272).
- [7] Balkhi, Z.T., Foul, A. (2009). A multi-item production lot size inventory model with cycle dependent parameters, *International Journal of Mathematical Models and Methods in Applied Sciences*, Vol. 3, No. 2, 94-104.
- [8] Rahmani, D., Ramezani, R., Fattahi, P., Heydari, M. (2013). A robust optimization model for multi-product two-stage capacitated production planning under uncertainty, *Applied Mathematical Modelling*, Vol. 37, No. 20-21, 8957-8971, doi: [10.1016/j.apm.2013.04.016](https://doi.org/10.1016/j.apm.2013.04.016).
- [9] Chiu, Y.-S.P., Chiang, K.-W., Chiu, S.W., Song, M.-S. (2016). Simultaneous determination of production and shipment decisions for a multi-product inventory system with a rework process, *Advances in Production Engineering & Management*, Vol. 11, No. 2, 141-151, doi: [10.14743/apem2016.2.216](https://doi.org/10.14743/apem2016.2.216).
- [10] Caggiano, K.E., Jackson, P.L., Muckstadt, J.A., Rappold, J.A. (2009). Efficient computation of time-based customer service levels in a multi-item, multi-echelon supply chain: A practical approach for inventory optimization, *European Journal of Operational Research*, Vol. 199, No. 3, 744-749, doi: [10.1016/j.ejor.2008.08.002](https://doi.org/10.1016/j.ejor.2008.08.002).
- [11] Björk, K.-M. (2012). A multi-item fuzzy economic production quantity problem with a finite production rate, *International Journal of Production Economics*, Vol. 135, No. 2, 702-707, doi: [10.1016/j.ijpe.2011.10.003](https://doi.org/10.1016/j.ijpe.2011.10.003).
- [12] Ma, W.-N., Gong, D.-C., Lin, G.C. (2010). An optimal common production cycle time for imperfect production processes with scrap, *Mathematical and Computer Modelling*, Vol. 52, No. 5-6, 724-737, doi: [10.1016/j.mcm.2010.04.024](https://doi.org/10.1016/j.mcm.2010.04.024).
- [13] Guerrero, W.J., Yeung, T.G., Guéret, C. (2013). Joint-optimization of inventory policies on a multi-product multi-echelon pharmaceutical system with batching and ordering constraints, *European Journal of Operational Research*, Vol. 231, No. 1, 98-108, doi: [10.1016/j.ejor.2013.05.030](https://doi.org/10.1016/j.ejor.2013.05.030).
- [14] Chiu, Y.-S.P., Sung, P.-C., Chiu, S.W., Chou, C.-L. (2015). Mathematical modeling of a multi-product EMQ model with an enhanced end items issuing policy and failures in rework, *SpringerPlus*, Vol. 4, No. 1, 679, doi: [10.1186/s40064-015-1487-4](https://doi.org/10.1186/s40064-015-1487-4).
- [15] Gerchak, Y., Magazine, M.J., Gamble, B.A. (1988). Component commonality with service level requirements, *Management Science*, Vol. 34, No. 6, 753-760, doi: [10.1287/mnsc.34.6.753](https://doi.org/10.1287/mnsc.34.6.753).
- [16] Garg, A., Tang, C.S. (1997). On postponement strategies for product multiple points of differentiation, *IIE Transactions*, Vol. 29, No. 8, 641-650, doi: [10.1080/07408179708966374](https://doi.org/10.1080/07408179708966374).
- [17] Graman, G.A. (2010). A partial-postponement decision cost model, *European Journal of Operational Research*, Vol. 201, No. 1, 34-44, doi: [10.1016/j.ejor.2009.03.001](https://doi.org/10.1016/j.ejor.2009.03.001).
- [18] Collier, D.A. (1982). Aggregate safety stock levels and component part commonality, *Management Science*, Vol. 28, No. 11, 1296-1303, doi: [10.1287/mnsc.28.11.1296](https://doi.org/10.1287/mnsc.28.11.1296).

- [19] Swaminathan, J.M., Tayur, S.R. (1998). Managing broader product lines through delayed differentiation using vanilla boxes, *Management Science*, Vol. 44, No. 12 (Part 2), S161-S172.
- [20] Swaminathan, J.M., Tayur, S.R. (2003). Models for supply chains in e-business, *Management Science*, Vol. 49, No. 10, 1387-1406, doi: [10.1287/mnsc.49.10.1387.17309](https://doi.org/10.1287/mnsc.49.10.1387.17309).
- [21] Bernstein, F., DeCroix, G.A., Wang, Y. (2011). The impact of demand aggregation through delayed component allocation in an assemble-to-order system, *Management Science*, Vol. 57, No. 6, 1154-1171, doi: [10.1287/mnsc.1110.1340](https://doi.org/10.1287/mnsc.1110.1340).
- [22] Shih, W. (1980). Optimal inventory policies when stock-outs result from defective products, *International Journal of Production Research*, Vol. 18, No. 6, 677-686, doi: [10.1080/00207548008919699](https://doi.org/10.1080/00207548008919699).
- [23] Makis, V. (1998). Optimal lot sizing and inspection policy for an EMQ model with imperfect inspections, *Naval Research Logistics*, Vol. 45, No. 2, 165-186, doi: [10.1002/\(SICI\)1520-6750\(199803\)45:2<165::AID-NAV3>3.0.CO;2-6](https://doi.org/10.1002/(SICI)1520-6750(199803)45:2<165::AID-NAV3>3.0.CO;2-6).
- [24] Ojha, D., Sarker, B.R., Biswas, P. (2007). An optimal batch size for an imperfect production system with quality assurance and rework, *International Journal of Production Research*, Vol. 45, No. 14, 3191-3214, doi: [10.1080/00207540600711853](https://doi.org/10.1080/00207540600711853).
- [25] Chiu, Y.-S.P., Wu, M.-F., Cheng, F.-T., Hwang, M.-H. (2014). Replenishment lot sizing with failure in rework and an enhanced multi-shipment policy, *Journal of Scientific & Industrial Research*, Vol. 73, 648-652.
- [26] Khan, M., Jaber, M.Y., Ahmad, A.-R. (2014). An integrated supply chain model with errors in quality inspection and learning in production, *Omega*, Vol. 42, No. 1, 16-24, doi: [10.1016/j.omega.2013.02.002](https://doi.org/10.1016/j.omega.2013.02.002).
- [27] Yeh, T.-M., Pai, F.-Y., Liao, C.-W. (2014) Using a hybrid MCDM methodology to identify critical factors in new product development, *Neural Computing and Applications*, Vol. 24, No. 3, 957-971, doi: [10.1007/s00521-012-1314-6](https://doi.org/10.1007/s00521-012-1314-6).
- [28] Pal, S., Mahapatra, G.S., Samanta, G.P. (2015). A production inventory model for deteriorating item with ramp type demand allowing inflation and shortages under fuzziness, *Economic Modelling*, Vol. 46, 334-345, doi: [10.1016/j.econmod.2014.12.031](https://doi.org/10.1016/j.econmod.2014.12.031).
- [29] Schwarz, L.B. (1973). A simple continuous review deterministic one-warehouse N-retailer inventory problem, *Management Science*, Vol. 19, No. 5, 555-566, doi: [10.1287/mnsc.19.5.555](https://doi.org/10.1287/mnsc.19.5.555).
- [30] Goyal, S.K., Gupta, Y.P. (1989). Integrated inventory models: The buyer-vendor coordination, *European Journal of Operational Research*, Vol. 41, No. 3, 261-269, doi: [10.1016/0377-2217\(89\)90247-6](https://doi.org/10.1016/0377-2217(89)90247-6).
- [31] Hill, R.M. (1996). Optimizing a production system with a fixed delivery schedule, *Journal of the Operational Research Society*, Vol. 47, No. 7, 954-960, doi: [10.1057/jors.1996.121](https://doi.org/10.1057/jors.1996.121).
- [32] Thomas, D.J., Hackman, S.T. (2003). A committed delivery strategy with fixed frequency and quantity, *European Journal of Operational Research*, Vol. 148, No. 2, 363-373, doi: [10.1016/S0377-2217\(02\)00398-3](https://doi.org/10.1016/S0377-2217(02)00398-3).
- [33] Çömez, N., Stecke, K.E., Çakanyildirim, M. (2012). Multiple in-cycle transshipments with positive delivery times, *Production and Operations Management*, Vol. 21, No. 2, 378-395, doi: [10.1111/j.1937-5956.2011.01244.x](https://doi.org/10.1111/j.1937-5956.2011.01244.x).
- [34] Wu, M.-F., Chiu, Y.-S.P., Sung, P.-C. (2014). Optimization of a multi-product EPQ model with scrap and an improved multi-delivery policy, *Journal of Engineering Research*, Vol. 2, No. 4, 103-118, doi: [10.7603/s40632-014-0027-7](https://doi.org/10.7603/s40632-014-0027-7).
- [35] Safaei, M. (2014). An integrated multi-objective model for allocating the limited sources in a multiple multi-stage lean supply chain, *Economic Modelling*, Vol. 37, 224-237, doi: [10.1016/j.econmod.2013.10.018](https://doi.org/10.1016/j.econmod.2013.10.018).
- [36] Chiu, S.W., Sung, P.-C., Tseng, C.-T., Chiu, Y.-S.P. (2015). Multi-product FPR model with rework and multi-shipment policy resolved by algebraic approach, *Journal of Scientific & Industrial Research*, Vol. 74, No. 10, 555-559.
- [37] Tseng, C.-T., Wu, M.-F., Lin, H.-D., Chiu, Y.-S.P. (2014). Solving a vendor-buyer integrated problem with rework and a specific multi-delivery policy by a two-phase algebraic approach, *Economic Modelling*, Vol. 36, 30-36, doi: [10.1016/j.econmod.2013.09.013](https://doi.org/10.1016/j.econmod.2013.09.013).
- [38] Hishamuddin, H., Sarker, R.A., Essam, D. (2014). A recovery mechanism for a two echelon supply chain system under supply disruption, *Economic Modelling*, Vol. 38, 555-563, doi: [10.1016/j.econmod.2014.02.004](https://doi.org/10.1016/j.econmod.2014.02.004).
- [39] Chiu, S.W., Huang, C.-C., Chiang, K.-W., Wu, M.-F. (2015). On intra-supply chain system with an improved distribution plan, multiple sales locations and quality assurance. *SpringerPlus*, Vol. 4, No. 1, 687, doi: [10.1186/s40064-015-1498-1](https://doi.org/10.1186/s40064-015-1498-1).
- [40] Pai, F.-Y. (2015). How supplier exercised power affects the cooperative climate, trust and commitment in buyer-supplier relationships, *International Journal of Business Excellence*, Vol. 8, No. 5, 662-673, doi: [10.1504/IJBEX.2015.071275](https://doi.org/10.1504/IJBEX.2015.071275).
- [41] Ocampo, L.A. (2015). A hierarchical framework for index computation in sustainable manufacturing, *Advances in Production Engineering & Management*, Vol. 10, No. 1, 40-50, doi: [10.14743/apem2015.1.191](https://doi.org/10.14743/apem2015.1.191).
- [42] Šarić, T., Šimunović, K., Pezer, D., Šimunović, G. (2014). Inventory classification using multi-criteria ABC analysis, neural networks and cluster analysis, *Technical Gazette - Tehnički vjesnik*, Vol. 21, No. 5, 1109-1115.
- [43] Kaveh, M., Dalfard, V.M. (2012). A study on the effect of inflation and time value of money on lot sizing in spite of reworking in an inventory control model, *Technical Gazette - Tehnički vjesnik*, Vol. 19, No. 4, 819-826.
- [44] Al-Hawari, T., Ahmed, A., Khrais, S., Mumani, A. (2013). Impact of assignment, inventory policies and demand patterns on supply chain performance, *International Journal of Simulation Modelling*, Vol. 12, No. 3, 164-177, doi: [10.2507/IJSIMM12\(3\)3.235](https://doi.org/10.2507/IJSIMM12(3)3.235).
- [45] Rardin, R.L. (1998). *Optimization in Operations Research*, Prentice-Hall, New Jersey, USA.

Experimental modeling of fluid pressure during hydroforming of welded plates

Karabegović, E.^{a,*}, Poljak, J.^a

^aFaculty of Technical Engineering, University of Bihać, Bihać, Bosnia and Herzegovina

ABSTRACT

The procedure of hydroforming belongs to one of the modern methods of sheet and tube design, usually of complex configuration. Research in the field of plastic forming using fluids usually relates to the analysis of important parameters that would enable high-quality design of elements and execution of the process in stable conditions. The hydroforming process of welded sheets found its application in manufacturing of tanks and other sheet parts in automotive industry, where, in addition to technical and technological characteristics of the obtained piece, it is necessary to achieve stability of the process and its economic feasibility. Experimental research in this paper had been aimed at the analysis of results and modeling of working fluid pressure during hydroforming of welded sheets of two kinds of material (St 37 and Al 99.5) for two sheet thicknesses (1.5 mm and 2.0 mm). Modeling was done by regression method, whose analysis is the determination of functional relationships between a dependent variable and two independent variables. Application of mathematical modeling method enabled working fluid pressure which confirmed the impact of input variables of hydroforming process (yield strength and sheets thickness) onto the values of working fluid pressure. Experimental results obtained for working fluid pressure enabled easier planning and projection of hydroforming process.

© 2016 PEI, University of Maribor. All rights reserved.

ARTICLE INFO

Keywords:
Forming
Hydroforming
Welding sheet metal
Fluid pressure
Modelling
Regression

**Corresponding author:*
edina-karabeg@hotmail.com
(Karabegović, E.)

Article history:
Received 15 September 2016
Revised 20 November 2016
Accepted 24 November 2016

1. Introduction

The development of the automotive industry is based on the emergence of new materials and technologies for their processing. New methods of processing materials enable the achievement of technical and technological characteristics required by the market of the finished product.

Hydroforming is the process of forming sheets and tubes during which, by function of fluids under pressure, pieces, most often of complex shapes, are formed for the automotive industry [1-4].

The process is quick, inexpensive and meets the quality of shaped elements. So far, a number of studies have been conducted that included analytical, experimental, numerical, mathematical and other analyses of various treatment processes [5-10]. Hein and Vollertsen (1999) have conducted experimental and numerical research in order to establish the technological and economic characteristics of the process during hydroforming of double sheets [11]. The analysis and comparison of conventional deep drawing and process of sheet element hydroforming by using the finite element method [12] is the area of research of Chang et al. (2001). By application of CCD (Charge Coupled Device) camera, Groche, P. et al. (2007) conducted the control of sealing system during the execution of sheet hydroforming process.

The control of fluid pressure upon hydroforming of double sheets is an area of research of Assempour and Emami (2009) [13]. In their paper Ertugrul et al. (2009) analyzed hydroforming of laser welded sheets [14].

In addition, Liewald and Bolay (2010) in their paper state the analysis of hydroforming process of double sheets [15]. By application of finite element method (FEM) Zhang et al. (2015) analyzed the impact of stress or pressure of fluids on the improvement of quality of the double sheets hydroforming [16]. As can be seen, there is a constant need to improve the technical conditions and methods for execution of the hydroforming process.

This paper gives the analysis of the experimental execution of hydroforming process of welded sheets of two types of materials with different thicknesses. During hydroforming of pieces with defined size and shape, we have measured the working fluid pressure and displacement (expansion) of welded sheets. The experimental results were used in the process of mathematical modeling. Mathematical model for working fluid pressure was obtained for defined conditions of process execution.

2. The hydroforming process

Hydroforming of connected sheets is a technique of forming by effect of fluid pressure in the interior of the welded sheets. Thereby, the sheets are deformed (spread) to the interior shape of the die which defines the shape and dimensions of the finished piece. The hydroforming process of welded sheets is used for making fuel tanks, the car doors, etc.

Execution process scheme is given in four phases, as shown in Fig. 1:

- a) Placement of welded sheets into a die (matrix),
- b) Activation of pressure and pre-forming,
- c) Calibration with final pressure of the fluid,
- d) The finished piece is removed from the die.

With this process it is possible to form welded sheets of the same or different material and thickness. For the analysis in this paper, we conducted hydroforming of work element of the defined shape.

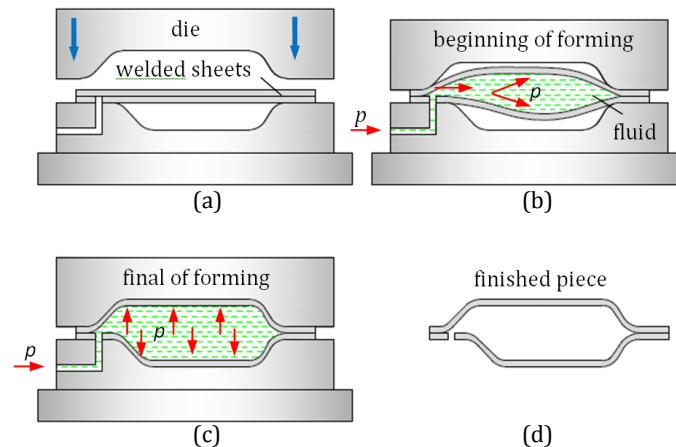


Fig. 1 Scheme of welded sheet hydroforming process

3. Experimental measurement of working fluid pressure

The following parameters were defined for the execution of the experiment:

- Geometrical shape and dimensions of finished pieces,
- Material (sheet) to produce beginning piece,
- Method of sheet welding,
- Tools for hydroforming and fluid,

- Pressure system or measuring amplifier device (pump),
- System for control and measurement of process parameters: computer and measurement equipment for information gathering.

Fig. 2 gives geometric shape and dimensions of the finished piece to be formed [17].

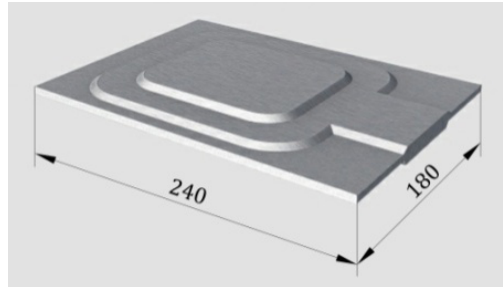


Fig. 2 Geometric shape and dimension of finished piece

3.1 Beginning piece and tools for hydroforming

When producing pieces (beginning piece), two types of materials (sheets) were applied, aluminum (99.5 %) and steel (St 37). Raw parts were produced from cold rolled sheets with thickness: $s = 1.5 \text{ mm}$ and $s = 2.0 \text{ mm}$. Mechanical properties of the material for raw parts are given in Table 1.

Table 1 Mechanical properties of materials

Types of materials	Yield strength, N/mm ²	Mechanical strength, N/mm ²	Modulus of elasticity, N/mm ²
Steel St 37	235	410	$2.1 \cdot 10^6$
Aluminium 99.5	100	120	$0.7 \cdot 10^4$

MIG welding procedure (protective argon gas) was selected for welding of the two materials.

Fig. 3 depicts the position of raw part in the tool for hydroforming of welded sheets.

Tool for hydroforming of welded sheets was produced from structural steel St 37 and consists of two parts (upper and lower matrix) and connection bolts.

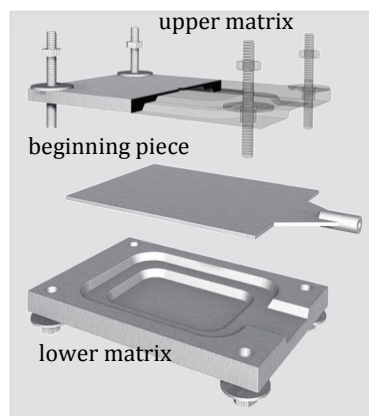


Fig. 3 The position of beginning piece in the tool for hydroforming of welded sheets

3.2. Pump for achieving working fluid pressure

Hydraulic high-pressure pump $p_{\max} = 3 \cdot 10^7 \text{ Pa}$ was used for the execution of the experiment. Working fluid for hydroforming is oil „Inol hidrol-X 46“, of density 0.884 g/cm^3 ($20 \text{ }^\circ\text{C}$).

3.3 Measuring equipment

Measuring amplifier device "Spider 8" with eight independent measuring channels was used for the measurement of working fluid pressure and displacement (expansion) of sheets, as shown in Fig. 4.

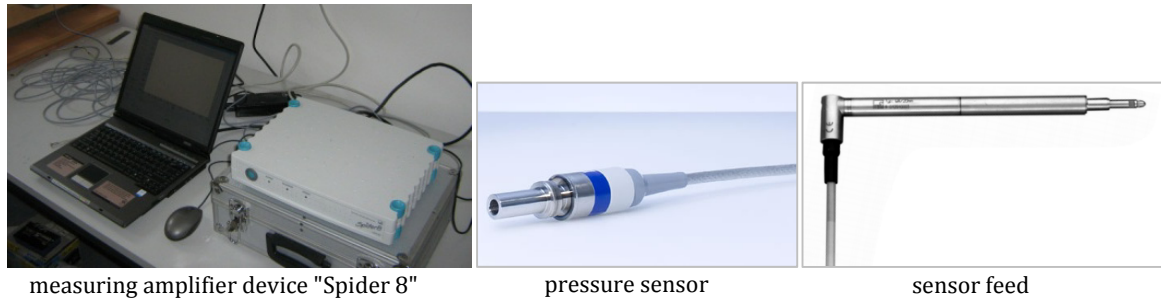


Fig. 4 Measuring equipment

Applied sensor for the measurement of the working pressure-P8AP, given in Fig. 5, operates on the principle of strain gauges. The nominal sensitivity of the sensor is 2 mV/5·10⁷ Pa. Sensor measuring range is 0-5·10⁷ Pa.

Displacement sensor-WA20, shown in Fig. 4, operates on inductive principle. Nominal sensitivity of the sensor is 80 mV/20 mm. Measuring range of the sensor is 0-20 mm.

Fig. 5 depicts the position of the sensor for measuring fluid pressure and displacement (expansion) of sheets during hydroforming of welded sheets.

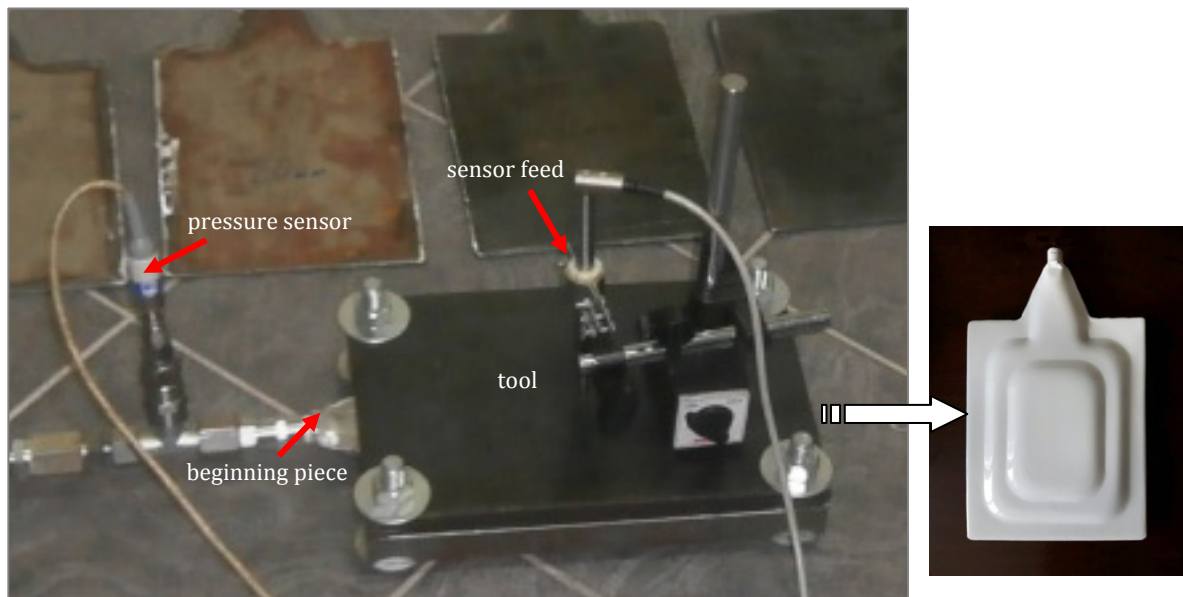


Fig. 5 The position of sensors during hydroforming of welded sheets and shaped piece

3.4 Number of tests in the experiment

Experimental measurements of the defined parameters are aimed at practical application of the results obtained in the planning, design and implementation process. Research and analysis of processes are important for achieving greater process stability in the given circumstances.

Number of probes in this experiment was determined by the rotatable plan of the experiment and expression:

$$N = 2^{k-p} + 2k + n_0 = n_k + n_\alpha + n_0 = 2^2 + 2 \cdot 2 + 5 = 13 \quad (1)$$

where N is total number of experiments, n_k is number of change of variables, n_0 is number of repetitions in plan center, and n_a is number of symmetrically positioned points at plan center. Experiment plan matrix has the shape presented in Table 2. Experiment was conducted in the laboratory of the Faculty of Technical Engineering of the University of Bihac.

Table 2 Experiment plan matrix

Trial No.	Input variables of the process Physical values		Coded values						Vector output Y_i
	Yield strength, N/mm^2 ($\sigma_{0.2}$)	Thickness, mm (s_i)	X_0	X_1	X_2	$X_1 X_2$	X_1^2	X_2^2	
1	100	1.5	1	-1	-1	1	1	1	Y_1
2	235	1.5	1	1	-1	-1	1	1	Y_2
3	100	2.0	1	-1	1	-1	1	1	Y_3
4	235	2.0	1	1	1	1	1	1	Y_4
5	168	1.75	1	0	0	0	0	0	Y_5
6	168	1.75	1	0	0	0	0	0	Y_6
7	168	1.75	1	0	0	0	0	0	Y_7
8	168	1.75	1	0	0	0	0	0	Y_8
9	168	1.75	1	0	0	0	0	0	Y_9
10	263	1.75	1	1.414	0	0	2.0	0	Y_{10}
11	72	1.75	1	-1.414	0	0	2.0	0	Y_{11}
12	168	2.10	1	0	1.414	0	0	2.0	Y_{12}
13	168	1.39	1	0	-1.414	0	0	2.0	Y_{13}

4. Measurement results

Experimental results of working fluid pressure and displacement (expansion) of sheets during hydroforming of welded aluminum and steel sheets, with thickness of 1.5 mm and 2.0 mm, are given in Fig. 6.

Experimental results of working fluid pressure for hydroforming of welded aluminum sheets are given in Fig. 7.

Experimental results of working fluid pressure for hydroforming of welded steel St 37 sheets are given in Fig. 8.

Comparative results of the working fluid pressure for hydroforming of welded sheets of aluminum and steel with 1.5 mm thickness are given in Fig. 9.

Comparative results of the working fluid pressure for hydroforming of welded sheets of aluminum and steel with 2.0 mm thickness are given in Fig. 10.

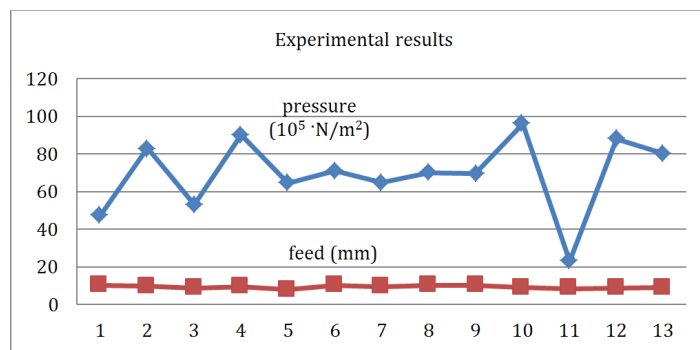


Fig. 6 Experimental results of working fluid pressure and displacement during hydroforming of welded sheets

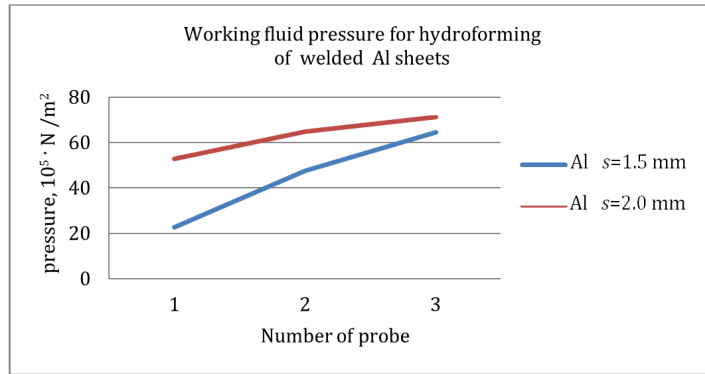


Fig. 7 Working fluid pressure for hydroforming of welded aluminum sheets

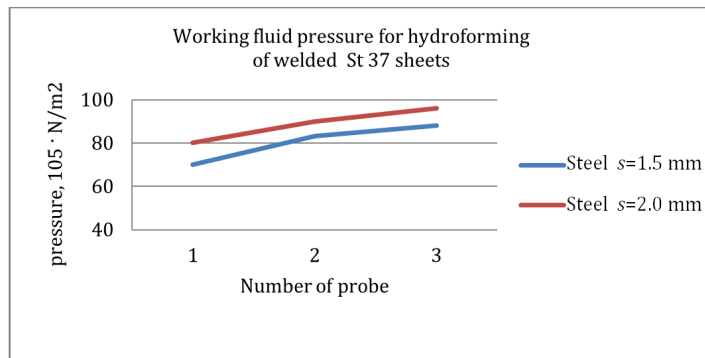


Fig. 8 Working fluid pressure for hydroforming of welded steel sheets

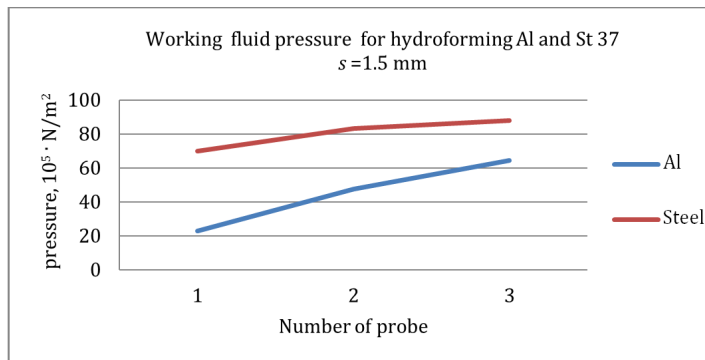


Fig. 9 Comparative results of working fluid pressure for aluminum and steel sheets with 1.5 mm thickness

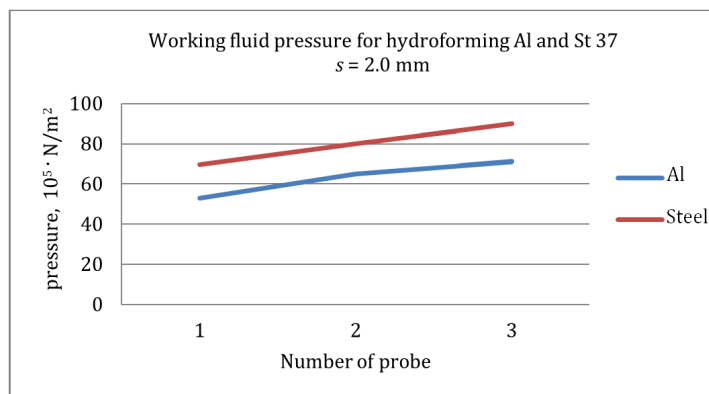


Fig. 10 Comparative results of working fluid pressure for aluminum and steel with 2.0 mm thickness

Analysis of the experiment results

The analysis of the obtained experimental values of the working fluid pressure for 13 samples (welded sheet 1.5 mm and 2.0 mm thickness, aluminum Al 99.5 % and steel St 37) provides the following conclusions:

- Average value of the working fluid pressure to form 2.0 mm thick aluminum sheet compared to the sheet thickness of 1.5 mm is higher for around 10.38 %,
- Average value of the working fluid pressure to form 2.0 mm thick steel sheet compared to the sheet thickness of 1.5 mm is higher for around 7.67 %,
- Increase in the working fluid pressure in both materials is the result of an increase in the thickness of welded sheets,
- The design of welded 1.5 mm thick steel sheet requires higher values of the working fluid pressure for around 42.84 % compared to welded aluminum sheets of the same thickness,
- The design of welded 2.0 mm thick steel sheet requires higher values of the working fluid pressure for around 41.12 % compared to welded aluminum sheets of the same thickness,
- Increase in the working fluid pressure during hydroforming of welded steel sheets is justified due to the differences in the mechanical properties of steel and aluminum,
- Average value of displacement deviations for 13 samples is about 7 %, which is caused by changes in the structure and quality of the sheet.

5. Modeling of working fluid pressure during hydroforming of welded sheets

The measured values of the working fluid pressure and displacement after conducted 13 experiments will be used to define a mathematical model that, in the appropriate level of accuracy, adequately describes the hydroforming process of welded sheets with defined shape and conditions of the process execution.

The model would be used in the design phase of the process, in analyzing and forecasting the state of the process [18].

The analysis of the stochastic process starts from the general functional relationship between the dependent variable size (Y_i) and independent variables (x_i), which can be presented with the model as follows:

$$Y_i = f(x_i) = f(x_1, x_2) \tag{2}$$

$$\text{i.e. } Y = p = f(\sigma_{0.2}, s) \tag{3}$$

Coded values of physical quantities are obtained using the following expressions:

$$X_1 = 1 + 2 \frac{\ln \sigma_{0.2i} - \ln \sigma_{0.2imax}}{\ln \sigma_{0.2max} - \ln \sigma_{0.2min}}; X_2 = 1 + 2 \frac{\ln s_i - \ln s_{imax}}{\ln s_{max} - \ln s_{min}} \tag{4}$$

Table 3 gives the physical and coded values of input parameters for hydroforming of welded sheets.

Table 3 Physical and coded values of the input variables

Input variables of the process		Coded values				
		$-\sqrt{2}$	-1	0	1	$\sqrt{2}$
Physical values	$x_1 = \sigma_{0.2}$ N/mm ²	72.0	100.0	168	235	263
	$x_2 = s_i$ mm	1.39	1.5	1.75	2.0	2.10

For the analysis of the process, the most commonly used form is polynomial function, so the impact of independent variable parameters onto output variable can be displayed in a polynomial mathematical model of the second order:

$$Y = b_0 + b_1x_1 + b_2x_2 + b_{12}x_1x_2 + b_{11}x_1^2 + b_{22}x_2^2 \quad (5)$$

Testing the importance of coefficients ($b_0, b_1, b_2, b_{12}, b_{11}, b_{22}$) and the adequacy of the mathematical model was established with the system of experiment repetition in the central point of the plan.

$$Y = 68.04 + 22.01X_1 + 2.95X_2 - 5.21X_{11}^2 + 7.12X_{22}^2 \quad (6)$$

Testing of adequacy was conducted with mathematical analysis according to F-criterion Fisher. The condition $F_a \leq F_t$ is satisfied.

$$F_a = 5.04 \leq F_t = 9.12 \quad (7)$$

in which F_a – adequacy according to Fisher criterion, and F_t – tabulated values according to Fisher criterion.

Testing the multiple regression coefficients R provided additional adequacy indicator of the obtained mathematical model:

$$R = \sqrt{1 - \frac{\sum_{j=1}^N (y_j^E - y_j^R)^2}{\sum_{j=1}^N (y_j^E - \bar{y}^E)^2}} = 0.981 \quad (8)$$

in which:

y_j^E – Values of experimental results,

y_j^R – Calculation values of the obtained model, and

$\bar{y}^E = \frac{\sum_{i=1}^N y_j^E}{N}$ – Arithmetic mean of all experimental results.

The value of $R = 0.981$ ($0 \leq R \leq 1$) indicates that the model positively describes the results of the experiment which confirms the interdependence between the input variables and goal functions (working fluid pressure).

The coefficient of determination R^2 is determined by the quality and reliability of the model.

$$R^2 = 0.962 \quad (9)$$

The obtained results of the coefficient of determination R^2 indicate that 96.2 % of the variability is attributed to the operation of the input variables (X_i).

Final, decoded form of mathematical model for working fluid pressure is given in expression:

$$Y = p = -28.55 \ln(\sigma_{0.2})^2 + 348.25 + 338.84 \ln(\sigma_{0.2}) - 362.35 \ln(s) - 820.3 \quad (10)$$

The fluid pressure values obtained by mathematical modeling, in regard to the change of sheet thickness and yield strength, are given in Fig. 11.

Comparative values of fluid pressure obtained by modeling and experimental measurements are presented in Fig. 12.

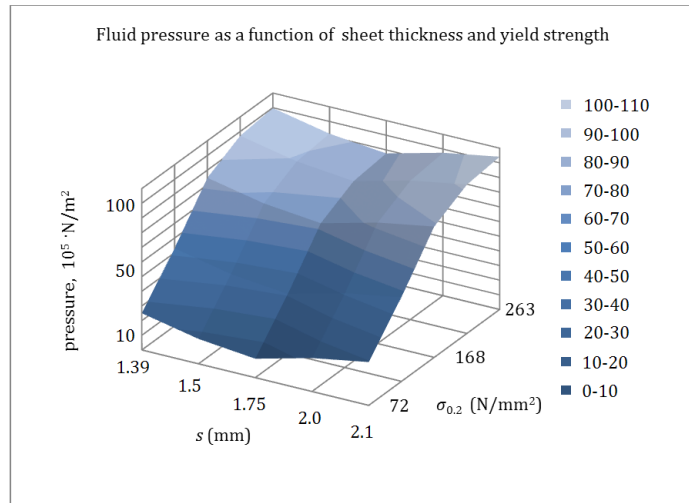


Fig. 11 Chart of the fluid pressure as a function of the sheet thickness and yield strength by model

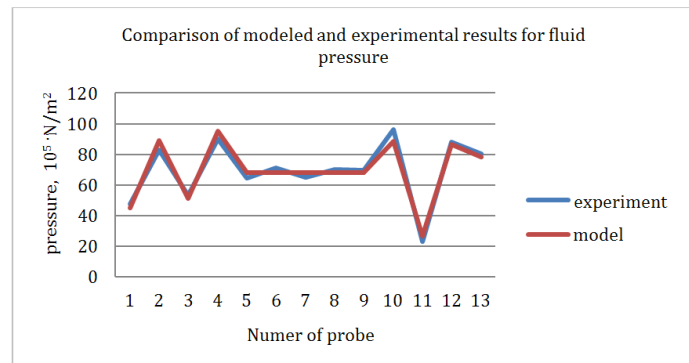


Fig. 12 Comparison of modeled and experimental results for fluid pressure during hydroforming of welded sheets

6. Conclusion

Accuracy, quality and ability to create very complex sheet pieces in one phase justify the fact that about 20 % of the parts in the automotive industry are obtained by applying sheet hydroforming process. The result is an increase in the number of research and development of hydroforming process. Experimental research in the paper aimed to obtain a mathematical model to determine the working pressure of the fluid, which would be applied in the design of hydroforming process of welded sheets of steel St 37 and Al 99.5, with sheet thickness of 1.5 mm and 2.0 mm. Analysis of the results was conducted after planning and execution of the experiment, confirming the influence of mechanical properties of materials (yield strength) and the geometric sizes (thickness of the sheet) on the value of the experimentally obtained working fluid pressure.

The experimental results were applied to mathematical modeling. A series of mathematical verifications referring to the uniformity of results, reliability and checking the adequacy of the mathematical model were conducted in order to obtain the resulting mathematical model.

The quality and reliability of the model has been confirmed by the coefficient of determination, which shows that 96.2 % of the variability is attributed to the influence of input variables, yield strength and thickness of the sheet. Comparative overview of the results (Fig. 12) indicates that the deviation in the values of working fluid pressure obtained by mathematical modeling is very small compared to the values obtained experimentally.

The resulting mathematical model will be used in the design of hydroforming process of welded sheets, and optimization of the working pressure of the fluid.

References

- [1] Harjinder, S. (2003). *Fundamentals of Hydroforming*, Society of Manufacturing Engineers, Michigan, USA.
- [2] Jurković, M., Mamuzić, I., Karabegović, E. (2004). The sheet metal forming with hydraulic fluid pressure, *Metallurgija*, Vol. 43, No. 4, 315-322.
- [3] Karabegović, E., Brezocnik, M., Mahmić M., Karabegović, I., Pašić, S., Isić, S. (2014). *Nove tehnologije u proizvodnim procesima – Razvoj i primjena (New technologies in production processes – Development and application)*, Mašinski fakultet Mostar, Mostar, Bosnia and Herzegovina.
- [4] Karabegović, E., Stupac, K., Poljak, J. (2013). Process of sheet and tube hydroforming, *International Journal of Engineering and Technology*, Vol. 3, No. 8, 826-828.
- [5] Parsa, M.H., Darbandi, R. (2008). Experimental and numerical analyses of sheet hydroforming process for production of an automobile body part, *Journal of materials processing technology*, Vol. 198, No. 1-3, 381-390, doi: [10.1016/j.jmatprotec.2007.07.023](https://doi.org/10.1016/j.jmatprotec.2007.07.023).
- [6] Gelin, J.C., Labergère, C., Thibaud, S. (2006). Modelling and process control for the hydroforming of metallic liners used for hydrogen storage, *Journal of Materials Processing Technology*, Volume 177, No. 1-3, 697-700, doi: [10.1016/j.jmatprotec.2006.04.109](https://doi.org/10.1016/j.jmatprotec.2006.04.109).
- [7] Yaghoobi, A., Bakhshi-Jooybari, M., Gorji, A., Baseri, H. (2016). Application of adaptive neuro fuzzy inference system and genetic algorithm for pressure path optimization in sheet hydroforming process, *International Journal of Advanced Manufacturing Technology*, Vol. 86, No. 9, 2667-2677, doi: [10.1007/s00170-016-8349-2](https://doi.org/10.1007/s00170-016-8349-2).
- [8] Ashrafi, A., Khalili, K. (2016). Investigation on the effects of process parameters in pulsating hydroforming using Taguchi method, *Proceedings of the Institution of Mechanical Engineers, Part B: Journal of Engineering Manufacture*, Vol. 230, No. 7, 1203-1212, doi: [10.1177/0954405415597831](https://doi.org/10.1177/0954405415597831).
- [9] Zhang, F.F., Chen, J., Chen, J.S., Lu, J., Liu, G., Yuan, S.J. (2012). Overview on constitutive modeling for hydroforming with the existence of through-thickness normal stress, *Journal of Materials Processing Technology*, Vol. 212, No. 11, 2228-2237, doi: [10.1016/j.jmatprotec.2012.06.018](https://doi.org/10.1016/j.jmatprotec.2012.06.018).
- [10] Yang, L., Tao, Z., He, Y. (2015). Prediction of loading path for tube hydroforming with radial crushing by combining genetic algorithm and bisection method, *Journal of engineering manufacture*, Vol. 229, No. 1, 110-121, doi: [10.1177/0954405414523752](https://doi.org/10.1177/0954405414523752).
- [11] Hein, P., Vollertsen, F. (1999). Hydroforming of sheet metal pairs, *Journal of Materials Processing Technology*, Vol. 87, No. 1-3, 154-164, doi: [10.1016/S0924-0136\(98\)00347-1](https://doi.org/10.1016/S0924-0136(98)00347-1).
- [12] Chang, J.C., Lei, L.P., Kang, B.S. (2001). Finite element analysis of hydroforming process for sheet metal pairs, In: Mori, K.-I. (ed.), *Simulation of Materials Processing: Theory, Methods and Applications*, 873-877.
- [13] Assempour, A., Emami, R.M. (2009). Pressure estimation in the hydroforming process of sheet metal pairs with the method of upper bound analysis, *Journal of Materials Processing Technology*, Vol. 209, No. 5, 2270-2276, doi: [10.1016/j.jmatprotec.2008.05.020](https://doi.org/10.1016/j.jmatprotec.2008.05.020).
- [14] Ertugrul, M., Groche, P. (2009). Hydroforming of laser welded sheet stringers, *Key Engineering Materials*, Vol. 410-411, 69-78, doi: [10.4028/www.scientific.net/KEM.410-411.69](https://doi.org/10.4028/www.scientific.net/KEM.410-411.69).
- [15] Liewald, M., Bolay, C. (2010). Manufacturing of shell structures by means of double sheet hydroforming, In: 10th Stuttgart International Symposium Automotive and Engine Technology, (10. Internationales Stuttgarter Symposium 2010 Automobil- und Motorentechnik), Stuttgart, Research Institute for Automotive and Automobile Engine Technology, Stuttgart, Germany, 641-656.
- [16] Zhang, F., Li, X., Xu, Y., Chen, J., Chen, J., Liu, G., Yuan, S. (2015). Simulating sheet metal double-sided hydroforming by using thick shell element, *Journal of Materials Processing Technology*, 221, 13-20 doi: [10.1016/j.jmatprotec.2015.02.001](https://doi.org/10.1016/j.jmatprotec.2015.02.001).
- [17] Poljak, J. (2014). *Matematičko modeliranje i optimizacija pritiska fluida kod hidrooblikovanja limova (Mathematical modeling and optimization of fluid pressure in hydroforming of sheets)*, Master thesis, University of Bihać, Bosnia and Herzegovina.
- [18] Jurković, M. (1999). *Matematičko modeliranje inženjerskih procesa i sistema, (Mathematical modeling of engineering processes and systems)*, University of Bihać, Bosnia and Herzegovina.

An integrated lean approach to Process Failure Mode and Effect Analysis (PFMEA): A case study from automotive industry

Banduka, N.^{a, b, *}, Veža, I.^a, Bilić, B.^a

^aUniversity of Split, Faculty of Electrical Engineering, Mechanical Engineering and Naval Architecture, Split, Croatia

^bUniversity of Kragujevac, Faculty of Engineering, Kragujevac, Serbia

ABSTRACT

Every automotive company is using ISO/TS 16949 standard for automotive industry. According to this standard of Process failure mode and effect analysis (PFMEA), is obligatory. Also, the application of lean in automotive industry is a trend nowadays. Both, PFMEA and lean have the same main purpose – identification, prevention, and correction of failures during the production process. But, PFMEA have many shortcomings. In this paper, an integrated lean approach to PFMEA for solving specific shortcomings, is presented. This approach is new and it has not been used until now. Lean approach (tools and principles), were integrated in PFMEA. The new approach to solving PFMEA was presented in algorithm form. Some of those lean tools and principles integrated in PFMEA are: Genchi Genbutsu, Kaizen, standardized work, Jidoka, and 5 why. The approach presented was realized in a case study from automotive industry where traditional approach to PFMEA was compared to the new lean approach integrated to PFMEA. Changed and improved conditions were: number of team members, the actions taken, identification of failures, change of Severity (S), Occurrence (O), detection (D) and risk priority number (RPN) values, reduced S, O, D, and RPN values after taken actions, RPN with value over 100, and S, O, D indexes with value over 8.

© 2016 PEI, University of Maribor. All rights reserved.

ARTICLE INFO

Keywords:

Lean approach
Process failure mode and effect analysis (PFMEA)
Automotive industry

*Corresponding author:

nikola.banduka90@gmail.com
(Banduka, N.)

Article history:

Received 8 July 2016
Revised 19 November 2016
Accepted 21 November 2016

1. Introduction

In many cases from the automotive industry, the largest number of automobile parts (about 70%), is produced by suppliers. Since that, design and design risk analysis are usually conducted inside car manufacturer's companies. Suppliers' job is widely related to production or assembly process, so it is very important to predict and eliminate potential defects (failures) during the process. Failures reduce product's quality, leading to production delay due to rework or additional production that leads, once more, to additional costs. With more time needed to find failures, costs are much bigger. The recommendation would be to eliminate failures with quality system on source, with prevention rather than detection [1, 2]. Therefore, if companies want to sustain market competitiveness, they have to install proactive systems for prevention of failures. According to ISO 9000 and ISO/TS 16949 standards, best classified analysis for prevention of failures during the production process is Process failure mode and effect analysis (PFMEA) [3, 4].

According to many authors, PFMEA is a very subjective method with many shortcomings, so reliability of its results is variable [2, 5, 6]. Case study for PFMEA conducted in 150 supplier

companies from automotive industry shows that the biggest part of surveyed suppliers sees PFMEA as additional administrative work which wastes a lot of time, and gives back less benefits [5]. Obviously it is a problem in misunderstanding or in inadequate use of PFMEA by users. Therefore, there is still lot of space for improvement of this analysis.

From the other side, lean was created due to the need for automotive industry to progress. Main purpose of lean was identification, prevention and correction of the problems in industry. Nowadays, a wide application of lean can be found in automotive companies all over the world. From the case study carried out on 300 manufacturers, it is evident that 90 % of them are applying lean [7]. Also, according to the recent research from 2015 published by Boston Consulting Group, 30 % of the world's original equipment manufacturers use lean tools in their production systems [8]. With this data, the theory about wide application of lean approach in automotive industry, is confirmed.

Since lot of automotive companies are using lean approach and PFMEA for prevention of failures, methodology for realization of PFMEA with integrated lean approach, will be presented in this paper. Also, a case study in one specific automotive company will be realized. In a Case study, results from reports of already realized traditional PFMEA and new PFMEA with integrated lean approach, will be compared.

2. PFMEA in automotive industry

The main objective of PFMEA is to identify potential failures, evaluate causes and effects of these failures, and to propose solutions to prevent these potential failures. The ultimate goal is a failure-free product in production process. PFMEA is one of two main types of failure mode and effect analysis (FMEA). Two main types are defined according to the phase where the product currently is. That could be design or production phase. According to this FMEA, the analysis related to design phase is a Design failure mode and effect analysis (DFMEA) and FMEA related to process is PFMEA. One of the differences between these two types is that for DFMEA the end user is a customer, but for PFMEA it can be the next user in a process. Also, PFMEA is more complicated and time-consuming than DFMEA. This analysis is a living document, which means that it has to be upgraded with new information or changed due to changes of product or process. For PFMEA report in automotive industry, a standard report form is usually used. This form is proposed in reference manual by Chrysler LLC, Ford Motor Company, and General Motors Corporation in 2008 [9]. Traditional risk priority number (RPN) is calculated by multiplication of Severity (S), Occurrence (O), and Detection (D) as it is shown on Eq. 1. These three indexes S, O, D and RPN are also defined according to standard tables for automotive industry proposed in the same reference manual. RPN goes from 1-1000 and S, O, D indexes from 1-10. Corrective actions should be taken any time, but especially when RPN exceeds 100 or one of indexes S, O or D exceeds 8. PFMEA is mostly conducted in team, with classic brainstorming technique while some standards obligate companies to realize PFMEA reports in a team [3, 4].

$$S \cdot O \cdot D = RPN \quad (1)$$

In 1973, Ford Motor Company was among the first users of PFMEA in automotive industry for preventive maintaining quality [10]. Later in the 1990s, PFMEA became the standard practice in most majority automotive companies and their suppliers, until today. Three most prestigious automotive manufacturers from USA (Chrysler LLC, Ford Motor Company, and General Motors Corporation), set PFMEA as a mandatory to their suppliers in 1990s. Because of this, suppliers had a lot of problems due to the regulations disagreement. So, in 1993 (Automotive Industry Agency Group) AIAG integrated different FMEA regulations into one uniformed document. This resulted with publishing guide reference manual [9, 11]. Today, the fourth edition of this guide from 2008 is actual [9]. The Case study from 2003 presented various use of traditional PFMEA in automotive industry in Europe [5]. Also, in review paper from 2013 a wide use of PFMEA is presented in industry, especially in automotive industry [6]. This means that a proper use of PFMEA could be of a great importance for automotive industry.

Traditional PFMEA approach have many shortcomings. Some of these shortcomings were identified in the case study realized on 150 automotive supplier companies from United Kingdom and Central Europe [5]. This case study also highlighted main opportunities for improvements: costs, S, O, and D data, technical and resource, standardization, training, PFMEA software. There is also one review paper which highlighted problems related to traditional RPN [6]. This study shows about 75 articles related to RPN improvements or alternative ways to RPN calculation. In this paper, various authors were using artificial intelligence, multi-criteria decision making, mathematical programming, hybrid approaches, and other approaches like cost-based approaches, Monte Carlo simulations, etc. All these approaches were giving more precise RPN but increasing time-consuming of PFMEA realization and therefore were very hardly applicable in real-world cases. All these improvements and different approaches are partially solving PFMEA shortcomings which was the biggest problem for its application.

Companies have to respond to customers demand fast, with right quality and with acceptable price. That means that the PFMEA team will not have the time to realize all these complicated and time-consuming methods partially. Industry has the need for comprehensive solution which will satisfy all three mentioned factors (time, quality, and cost).

3. Lean approach

Lean is American term to describe the Toyota production system (TPS). The advent of TPS is related to period after World War II. This Company was in need of a great solution which will turn the company on and make it more competitive on the market. TPS was that solution. Mass production which was widely used all over the world, was changed with "pull system", or production of the customer demanded products only [12]. Company focus were changed to continuous improvement and quality management in every step. TPS was not famous beside the Toyota company and its suppliers until 1943, when first oil crisis attacked the world. The most important fact is that the TPS led Toyota company to the first place on world's car manufacturers list. Lean became popular worldwide in the 1990s, when many companies started applying it [13].

The lean approach in this paper is approach made of using lean thinking, principles and tools for solving PFMEA. Lean principles can be understood best through 4 basic Toyota principles: Genchi Genbutsu (go and see for yourself), Kaizen (continuous improvement), team work and respect for people, and challenge. Based on this 4 principles, Liker, J. K. [13] preformed his own 4 principles known as 4P: philosophy, process, people and partners, and problem solving. Lean approach could be applied to any other business aspect or in any business situation [13]. Firstly, lean approach have been applied to manufacturing process – lean manufacturing. But nowadays, lean approach is applicable in many other aspects like: lean enterprise, lean office, lean start-up, lean development, lean system, etc. Lean approach in automotive industry is mostly used for production process improvements. For these improvements, various lean tools are commonly used. For example: Jidoka, Poka-Yoke, Kanban, single minute exchange of die (SMED), just in time (JIT), 5S, standardized work, 5 why, total productive maintenance (TPM), PDCA, etc.

Main purposes of lean are in identifying, preventing and correcting of failures and problems. According to that, lean approach have almost the same purpose in production process as PFMEA. Therefore, there is a lot of space for integration of lean approach in PFMEA for failure prevention improvement.

4. Integrated lean approach in PFMEA

This is the new approach in science until now. Various authors conducted several research on similar but reverse approach. They were using FMEA as a tool to improve lean system. This is not necessary, because companies which are using lean approach does not need FMEA to prevent risks and failures. Automotive company is the unique example, because PFMEA is obligatory, with most of them using lean approach also.

Shekari, A. et al. [15] were using FMEA as a tool for failure detection to improve lean system. Sawhney, R. et al. [16] presented modified FMEA approach for reliability improvements of lean

system. Then, Shahrabi, M., et al. [17] applied FMEA and AHP methods for improvements due to maintenance of lean system. These papers were related to the use of FMEA in order to improve lean systems. There was one example of using lean tools to improve FMEA. Pavanasvaran, P., et al. [18, 19] used lean tool named Poka-Yoke to improve FMEA. But this tool was used separately, not as a whole lean approach.

Idea is to integrate lean approach into steps to PFMEA realization. But firstly, shortcomings which occur during PFMEA realization have to be identified and fixed with lean approach. For many of these shortcomings various solutions have been already found. For example, for RPN, costs, S, O, D indexes, etc. lot of solutions have been found. But, there is still a lot of space for improvements. Specified shortcomings identified in literature, which can be fixed with lean approach are presented in Table 1. These shortcomings are defined by various authors and they are presented in the left column. In the right column, the lean approach solutions for fixing of specified shortcomings are presented.

As it can be noticed, each of the shortcomings is solved with lean approach. Some of the used lean tools are: standardized work, Kaizen, Jidoka, and 5 why. One of principles used was – Genchi Genbutsu. These tools and the principle will be integrated as a lean approach into PFMEA, resulting with the new PFMEA approach.

The new PFMEA approach is proposed in algorithm form on Fig. 1. Proposed algorithm is divided in four phases of Deming's PDCA cycle for problem solving. Plan (P), do (D), check (C), act (A) is a four-phase-cycle for problem solving which Deming proposed in 1950 [23]. Plan phase is broken down in several segments for detailed analysis. Do phase is related to plan execution. Check phase is needed for checking of every progress. Act phase is related to recognized and standardized solution. PDCA cycle is the approach to problem solving frequently used in lean approach.

Table 1 Application of lean approach for fixing the specific PFMEA's shortcomings

Shortcomings	Lean approach for fixing the shortcomings
Wrong approach to detecting failures of root cause [5]	Root cause of failure can be identified with lean tool for identification of root cause of problem – 5 why
Unutilized existing resources [5]	There are many resources unutilized in companies which can be used for improvements during PFMEA realization. One of the most unused resources are people in company. In lean systems, all employees should be involved in improvements – Lean approach
Problem during defining RPN actions [6]	Failures should be treated respectively with higher RPN. Surely, all failures need to be solved or reduced due to the “zero failure” goal of lean approach – Kaizen
Repeating of failures in next row [6]	Failures should be solved with solutions consequently standardized. Data base also needs to avoid failure repeating – standardized work
Traditional brainstorming is boring and time consuming [11].	Failure identification should be done directly in shop floor and workers should be also involved in analysis – Genchi Genbutsu
It's impossible to use again FMEA report [20].	Use of software with tables in which revision can be done that imply a constant improvement – software solution and Kaizen
FMEA report fulfilment is very time consuming [21, 22].	Lean should be accessed slowly and thoroughly, rather than fast and superficially. Standardization of PFMEA failures will mean less failures to improve. So PFMEA realization will go faster - lean approach.

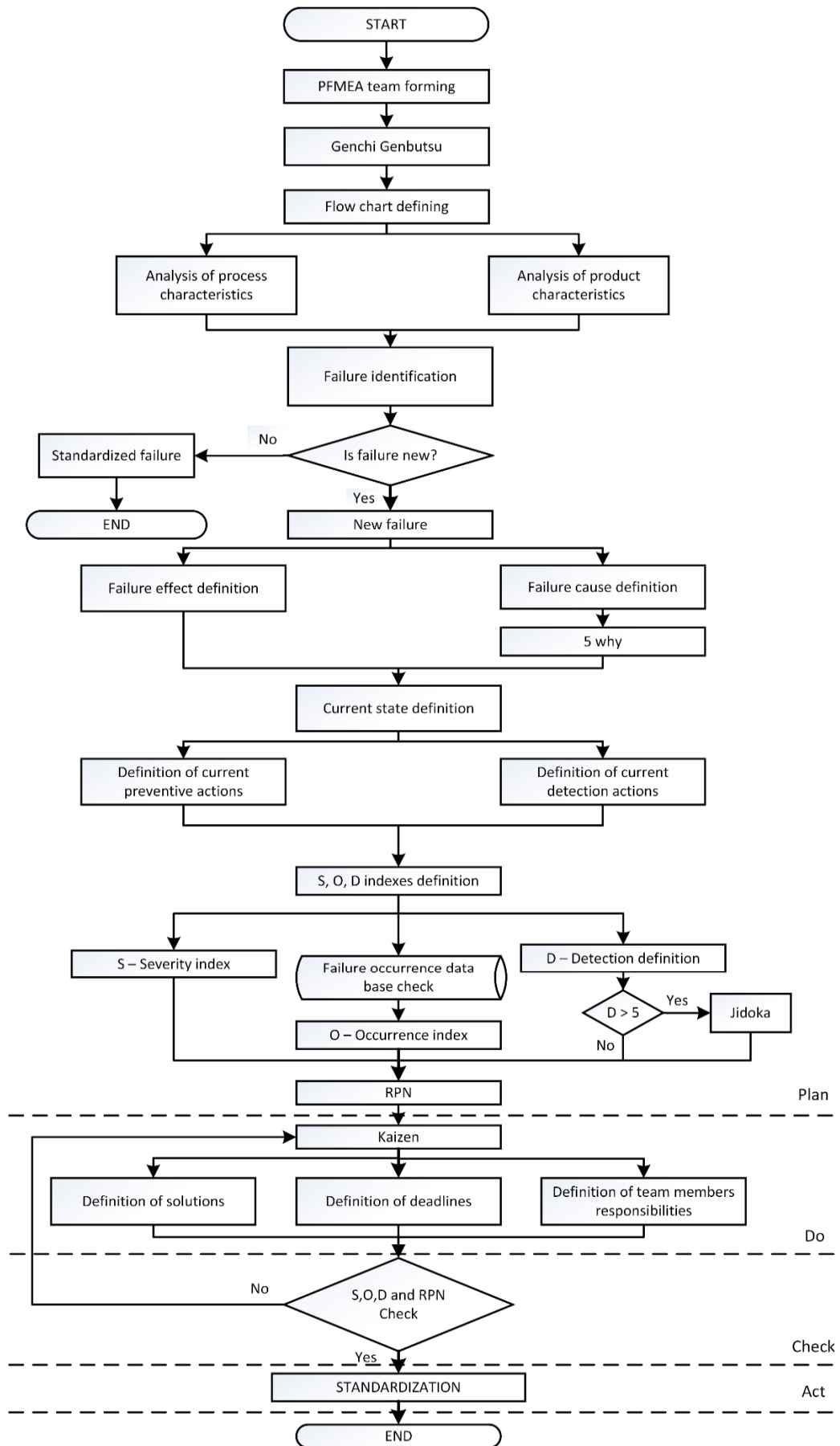


Fig. 1 Algorithm model for PFMEA with integrated lean approach

New PFMEA approach is starting with multidisciplinary team forming. When the team is formed, identification of problems should start. Firstly, team have to go directly to the place where the process is going to be performed and observe how the process really looks like – Genchi Genbutsu. Also, it is highly recommended to include shop floor workers in decision making process. Workers are directly in contact with the process, and they usually know best what kind of problems may occur. When these terms are satisfied, team should propose process flow chart. After flow chart definition, process and product characteristics should be deeply analysed. Identification of failures is one of the most important steps, because it directly depends on team members' opinion. There are two types of failures: standardized failures and the new one failures. Standardized failures are already known and they exist in data base. New failures, occurring for the first time, have to be defined, solved and standardized. For these new failures effects and causes of failures have to be identified. Team is often blending effects and causes which is a very big problem [5]. For all causes, one lean tool is specified for finding a root cause of the problem – 5 why. According to the current state, S, O, and D indexes should be defined. For O index, a special data base is needed. This data base should contain the amount of same or similar problem occurrence. D is another index with special issue, due to the lean approach purpose of producing in quality, so quality have to be provided on source - Jidoka. For the case of automotive industry, in detection table from fourth edition of reference manual guide for automotive industry, automatized control for first 5 indexes, is predicted [9]. Over 5 isn't automatized, so if $D > 5$ then Jidoka or quality on source, should be applied. With all three indexes defined, RPN can be calculated as the end of the plan phase.

After the plan phase, do phase or realization phase follow. For all defined RPN, corrective actions or Kaizen, should be taken. Suggested improvements had to be set on a list of solutions, with exact deadlines and with responsible team members.

Third phase is check phase where the action taken has to be checked with repeating of RPN calculation. If there is no progress, then Kaizen should be performed again. This check phase have to be realized very carefully, because after this phase failure should be standardized.

Last phase is act phase. When the solution is finally found and the progress has been made, failure and elected solution have to be standardized and ready to use.

5. The new PFMEA approach: Case study from automotive industry

The company elected for the case study is automotive company which produce electronic circuit boards and electronic cables for automobiles. Company is supplying automotive suppliers and corporations all over the world. This company applies lean approach in their production system for a long time and also use PFMEA for prevention of failures and risks. The use of PFMEA in this company is obligatory according to ISO9000 and ISO TS16949 standards.

PFMEA for product MSM6BL was already realized on traditional way. Results are presented in Table 2. Measured conditions taken for comparison are: number of team members, identification of failures, change of S, O, D and RPN values, reduced S, O, D, and RPN values after taken actions, RPN value over 100, and S, O, D value over 8. These conditions are measured in total amount for whole PFMEA. The goal is to compare them with the new approach and see the differences after its implementation. S, O, D and RPN value changes are also calculated in total change regardless if it is increased or reduced value.

Methodology set in algorithm form from Fig.1 is used for realization of PFMEA. Realized PFMEA report is shown in Appendix 1. The changes made after the new approach are painted in grey in Appendix 1. They have been implemented and used for calculation. The data for a new state are presented in Table 2. These data were taken from Appendix 1, also. After this step, the comparison between the state after traditional approach to PFMEA realization and the new approach to PFMEA realization with integrated lean approach, was made. These results are also presented in Table 2.

From Table 2, it can be seen that almost all conditions are changed, except one - S. Two conditions; the actions taken and identification of failures, are very important for analysis because they are related to the purpose of analysis to detect a failure and take action to improve it. Gen-

chi Genbutsu have mostly contributed to these changes. Lean approach stimulated involvement of more employees, including six workers. As it was predicted, workers contributed a lot to failure identification because they are directly involved in a process. But Genchi Genbutsu stimulated PFMEA team to go directly in process and observe an actual status. Increased identification of failures and the taken action can avoid hidden failures reaching customer. Also, they affected the changes of S, O, D indexes and RPN values. Moreover, during these changes, value of some S, O, D indexes exceeded 8 and RPN values exceeded 100. The lack of situations when S, O, D and RPN exceed predicted values for improvements, may cause problems if failures reach a customer. Only one condition which is not reduced is S index due to the actions taken, which is not a big issue due to the O and D indexes reduction for that failures. This was achieved due to the application of Kaizen. Also, some of D indexes were reduced due to the application of Jidoka. Causes of failures were superficially defined and some resulted with mixing of causes and effects. With application of lean tool - 5 why, root causes of failures were deeply analysed. The actions taken were oriented on fixing root causes of failure, not effects. One more lean tool used in this case study, is standardized work. Some of failures were standardized. This means that in the next PFMEA for some of the new processes or products, standardized solution will be used. That will save a lot of time. Along these integrated lean tools into PFMEA, Poka-Yoke and 5S were also used as the lean tool for recommended actions during PFMEA realization.

Table 2 Comparison of state before and after lean approach integration in PFMEA

Measured conditions	State after traditional approach	New state after lean approach	Improvements (%)
Number of team members	2	9+6 workers	85
The actions taken	1	19	95
Identification of failures	18	27	33
Change of S value	155	227	32
Change of O value	64	105	39
Change of D value	85	161	47
Change of RPN value	1642	3720	56
Reduced RPN value due to taken actions	2602	3366	23
Reduced S value due to taken actions	226	226	/
Reduced O value due to taken actions	80	127	37
Reduced D value due to taken actions	121	139	13
RPN value over 100	/	16	100
S, O, D values over 8	/	3	100

6. Conclusion

The new approach with the integration of lean approach into PFMEA for improvement of specific shortcomings, is presented in this paper. This new PFMEA approach has proven to be very good and practical combination for identifying and fixing problems and failures. The case study realized from the automotive industry was used for the new approach testing. The state with traditional PFMEA is compared with the new state where almost all measured conditions were changed and improved. Therefore, this approach was practically approved.

The main advantage of this approach was in improvement of process and product quality, which is mostly important for customers. For a change, this approach is applicable in real-world cases in every process or industry where the lean approach is implemented. Also, it is very simple and practical to use and does not require big investments, implementation of new technology and complicated additional education. The way this approach has stopped potential failures to reach a customer was not identified with traditional approach. This was presented on practical example. Therefore, this new approach increased identification and prevention possibilities as well.

This new approach have also few constraints. It is used for specific group of shortcomings and it is not comprehensive. Also cannot be applicable in processes and industries where the lean approach has not been implemented. Costs are not included and there is different aspect of looking on it from perspective of PFMEA and lean approach.

Future work should be oriented to fixing all other shortcomings of PFMEA, costs especially. Lean approach is oriented to long term thinking about costs. From PFMEA team perspective is different. During PFMEA realization team have to percept immediately if the solution is profitable. Thus in further research, the balance should be found between urgent need for costs from PFMEA aspect and long term thinking profitability from the lean approach aspect.

Acknowledgement

This paper has been supported by Croatian Science Foundation under the project Innovative Smart Enterprise – INSENT (1353). This publication also has been supported by the European Commission under the Erasmus Mundus project Green-Tech-WB:Smart and Green technologies for innovative and sustainable societies in Western Balkans (551984-EM-1-2014-1-ES-ERA MUNDUS-EMA2).

References

- [1] Harrison, A., van Hoek, R. (2005). *Logistics management and strategy*, Pearson Education, Harlow, England.
- [2] Stamatis, D.H. (2003). *Failure mode and effect analysis: FMEA from theory to execution*, ASQ Quality Press, Milwaukee, Wisconsin, USA.
- [3] ISO 9000. Quality management systems – Fundamentals and vocabulary, FMEA obligations, from http://www.bti.secna.ru/education/smq/docs/news/iso_9000_2005_e.pdf, accessed October 30, 2016.
- [4] ISO/TS 16949:2002(E). Quality management systems – Particular requirements for the application of ISO 9001: 2000 for automotive production and relevant service part organizations, FMEA obligations, from <https://ciiias.files.wordpress.com/2007/11/iso-ts-16949-2002.pdf>, accessed June 13, 2016.
- [5] Johnson, K.G., Khan, M.K. (2003). A study into the use of the process failure mode and effects analysis (PFMEA) in the automotive industry in the UK, *Journal of Materials Processing Technology*, Vol. 139, No. 1-3, 348-356, doi: [10.1016/S0924-0136\(03\)00542-9](https://doi.org/10.1016/S0924-0136(03)00542-9).
- [6] Liu, H.C., Liu, L., Liu, N. (2013). Risk evaluation approaches in failure mode and effects analysis: A literature review, *Expert systems with applications*, Vol. 40, No. 2, 828-838, doi: [10.1016/j.eswa.2012.08.010](https://doi.org/10.1016/j.eswa.2012.08.010).
- [7] Biddle, J. The lean benchmark report, from <http://consumergoods.edgl.com/column/The-Lean-Benchmark-Report48987>, accessed June 13, 2016.
- [8] Lorenc, M., Jentzsch, A., Andersen, M., Noack, B., Waffenschmidt, L., Schuh, G., Rudolf, S. The lean advantage in engineering: developing better products faster and more efficiently, from <https://www.bcgperspectives.com>, accessed June 13, 2016.
- [9] Chrysler LLC, Ford Motor Company, General Motors Corporation, Potential failure mode and effect analysis (FMEA), Reference Manual, 4th edition, from www.engmatl.com/home/finish/20-engineering.../160-fmea-manual, accessed June 13, 2016.
- [10] Korenko, M., Krocko, V., Kaplík, P. (2012). Use of FMEA method in manufacturing organization, *Journal of Manufacturing and Industrial Engineering*, Vol. 11 No. 2, 48-50.
- [11] Montgomery, T.A., Pugh, D.R., Leedham, S.T., Twitchett, S.R. (1996). FMEA automation for the complete design process, In: *Proceedings of Reliability and Maintainability Symposium – International Symposium on Product Quality and Integrity*, IEEE, Las Vegas, NV, USA, 30-36.
- [12] Vujica-Herzog, N., Tonchia, S. (2014). An instrument for measuring the degree of lean implementation in manufacturing, *Strojniški vestnik – Journal of Mechanical Engineering*, Vol. 60, No. 12, 797-803, doi: [10.5545/sv-jme.2014.1873](https://doi.org/10.5545/sv-jme.2014.1873).
- [13] Liker, J.K. (2004). *The Toyota way*, 14 management principles from the world's freest manufacturer, McGraw-Hill, New York, USA.
- [14] Womack, J.P., Jones, D.T. (2010). *Lean thinking: Banish waste and create wealth in your corporation*, Simon and Schuster, New York, USA.
- [15] Shekari, A., Fallahian, S. (2007). Improvement of lean methodology with FMEA, In: *Proceedings of the 18th Annual Conference – POMS (Production and Operation Management Society)*, Texas, USA, 007-0520.
- [16] Sawhney, R., Subburaman, K., Sonntag, C., Rao Venkateswara Rao, P., Capizzi, C. (2010). A modified FMEA approach to enhance reliability of lean systems, *International Journal of Quality & Reliability Management*, Vol. 27, No. 7, 832-855, doi: [10.1108/02656711011062417](https://doi.org/10.1108/02656711011062417).
- [17] Shahrabi, M., Shojaei, A.A. (2014). Application of FMEA and AHP in lean maintenance, *International journal of Modern Engineering Science*, Vol. 3, No. 1, 61-73.
- [18] Puvanasvaran, A.P., Jamibollah, N., Norazlin, N., Adibah, R. (2014). Poka-Yoke Integration into process FMEA, *Australian Journal of Basic and Applied Sciences*, Vol. 8, No. 7, 66-73.

- [19] Puvanasvaran, A.P., Jamibollah, N., Norazlin, N. (2014). Integration of POKA YOKE into process failure mode and effect analysis: A case study, *American Journal of Applied Sciences*, Vol. 11 No. 8, 1332-1342, [doi: 10.3844/ajassp.2014.1332.1342](https://doi.org/10.3844/ajassp.2014.1332.1342).
- [20] Teoh, P.C., Case, K. (2007). An evaluation of failure modes and effects analysis generation method for conceptual design, *International Journal of Computer Integrated Manufacturing*, Vol. 18, No. 4, 279-293, [doi: 10.1080/0951192042000273122](https://doi.org/10.1080/0951192042000273122).
- [21] Arabian-Hoseynabadi, H., Oraee, H., Tavner, P.J. (2010). Failure modes and effects analysis (FMEA) for wind turbines, *International Journal of Electrical Power & Energy Systems*, Vol. 32 No. 7, 817-824, [doi: 10.1016/j.ijepes.2010.01.019](https://doi.org/10.1016/j.ijepes.2010.01.019).
- [22] Moore, C. Failure Modes and Effects Analyses (FMEA) and critical items list (CIL) for the ECS project; EOSDIS core system project, from https://prod.nais.nasa.gov/eps/eps_data/161793-AMEND-002-002.pdf, accessed November 13, 2016.
- [23] Liker, J., Convis, G.L. (2011). *The Toyota way to lean leadership: Achieving and sustaining excellence through leadership development*, McGraw Hill Professional, New York, USA.

Appendix 1

FMEA Number	51					Part Name/Part No	BSH MSM6BL				E index: A1	Realized by: Project manager										
FMEA Date (Orig)	2/18/2015					FMEA Revision Date	20.04.2015. Rev.02				Prepared by: Project Leader											
FMEA Team	Project Leader x2, Project manager, Quality manager, Logistics manager, Procurement manager, R&Dx2, Maintenance manager + 6 workers																					
Process No./Function	Requirements	Potential Failure Mode	Potential Effect(s) of Failure	Severity	Classification	Potential Cause(s) of Failure	Occurrence	Current Process Controls: Prevention	Current Process Controls: Detection	Detection	RPN	Recommended Action(s)	Responsibility	Target Completion Date	Action Results							
															Actions Taken	Effective Date	Occurrence	Severity	Detection	RPN		
E110	Axial insertion																					
E110	Axial insertion	Component failed	PCB with failed function; No function	6		No components in storage	2	Intern schooling, working instruction	Process approved	6	72	No								0		
E110	Axial insertion	Component with false value	Badly equipped PCB; PCB with failed function; No function	6		Wrong components in storage	2	Intern schooling, working instruction	Process approved	6	72	No								0		
E110	Axial insertion	Wrong orientation of	Incorrect or no function	6		Machine failure	2	Intern schooling, working instruction	Process approved	6	72	No								0		
E412	Manual inserting																					
E412	Manual inserting	Mechanical damaged component	Trouble in process	5		Inattention	4	Intern schooling, working instruction	Visual control; Process approved	6	120	Increase workers precaution	Project manager	Work instructions					5	1	6	30
E412	Manual inserting	Component failed on PCB	PCB with failed function, no function	5		Inattention	5	Visual inspection before use	Visual inspection by end inspection	5	125	Poka yoke	Project manager	Additional tool for check out of components					5	1	6	30
E412	Manual inserting	Wrong component	PCB with false components	7		Inattention	4	Intern schooling, working instruction	Process approved	8	224	kaizen workshop	Project manager	Process improvement + check out after component selection					7	1	8	56

PFMEA report 1/4

Process No./Function	Requirements	Potential Failure Mode	Potential Effect(s) of Failure	Severity	Classification	Potential Cause(s) of Failure	Occurrence	Current Process Controls: Prevention	Current Process Controls: Detection	Detection	RPN	Recommended Action(s)	Responsibility	Target Completion Date	Action Results					
															Actions Taken	Effective Date	Occurrence	Severity	Detection	RPN
E412	Manual inserting	Contact badly placed	Trouble in process	8		Inattention	4	Intern schooling, working instruction	Visual control; Process approved	8	256	Kaizen + poka yoke	Project manager		Process improvement + tool for contact set up	8	1	8	64	
E500	Wave soldering	Too much solder on solder joint	Short circuit on PCB	7		False setting the process parameter - speed of soldering line is wrong	4	Intern schooling, working instruction	Visual inspection, check the parameter before use	5	140	Preventive machine maintenance	Maintenance manager		Check out of parameters before start of machine	7	1	4	28	
E500	Wave Soldering	Use of false temperature profil	Bad or not soldered joints between pads and component	8	§	Inattention, false setting of machine parameters	5	Intern schooling, working instruction	Visual inspection	5	200	Preventive machine maintenance	Maintenance manager		Check out of parameters before start of machine	8	1	6	48	
E500	Wave Soldering	Uncorect solder joint	Unreliable joint - unreliable function	8		False setting the process parameter -	5	Intern schooling, working instruction	Visual inspection, check the parameter before use	5	200	Preventive machine maintenance	Maintenance manager		Check out of parameters before start of machine	8	1	6	48	
E500	Wave Soldering	Not enough solder on solder joint	Bad solder joint	8		False setting the process parameter	4	Intern schooling, working instruction	Visual inspection - check the parameter before use	5	160	Preventive machine maintenance	Maintenance manager		Check out of parameters before start of machine	8	1	5	40	
E500	Wave Soldering	Cold contact	Bad solder joint	7		False setting the process parameter	4	Intern schooling, working instruction	Visual inspection, check the parameter before use	5	140	Preventive machine maintenance	Maintenance manager		Check out of parameters before start of machine	7	1	5	35	
E650	Function test	Skipped the final control	Bad parts can be sent to the customer	8		Inattention	3	Intern schooling, working instruction	Process approved	8	192	One piece flow	Worker		Work instructions	7	1	5	35	
E521	Rework; visual inspection Zabranjeno je neovlašćeno kopiranje i prenošenje prava trećim licima!																			

PFMEA report 2/4

Process No./Function	Requirements	Potential Failure Mode	Potential Effect(s) of Failure	Severity	Classification	Potential Cause(s) of Failure	Occurrence	Current Process Controls: Prevention	Current Process Controls: Detection	Detection	RPN	Recommended Action(s)	Responsibility	Target Completion Date	Action Results					
															Actions Taken	Effective Date	Occurrence	Severity	Detection	RPN
E521	Rework; visual inspection	Not sensed missing element	PCB with false function	7		Inattention	3	Intern schooling, working instruction, changing workers	Visual inspection	5	105	Kaizen + poka yoke	Project manager		Process improvement + tool for contact set up	7	1	4	28	
E521	Rework; visual inspection	Not sensed wrong orientated element	PCB with false function	7		Inattention	2	Intern schooling, working instruction, changing workers	Visual inspection; Function test	5	70	No							0	
E521	Rework; visual inspection	Not sensed mechanical damages	No function	6		Inattention	2	Intern schooling, working instruction	Visual inspection	5	60	No							0	
E521	Rework; visual inspection	Not sensed shoort circuit	No function	8		Inattention	3	Intern schooling, working instruction, changing workers	Visual inspection; Function test	6	144	Jidoka	Project manager		Implement testing of current flow	8	1	4	32	
E521	Rework; visual inspection	Not sensed broken connections	No function	8		Inattention	3	Intern schooling, working instruction, changing workers	Visual inspection; Function test	6	144	Isolation of part for special inspection	QS		Rework after check	8	1	8	64	
E710	Marking	No data about the product	Bad tracking of product, tracking unpossible	4		Inattention	2	Intern schooling, working instruction	Visual inspection	5	40	No							0	
E710	Marking	In the wrong place labeled product	Unwilling customer, customer reclamation	4		Inattention	2	Intern schooling, working instruction	Visual inspection	5	40	No							0	

PFMEA report 3/4

Process No./Function	Requirements	Potential Failure Mode	Potential Effect(s) of Failure	Severity	Classification	Potential Cause(s) of Failure	Occurrence	Current Process Controls: Prevention	Current Process Controls: Detection	Detection	RPN	Recommended Action(s)	Responsibility	Target Completion Date	Action Results						
															Actions Taken	Effective Date	Occurrence	Severity	Detection	RPN	
E710	Marking	Wrong data on product	Bad tracking of product, tracking impossible	4		Inattention	2	Intern schooling, working instruction	Visual inspection	5	40	No									0
E531 PCB separation																					
E531	PCB separation	Damage the PCB, outline is not clear	Trouble by assembling in housing	6		Innatenation, damaged tooling	6	Intern schooling, working instruction	Visual inspection	5	180	Jidoka	Project manager + workers		Kvalitet na izvorištu		6	1	8	48	
E531	PCB separation	Break the PCB	Useless of PCB	8			3	Intern schooling, working instruction	Visual inspection	5	120	kaizen workshop	Project manager + R&D		Made tools for automatic removing of excess		8	1	2	16	
E900 Final control and packing																					
E900	Final control and packing	Mixed products in the box	Unwilling customer, customer reclamation	2		Operator error, mess at the working place	2	Intern schooling	Visual final inspection	9	36	5S + Work instructions	Project manager + workers		organisation of work place + additional worker education		2	2	8	32	
E900	Final control and packing	Quantity is false	Unwilling customer, customer reclamation	2		Inattention	2	Intern schooling	Visual final inspection	9	36	5S + Work instructions	Project manager + workers		organisation of work place + additional worker education		2	2	8	32	
E900	Final control and	VDA label is uncorrect full field	Identificatio n, traceability is not assure	2		Mistake in system, not enough datas	2	Intern schooling	Visual final inspection	9	36	Kaizen	Project manager + workers		System for VDA markers chose		2	1	1	2	
E900	Final control and packing	Wrong products in the box	Unwilling customer, customer reclamation	8		Operator error, mess at the working	2	Intern schooling	Visual inspection	8	128	Jidoka	Project manager + workers		Kvalitet na izvorištu		8	1	8	64	

PFMEA report 4/4

Multi-objective optimization of the turning process using a Gravitational Search Algorithm (GSA) and NSGA-II approach

Klančnik, S.^{a,*}, Hrelja, M.^{a,b}, Balic, J.^a, Brezocnik, M.^a

^aProduction Engineering Institute, Faculty of Mechanical Engineering, University of Maribor, Maribor, Slovenia

^bAVL, Piezocryst: Advanced Sensorics GmbH, Graz, Austria

ABSTRACT

In this paper, we proposed a Gravitational Search Algorithm (GSA) and an NSGA-II approach for multi-objective optimization of the CNC turning process. The GSA is a swarm intelligence method exploiting the Newtonian laws on elementary mass objects interaction in the search space. The NSGA-II is an evolutionary algorithm based on non-dominated sorting. On the basis of varying values of the three independent input machining parameters (i.e., cutting speed, depth of cut, and feed rate), the values of the three dependent output variables were measured (i.e., surface roughness, cutting forces, and tool life). The obtained data set was divided further into two subsets, for the training data and the testing data. In the first step of the proposed approach, the GSA and the training data set were applied to modelling a suitable model for each output variable. Then the accuracies of the models were checked by the testing data set. In the second step, the obtained models were used as the objective functions for a multi-objective optimization of the turning process by the NSGA-II. The optimization constraints relating to intervals of dependent and independent variables were set on the theoretical calculations and confirmed with experimental measurements. The goal of the multi-objective optimization was to achieve optimal surface roughness, cutting forces, and increasing of the tool life, which reduces production costs. The research has shown that the proposed integrated GSA and NSGA-II approach can be implemented successfully, not only for modelling and optimization of the CNC turning process, but also for many other manufacturing processes.

© 2016 PEI. University of Maribor. All rights reserved.

ARTICLE INFO

Keywords:

Turning
Multi-objective optimization
Evolutionary algorithms
Particle swarm
Gravitational Search Algorithm
NSGA-II algorithm

*Corresponding author:

simon.klančnik@um.si
(Klančnik, S.)

Article history:

Received 8 July 2016
Revised 19 November 2016
Accepted 21 November 2016

1. Introduction

Advances in existing production are measured in terms of the flexibility, autonomous functioning and extent of automation. Modernisation of production covers the modernisation and integration of the latest technologies into production systems so that the companies remain competitive. Integration of advanced technologies results in shorter manufacturing times, higher capacities and reduction of production costs. Because of the dynamics and increase in the amount of input parameters or data, the optimization of systems has become more difficult than previously. Because of high quantities of data, the optimal functioning of production can often be reached no more by conventional methods; therefore, more advanced methods are applied to acquire new and better solutions in the optimization of production systems.

The research is aimed at conceiving an advanced system for modelling of CNC machining operations and subsequent optimization of machining parameters by the use of the developed machining models. In the past, a lot of researches have been executed in the field of optimization

and modelling of the CNC machining operations [1-3]. Important researches in this field have been carried out for optimization of milling [4], turning [5], laser cutting and water jet cutting [6]. Successful optimization relies on the use of the training and testing databases [7] comprised of the values measured in experiments [8, 9]. The training and testing databases allow the training of algorithms and testing of correctness of the models developed. The development of modern methods of optimizing and modelling of complex production systems requires know-how from the area of intelligent systems, which presupposes incorporation of artificial intelligence into solving complex engineering problems. One of the most widespread nondeterministic approaches for solving complex engineering problems is evolutionary computation, especially genetic algorithms and genetic programming [10]. There are many works where genetic algorithms, as well as other nondeterministic methods (e.g., Artificial Neural Networks – ANN) were implemented for solving various problems in cutting systems, including surface roughness optimization and optimal tool selection (see for example [1, 14-21]). Another artificial intelligence method used frequently is swarm intelligence. Swarm intelligence is only a covering term and is divided into many sub-types [22]. Often, the authors refer to intelligence adopted from biological aspects, e.g. bee swarms, bird flights or ant colonies [23]. A relative novelty in the swarm intelligence methods is the Gravitational Search Algorithm (GSA) working on the principle of the interaction of masses [24]. A review of the literature reveals that, so far, the GSA has not been reported frequently for optimization of manufacturing technologies.

This paper proposed an effective approach for modelling and multi-objective optimization of CNC machining processes by the GSA and NSGA-II. Data gained on the basis of experimental measurements were used for training and testing of the model developed by the GSA. After modelling, the multi-objective optimization of the cutting parameters was done on the basis of CNC cutting models developed by the GSA. The NSGA-II algorithm was implemented for the multi-objective optimization. The system is generally convenient for different CNC machine tools and can be adapted to several different materials' removing processes, e.g. milling and laser cutting. However, our research was restricted to turning as far as training of the system and testing of its effectiveness are concerned.

The article is composed as follows: Section 2 presents detailed descriptions of the experimental setup, Gravitational Search Algorithm, and elitist Non-dominated Sorting Genetic Algorithm's (NSGA-II) background. The results and discussion are presented in Section 3. The article ends with a short Conclusion.

2. Materials and methods

2.1 Experimental setup and results

Models of the turning process were created by means of experimental measurements of the output parameters of machining operations depending on the input parameters, in accordance with the work of Jurkovic [25]. The experiment was carried out during a fine turning operation on the CNC lathe Georg Fischer NDM-16. Samples from the material C45E were used for execution of the experiment. This is a hot rolled structural steel. The workpiece diameter for machining was $\varnothing 10 \text{ mm} \times 380 \text{ mm}$. The tool used for the test samples was the cutting insert Sandvik Coromant DNMG 150608-PM4025. The following equipment was used for proper measuring of tool wear, machining forces, and surface roughness:

- Measuring of cutting forces:
Force meter Kistler 9257A. Measuring range $F_{x,y,z} = 5 \text{ kN}$ allowing capturing, displaying and processing of resulting cutting forces with the aid of the programme package Labview™.
- Surface roughness:
Roughness meter R_a produced by Mitutoyo SJ-201P.
- Tool wear:
Microscope Carl Zeiss with magnification 30 \times and 0.0001 mm resolution.

The input data for execution of the experiment were as follows:

- Cutting speed V_c (m/min)
- Feed rate f (mm/rew) and
- Cut depth a_p (mm).

The output data were gained from the input data, as the latter have direct impact on their values. The output data and/or the experiment results were:

- Main cutting force F_c (N)
- Surface roughness R_a (μm) and
- Tool resistance time T (min).

The experimental results obtained during the fine turning are presented in Table 1.

Table 1 The results of the experiment

Trial No.	Input data			Output data			
	V_c (m/min)	f (mm/rev)	a_p (mm)	F_c (N)	R_a (μm)	T (min)	
1	400	0.100	0.40	128.893	0.77	32.66	Training data
2	500	0.100	0.40	130.755	0.80	11.15	
3	400	0.200	0.40	201.899	1.70	25.89	
4	500	0.200	0.40	202.200	1.67	7.450	
5	400	0.100	1.20	337.859	1.11	28.43	
6	500	0.100	1.20	330.745	1.19	9.230	
7	400	0.200	1.20	492.945	2.14	20.74	
8	500	0.200	1.20	550.848	1.77	5.610	
9	450	0.150	0.80	299.005	1.26	14.44	
10	450	0.150	0.80	301.647	1.30	14.38	
11	450	0.150	0.80	304.772	1.29	14.39	
12	450	0.150	0.80	299.519	1.28	14.48	
13	450	0.150	0.80	299.875	1.27	14.43	
14	450	0.150	0.80	303.832	1.28	14.46	
15	366	0.150	0.80	313.225	1.37	34.46	
16	534	0.150	0.80	307.622	1.31	6.120	Testing data
17	450	0.066	0.80	174.024	1.21	20.25	
18	450	0.234	0.80	406.719	2.32	10.93	
19	450	0.150	0.13	61.2230	1.17	12.18	
20	450	0.150	1.47	497.895	1.13	10.05	

2.2 Gravitational Search Algorithm background

In the Gravitational Search Algorithm, a set of objects with relevant atomic masses is concerned, the objects representing the search mechanism [24]. Those objects find the proper solution during the searching process. The search mechanism works on the principle of Newtonian gravitation laws and laws of motion and, on the basis of gravitational attraction, it searches for the optimum solution in the multitude of potential solutions, where each of the solutions has a specific mass. All particles within the population are attracted by mutual gravitational forces according to Eq. 1 and 2, which causes global motion of objects in the system, heavier objects attracting lighter objects to a larger extent. The objects communicate mutually by means of the gravitational force. Larger masses result faster in a better solution, but they move more slowly than lower masses with worse solutions. In the GSA, each particle has four basic properties: Location, inertial mass, active gravitational mass and passive gravitational mass. The location of mass coincides with the location of the result of the problem. With the aid of the active, passive and inertia masses, it is also possible to write the mathematical function. In that way, the algorithm is guided through the space of solutions by means of mutual effects of gravitational and inertia masses. After expiration of the search time, the solutions are expected to start tending to the

largest mass in the system, that mass increasing during the search process and representing the optimum solution in the search space. The search space represented by the algorithm is not influenced by the external masses so that only two physical laws, i.e. the gravitation law and the law of motion act on it. In a system of two or more bodies, it is the active gravitational mass M_A that affects most the remaining bodies inside the system with its gravitational field, which means that it has the greatest mass. The passive gravitational mass M_P represents the gravitational field of the body with less mass and affects the gravitational field of the more massive object passively only and has a lesser mass. The system of several bodies must be calculated in pairs, two by two bodies simultaneously. The inertia gravitational mass M_I is the mass with which the object in the system resists the position change, if acted upon by a specific mass. The body having larger inertia mass changes the direction of motion slower than the body with smaller mass, as the force must act on the body longer in order to direct the body into a new direction. If the Newtonian equations are written by using newly named masses in combination with two bodies, the result is as follows:

$$F_{12} = G \frac{M_{A2} \cdot M_{P1}}{R^2} \quad (1)$$

where:

- F_{12} – Attraction with which the second body acts on the first body
- G – Gravitational constant
- M_{A2} – Active mass of second object
- M_{P1} – Passive mass of first object
- R – Distance between the two objects

Consequently, the gravitational force F_{12} acting on the first object with the mass of the second object is proportional to the product of the active part of gravitational mass in the system with the passive part of gravitational mass, and inversely proportional to the distance between the two objects. The acceleration with which the body moves and/or the effect of the second on the first body can be written with the equation:

$$a_1 = \frac{F_{12}}{m_{I1}} \quad (2)$$

- a_1 – Acceleration with which the body moves; effect of the second on the first body
- F_{12} – Attraction with which the second body acts on the first body
- m_{I1} – Inertia mass of the first body

Transformation of the system by means of a random component ensures random motion of mass bodies.

$$F_a^n(t) = \sum_{b=1, b \neq i}^N rand_b \cdot F_{ab}^n(t) \quad (3)$$

where:

- $F_a^n(t)$ – Force with stochastic characteristic in given time t
- $rand_b$ – Random number at interval $[0,1]$ ensures randomization
- $F_{ab}^n(t)$ – Force which is caused by the b -th mass particle and acts on the a -th mass particle in time t

As the stochastic mode of operation of gravitational force has been given, the same must be effected also on the gravitational acceleration and, thus, Eq. 2 is transformed to an n -dimensional equation in specific time t :

$$a_a^n(t) = \frac{F_a^n(t)}{M_{ia}(t)} \quad (4)$$

where:

- $a_a^n(t)$ – Gravitational acceleration of body a in the n -dimension space
 $F_a^n(t)$ – Force with stochastic characteristic in specific time t
 $M_{ia}(t)$ – Inertia mass of body a in specific time t

On the basis of the updated equation for the force with stochastic characteristic in specific time t , and on the basis of the gravitational acceleration of body a in the d -dimension space, the new velocity of particle or body in the space with n -dimensions – Eq. 5, can be expressed; the same also applies to the newly calculated position of the body in the solution space – Eq. 6:

$$v_a^n(t+1) = rand_a \cdot v_a^n(t) + a_a^n(t) \quad (5)$$

$$x_a^n(t+1) = x_a^n(t) + v_a^n(t+1) \quad (6)$$

Terms in Eq. 5 and 6:

- $v_a^n(t+1)$ – New velocity of body a in newly calculated time $t+1$
 $x_a^n(t+1)$ – New position of body a in newly calculated time $t+1$
 $rand_a$ – Random number at interval $[0,1]$ ensures randomization
 $v_a^n(t)$ – Velocity of motion of body a in specific time t
 $a_a^n(t)$ – Acceleration of body a in specific time t
 $x_a^n(t)$ – Position of body a in specific time t
 n – Index n stands for the n -dimension space with solutions

Gravitational and inertia masses of bodies in the system can also be written as a fitness function to define the success of the algorithm in searching for the solution. It must be borne in mind that larger masses are better indicators of solutions and are more effective; however, as those bodies have larger mass, they move slower in the space with solutions. That phenomenon is compensated for by a random number of lighter bodies representing worse solutions but, in combination with heavier bodies, they take part in converging to proper solutions much faster. If it is assumed that gravitational and inertia masses are identical, they can be written in the form of an equation. Updated equations of the mass system are:

$$M_{an} = M_{pn} = M_{in} = M_n \cdot n = 1, 2, \dots, N \quad (7)$$

$$m_a(t) = \frac{fit_a(t) - worst(t)}{best(t) - worst(t)} \quad (8)$$

$$M_a(t) = \frac{m_a(t)}{\sum_{b=1}^N m_b(t)} \quad (9)$$

where $fit_a(t)$ stands for the fitness value of body a in specific time t , while $best(t)$ and $worst(t)$ are values representing the best and worst current values of results and can be written even in more detail, particularly, when searching for minimums and maximums.

For minimum:

$$\begin{aligned} best(t) &= \min_{j \in \{1, 2, \dots, N\}} fit_b(t) \\ worst(t) &= \max_{j \in \{1, 2, \dots, N\}} fit_b(t) \end{aligned} \quad (10)$$

For maximum:

$$\begin{aligned} best(t) &= \max_{j \in \{1, \dots, N\}} fit_b(t) \\ worst(t) &= \min_{j \in \{1, \dots, N\}} fit_b(t) \end{aligned} \quad (11)$$

To avoid efficiently the local minimums at the beginning of the algorithm start-up the research principle must be introduced, whereas, after n -iterations, the research limit is dimmed by means of elimination and the system of algorithm functioning passes into the search mode. That is reached by gradual elimination and each subsequent algorithm iteration assures better convergence of solutions. Each subsequent potential optimal solution can be designated N -best, where each iteration changes the action of the virtual gravitational force with which it affects all the remaining bodies in the space of solutions. Consequently, N -best is the time function having

the value No at the beginning of time t . In that way, at the beginning of the algorithm, all elements act with gravitational force on all remaining bodies, while the force decreases linearly with the reduction of the number of objects in the system and/or convergence of solutions to one point, which can also be described by means of gravitational collision of two bodies. The algorithm finalises the optimization, when only one body is still available with the greatest possible mass with which it acted on the remaining bodies and attracted them gravitationally. In that way, the Eq. 3 can be transformed and the result is:

$$F_a^n(t) = \sum_{b \in N - \text{best}, b \neq a} rand_b F_{ab}^n(t) \quad (12)$$

$F_a^n(t)$ – Force with stochastic characteristic in specific time t

$rand_b$ – Random number at interval $[0,1]$, it assures randomization

$F_{ab}^n(t)$ – Force which is caused by the b -th mass particle and acts on the a -th mass particle in time t

N -best – Set of first bodies with largest mass and highest fitness value

The pseudocode of the GSA algorithm is presented in Fig. 1.

```

1: Start GSA
2: Set-up search space
3: For each particle
4:   Initialize mass particle
5:   Start regression analysis module/with measured experimental data
6: END
7: Do
8:   For each particle/import measured experimental data
9:     Calculate capacity/fitness function of particle
10:    Capacity of particle > best capacity of particle (best (t)) → new best
11:    Evaluate worst values as worst (t)
12:  END
13:  For each particle
14:    Calculate velocity, masses and accelerations of mass particle
15:    Update particle position and velocity
16:  END
17: While → number N of iterations is reached
18: END GSA

```

Fig. 1 Pseudocode of the GSA algorithm

2.3 NSGA-II algorithm background

The NSGA-II (elitist Non-dominated Sorting Genetic Algorithm) is a genetic algorithm designed for multi-objective optimization [26]. The algorithm uses the crowding distance metric and non-dominated sorting as its main features. Fig. 2 presents the algorithm's pseudocode.

Roughly speaking, an algorithm consists of initialization, selection and re-combination. Selection and re-combination are the main algorithm steps (see Fig. 2). In the first step, the old population of parents and descendants is combined into a joint population of size $2n$. In the next step, the subjects from that combined population R_{t-1} are sorted front by front using non-dominated sorting. Subjects not dominated by any other subject go into the first front. The first i fronts still going whole into the new parent population P_t are written into that population. The first next front (front $i+1$) not going whole into the newly created population is sorted by using the crowding metric. The least crowded subjects from front $i+1$ are added to the new population P_t . The solutions have the largest range if the extreme subjects in the front are evaluated as best when sorting with the crowding metric. Evaluation of the remaining subjects in the front is performed by calculating the distance to its nearest neighbours.

-
- 1: Randomly generate and evaluate initial population of parents P_0 .
 - 2: Prepare empty initial population of descendants Q_0 .
 - 3: Setup $t = 0$.
 - 4: Until stopping criterion has been fulfilled, repeat:
 - 5: Setup $t = t + 1$.
 - 6: Unite two old populations of parents and descendants: $R_{t-1} = P_{t-1} \chi Q_{t-1}$.
 - 7: Perform non-dominated sorting on R_{t-1} and determine fronts $F_i, i = 1, 2, \dots$
 - 8: Prepare new empty population of parents P_t .
 - 9: Put into population P_t the first i front fronts still fitting whole into it.
 - 10: With the use of crowding distance metric sort front F_{i+1} no more fitting whole into population P_t
 - 11: Add the least crowded subjects from F_{i+1} to population P_t
 - 12: Generate population of descendants Q_t from parent population P_t by using tournament selection, crossover and mutations.
 - 13: Evaluate subjects from population of descendants Q_t .
-

Fig. 2 Pseudocode of the NSGA-II algorithm

When optimising k criteria, k subjects are first sorted according to growing evaluating values f_j for each criterion $j = 1, 2, \dots, k$. In the next step for each subject i , the distance between its two neighbours u and v is calculated according to the following equation:

$$d_j(i) = \frac{f_j(u) - f_j(v)}{f_j^{max} - f_j^{min}} \quad (13)$$

where f_j^{max} and f_j^{min} are the maximum and the minimum values of the j -th criterion, respectively.

The following must apply:

$$f_j(u) \leq f_j(i) \leq f_j(v) \quad (14)$$

As already mentioned, the highest possible distance is assigned to the two extreme subjects (with respect to the j criterion). For all remaining subjects, the crowding metric for subject i is equal to the sum of those distances according to all criteria:

$$c(i) = \sum_{j=1}^k d_j(i) \quad (15)$$

The parent population P_t is obtained in the manner described above. In the next steps, the descendant population is generated from that population by using tournament selection, crossover and mutation. Out of two random subjects, the subject classified into the front with lower consecutive value, wins in the selection. If two subjects taking part in selection come from an equal front, then the subject better evaluated by the crowding metric is chosen. The descendant population is designated Q_t . Each subject from the descendant population is evaluated in the last step of the NSGA-II algorithm. That estimate is used in the next generation for non-dominated sorting of subjects. The algorithm is repeated until the maximum number of generations has been reached or until another stopping criterion has been reached.

3. Results and discussion

3.1 Modelling of turning process by the Gravitational Search Algorithm

For processing experimental data the GSA method was used for the purposes of turning system modelling. For the modelling process the following control parameters of the GSA optimization algorithm were used:

- Number of mass bodies: 210
- Number of iterations: 1000
- Size of mass body (dimension): 10
- Power of Euclidean distance between mass bodies: 1

- Power factor α : 20
- Gravitational constant G_0 : 100

In particular, the two random factors α and G_0 must be pointed out. Both of them are inter-related and form the refreshment of iteration within the scope of the gravitational constant, where the G_0 value is the initial value of the gravitational constant and is changed exponentially on the basis of factor α which, in combination with the ratio of consecutive iteration and total number of iterations, affects the contingency of gravitational constant values additionally during each iteration. The mass particle size and/or the properties of solutions written in the mass particle are represented with a dimension which also defines the number of coefficients in the polynomial representing the model of the individual machining operation. A prerequisite for successful execution of modelling was correct selection of the polynomial optimized by means of GSA. Eq. 16 shows the form of a ten-coefficient polynomial which proved to be a good choice for prediction of output variables.

$$f(x_1, x_2, x_3) = k_1 + k_2 \cdot x_1 + k_3 \cdot x_2 + k_4 \cdot x_3 + k_5 \cdot x_1 \cdot x_2 + k_6 \cdot x_1 \cdot x_3 + k_7 \cdot x_2 \cdot x_3 + k_8 \cdot x_1 \cdot x_1 + k_9 \cdot x_2 \cdot x_2 + k_{10} \cdot x_3 \cdot x_3 \quad (16)$$

where x_1 is cutting speed v_c , x_2 is feed rate f , and x_3 is depth of cut a_p .

The polynomial represents the core of the system round which the optimization process is designed. Input and output experimental values are inserted into the polynomial, while the optimization process optimises the coefficients in such a manner that the predictions given by the polynomial model are as near the experimental values as possible. Out of all the experimental measurements performed, fifteen measurements were chosen at random for the process of optimising of the polynomial coefficients, while the remaining 5 measurements were used for result verification. The results of optimization are polynomial models for the calculation of cutting force, surface roughness and tool wear (Eq. 17-19).

$$F_c = 523.66 - 1.89 \cdot x_1 - 813.18 \cdot x_2 + 48.88 \cdot x_3 + 3.05 \cdot x_1 \cdot x_2 + 0.29 \cdot x_1 \cdot x_3 + 1439.13 \cdot x_2 \cdot x_3 + 0.0014 \cdot x_1 \cdot x_1 - 1257.73 \cdot x_2 \cdot x_2 - 43.70 \cdot x_3 \cdot x_3 \quad (17)$$

$$R_a = 3.74 - 0.01 \cdot x_1 - 4.25 \cdot x_2 + 1.53 \cdot x_3 - 0.01 \cdot x_1 \cdot x_2 - 0.001 \cdot x_1 \cdot x_3 - 1.03 \cdot x_2 \cdot x_3 + 0.00002 \cdot x_1 \cdot x_1 + 68.81 \cdot x_2 \cdot x_2 - 0.31 \cdot x_3 \cdot x_3 \quad (18)$$

$$T = 294.77 - 0.95 \cdot x_1 - 242.17 \cdot x_2 - 4.60 \cdot x_3 + 0.24 \cdot x_1 \cdot x_2 + 0.02 \cdot x_1 \cdot x_3 - 9.20 \cdot x_2 \cdot x_3 + 0.0007 \cdot x_1 \cdot x_1 + 287.75 \cdot x_2 \cdot x_2 - 5.37 \cdot x_3 \cdot x_3 \quad (19)$$

Testing of the developed models was recorded as a comparison of experimental values, predictions and percent deviation; experimental value \rightarrow prediction \rightarrow percent deviation:

- Principal cutting force (Eq. 17)
Lowest deviation with measured value: 550.848 N \rightarrow 557.877 N \rightarrow 1.28 %
Highest deviation with measured value: 174.024 N \rightarrow 189.579 N \rightarrow 8.94 %
Average deviation of all twenty measurements with ten predictions: 3.57 %
- Surface roughness (Eq. 18)
Lowest deviation with measured value: 2.32 μm \rightarrow 2.31 μm \rightarrow 0.43 %
Highest deviation with measured value: 1.31 μm \rightarrow 1.48 μm \rightarrow 13.30 %
Average deviation of all twenty measurements with ten predictions: 4.02 %
- Tool life (Eq. 19)
Lowest deviation with measured value: 10.93 min \rightarrow 10.77 min \rightarrow 1.49 %
Highest deviation with measured value: 28.43 min \rightarrow 26.45 min \rightarrow 6.97 %
Average deviation of all twenty measurements with ten predictions: 4.50 %

In this case, the deviation was within the acceptable ten percent. In any case, the lowest possible deviations are desirable, but the size of deviations depends primarily on the number of

measurements. The experiment assured only 20 results of finishing machining, therefore, the final average of results can be assumed to be acceptable.

3.2 Multi-objective optimization by the NSGA-II algorithm

On the basis of models created by means of the GSA algorithm and outlined in the previous subsection, in this paragraph, a set of optimal solutions for the chosen machining operation will be searched for. In our case, the resulting models for force, roughness and tool resistance represent three objective (criteria) functions having to satisfy also the limitations stated below. In this research, the aim of multi-objective optimization by the NSGA-II method was to determine such a combination of independent input variables (i.e. cutting force, feed rate and cut depth) at chosen intervals, that optimal values of criteria functions will be reached and the limitations prescribed satisfied. On the basis of theoretical calculations of limitations, and on the basis of experimental data, the optimization limitations of cutting force F_c , roughness R_a and tool resistance T were determined:

- $F_c \leq 450.0$ N
- $1.0 \leq R_a \leq 1.6$ μm
- $15.0 \leq T \leq 20.0$ min

According to the theoretical calculations and experimental data, the intervals of independent variables of cutting speed v_c , feed rate f and cut depth a_p were also prepared:

- $366.0 < v_c < 540.0$ $\frac{\text{m}}{\text{min}}$
- $0.10 < f < 0.18$ $\frac{\text{mm}}{\text{rev}}$
- $0.2 < a_p < 1.2$ mm

The results of the fine turning operation are presented by means of a Pareto optimal front. Minimal surface roughness has priority as fine machining is aimed at securing final shapes and dimensions. Fig. 3 shows the results of optimization developed by using the GSA algorithm.

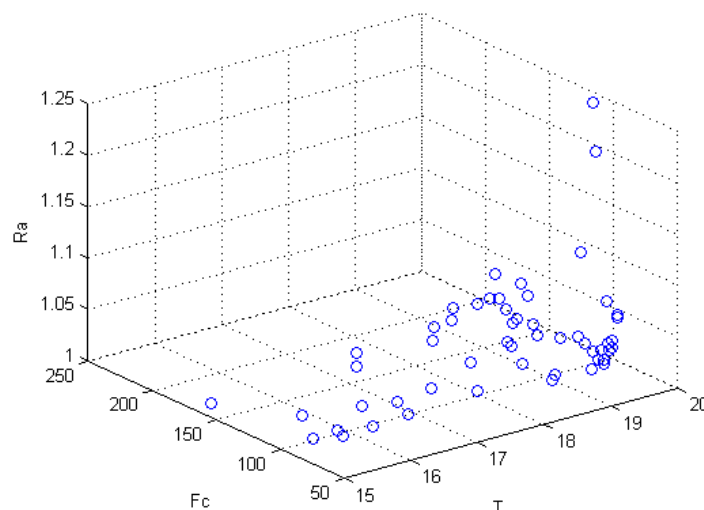


Fig. 3 Pareto optimal front

The Pareto optimal front contains 53 equivalent solutions. The most successful optimal combination is proposed, where:

Independent parameters:

$$x_1 = v_c = 439.9 \text{ m/min}$$

$$x_2 = f = 0.11 \text{ mm/rev}$$

$$x_3 = a_p = 0.62 \text{ mm}$$

Dependent parameters:

$$F_c = 201.36 \text{ N}$$

$$R_a = 1 \mu\text{m}$$

$$T = 19.53 \text{ min}$$

4. Conclusion

In the first step of the research an intelligent system was devised, ensuring effective modelling of the CNC machining process by the use of a GSA. The relevant GSA was developed, with an added regression analysis module allowing wider algorithm functioning for modelling machining operations with a training base. The developed system is useful in all standard machining processes, e.g. turning, milling, drilling, but, for the purpose of this research, the models of the CNC turning process have been developed with the use of experimental measurements relating to the turning process, and their accuracy tested. Results have confirmed that the CNC machining process can be modelled effectively by using a GSA.

In the second step, the models of CNC turning were used for multi-objective optimization of machining parameters by the NSGA-II algorithm. The result of multi-objective optimization of machining parameters was the Pareto front of optimal solutions, out of which the solution most suitable in practice can be selected for the chosen machining operation. For example, if fine machining parameters are looked for, the solution, giving priority to minimum surface roughness, will be selected, as the aim of fine machining is securing final shapes and dimensions.

Prospective further researches could focus on the enhancement of the training and testing base with new measurements, and on repetition of the whole experiment with other materials and tools. The use of appropriate machine tools and sensors could also ensure current measuring of cutting force which would be transmitted via computer communication into the base on an intermediate server or computer.

Acknowledgement

We would like to thank the Slovenian Research Agency (ARRS) for the financial support for execution of the presented research.

References

- [1] Hrelja, M., Klančnik S., Balic J., Brezocnik M. (2014). Modelling of a turning process using the gravitational search algorithm, *International Journal of Simulation Modelling*, Vol. 13. No. 1, 30-41, [doi: 10.2507/IJSIMM13\(1\)3.248](https://doi.org/10.2507/IJSIMM13(1)3.248).
- [2] Lestan, Z., Klančnik, S., Balic, J., Brezocnik, M. (2015). Modeling and design of experiments of laser cladding process by genetic programming and nondominated sorting, *Materials and Manufacturing Processes*, Vol. 30, No. 4, 458-463, [doi: 10.1080/10426914.2014.973586](https://doi.org/10.1080/10426914.2014.973586).
- [3] Ficko, M., Palcic, I. (2013). Designing a layout using the modified triangle method, and genetic algorithms, *International Journal of Simulation Modelling*, Vol. 12, No. 3, 237-251, [doi: 10.2507/IJSIMM12\(4\)3.244](https://doi.org/10.2507/IJSIMM12(4)3.244).
- [4] Alberti, M., Ciurana, J., Casadesús, M. (2005). A system for optimising cutting parameters when planning milling operations in high-speed machining, *Journal of Materials Processing Technology*, Vol. 168, No. 1, 25-35, [doi: 10.1016/j.jmatprotec.2004.09.092](https://doi.org/10.1016/j.jmatprotec.2004.09.092).
- [5] Bharathi Raja, S., Baskar, N. (2011). Particle swarm optimization technique for determining optimal machining parameters of different work piece materials in turning operation, *The International Journal of Advanced Manufacturing Technology*, Vol. 54, No. 5, 445-463, [doi: 10.1007/s00170-010-2958-y](https://doi.org/10.1007/s00170-010-2958-y).
- [6] Zain, A.M., Haron, H., Sharif, S. (2011). Optimization of process parameters in the abrasive waterjet machining using integrated SA-GA, *Applied Soft Computing*, Vol. 11, No. 8, 5350-5359, <https://doi.org/10.1016/j.asoc.2011.05.024>.
- [7] Billatos, S.B., Tseng, P.-C. (1991). Knowledge-based optimization for intelligent machining, *Journal of Manufacturing Systems*, Vol. 10, No. 6, 464-475, [doi: 10.1016/0278-6125\(91\)90004-L](https://doi.org/10.1016/0278-6125(91)90004-L).
- [8] Byrne, G., Dornfeld, D., Inasaki, I., Ketteler, G., König, W., Teti, R. (1995). Tool condition monitoring (TCM) – The status of research and industrial application, *CIRP Annals – Manufacturing Technology*, Vol. 44, No. 2, 541-567, [doi: 10.1016/S0007-8506\(07\)60503-4](https://doi.org/10.1016/S0007-8506(07)60503-4).
- [9] Chua, M.S., Rahman, M., Wong, Y.S., Loh, H.T. (1993). Determination of optimal cutting conditions using design of experiments and optimization techniques, *International Journal of Machine Tools and Manufacture*, Vol. 33, No. 2, 297-305, [doi: 10.1016/0890-6955\(93\)90081-5](https://doi.org/10.1016/0890-6955(93)90081-5).
- [10] Yusup, N., Zain, A.M., Hashim, S.Z.M. (2012). Evolutionary techniques in optimizing machining parameters: Review and recent applications (2007-2011), *Expert Systems with Applications*, Vol. 39, No. 10, 9909-9927, [doi: 10.1016/j.eswa.2012.02.109](https://doi.org/10.1016/j.eswa.2012.02.109).
- [11] Zain, A.M., Haron, H., Sharif, S. (2010). Application of GA to optimize cutting conditions for minimizing surface roughness in end milling machining process, *Expert Systems with Applications*, Vol. 37, No. 6, 4650-4659, [doi: 10.1016/j.eswa.2009.12.043](https://doi.org/10.1016/j.eswa.2009.12.043).

- [12] D'Addona, D.M., Teti, R. (2013). Genetic algorithm-based optimization of cutting parameters in turning processes, *Procedia CIRP*, Vol. 7, 323-328, doi: [10.1016/j.procir.2013.05.055](https://doi.org/10.1016/j.procir.2013.05.055).
- [13] Khaider, B., Asma, T. (2016). Hard turning behavior improvement using NSGA-II and PSO-NN hybrid model, *The International Journal of Advanced Manufacturing Technology*, Vol. 86, No. 9, 3527-3546, doi: [10.1007/s00170-016-8479-6](https://doi.org/10.1007/s00170-016-8479-6).
- [14] Krimpenis, A., Vosniakos, G.-C. (2009). Rough milling optimisation for parts with sculptured surfaces using genetic algorithms in a Stackelberg game, *Journal of Intelligent Manufacturing*, Vol. 20, No. 4, 447-461, doi: [10.1007/s10845-008-0147-8](https://doi.org/10.1007/s10845-008-0147-8).
- [15] Suresh, P.V.S., Venkateswara Rao, P., Deshmukh, S.G. (2002). A genetic algorithmic approach for optimization of surface roughness prediction model, *International Journal of Machine Tools and Manufacture*, Vol. 42, No. 6, 675-680, doi: [10.1016/S0890-6955\(02\)00005-6](https://doi.org/10.1016/S0890-6955(02)00005-6).
- [16] Mizugaki, Y., Hao, M., Sakamoto, M., Makino, H. (1994). Optimal tool selection based on genetic algorithm in a geometric cutting simulation, *CIRP Annals – Manufacturing Technology*, Vol. 43, No. 1, 433-436, doi: [doi:10.1016/S0007-8506\(07\)62247-1](https://doi.org/10.1016/S0007-8506(07)62247-1).
- [17] Jurkovic, Z., Cukor, G., Brezocnik, M., Brajkovic, T. (2016). A comparison of machine learning methods for cutting parameters prediction in high speed turning process, *Journal of Intelligent Manufacturing*, (in Press), doi: [10.1007/s10845-016-1206-1](https://doi.org/10.1007/s10845-016-1206-1).
- [18] Cukor, G., Jurkovic, Z. (2010). Optimization of turning using evolutionary algorithms, *Engineering Review*, Vol. 30, No. 2, 1-10.
- [19] Mocnik, D., Paulic, M., Klančnik, S., Balic, J. (2014). Prediction of dimensional deviation of workpiece using regression, ANN and PSO models in turning operation, *Tehnički vjesnik – Technical Gazette*, Vol. 21, No. 1, 55-62.
- [20] El-Mounayri, H., Kishawy, H., Briceno, J. (2005). Optimization of CNC ball end milling: A neural network-based model, *Journal of Materials Processing Technology*, Vol. 166, No. 1, 50-62, doi: [10.1016/j.jmatprotec.2004.07.097](https://doi.org/10.1016/j.jmatprotec.2004.07.097).
- [21] Muñoz-Escalona, P., Maropoulos, P.G. (2010). Artificial neural networks for surface roughness prediction when face milling Al 7075-T7351, *Journal of Materials Engineering and Performance*, Vol. 19, No. 2, 185-193, doi: [10.1007/s11665-009-9452-4](https://doi.org/10.1007/s11665-009-9452-4).
- [22] Zhang, Y., Gong, D.-W., Ding, Z.-H. (2011). Handling multi-objective optimization problems with a multi-swarm cooperative particle swarm optimizer, *Expert Systems with Applications*, Vol. 38, No. 11, 13933-13941, doi: [10.1016/j.eswa.2011.04.200](https://doi.org/10.1016/j.eswa.2011.04.200).
- [23] Chiang, F., Braun, R., Agbinya, J.I. (2007). Self-configuration of network services with biologically inspired learning and adaptation, *Journal of Network and Systems Management*, Vol. 15, No. 1, 87-87, doi: [10.1007/s10922-006-9056-3](https://doi.org/10.1007/s10922-006-9056-3).
- [24] Rashedi, E., Nezamabadi-pour, H., Saryazdi, S. (2009). GSA: A gravitational search algorithm, *Information Sciences*, Vol. 179, No. 13, 2232-2248, doi: [10.1016/j.ins.2009.03.004](https://doi.org/10.1016/j.ins.2009.03.004).
- [25] Jurkovic, Z. (2007). *Modeliranje i optimizacija parametara obrade primjenom evolucijskih algoritama kod inteligentnih obradnih sustava*, PhD thesis, University of Rijeka, Rijeka, Croatia.
- [26] Wang, L., Wang, T.-G., Luo, Y. (2011). Improved non-dominated sorting genetic algorithm (NSGA)-II in multi-objective optimization studies of wind turbine blades, *Applied Mathematics and Mechanics*, Vol. 32, No. 6, 739-748, doi: [10.1007/s10483-011-1453-x](https://doi.org/10.1007/s10483-011-1453-x).

Calendar of events

- International Conference on Manufacturing Technologies, San Diego, USA, January 19-21, 2017.
- The 7th International Conference on Advanced Materials Research, Hong Kong, China, January 20-22, 2017.
- 8th International Conference on Mechatronics and Manufacturing, Tokyo, Japan, January 20-22, 2017.
- The 8th International Conference on Mechanical and Intelligent Manufacturing Technologies, Cape Town, South Africa, February 3-6, 2017.
- European Conference on Materials, Mechatronics and Manufacturing, Paris, France, February 15-17, 2017.
- 2nd International Conference on Mechanical, Manufacturing, Modeling and Mechatronics, Kortrijk, Belgium, February 24-26, 2017.
- 5th Annual International Conference on Operational Research and Statistics, Singapore, March 6-7, 2017.
- 19th International Conference on Production Engineering and Management, Boston, USA, April 24-25, 2017.
- 10th International Conference on Industrial Tools and Advances Processing Technologies, Ljubljana, Slovenia, April 24-26, 2017.
- 7th International Conference on Simulation and Modeling Methodologies, Technologies and Applications, Madrid, Spain, July 29-31, 2017.

This page intentionally left blank.

Notes for contributors

General

Articles submitted to the *APEM journal* should be original and unpublished contributions and should not be under consideration for any other publication at the same time. Manuscript should be written in English. Responsibility for the contents of the paper rests upon the authors and not upon the editors or the publisher. Authors of submitted papers automatically accept a copyright transfer to *Production Engineering Institute, University of Maribor*. For most up-to-date information on publishing procedure please see the *APEM journal* homepage apem-journal.org.

Submission of papers

A submission must include the corresponding author's complete name, affiliation, address, phone and fax numbers, and e-mail address. All papers for consideration by *Advances in Production Engineering & Management* should be submitted by e-mail to the journal Editor-in-Chief:

Miran Brezocnik, Editor-in-Chief
UNIVERSITY OF MARIBOR
Faculty of Mechanical Engineering
Production Engineering Institute
Smetanova ulica 17, SI – 2000 Maribor
Slovenia, European Union
E-mail: editor@apem-journal.org

Manuscript preparation

Manuscript should be prepared in *Microsoft Word 2007* (or higher version) word processor. *Word .docx* format is required. Papers on A4 format, single-spaced, typed in one column, using body text font size of 11 pt, should not exceed 12 pages, including abstract, keywords, body text, figures, tables, acknowledgements (if any), references, and appendices (if any). The title of the paper, authors' names, affiliations and headings of the body text should be in *Calibri* font. Body text, figures and tables captions have to be written in *Cambria* font. Mathematical equations and expressions must be set in *Microsoft Word Equation Editor* and written in *Cambria Math* font. For detail instructions on manuscript preparation please see instruction for authors in the *APEM journal* homepage apem-journal.org.

The review process

Every manuscript submitted for possible publication in the *APEM journal* is first briefly reviewed by the editor for general suitability for the journal. Notification of successful submission is sent. After initial screening, and checking by a special plagiarism detection tool, the manuscript is passed on to at least two referees. A double-blind peer review process ensures the content's validity and relevance. Optionally, authors are invited to suggest up to three well-respected experts in the field discussed in the article who might act as reviewers. The review process can take up to eight weeks. Based on the comments of the referees, the editor will take a decision about the paper. The following decisions can be made: accepting the paper, reconsidering the paper after changes, or rejecting the paper. Accepted papers may not be offered elsewhere for publication. The editor may, in some circumstances, vary this process at his discretion.

Proofs

Proofs will be sent to the corresponding author and should be returned within 3 days of receipt. Corrections should be restricted to typesetting errors and minor changes.

Offprints

An e-offprint, i.e., a PDF version of the published article, will be sent by e-mail to the corresponding author. Additionally, one complete copy of the journal will be sent free of charge to the corresponding author of the published article.

APEM

journal

Advances in Production Engineering & Management

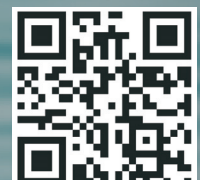
Production Engineering Institute (PEI)
University of Maribor
APEM homepage: apem-journal.org

Volume 11 | Number 4 | December 2016 | pp 255-380

Contents

Scope and topics	258
A combined zone-LP and simulated annealing algorithm for unequal-area facility layout problem Xiao, Y.J.; Zheng, Y.; Zhang, L.M.; Kuo, Y.H.	259
A new multi-objective Jaya algorithm for optimization of modern machining processes Rao, R.V.; Rai, D.P.; Ramkumar, J.; Balic, J.	271
Finite element method for optimum design selection of carport structures under multiple load cases Özkal, F.M.; Cakir, F.; Arkun, A.K.	287
Applying multi-phase particle swarm optimization to solve bulk cargo port scheduling problem Tang, M.; Gong, D.; Liu, S.; Zhang, H.	299
A case-based reasoning approach for non-traditional machining processes selection Boral, S.; Chakraborty, S.	311
Dimensional accuracy of camera casing models 3D printed on Mcor IRIS: A case study Mandić, M.; Galeta, T.; Raos, P.; Jugović, V.	324
Effect of delayed differentiation on a multiproduct vendor-buyer integrated inventory system with rework Chiu, Y.-S.P.; Kuo, J.-S.; Chiu, S.W.; Hsieh, Y.-T.	333
Experimental modeling of fluid pressure during hydroforming of welded plates Karabegović, E.; Poljak, J.	345
An integrated lean approach to Process Failure Mode and Effect Analysis (PFMEA): A case study from automotive industry Banduka, N.; Veža, I.; Bilić, B.	355
Multi-objective optimization of the turning process using a Gravitational Search Algorithm (GSA) and NSGA-II approach Klancnik, S.; Hrelja, M.; Balic, J.; Brezocnik, M.	366
Calendar of events	377
Notes for contributors	379

Copyright © 2016 PEI. All rights reserved.



apem-journal.org